PROCESSING MELT BLENDED POLYMER NANOCOMPOSITES USING A NOVEL LABORATORY MINI-MIXER

Development of polymer nanocomposites in the melt phase using a novel mini-mixer

Atif Hussain KHAN (BEng, MSc, IMechE)

Submitted for degree of doctor of philosophy

School of Engineering, Design and Technology

University of Bradford

2012

ABSTRACT

Name: Atif Hussain Khan

Title: Processing Melt Blended Polymer Nanocomposites Using a Novel Laboratory Mini-mixer

Keywords: Nanocomposites, Nanoclay, Intercalation, Exfoliation, Polypropylene, Mixing, Extrusion, Stretching, Rheology

Research into the processing conditions and parameters of polymeric nanocomposites has always been challenging to scientists and engineers alike. Many have developed tools and procedures to allow materials to be exploited and their properties improved with the addition of nanofillers to achieve the desired end material for various applications. Initial trials are mostly conducted using conventional small scale experiments using specialised equipment within the laboratory that can replicate the larger industrial equipment. This is a logical approach as it could save time and costs as many nanocomposites are relatively expensive to produce. Experiments have previously been done using the likes of the Haake twin screw extruder to manufacture nanocomposites within the laboratory but this research project has used a novel minimixer specifically developed to replicate mixing like large twin screw extrusion machines. The minimixer uses a twin paddle system for high shear mixing in conjunction with a single screw thus theoretically allowing an infinitely long recirculation. It is this ability to mix intensely whilst allowing for as long as desired recirculation which enables the replication in this very small mixer (10-30g capacity) of the mixing conditions in a large twin screw extruder. An added feature of the minimixer is that it can undertake inline data analysis in real time.

The main experiments were conducted using a comprehensive DOE approach with several different factors being used including the temperature, screw speed, residence time, clay and compatibiliser loading and two polymer MFI's. The materials used included PP, Cloisite 20A, Polybond 3200, PET, Somasif MTE, Polyurethane 80A and Single / Multi-walled Carbon nanotubes.

Detailed experimental results highlighted that rheological analysis of the nanocomposite materials as an initial testing tool were accurate in determining the Elastic and Loss modulus values together with the Creep and Recovery, Viscosity and Phase Angle properties in the molten state. This approach was also used in an additional set of experiments whereby the temperature, speed, residence time and compatibiliser were kept constant but the clay loading was increased in 1% wt. increments. These results showed that the G' & G'' values increased with clay loading. Another important finding was the bi-axial stretching step introduced after the processing stage of the nanocomposite materials which highlighted a further improvement in the modulus values using rheological testing. Other tests included using inline monitoring to look into both the viscosity and ultrasound measurements in real time of the molten polymer nanocomposite through a slit die attachment to the minimixer.

ACKNOWLEDGEMENTS

I would like to thank everyone for supporting me in my efforts of making this report possible.

I am especially grateful to my supervisors Prof. Hadj Benkreira & Dr Raj Patel who have continually helped and guided me in the right direction together with Prof. Phil Coates. I would also like to thank David Steele and the other staff & technicians in the IRC department for their help and expertise when most needed and EPSRC for the grant that made all this possible for me.

Finally I would like to express gratitude to my family who morally supported me and gave me the time to complete the work.

CONTENTS

Chapter 1 : INTRODUCTION 1
1.1 Introduction 1
1.2 Background history of composite materials 3
1.3 The formation of nanocomposite materials 7
1.4 Equipment for processing nanocomposite materials 10
1.5 Characterising a polymer nanocomposite 13
1.6 Aim and objectives of the research 14
Chapter 2 : LITERATURE REVIEW 18
2.1 Introduction 18
2.2 Polymer nanocomposite variations 18
2.3 PP-Clay nanocomposites 22
2.3.1 Nanoclays 26
2.3.2 Role of Compatibilisers 27
2.4 Processing stages of polymer nanocomposites 29
2.4.1 Small scaled production of NC 30
2.4.2 Large scaled production of NC 37
2.5 The Minimixer at Bradford 40
2.6 Studies on development of PP nanocomposites 43
2.7 Assessing properties of PP nanocomposites 49
2.7.1 X-Ray Diffraction (XRD) 50
2.7.2 SEM / TEM 51
2.7.3 Mechanical Testing 51
2.7.4 Differential Scanning Calorimetry (DSC) 52
2.7.5 Dynamic Mechanical Analyser (DMA) 52
2.7.6 Rheology 53
2.8 Additional work on PP nanocomposites 54
2.8.1 Biaxial stretching of polymer nanocomposites 54
2.8.2 Recycling polymer nanocomposites 57
2.8.3 Inline Monitoring 59
2.9 Conclusions 60
Chapter 3 : EXPERIMENTAL METHOD 64
3.1 Introduction 64

3.2 The mini-mixer: Design and Operation Features 65
3.2.1 The original mini-mixer 65
3.2.2 New Instruments Data Logging of the mini-mixer 68
3.3 Polymers & nano-additives used and their preparation 72
3.3.1 Materials Used 73
3.3.2 Material preparation before extrusion 73
3.3.3 Extrudate samples preparation for testing 74
3.4 Experiments for producing nanocomposites 76
3.4.1 Design of Experiments for PP 76
3.4.2 Additional PP runs 78
3.4.3 Design of Experiment (DOE) for PET 81
3.4.4 Experiments with PU and Carbon Nanotubes 84
3.5 Characterisation of nanocomposites obtained 87
3.5.1 Microscopy 87
3.5.2 Off-line rheology 87
3.5.3 In-line rheology 91
3.5.4 Ultrasound measurements 94
3.5.5 Mechanical and Crystallisation properties measurements 95
3.6 Stretching experiments 96
3.7 Extrusion scale-up: Equipment & method 98
Chapter 4 : RESULTS / DISCUSSION 101
4.1 Introduction 101
4.2 Results of DOE programme on PP in the Minimixer 101
4.2.1 Rheological Data of Nanocomposites Obtained 102
4.2.2 Mechanical Properties of the Nanocomposites Obtained 110
4.2.3 Microscopic Evaluation of the Nanocomposites Obtained 112
4.3 Rheological Evaluation at Optimum DOE conditions 114
4.4 Effect of Stretching on Nanocomposites 120
4.5 Further Evaluation of Mixing Processes 143
4.5.1 Effect of Mixing Materials Prior to Feeding into Mini-mixer (Extrusion) 143
4.5.2 Effect of Nanoclay Type 144
4.6 Repeatability Tests of Rheological Evaluation 155
4.7 In-Line Rheological Evaluation using a Slit Die 162
4.8 In-line Evaluation of Nanocomposites using Ultrasound 166
Chapter 5 : CONCLUSION / RECOMMENDATIONS 168

REFERENCES 172
APPENDICES 183
DSC Results 183
DMA Results 185
PET DOE trials 187
Polyurethane and Carbon nanotube trials 198

LIST OF FIGURES

Figure 1.1: Various nanofiller particle profiles [1] 2
Figure 1.2: A selection of composite materials [6] 5
Figure 1.3: Formation of polymer nanocomposites 8
Figure 1.4: The Haake Minilab II Micro Compounder 11
Figure 1.5: Internal layout of the minimixer showing the 3 screw design 13
Figure 2.1: Different types of nanofillers [27] 19
Figure 2.2: Stages of nanocomposite formation 21
Figure 2.3: Ziegler-Natta Polymerisation 23
Figure 2.4: Dispersive and Distributive mixing [46] 30
Figure 2.5: Typical illustration of co and counter rotating screw layout 32
Figure 2.6: The Haake type TS laboratory extruder 34
Figure 2.7: The Brabender type TS extruder 36
Figure 2.8: A typical extruder 38
Figure 2.9: Illustration of the Mini-Mixer [24] 42
Figure 2.10: Screw design layout 43
Figure 2.11: G'of PP/PPg vs.Strain at $1s^{-1}$and $180^{o}C$ [52] 45
Figure 2.12: G' & tan δat $180^{o}C$ [52] 46
Figure 2.13: E'& Impact Strength of TPO vs. OMMT content [53] 47
Figure 2.14: η* of various nanocomposites at $190^{o}C$ [54] 49
Figure 2.15: TEM Images of PP / Nanoclay materials with different Stretching Ratio's (Courtesy of QUB) 55
Figure 2.16: Diagram of the blown film process [73] 57
Figure 2.17: Inline monitoring setup 59
Figure 2.18: Shearing effect of clay platelets 61
Figure 3.1: Designs of the minimixer showing various arrangements for operation. 67
Figure 3.2: The limitation of commercial minimixer (unequal mixing history in recirculation channel. 67
Figure 3.3: The minimixer setup in its entirety 68
Figure 3.4: Picture of the NI-cDAQ-9172 and overall data acquisition setup 69
Figure 3.5: Front panel of VI for data acquisition Labview software 71
Figure 3.6: Block Diagram Containing Source Code of Labview software 71
Figure 3.7: Picture of the hot press 76
Figure 3.8: Bohlin CVO120 Rheometer 89
Figure 3.9: Slit die in bare form and in use 91
Figure 3.10: Slit die with pressure transducers 93
Figure 3.11: Slit die with ultrasound probes attached in parallel and Oscilloscope 94
Figure 3.12: Picture of a cut out T-bar and Instron Machine clamps 95
Figure 3.13: Setup of the biaxial stretcher 97
Figure 3.14: Different stages of the stretched samples 98
Figure 3.15: Picture of the APV twin screw extruder 99
Figure 3.16: Illustration of shear rates within minimixer 100
Figure 3.17: The different colour complexity of each run after extrusion in the APV 100
Figure 4.1: G' vs. strain rate from AS test 103
Figure 4.2: G' organised in descending order for AS 104

Figure 4.3: G' vs. frequency from FS tests 105
Figure 4.4: G' organised in descending order for FS 106
Figure 4.5: G'' organised in descending order for FS 106
Figure 4.6: η* organised in descending order for FS 107
Figure 4.7: δ^{o}organised in descending order for FS 107
Figure 4.8: Creep & Recovery vs. Time 108
Figure 4.9: Creep tests in descending order 109
Figure 4.10: Recovery tests in descending order 109
Figure 4.11: Tensile modulus of DOE runs in ascending order 111
Figure 4.12: Tensile strength of DOE runs in ascending order 111
Figure 4.13: Mechanical properties of compression moulded samples 112
Figure 4.14: TEM images of various DOE runs 114
Figure 4.15: G' vs. Strain rate from AS test at 190^{o}C and clay loading 0-10% 116
Figure 4.16: G' vs. Frequency from FS test at 190^{o}C and clay loading 0-10% 116
Figure 4.17: G'' vs. Frequency from FS test 117
Figure 4.18: η* vs. Frequency from FS test 117
Figure 4.19: δ^{o} vs. Frequency from FS test 118
Figure 4.20: J_C& J_R vs. Time from CR test and clay loading 0-10% 118
Figure 4.21: E' vs. % clay for PP 119
Figure 4.22: % Elongation vs. % clay for PP 119
Figure 4.23: SEM images of fracture surface for 1% clay 120
Figure 4.24: SEM images of fracture surface for 6% clay 120
Figure 4.25:G' vs. Strain rate from AS test (2:1) 126
Figure 4.26: G' vs. Strain rate from AS test (4:1) 126
Figure 4.27: AS comparison chart for G' 127
Figure 4.28: G' vs. Frequency from FS test (2:1) 127
Figure 4.29: G' vs. Frequency from FS test (4:1) 128
Figure 4.30: FS comparison chart for G' 128
Figure 4.31: FS comparison chart for G'' 129
Figure 4.32: η* vs. Frequency from FS test (2:1) 129
Figure 4.33: η* vs. Frequency from FS test (4:1) 130
Figure 4.34: FS comparison chart for η* 130
Figure 4.35: δ^{o} vs. Frequency from FS test (2:1) 131
Figure 4.36: δ^{o} vs. Frequency from FS test (4:1) 131
Figure 4.37: FS comparison chart for δ^{o} 132
Figure 4.38: J_C& J_R vs. Time from CR test (2:1) 132
Figure 4.39: J_C& J_R vs. Time from CR test (4:1) 133
Figure 4.40: Creep tests comparison chart 133
Figure 4.41: Recovery tests comparison chart 134
Figure 4.42: E' vs. % clay for unstretched PP 134
Figure 4.43: E' vs. % clay for 2:1 stretched PP 135
Figure 4.44: E' vs. % clay for 4:1 stretched PP 135
Figure 4.45: % Elongation vs. % clay for unstretched PP 136
Figure 4.46: % Elongation vs. % clay for 2:1 stretched PP 136
Figure 4.47: % Elongation vs. % clay for 4:1 stretched PP 137
Figure 4.48: % Crystallinity from DSC data 138

Figure 4.49: G' vs Strain from dual processing of run 4 140
Figure 4.50: G' vs Frequency from dual processing of run 4 140
Figure 4.51: η* vs Frequency from dual processing of run 4 141
Figure 4.52: J_C &J_R vs Time from dual processing of run 4 (AS test).....141
Figure 4.53: E' from tensile tests of dual processed run 4.....142
Figure 4.54: % Elongation from tensile tests of dual processed run 4 142
Figure 4.55: G' vs. Strain for unmixed samples.....146
Figure 4.56: G' vs. Frequency for unmixed samples.....146
Figure 4.57: G'' vs. Frequency for unmixed samples 147
Figure 4.58: η* vs. Frequency for unmixed samples.....147
Figure 4.59: J_C& J_R vs. Time for unmixed samples 148
Figure 4.60: G' vs. Strain for Cloisite 10A.....149
Figure 4.61: G' vs. Frequency for Cloisite 10A.....149
Figure 4.62: G'' vs. Frequency for Cloisite 10A 150
Figure 4.63: η* vs. Frequency for Cloisite 10A.....150
Figure 4.64: J_C & J_R for Cloisite 10A 151
Figure 4.65: G' vs. Strain for Cloisite 10A (3:1) 151
Figure 4.66: G' vs. Frequency for Cloisite 10A (3:1) 152
Figure 4.67: G'' vs. Frequency for Cloisite 10A (BS 3:1) 152
Figure 4.68: η* vs. Frequency for Cloisite 10A (BS 3:1).....153
Figure 4.69: J_C& J_R for Cloisite 10A (BS 3:1).....153
Figure 4.70: E' from tensile tests of Cloisite 10A.....154
Figure 4.71: % Elongation from tensile tests of Cloisite 10A 154
Figure 4.72: G' vs. Strain using Anton Paar 157
Figure 4.73: G'' vs. Strain using Anton Paar.....157
Figure 4.74: G' vs. Frequency using Anton Paar 158
Figure 4.75: G'' vs. Frequency using Anton Paar.....158
Figure 4.76: η* vs. Frequency using Anton Paar 159
Figure 4.77: Torque vs. Frequency using Anton Paar 159
Figure 4.78: G'' vs. Strain using Anton Paar.....160
Figure 4.79: G'' vs. Frequency using Anton Paar.....160
Figure 4.80: η* vs. Frequency using Anton Paar 161
Figure 4.81: Torque vs. Frequency using Anton Paar 161
Figure 4.82: Viscosity vs. Shear rate from Pressure measurements.....163
Figure 4.83: Inline Torque measurement in real time 163
Figure 4.84: Viscosity vs. Shear Rate comparison.....164
Figure 4.85: Temperature along slit die 165
Figure 4.86: Ultrasound measurements of PP 0-10%wt Clay.....166
Figure 4.87: Ultrasound measurements of 0-10% clay samples 167
Figure 4.88: Ultrasound measurements of 0-10% clay samples 167

LIST OF TABLES

Table 2.1: Development of nanocomposites 37
Table 2.2: Organo-modified clays used to prepare the PNCs [52] 44
Table 2.3: TGA and XRD results [54] 44
Table 2.4: E', yield and impact strength of nanocomposites [53] 47
Table 2.5: Pure PP, PP-g-MAH Compatibilizer & Organoclay (wt %) [54] 48
Table 2.6: Effects of different stretch ratios on properties 55
Table 3.1: Table of different factors and their levels 77
Table 3.2: Complete DOE runs 77
Table 3.3: Additional PP runs 79
Table 3.4: Different factors used for PET runs 81
Table 3.5: PET NC observations 82
Table 3.6: PET runs 83
Table 3.7: Additional PET runs 84
Table 3.8: PU/CNT runs 86
Table 3.9: Pressure measurement calculations 93
Table 3.10: Deriving Viscosity from Pressure data 93
Table 3.11: Scaled up runs undertaken on APV extruder 99
Table 4.1: Table of different DOE factors and their levels 101
Table 4.2: DOE Runs 102
Table 4.3: DoE outcomes – responses 113
Table 4.4: Crystallinity and Standard Heat values 138

KEYWORDS

Nanocomposites, Nanoclay, Intercalation, Exfoliation, Polypropylene, Mixing, Extrusion, Stretching, Rheology

Nomenclature:

D	Diffusivity
d	Spacing between diffractional lattice planes
DMA	Dynamic mechanical analysis
DOE	Design of experiments
DSC	Differential scanning calorimetry
E' (MPa)	Storage modulus under bending mode
E'' (MPa)	Loss modulus under bending mode
G' (Pa)	Storage modulus under tensile mode
G'' (Pa)	Loss modulus under tensile mode
MMT	Montmorillonite
Clay	Organo-modified clay
OMLS	Organo-modified layered silicate, organosilicate,
P	Permeability
PCN	Polymer–clay nanocomposite
PET	Poly(ethylene terephthalate)
PLS	Polymer–layered silicate nanocomposite
PMMA	Polymethyl methacrylate
PP	Polypropylene
PP-MA/PP-g-MA	Maleic anhydride-grafted polypropylene
PU	Polyurethane
S	Solubility
SEM	Scanning electron miscroscope
T_c	Crystallisation temperature
TEM	Transmission electron microscopy
T_g	Glass transition temperature
TGA	Thermogravimetric analysis
WAXD/WAXS	Wide angle X-ray diffraction or scattering
XRD	X-ray diffraction

Chapter 1 : INTRODUCTION

1.1 Introduction

The term ‘nano’ is being used more prevalently as people come to terms with the nanotechnology revolution and its links to the development of new materials and technologies. Anything linked with this term is deemed very small however it is important to state that nanoparticles are not as small as atomic scale objects so in principle they are comparatively easy to measure, being one thousand of a micron in size [1]. As technological advances in new generation materials increase with lighter and stronger materials for demanding applications, the research into this area is ever expanding with research focusing into the microstructure of these materials and how this can influence their properties [1].

The main focus in the past few years has been on polymer based materials which are abundantly available at a low cost and trying to improve their properties by the addition of different nano sized fillers as shown in figure 1.1. The addition of a foreign material that is within the nano range to the main material is termed a nanocomposite and these are the new materials that are emerging as winners with their new and improved properties [1-2]. The dimensional feature that makes nanoparticles unique is that it is only necessary to use a very small amount; typically 5% into a polymer melt, to produce a huge interfacial area between the nano-additives and the polymer. In other words, nanoparticles provide surface area / volume ratios that are extremely high, typically of the order one billion times larger when you decrease the particle size from 1 micron to 1 nanometre. This large interface area

promotes strong interactions between the polymer and the nanoparticles leading to the unique properties observed with the nanocomposites [2].

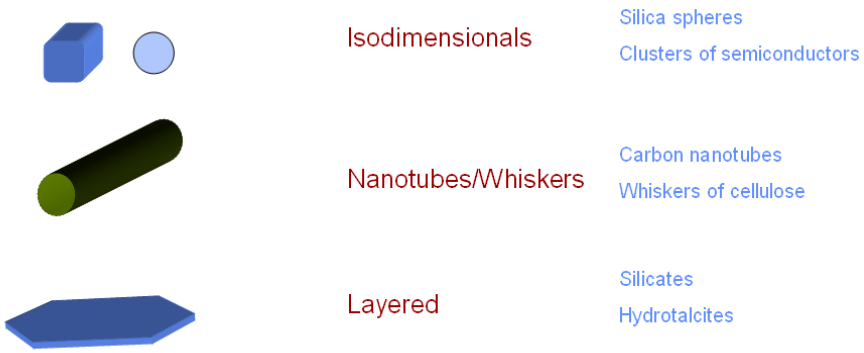

Figure 1.1: Various nanofiller particle profiles [1]

Since nanocomposites can be derived from many different combinations of materials i.e. metals, plastics, glass and even fibres, the scope of these new materials is huge therefore this research here will focus on polymer nanocomposites only.

Today polymers are broadly used in everyday applications and are essentially an indispensable commodity with great attention having been focused on making the materials more user friendly for the desired markets together with cost savings. The main advantages are the cheap prices and the vast availability of the raw materials together with easy processing making them a good all-round commodity. However more specialised and high end products made from polymers require additional features and improvements in various properties and this is where nanofillers come into play. For example, since some polymers have a low tensile strength, the addition of nanofillers can cause a reinforcement type effect at the microscopic level thus transforming them into a more advanced material with improved properties and features [2-3].

The first recording of modern polymer nanocomposites being used in industry started in 1990 when the multinational car maker Toyota first used clay/nylon-6 nanocomposites for timing belt covers [2-3]. Other car manufacturers followed suit and started implementing these new super-polymers into car appliances that demanded more than just typical polymers. Companies started to see the potential of these so called nanocomposites and research resulted in applications for packaging (increased barrier properties against moisture & air) and medical devices etc. Since then the area associated with polymer nanocomposites has seen a massive upsurge in research within this broad area. Developments have begun on manufacturing new grade materials with improved properties and which are low cost and eco-friendly and that use less natural resources or cause less waste and pollution together with recyclability benefits. The range of nanocomposite materials is vast and ever increasing with different materials being formulated by using various polymer/nanofiller blends. These include fibres, clays, metals, carbon nanotubes and many more that are being developed.

1.2 Background history of composite materials

The discovery of composite materials also termed hybrids has not been anything new. These materials have been found in many forms both naturally occurring or artificially made and date back many centuries. The natural fibres of cellulose and lignin combine to form wood, bamboo and various other plant species and could be considered composite materials. These consist of a fibrous and glue combination to give plants and trees their robust properties and with evolution many other plant and tree species have

evolved to make themselves lighter and stronger with complex structures of fibres or hollow centres to allow them to adapt to various conditions around the globe [4].

Other natural composite materials include human or animal bone, teeth and muscle fibres to name but a few that have a complex composition of various materials and structures resulting in very good properties. Most of these materials have constituents at the macro scale but some are of the nano scale and contribute to the robust properties of the structure.

For man-made composites, these have gone back centuries with the Japanese making samurai swords consisting of soft wrought iron and hardened steel that was formed into sheets and repeatedly folded. This gave the composite material extra strength due to the multi-layered structure. The early Egyptians made bricks from clay mud and reinforced it with straw as a binder to form a solid entity that was durable. Modern day examples have followed suit with hybrid materials following a similar pattern such as cement with sand used as an additive to bind and give overall strength and flexibility to the material for end usage. Many other ancient civilizations used composite technologies to generate new strains of materials for their needs either for hunting or for wars. For example, the Mongols were masters in archery with bow and arrows developed from animal bones, bamboo and fabrics to give strength and increase the distance of the arrows. The Romans used combinations of metals and fabrics to make weapons and armaments that had the advantage over their enemies with stronger and lighter weaponry. The Europeans made stained glass for use in churches which consisted of micro-particles that could be used in different colour contexts. The Chinese also developed hybrid materials including many innovative fibres but one great achievement was the discovery of gunpowder which consisted of sulphur,

charcoal and potassium nitrate blended together to form a material with powerful explosive properties that would last for centuries [5-6]. Some examples are shown in figure 1.2.

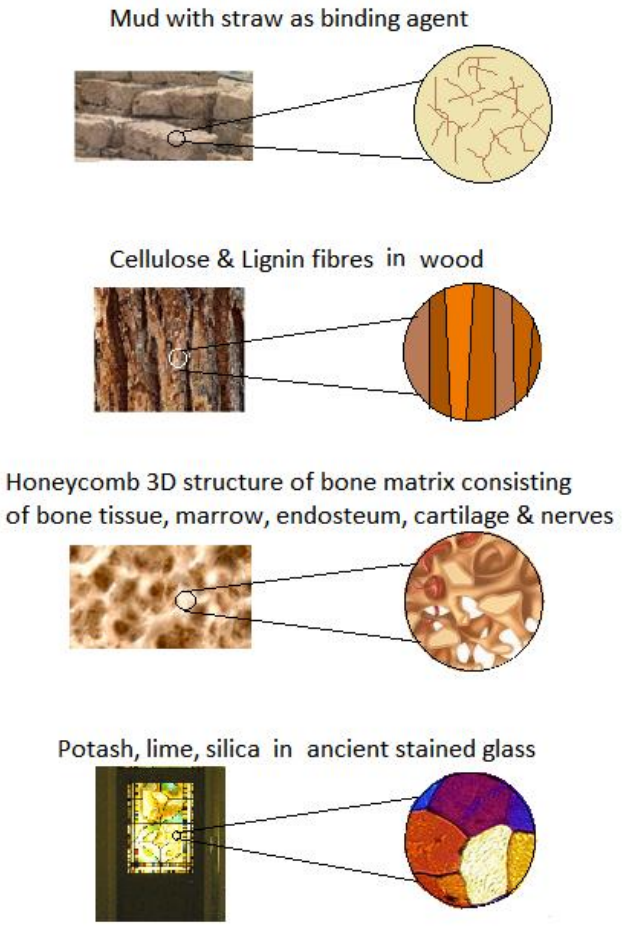

Figure 1.2: A selection of composite materials [6]

Moving onto modern day composites, a lot of research activity occurred during the start of the twentieth century with the discovery of oil and its constituents which led to the development of polymers. This saw a boom in new material and product development especially during World War 2 when different countries were trying to gain the upper hand in the war by developing new materials for military purposes. This saw the start of a new

phase in polymer development whereby new strains of polymer composite materials boomed before and after the war period. This trend was followed since then until the discovery of polymer nanocomposites within the last few years [7].

With the emergence of new technologies and advanced testing strategies of materials during the past few decades and the emergence of sophisticated computers and software packages, the techniques of new material development and testing has also increased. It was easier to undertake experiments within the laboratory environment and test the end material using sophisticated equipment that would have only been available to large companies or governmental institutions [7-8]. The 1990's saw the emergence of one particular new material whereby Toyota researchers worked on Nylon-6–clay thermoplastic nanocomposites technology to develop timing belt covers and later in other automotive part development which brought about a mini revolution in polymer nanocomposites. They found that with the addition of approximately 4wt% clay, the strength of the base material increased by 50% and the modulus doubled [9]. Since this discovery the research into polymer nanocomposite materials has seen a boom with many new materials and products being developed for various markets including the military, medical, automotive, aerospace and packaging fields. Work undertaken by Usuki et al. [9] found that organophilic clay that had been ion-exchanged with 12-amino-dodecanoic acid could be swollen by moltencaprolactam, thus expanding the basal spacing by approximately twice its original value [9-10]. Caprolactam was then polymerised in the clay gallery and the silicate layers were dispersed in nylon 6 to yield a nylon 6-clay hybrid [8]. The properties of the nylon 6-clay hybrid material showed drastic improvement within its modulus increasing by 1.5 times that of the base polymer, gas permeability was halved and the heat distortion

temperature increased from 65^{o}C to 140^{o}C with 2 wt% clay loading [11].This was officially the first time an industrial clay based polymer nanocomposite was formed. During the same time period, Ijima et al. [12] undertook research work on producing finite carbon structures also known as carbon nanotubes using an arc-discharge evaporation method similar to that used for fullerene synthesis. This discovery paved the way for research activity in the field of nano-particles since they had unique attributes of drastically improving the properties of base polymers by using small quantities [12]. These and other discoveries soon found that blending nanofillers into polymer matrices using the correct techniques and equipment improved the strength and stiffness properties while reducing the weight, improving air/moisture barrier properties of the base polymer and various other specific improvements were noted [13-14]. Hussain, et. al. [15] stated that the transition from micro-particles to nano-particles had a greater effect on the physical properties of polymers due to their large surface area for a given volume.

1.3 The formation of nanocomposite materials

A nanocomposite can be defined as a broad range of materials consisting of two or more components, with at least one component having dimensions in the nm range between 1 and 100 nm [15]. Material variables which can be controlled and which can have a profound influence on the nature and properties of the final nanocomposite include the type of nanofiller, the choice of pre-treatment, the type of equipment used for processing and the factors/settings used i.e. temperature, speed, residence time.

The addition of specialised clays to polymers enhances their properties making them better for specific applications i.e. improved air and moisture barrier properties, increased tensile

strength, higher modulus etc. [16-17]. In line with this, nanocomposites containing carbon nanotubes within a polymer lattice have also proved to be highly successful, reinforcing them in an elastic manner. Since carbon nanotubes have long chains and can consist of single and twinned walls, they have shown to drastically improve the primary material in many ways, including electrical conductivity in plastics and improved tensile strength and elasticity. Many successful products have been launched with such materials including medical implants and electronic devices whereby the carbon nanotubes have brought about beneficial changes to the base polymer materials at the molecular level.

For nanoclays, intercalation and/or exfoliation of layered silicates in polymers have proven to be the ideal characteristics of achieving the best properties from polymer clay nanocomposites [17]. The preparation methods for this are divided into three main techniques also shown in figure 1.3.

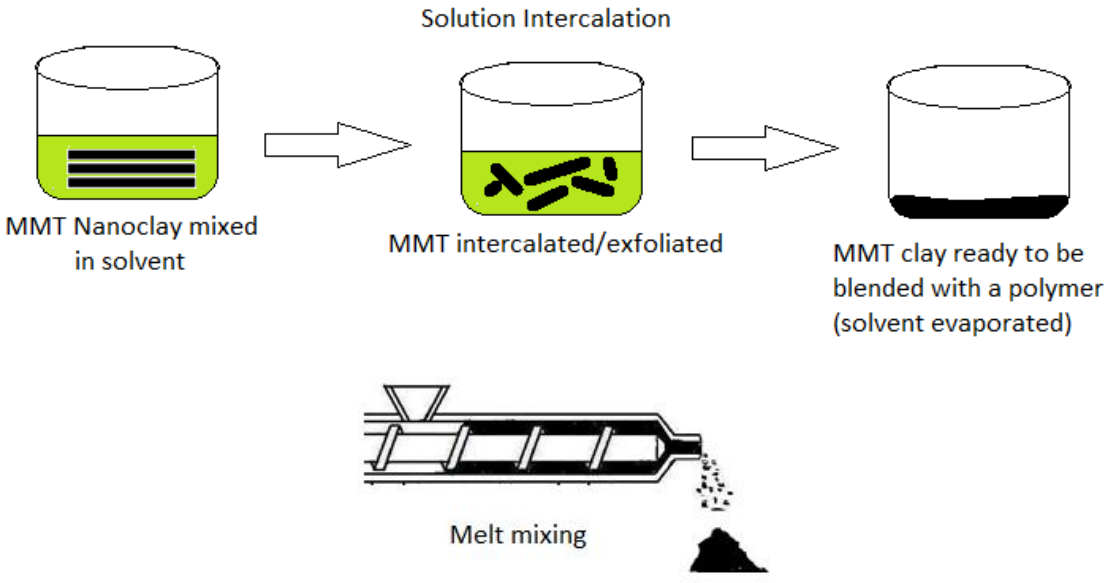

Figure 1.3: Formation of polymer nanocomposites

Solution Intercalation of polymer: This technique is based on a solvent system in which the polymer is soluble and the silicate layers are swellable. The layered silicate is first swollen in a solvent, such as water or toluene. When the polymer and layered silicate solutions are mixed, the polymer chains intercalate and displace the solvent within the interlayer of the silicate. Upon solvent removal, the intercalated structure remains, resulting in a nanocomposite.

In situ intercalative polymerisation technique: In this method, the layered silicate is swollen in the liquid monomer or it can be done in a monomer solution so that the polymer formation can occur between the layered sheets. Polymerisation can be done either by heat or radiation, by the diffusion of a suitable initiator, or by an organic initiator or catalyst.

Melt intercalation method: This method is the most common and prevalent and involves annealing under shear a mixture of the polymer above its melting point. This method has advantages over the other two processes by being environmentally friendly because of the absence of organic solvents and, it is compatible with current industrial processes, such as extrusion and injection moulding [18].

Since Polypropylene (PP) is one of the most commonly used polymers for making household items, packaging and plastic parts, it is the most likely to undergo changes to further enhance its properties to manufacture high end products. The best approach is with the addition of silicate based nanoclays. PP however is a hydrophobic polymer and does not have a polar group and on the other hand nanoclays are organophilic so the two are incompatible with one another and would show no benefit if melt blended together. A solution to this is the addition of a compatibilising agent which contains polar groups thus

forming hydrogen that could bond onto the oxygen of the silicate clay surface thus allowing both to be miscible with one another [19].

Another problem is how do we overcome the problem of breaking apart the stacks of clay layers and distribute the clay platelets so as to cause exfoliation thus allowing the full potential of the nanocomposite material to be utilised. To overcome this, using the "solution intercalation" or "in-situ intercalative polymerisation" techniques mentioned earlier could be adopted but an easier and cheaper solution would be by melt blending them using an appropriate mixer that could deliver high shear and elongational mixing to break the stacks of silicate layers and disperse the nanoclay platelets. It is important to state at the outset that as the nanoparticles will be highly agglomerated in their natural initial state, shear alone is insufficient to break them apart into their individual component or platelets. Elongational flows are better suited as these can create the stress required. Thus the required mixer must offer both good shear and good elongational mixing, first to break the agglomerate and intercalate them and then disperse and exfoliate them to produce the large interfacial area necessary to create the strong interaction between the particles and polymer to achieve the superior properties sought. In this research, we use precisely such a mixer to achieve nano-composition.

1.4 Equipment for processing nanocomposite materials

The processing of polymer nanocomposites has always been a challenge both industrially and within the laboratory environment because of the requirement of achieving the right level of intercalation and exfoliation consistently, product after product. Conducting experiments on a large scale is costly and time consuming. Clearly, smaller

scale experiments are favoured but only if they mimic the larger scaled equipment and conditions accurately for future scaling up. The challenge over the years has been to develop such small scale equipment.

The extrusion process is the preferred choice of processing polymer nanocomposites due to its versatility of being a solid melter, a pump, a mixer and an equipment to which dies can be attached to form different profiles. The twin screw extruder, because of its enhanced mixing capability, is the tool of choice [20]. Small scale versions of the larger single and twin screw extruders have become naturally the instruments used in the laboratory [20-21]. Examples include the Haake Minilab by Thermo-scientific Instruments shown in Figure 1.4. It is a conical twin-screw design with a recirculation channel and bypass to allow for the extrusion of a strand.

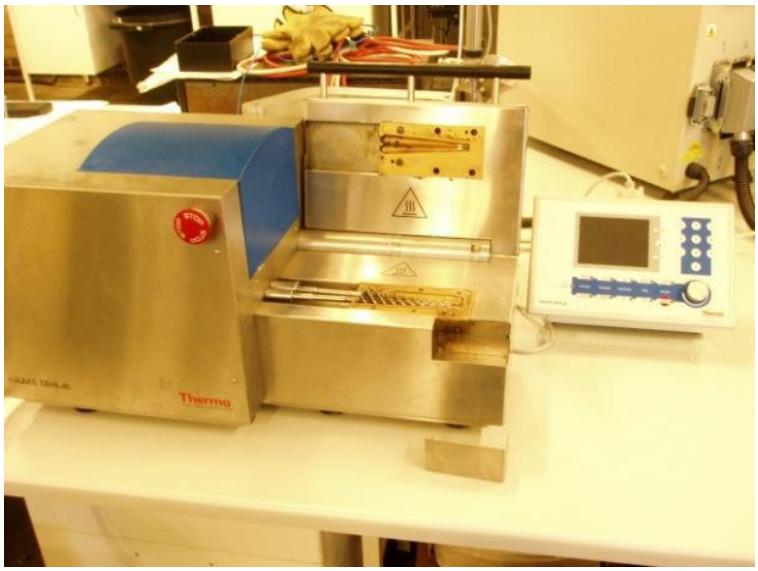

Figure 1.4: The Haake Minilab II Micro Compounder

Another instrument is the Mini-Max developed by Custom Scientific Instruments Inc. This device is essentially a heated cup-cylindrical rotor assembly which shear mix the polymer

and nano-additive. The Alberta Polymer Asymmetric mixer [21] has also a design similar to the Mini-Max and both operate on a batch basis, typically 10g. An axial discharge continuous mixer (LCMAX40) was used by Yao et al. [22] to determine dispersive mixing and compromised of two parallel and intermeshing two-lobe rotors that were co-rotating. This was an attempt to combine the features of a continuous mixer and a twin screw extruder. Another mini laboratory extruder developed by Covas et al. [23] used a single screw design held in a vertical position with the die fixed to a platform and it had the capability to extrude strands in the horizontal direction.

The examples given above show that there are available instruments but they all lack the required combination of mixing time, shear flow, elongational flow and uniformity of mixing. The Haake Minilab for example appears attractive but the fact that it has to re-circulate the material through an external channel indicate that the mixing cannot be uniform (high shear at the wall and zero shear at th e centre of the channel). Laboratory twin extruders suffer from the fact that the residence time is short (because of the short length of the screw-barrel). The novel mini-mixer developed at Bradford University resolved the issue regarding limited mixing time by using a three screw design, two screws operating as a twin screw extruder and the third screw recirculation the melt continuously (further details later) [24-25].

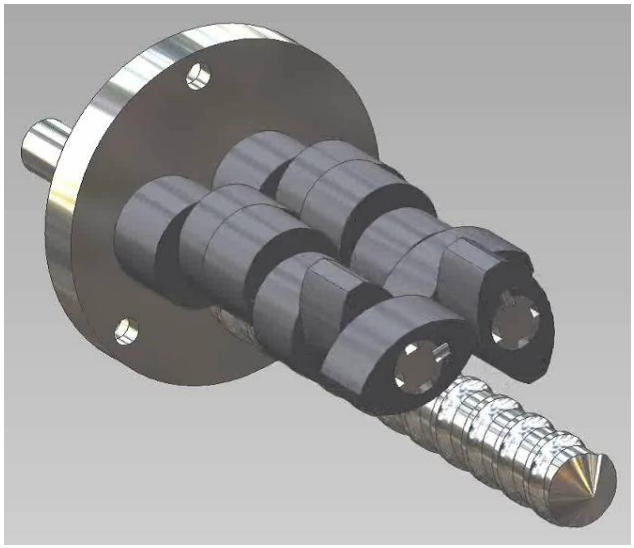

Figure 1.5: Internal layout of the minimixer showing the 3 screw design

1.5 Characterising a polymer nanocomposite

This generally consists of observing the microstructure using powerful microscopes (up to X 20,000) such as in Scanning Electron Microscopy (SEM) and Transmission Electron Microscopy (TEM) or observing the scattering of light through the material as in Wide Angle X-ray Diffraction (WAXD). One immediate problem is the choice of a representative sample since the observations are on a tiny microscopic sample. Also are the observations representative of the entire sample? Clearly for these methods to offer confidence in the final assessment, a large number of observations are necessary.

Another approach, more engineering based and aimed at assessing the performance of a much larger sample thus given a higher confidence level, is mechanical testing using the Instron machine or similar equipment to determine the tensile strength, percentage elongation or modulus properties of the samples in the solid state. This would enable the end user to distinguish if any improvements within the specific properties have occurred.

In recent years and with the advent of more accurate drives and torque measuring technique, rheology has become more increasingly used to test if a nano-composition state has been reached. The idea is that a change in rheology should occur as the level of intercalation-exfoliation increases thus affecting structural changes. The attractiveness of this technique is that it also provides information necessary to understand the flow and deformation as they occur. This information is necessary for design and operation of the equipment. Thus rheological testing provides both information on the "level" of nano-composition and flow and deformation.

More detailed information will be given in the Literature review section in regards to these testing strategies.

1.6 Aim and objectives of the research

A huge amount of research is being devoted to polymer nanocomposites. Limiting our consideration to the process engineering aspects, we note that previous work was in large parts concerned with assessing the effect of formulation on performance during extrusion, i.e. effect of % clay, % compatibiliser, processing temperature on properties (structural, mechanical or rheological). Such work of course is important but it does not inform on the effect of the mixing conditions. The design conditions are critical. What matters most during nano-composition is not how much % clay is added to reach a certain gain in say mechanical properties but how effective the extruder design is in intercalating-exfoliating that particular amount of clay added. If the optimum design conditions are reached, then the assessment of the benefit of adding say 2 or 3% clay to a particular

polymer become more tractable. In this research, we are concerned precisely with such an aspect.

Thus this research aims to highlight the importance of optimising the mixing conditions to ensure that a nanocomposite indeed forms. In all the previous studies with the various laboratory mixers used, there appears to be as if it is for certain that a nanocomposite "always" forms when it is highly likely that "*a*" state of nano-composition is reached rather than the ultimate, optimum state where complete intercalation and exfoliation is achieved. Thus a carefully designed experimental programme (Design of Experiments (DOE) approach) is necessary to test a range of operating conditions (temperature, mixing time, mixing speed, nano- particle loading, compatibiliser loading) to arrive at the optimum conditions. The use of a versatile mixer such as the mini-mixer developed at Bradford is very important as the experiments can be carried out consistently and over a wide range of processing conditions, including if necessary very long mixing times. In order to assess the effect at the larger scale and guide processing in larger machines, experiments on larger twin screw extruders will also be carried out. Also, the focus of the research will be on rheology as it is the "natural" tool to assess the extent of full mixing (intercalation/exfoliation) and to reveal a loading threshold at which a step change in rheological behaviour is measured. In this research, the rheological studies will be carried out off-line (on samples of nanocomposites formed) and in-line using a slit die attached to the mini-mixer to measure pressure drop data to be used for rheological characterisation. In developing this programme of work, it is hoped to provide industry and other researchers a bench mark on the link between various state of nano-compositions and rheological properties using a bench top mixer.

A detailed look at the different formation stages of these nanocomposites and how this could affect their properties and behaviour will also be investigated using extensive testing and measurement strategies both online and offline, including the use of ultrasound to assess changes in structure of the nanocomposites formed.

Another question raised during this research is can the mini-mixer produce enough dispersive power to break the clay platelets i.e. to intercalate and exfoliate the nano-additive?

Finally and following on the theme of the processing effect, the project will investigate the effect of biaxial stretching on "helping" the formation of improved nanocomposites. Here biaxial stretching is viewed not as reinforcing the structure by aligning polymer chains but by inducing further intercalation-exfoliation of the added clay. Thus the proposition tested in this research is "what happens to the mix issuing from the mini-mixer upon biaxial stretching in the cold phase?" "Does this additional processing enhance the formation of nanocomposites?" Again rheological testing will be used to assess this. It is important to note that the rheological measurements in this case will be carried out in the melt phase to remove the stretching aspect of the polymer matrix. So really we are only assessing if biaxial stretching actually leads to further dispersion of the clay within the polymer matrix.

<u>In summary, the aim of the project is:</u>

To develop a fuller understanding of the effects that the operating conditions of the mini-mixer have on the formation of polymer nanocomposites using PP as a polymer and clay as the nano-additive within a Design of Experiments (DOE) approach.

The objectives are:

- Carry out a comprehensive range of DOE testing in the mini-mixer and obtain the corresponding nanocomposite samples.
- Measure the rheological properties of these samples in the molten state and correlate with a variety of other data including the mechanical & barrier properties together with microscopic observations.
- From the above measurements, establish the optimum conditions to be operated for future use of the mini-mixer.
- Undertake scaled up trials using a larger twin screw laboratory mixer to establish scale-up of the mini-mixer operating conditions.
- As rheology will be used as the tool to measure the state of nano-composition, design and fit a slit die to measure rheology on-line in the mini-mixer.
- Subject a number of the nanocomposite samples to biaxial stretching and assess the effect on nano-composition using rheological testing. Establish the added effect of stretching on nano-composition.
- As preliminary work to further investigations, use the slit die in the mini-mixer to assess effect of ultra-sound waves.

Chapter 2 : LITERATURE REVIEW

2.1 Introduction

Since the subject area of polymer nanocomposites has attracted much attention and research, it is not the intention of this literature review to cover all research aspects related to their development. This research is concerned with the development of a certain category of nanocomposites; polypropylene-clay as these can serve as a model system, made within the laboratory, i.e. at the small scale so that their properties can be accurately measured. The making of such nanocomposites (NC) require an appropriate mixing system and the system studied here is a new minimixer developed at Bradford. The focus of this review must be thus to review other works that have investigated the development of similar NC using laboratory methods. Clearly before getting to this main aspect, this chapter gives background to put NC in perspective.

2.2 Polymer nanocomposite variations

Polymers have been around for many years and have the advantages of being a versatile range of materials with a wide variety of characteristics thus enabling them to be used in many applications. There are many different ways of processing polymers but the preferred choice is melt blending using the extrusion / injection moulding processes due to their ease and ability to mass manufacture in a short period of time. Since polymers tend to exhibit certain properties that are good, there are various limitations to their use. These could include high water absorption, low barrier properties and low tensile strength to

mention but a few flaws especially when it comes to using polymers for high demand applications [26-28].

Nano-additives come in all forms and sizes as shown in figure 2.1 and can be blended in with polymers to help overcome most of these issues and improve the properties of the final material. The most upto date fillers are commonly termed nanofillers and have had a significant effect on the plastics industry. These are materials which come in various shapes and forms and mainly comprise of inorganic materials. The main advantage of these nanofillers is their very fine particle structures (within the nanometre range), which can cause structural changes within the polymer matrix of the material possibly due to the high surface area that they possess [27]. This can thus bring about targeted improvements in certain physical or mechanical properties by various means i.e. formation of chemical bonds, orientation of the polymer structure or even filling in gaps within the matrix. Since there are many different types of polymers available together with a vast array of nanofillers (clay, metallic, glass based), it is not surprising that so much research has been undertaken in this field in the past few decades.

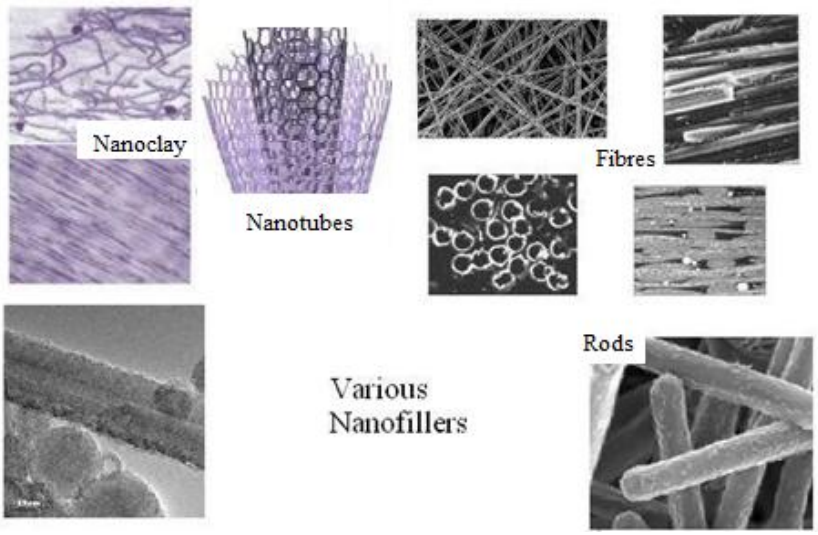

Figure 2.1: Different types of nanofillers [27]

Any polymer with the addition of any nanofiller is termed a nanocomposite (NC) and have been proven to exhibit improved tensile strength, air/water barrier and fire retardation properties depending on the combination of materials used. These improved properties can be directly related to the fact that once the nanofillers are evenly dispersed and distributed into the polymer matrix and are compatible with one another, the improvements can be achieved. Further observations looking into the chemistry of the blended elements and the achievement of a nano-composition state at the microscopic level is also a broad area.

A study undertaken by Lei et al. [28] looked into how nanofillers affected polymers at the chemistry level. They found that with the addition of various nanofillers into the polymer led to an improvement in the modulus properties and a decrease in the melting temperature. Ding et al. [29] undertook work into polypropylene (PP) / nanofiller materials using solid phase grafted PP as the compatibiliser and discovered that the strength and thermal stability was improved with the addition of the nanofiller. This also increased the crystallisation temperature of the PP possibly due to the addition of the nanofiller.

The main and most important focus on nanocomposite materials is usually based on the following conditions with an illustration shown in figure 2.2:

(a) Intercalation – This is whereby polymer within the melt phase is incorporated into the layers/pores of the nanofiller and causing it to expand thus enlarging its surface area. This scenario could thus be attributable to the improvement within certain properties of the base polymeric material.

(b) Exfoliation – This scenario is similar whereby the nanofiller platelets are expanded to such a high limit that they are sheared away completely thus leaving individual platelets

within the nano-range. This is caused by high shear mixing whereby the broken platelets are randomly distributed within the polymer matrix and thus causing a reinforcement type effect at the nano-scale. This is the preferred end result for most typical nanocomposites as it has been proved to drastically improve certain properties. This end result is however difficult to achieve and requires the precise processing conditions i.e. speed of the screws, temperature, percentage nanofiller and the correct material combinations and equipment.

(c) Agglomerates – These are caused by the grouping up of many nanofiller structures causing lumps to be formed within the polymer matrix due to poor mixing conditions. This could lead to a weakened nanocomposite due to trapped states and ageing [30].

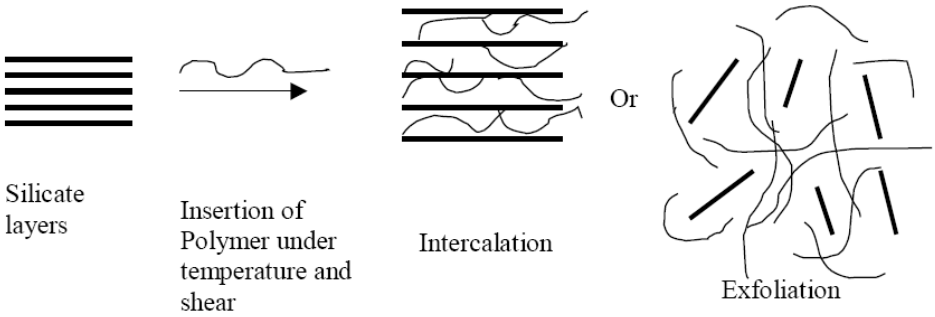

Figure 2.2: Stages of nanocomposite formation

A comprehensive study by Schmidt et al. [31] looked at the classification of typical nano-materials by using their geometries including nanoparticles, nanotubes, nanofibers, fullerenes. Silica nanoparticle and carbon black could be classified as nanoparticle reinforcing agents while carbon nanotubes could be classed as fibrous material.

Since nanofillers such as carbon nanotubes do not have intercalation or exfoliation properties but instead have long tubular structures with nano sized diameters, dispersion and distribution is very important as they can tangle up and cause agglomerates within the

polymer matrix if not mixed well enough thus resulting in voids throughout the polymer matrix and a weaker structure and worsening of specific properties [31].

With the abundance of different polymeric materials and nanofillers and the use of different equipment to process them, the development of new nanocomposite materials with improved properties has profoundly increased. Each nanocomposite material has its own unique properties dependent on the nanofiller used and at the correct concentration (which can be less than 5% volume) and given that thorough and substantial dispersion of the nanofiller has taken place. Melt processing, in situ polymerisation or solution induced intercalation are well established methods. Melt processing involves dispersing the nanoclay silicate layers (surface treated) into the polymer melt with good distribution and dispersion ratios. The in-situ polymerisation process involves dispersing clay layers into the polymer matrix by mixing the layers with a monomer and a catalyst/initiator.

Solution induced intercalation involves solubilising the polymer in an organic solvent and then dispersing the clay in the solution and then evaporating the solvent. This is not a very good technique as it results in poor distribution and dispersion and is reasonably expensive. Some of the nanofillers that can be added to polymers include: Carbon nanotubes, Carbon black, Clay nanofillers, Organo-clay nanofillers and silver nanofillers etc. As for the polymers used, these can include PP, PET, Nylon and Polyesters etc [32].

2.3 PP-Clay nanocomposites

Polypropylene is one of the most widely and commonly used thermoplastic polymers on a large scale due to its versatility of being easily processed into products ranging from everyday consumer merchandise to industrial and automotive components

and packaging films. It is also widely available and cheap to produce and possesses good mechanical and physical properties. It does however have some drawbacks including limited tensile strength and low density. With the availability of different grades of PP, selecting the correct type is important as this can affect specific properties and result in undesired features in the end product. Since PP has some good properties including high stiffness on part due to the high crystallinity content, its weaknesses are it is not prone to heat or light and this can alter the properties over a long term. An important feature for distinguishing different graded PP materials is using the MFI (Melt Flow Index) number which identifies the material by its molecular weight. It can determine the flow properties of the molten PP polymer.

PP was discovered by a couple of scientists, Karl Rehn and Giulio Natta during the 1950s by polymerising propylene to a crystalline isotactic polymer and this breakthrough was followed onto large scale commercial production of the material [33]. PP is a vinyl polymer and has a close resemblance to other polymers in the range including polyethylene but with the exception that carbon atoms in the backbone chain have a methyl group attachment. PP can be derived from the monomer propylene by Ziegler-Natta polymerisation and by metallocene catalysis polymerisation as shown in figure 2.3.

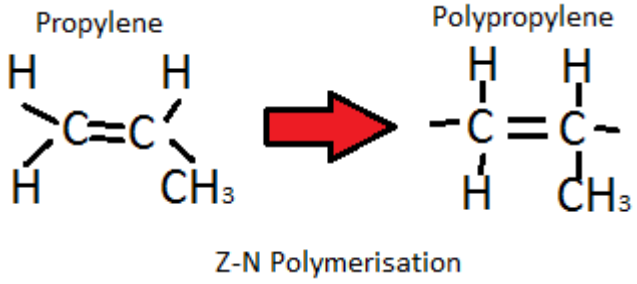

Figure 2.3: Ziegler-Natta Polymerisation

The majority of research trials into polymer nanocomposite formation have consisted of using montmorillonite (MMT) clay since it is fairly abundant and cheap. Other benefits have been the added advantages of using it with a range of polymers to increase specific properties and help develop more high end products with better properties. The main disadvantage has been the implementation of the MMT into the molten PP which can be challenging given the fact that the MMT is hydrophilic and PP is hydrophobic and this causes them not to mix well with one another. Basically it's like mixing water and oil and trying to see what happens. Mixing both MMT into PP would not constitute a NC material as this could result in the generation of agglomerates of the MMT or phase separation thus reducing the strength and various mechanical properties of the material [34]. As mentioned before, intercalation, exfoliation or both can result when PP-MMT NC are produced by good distributive and dispersive mixing processes.

The main ways of producing PP- MMT NC materials have been using in-situ intercalative polymerisation, intercalation of the polymer from solution or melt intercalation. These techniques have been shown from previous research to successfully allow the creation of NC materials within the laboratory. As this study will mainly focus on processing PP-MMT NC materials using a laboratory mixer to melt process the raw materials, this has been shown to be the most common and effective technique from literature. This aspect will be raised in this literature review so further comparisons can be made against our work.

A range of studies looking at PP-clay nanocomposites include:

- A study undertaken by Zhu et al. [35] looked at PP/MMT clay NC materials. An isotactic PP with a MFI of 2.5g/10 min was melt blended with and without a

surfactant that consisted of a compatibilising agent using a three section twin screw extruder. The temperature ranged from 175-190^{o}C and a screw speed of 200rpm was used. The material was characterised using Fourier transform infrared spectroscopy (FTIR), TGA, XRD, TEM, DSC, mechanical testing and rheology. It was found that the mechanical properties were significantly improved of Mt/PP and the impact testing showed an improvement of 1.95 and 2.77 than that of pure PP. The melt viscosity also reduced using rheological measurements of apparent viscosity.

- Another study using PP nanocomposites was prepared by Ellis et al. [36] using melt blending and contained 4.wt % organophilic montmorillonite clay. These samples were compared with some formed by using up to 40 wt% talc mixed with the PP to monitor the main differences between both types of fillers, one conventional and the other a nanofiller. The findings concluded that the nanoclay samples weighed less than the talc / PP samples and had higher elastic and loss modulus values. The stiffness was also slightly better in the nanoclay samples as compared to the talc samples.
- Demin et al. [37] undertook research work into the structural properties of PP/OMMT nanocomposite materials by using the melt intercalation processing method. The mechanical properties of pure PP and with the addition of 2 wt.% organo-clay compatibilised with PPgMA were compared. The findings revealed that the flexural modulus of the PP-Clay samples approximately doubled to 2.41 GPa in comparison to the pure PP. The mechanical properties also increased with

the addition of MMT clay and this could possibly be due to the onset of intercalation.

- Polypropylene with different molecular weights was investigated by Gianelli et al. [38] who used organoclay and PPgMA as a compatibilising agent using melt mixing. The modulus values were increased for the homo-polymers by approximately 50% in comparison to 30% for the heteropolymers with 3wt.% clay loading. This could have been due to the MFI values, thus the polymer with the higher MFI value had a higher modulus value because of better delamination of the clay. Other findings including the stiffness and elongation at break showed a similar pattern.

2.3.1 Nanoclays

The vast majority of clays are naturally occurring which require very little treatment from start to finish. Many of the clays have layered structures and consist of aluminosilicates (silica tetrahedra SiO4 bonded to alumina octahedra AlO6) but different clays also exist. The most commonly used clay has been montmorillonite which also has layers of platelets that are approximately 1nm in thickness and have high aspect ratios [39-40].

A very important issue with clays is that they are hydrophilic (charged) and therefore not compatible with most polymers which is a major issue. To overcome this, the clay polarity is changed to make it organophilic by ion exchange with an organic cation i.e. for montmorillonite the sodium ions in the clay can be exchanged for an amino acid such as 12-aminododecanoic acid (ADA) thus giving the following:

$$Na^{+}\text{-CLAY} + HO_2C\text{-R-}NH_3^{+}Cl^{-} \rightarrow .HO_2C\text{-R-}NH_3^{+}\text{-CLAY} + NaCl$$

There are many different types of clays and each one would have to depend on its intended purpose with the desired polymer and the specific properties that it would be required to achieve [40].

2.3.2 Role of Compatibilisers

The role of compatibilisers in processing nano-composite materials is their ability to allow the dispersion of clay within the polymer by creating more favourable polymer – clay interactions which may lead to the exfoliation of the nanoclay. Compatibilisers consist of an organophilic functional molecule which favours polymer molecules and a hydrophilic functional molecule which favours clay molecules; this in turn allows for easier dispersion of the clay within the polymer matrix. Early uses of compatibilisers in making nanocomposite materials were using amino acids in preparing Nylon 6 and clay materials [40]. There are many other compatibilisers in use today including alkyl ammonium ions and silanes.

A research study undertaken by Peter et al. [41] used octodecylamine treated montmorillonite and PP-g-maleic anhydride compatibiliser to produce clay-polypropylene nanocomposites by the in-situ intercalation technique. They reported that the morphology of the samples after extrusion was not stable and they also reported that annealing the samples at 120 °C for 200 minutes led to further exfoliation and self-assembly into skeleton structure of layered silicate at the same time. That is the thermal treatment of the nanocomposite samples during processing has the tendency to dramatically change the morphology of nanocomposites.

Due to the low polarity of most polymers, it is difficult to obtain polymeric nanocomposites with homogeneous dispersion of the silicate layer at the nanometre level in the polymer. Organoclay containing silicate layers modified by non-polar long alkyl groups are still relatively more polar and hence incompatible with polyolefin. Therefore, the main method to prepare polymer/clay nanocomposites is using a polar functional oligomer as a compatibiliser [42]. In this approach polyolefin oligomers with polar telechelic OH groups (PO–OH) and maleic-anhydride-modified PP oligomers are used. The driving force for the intercalation is assumed to originate from the strong hydrogen bonding between the OH groups of the PO–OH or maleic anhydride group or COOH group (generated from the hydrolysis of the maleic anhydride) and the oxygen groups of the silicates. The interlayer spacing of the clay increases and the interaction of the layers is weakened. The intercalated clay with the oligomers contacts PP under a strong shear field. If the miscibility of the oligomers with PP is good enough to disperse at the molecular level, exfoliation of the intercalated clay may occur [42].

Hoa et al. [43] processed PP/nanoclay nanocomposite materials by using a Brabender plasticorder to melt blend the samples. After undertaking DMA analysis on a range of samples prepared with different nanoclay types, all the samples showed higher storage modulus values. The sample with 3% wt. clay loading blended with modified quaternary ammonium had the highest modulus at 20% higher as compared to virgin PP.

For an ideal nanocomposite material the nanofiller would have had to be thoroughly dispersed and distributed throughout the base polymer matrix and preferably have undergone either intercalation, partial exfoliation or a mixture of both if possible. For a nanofiller to intercalate, the polymer would have to flow and distribute through the layers

of the clay thus expanding the spacing and increasing its surface area. To exfoliate would require the nanoclay layers also known as platelets to break apart by high shear strains and distribute them around the polymer matrix.

2.4 Processing stages of polymer nanocomposites

The processing stages of polymer nanocomposites are very crucial in achieving a "true" nano-composition state and help to improve specific properties. Nanocomposite production has been undertaken using many different means with the most prevalent being melt blending. Kawasumi et al. [44] melt blended organically modified clay with PP by mixing it with distearyldimethylammonium ion, and a polyolefin oligomer containing polar telechelic OH groups which was the compatibiliser. They found that by undertaking this process, the compatibiliser first intercalated the clay layers through strong hydrogen bonding between the OH groups of the compatibiliser and the oxygen groups on the silicate. This swelled the clay interlayer spacing and therefore allowed layer separation on introduction of the melted PP. Though this process yielded a positive outcome with improvement of the material properties, often more rigorous mixing would be required to exfoliate or disperse the nanofiller. This was demonstrated by Dennis et al. [45] who processed Nylon-6 nanocomposites by using laboratory mixing equipment to melt blend them. By using different screw designs and extruders they were able to study the effect that shear speed had on silicate dispersion. They found that both residence time in the extruder and shear speed had affected dispersion. Specifically they noted that high shear intensity was necessary to initiate the dispersion process, and that this high shear intensity reduced

the residence time requirement. At lower shear, longer residence times were required to disperse the layers. The main negative aspect of high shear mixing could result in the onset of degradation of the nanocomposite material thus losing most of the potential properties but this could be overcome by introducing chemical functionalities onto the clay surface, to provide interaction sites for the intercalating polymer [45].

Chin et al. [46] stated that exfoliated nanocomposites had higher phase homogeneity than their intercalated counterpart. Hence the exfoliated structure is more desirable in enhancing the properties of nanocomposite materials. Figure 2.4 highlights the different mixing patterns achievable through both dispersive and distributive mixing.

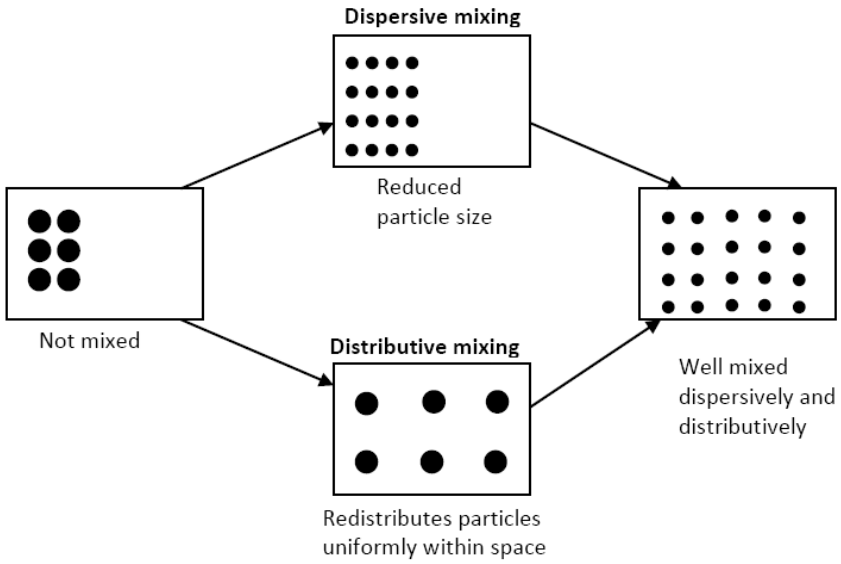

Figure 2.4: Dispersive and Distributive mixing [46]

2.4.1 Small scaled production of NC

Prior to undertaking the large scale production of nanocomposite materials using industrial means, they have on almost every occasion been developed and tested on a much smaller scale within the laboratory environment. This is due to many reasons including cost

savings since nanofillers are quite expensive, quicker production times, more flexibility in using different material/equipment combinations, availability of a range of small scaled processing equipment and most importantly of all is failure within the laboratory environment is less damaging than on the industrial production line. With all these reasons plus many more the ideal place for nanocomposite material generation is within the laboratory.

Many small scaled laboratory extruders include the Haake, Micro-extruder and the Minimax (detailed below) and these plus many more have been utilised to carry out small scaled trials of new generation nanocomposite materials [47]. They mainly rely on similar designs which incorporate twin screws together with a recirculation channel and occasionally online monitoring probes for real time data analysis (figure 2.4). They tend to process batch quantities of materials ranging from 10-30 grams and include settings for altering the temperature, speed and residence time.

The twin screw design and layout plays a major role in processing polymer and NC materials and can help achieve a good mixed material. The common two scenarios are co-rotating or counter-rotating screws. Basically the co-rotating screws rotate in the same direction and allow the material to flow from one screw to the other with ease together with the benefit of being evenly mixed with a continuously even shear mix. On the other hand in the counter-rotating design the screws rotate in the opposite directions thus conveying the material inwards. This generates high shear in the middle sections of the twin screws where they contact but lower shear on the outer sides. This therefore causes uneven shear mixing

and occasionally weaker mixing the other type [48]. A typical illustration is shown in figure 2.5.

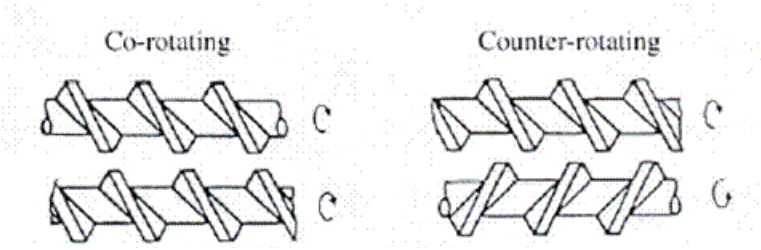

Figure 2.5: Typical illustration of co and counter rotating screw layout

An important issue which has to been considered is if the laboratory equipment can imitate and process the desired polymer nanocomposites in a similar manner as its larger industrial adversaries and try and achieve the same output of finished products.

Cho et al. [49] looked into how the mixing device and processing parameters affected the various properties of polymer nanocomposites. Using a single-screw extruder to process nanocomposite materials resulted in slight exfoliation of the clay platelets. This remained largely unchanged even after a second passing of the material through the extruder but with the exception that there was slight improvement observed in the tensile strength and modulus values. Using a twin screw extruder yielded much more favourable nanocomposite materials with better properties over a broad range of processing conditions. Other tests found that the screw speed or second pass through the extruder improved certain properties. This would therefore suggest that processing conditions are crucial in developing good quality nanocomposite materials.

Haake type TS extruder

This type of laboratory extruder is commonly used in research institutions to develop polymer NC materials. It has been proven to be an effective tool to process a variety of materials with results showing good dispersion and distribution aspects. Figure 2.6 shows a typical Haake laboratory extruder with the twin screw layout. The system typically consists of either co or counter rotating conical screws, pneumatic feeding system, LCD display, bypass for circulation of material, automatic control and air or water cooling capabilities. The twin screws intermesh and the conical design and overall geometry allows for high shear mixing of the materials. The bypass valve enables the user to specify whether to recirculate the material for any desired time period or discharge it through the die.

Park et al [50] used a Rheocord 90 Haake mixer to process three different polymer nanocomposites; PP, maleic anhydride modified PP (MAPP – also used as a compatibiliser) & polystyrene (PS) with 5wt.% cloisite 20A clay. These where prepared and then separated into three different classes, micro-composite, intercalated and partially exfoliated states. Screw speed was set at 50 rpm, with a mixing time of 20 min and 170^{o}C for PP and 200^{o}C for PS. The rheological, X-ray scattering and TEM results showed that the exfoliated nanocomposites had the overall optimum properties as compared to the other two.

Another study undertaken by Kim et al [51] used a Haake co-rotating twin screw extruder to melt compound PP, PP-g-MA and 1, 3, 5 & 7wt% organoclay. The temperature was set at 190^{o}C with a screw speed of 280rpm for 10 min. The morphological findings and quantitative particle analysis for the dispersed clay showed that aspect ratio for the clay

particles decreased with clay loading and PP-g-MA loading. Mechanical or modulus properties did not improve in all cases possibly due to a reduction in the matrix properties by PP-g-MA.

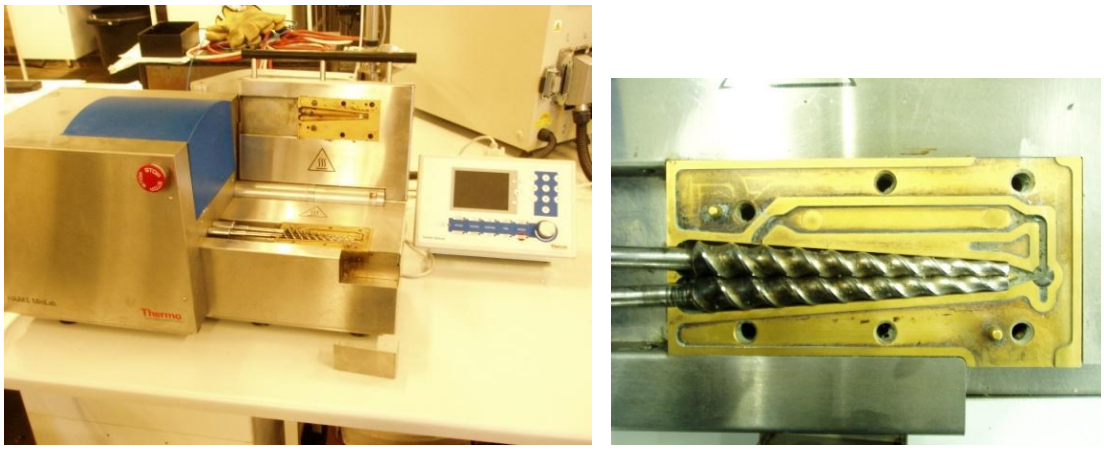

Figure 2.6: The Haake type TS laboratory extruder

From these and many other research papers it can be derived that a few factors are important in utilising the Haake equipment. The ***screw speeds, residence time, melting temperature*** as well as the overall ***screw and mixing element design*** are of major importance and play a significant role if one has to produce the ideal polymer nanocomposites. Many different designs and models of the Haake extruder are available so selecting the correct type is of real importance for its intended purpose and material processing.

Brabender type TS extruder

The Brabender is a miniature sized extruder mainly used for laboratory based trials and testing of materials with a range of different screw designs including cam-blades or co-rotating twin screws. There are many different models and designs available for specific

uses and it has been widely used to process polymer nanocomposite materials. The newer systems have a clamshell design with segmented screws and can achieve high screw speeds. The modular screw design can sufficiently process the materials using specific kneading, mixing, and shear elements located on the screws. Small scaled trials can be undertaken with small amounts of material and the screw configuration can be altered by changing the segmented screw elements.

Rohlmann et al. [52] used a Brabender Plastograph extruder to melt mix isotactic PP, Polybond 3200 as a compatibiliser together with 5 & 15wt% Cloisite nanoclay. The temperature was set at 185^{o}C and using a nitrogen atmosphere (remove any moisture in the air); small quantities of the materials were processed per batch using cam-blades rotating at 50rpm. The materials were removed using a spatula from the mixing chamber and the samples pressed. The XRD, SEM and rheological results showed that the material composition and processing affected the end product and its properties greatly. The major factor was the type of clay used and how well it was processed with the polymer to cause an intercalated state to improve the properties.

Hejazi et al [53] & Lee et al [54] also used Brabender mini laboratory extruders to process polymer/clay nanocomposites using melt mixing. PP was used in both cases with a variety of nanoclays and compatibilising agents. The settings of the equipment were also at 190^{o}C with a variety of speeds ranging from 60 to 100rpm and a range of percentage clay loadings added. The mixing times also varied for different experiments. The test results from both research studies showed that a good degree of dispersion of the clay was observed using XRD and TEM analysis. The mechanical properties and the modulus values were also seen to improve with clay loading.

Figure 2.7: The Brabender type TS extruder

Once again similarly to the Haake equipment a few parameters have been seen to be important in processing polymer nanocomposites using the Brabender laboratory extruders. The specific type of model used is important as the design layout of the screws varies for each different model. These could be ***twin screw co or counter rotating screws, cam-bladed, batch or continuous processers***. Then the temperature, speed, residence time and overall design are important features.

Other specific research studies using novel equipment have been developed. One such study by Mould et al [55] looked at attaching an Anton Paar rheometer testing head to the end of a conventional co-rotating twin screw extruder. The idea was to process a range of polymer materials using the twin screw extruder and allow the material to exit the die and feed directly onto the head of the rheometer where a range of tests could be conducted. The materials used were PS, PE & PP with nanoclay. Validations of the test rig were made against conventional rheological equipment and were found to be fairly successful.

Table 2.1: Development of nanocomposites

Processing Tool	Important Factors	Design Features	Additional Benefits
Haake	Screw speed, temperature control, residence time	Co-Counter rotating twin screws, continuous/batch processing, variable pitch distance, high shear mixing	LCD display, air/water cooled, partly automated
Brabender	High speed/shear mixing, precise processing, RPM & temperature control	Segmented screw, able to change screw configuration for kneading, mixing and shear, batch or continuous processing	Small, portable, very small quantities testing
Solution Intercalation	Material preparation, thorough solution mixing, compatibility, dry time, solvent evaporation	Typical laboratory equipment i.e. beakers, stirrer, oven, press	Tried and tested way of producing good quality NC materials without melt mixing. Shown to produce intercalated NC.
Other mixers	Online measurements in real time, high/low shear mixers, range of temperatures	Huge variety of design features, range of attachments i.e. slit die, pressure/ultrasound/infrared sensors, thermal analysis.	Huge scope and potential to identify specific features of NC processing routes

2.4.2 Large scaled production of NC

The production of polymer nanocomposites on a large scale using industrial means has always been a challenge for manufacturers trying to produce potentially premium graded material with specific properties to use in new product development areas. The availability of a range of nanocomposite materials has opened the market for a lot of research within this area that was considered a niche area some decades ago. Using different nanofillers and polymer combinations and altering certain factors or the addition of various chemicals or processes has generated a great demand for these materials. There

are many ways and techniques of manufacturing nanocomposite materials by industrial means but the most commonly used procedure is melt processing using twin screw extruders [56].

Twin screw extrusion is used extensively for mixing, compounding, or reacting polymeric materials. The flexibility of twin screw extrusion equipment allows this operation to be designed specifically for the formulation being processed. For example, the two screws may be co-rotating (rotating in the same direction) or counter-rotating (rotating in opposing directions), intermeshing (overlapping teeth) or non-intermeshing. In addition, the configurations of the screws themselves may be varied using forward conveying elements, reverse conveying elements, kneading blocks, and other designs in order to achieve particular mixing characteristics.

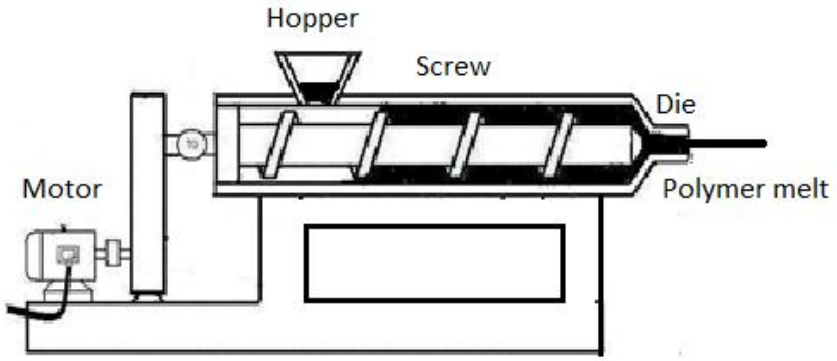

Figure 2.8: A typical extruder

The design of the twin screw extruder and its screw layout plays a significant role in the processing of the raw polymeric materials and is of great importance for the end product (figure 2.8).

The basic processing stages are as follows assuming a typical twin screw extruder is used:

(i) Firstly, health and safety is of paramount importance since the inhalation, ingestion or contact with many of the nanofillers is dangerous thus the correct clothing and equipment (masks, gloves) should be used.

(ii) The raw materials are thoroughly and precisely prepared and using the correct quantities to allow the materials to interact with the correct chemistry during the processing stage. This could include using the correct weight percentages for the different materials, chemical treatment, thorough mixing of raw ingredients or even removal of moisture by heating in a vacuum oven etc.

(iii) The factors used should be favourable for all the raw materials used and to allow the processing stage to assist them to form in the relevant manner and produce the idealistic nanocomposite material. This could include the setup temperature of the extruder in the different regions of the barrel which is probably one of the most important factors and could determine the overall properties of the material. Other factors could include the speed of the screws, the equipment design, the residence time of the materials within the extruder etc.

(iv) Once the material exits the extruder die, retrieving the material is also important. There are many ways to undertake this step including air cooling, water cooling, using haul offs at various speeds or simply a conveyor system.

(v) Any additional stages of processing the materials can be undertaken i.e. bi-axial stretching, pressing into sheets, injection moulding etc.

Each stage of the processing cycle is important and can have a tremendous effect on the final nanocomposite material and its properties. Examples include the design of the twin

screws; without the correct design the material would have little chance in achieving the desired mixing together with too much or too little shear stresses acting on the material causing flaws within the nanocomposite material. Using the wrong speed to operate the twin screw extruder could have more disadvantages than advantages and could easily over or under process the nanocomposite material. Setting the incorrect temperatures to process the nanocomposites outside their ranges could either lead to degradation of the material or unprocessed residue which would be of no value. Also the cooling period after exiting from the extruder die could have negative effects on the nanocomposite material. Bad preparation of the initial materials or using incompatible materials would deem the nanocomposite useless from the onset. All this therefore makes nanocomposite production a specialised area while upmost care and attention to detail has to be taken into consideration [56-57].

2.5 The Minimixer at Bradford

The design and development of the minimixer was unique and based at the University of Bradford with its initial intention to look into mixing capabilities of different polymer based materials with additives. It was widely used to undertake experiments to look at the dispersive and distributive aspects of the mixer and if it was effective enough to mix both polymers and additives to form viable materials. The main experiments included work undertaken by Butterfield et al. [24] on polymer and carbon black mixtures and their conductive properties together with the characterisation of flow properties of the polymers within the minimixer. They found that the minimixer has the capability of mixing different material blends thoroughly and that the polymer/carbon black composite materials became

conductive by using specific processing factors and material concentrations [24-25]. Figure 2.9 shows an illustration of the minimixer layout and its various sections. The challenging aspect was to determine if the minimixer had the scope to undertake mixing of more specialised materials and thus after winning a European grant proposal to undertake work on the minimixer to develop a range of polymer nanocomposites using a Design of Experiments (DOE) approach, its full potential was tested. The main conceptual challenge was to determine if the equipment could cope with the production of such specialised materials and if it was capable of producing good quality nanocomposite materials. This was a totally new concept for the mixer and involved certain modifications to it together with the attachment of additional online monitoring probes to undertake measurements in real time of the temperature, speed, torque and residence time. Other modifications would later include the addition of a specialised die that would allow the online monitoring of the pressure at two points along it together with ultrasound measurements. These would enable the user to establish the flow patterns of the molten polymer / clay nanocomposite materials and more importantly try and determine the viscosity of the materials and any specific patterns that could be observed with nanofiller loading. The minimixer used conventional extruding technology which included twin shaft paddles but the internal layout was modified to allow for a more innovative approach to material processing.

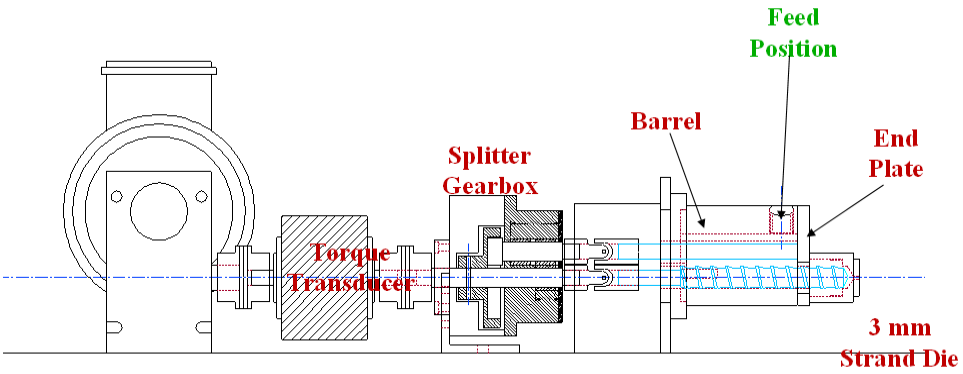

Figure 2.9: Illustration of the Mini-Mixer [24]

The main difference that this concept design had over its laboratory rivals was the design of the twin shaft paddles which would allow for high shear mixing in the reverse mode. This enabled with an indefinite time for mixing the material in 30 gram batches and the single screw located underneath for the extraction of the material in forward mode was unique (figure 2.10). Then the added highlight of online monitoring and data logging the temperature, speed and torque in real time was a big advantage. This layout would also require no specific pre-treatment of the polymer / nanofiller materials i.e. melt blending them in an aqueous solution for many hours and then feeding them through the extruder; as high shear rates together with thorough melt blending would be sufficient enough to process the materials to form a nanocomposite material.

Figure 2.10: Screw design layout

Another issue was to determine how well the minimixer could cope with developing new nanocomposite materials and if was capable of having the same processing capabilities as its other laboratory rivals. This would be addressed by conducting a few experiments using a different laboratory extruder, the APV extruder. The best and worst experimental runs would be taken from the DOE range of runs and repeated using the APV extruder. This would allow us to make direct comparisons between the APV and minimixer extruders and if they were similar in processing polymer nanocomposites based on the DOE range of experiments with the factors being kept as same as possible.

Further testing would be required to ensure if viable nanocomposites had been formed.

2.6 Studies on development of PP nanocomposites

Many experimental approaches have been undertaken in processing and testing PP nanocomposites with different variations in their development using equipment, materials and strategies.

An approach undertaken by Rohlmann et al [52] used PP, Polybond 3200 compatibiliser and 6 different OMMT clays as shown in table 2.2. The quantities used were 5wt% for each clay type and 15wt% for the polybond compatibiliser processed in 35g batches with the PP. The materials were melt mixed using a Brabender Plastograph for 15 minutes at 185^{o}C & 50rpm for all the samples.

Table 2.2: Organo-modified clays used to prepare the PNCs [52]

MMT	ID	Organic modifier (ID)	PSR[b] (μm)
Sodium Cloisite	Na^+Cloisite	–	2–13
Cloisite 10A	C10	Dimethyl benzyl hydrogenated tallow ammonium chloride (2MBHTA)[a]	2–13
Cloisite 15A	C15	Dimethyl dihydrogenated tallow ammonium chloride (2M2HTA)[a]	2–13
Cloisite 30B	C30	Methyl-tallow-bis,2-hidroxiethyl ammonium chloride (MT2EthOHA)[a]	2–13
Cloisite 93A	C93	Methyl dihydrogenated tallow ammonium sulfate (M2HTA)[a]	2–13
Nanomer I44	N44	Dimethyl dihydrogenated tallow ammonium chloride (2M2HTA)[a]	15–25
Sodium MMT from bentonite	Na^+B18	–	–
OMMT from bentonite	B18	Octadecylammonium chloride (ODA)	0.3–35

Their testing included thermo-gravimetric analysis (TGA), XRD, SEM and rheology. Table 2.3 shows some of the data generated from the TGA and XRD tests including observations taken from the SEM image analysis.

Table 2.3: TGA and XRD results [54]

Clay	Weight loss [a] (wt%)	Modifier concentration (meq/g of inorganic clay)		% of surface coverage	T_{decomp}[e] (°C)	Clay d_{001} (nm)	PNC d_{001} (nm)
		Nominal	Calculated				
Na^+Cloisite	5	–	–	–	–	1.1	–
C10	37.5	1.25[b]	1.45	150	165 (210)	2.0	1.7
C15	41.5	1.25[b]	1.24	130	195 (255)	3.3	3.4
C30	28	0.90[b]	0.93	100	170 (265)	1.8	1.4
C93	35	0.90[b]	0.94	100	215 (285)	2.5	2.4
N44	37	–[c]	1.04	70	200 (265)	2.6	3.3
Na^+B18	4	–	–	–	–	1.4	–
B18	32.5	1.62[d]	1.60	118	185 (280)	~2.6	2.6

Other research studies [58-59] have used a combination of PP, PPg and OMMTs to make successful NC materials with intercalated/exfoliated states. A maximum of 10 wt% of OMMT, a range of PPg/OMMT ratios and a variety of extruders or laboratory mixers with different processing conditions were used. An increase of the interlayer spacing and partial exfoliation of the clay in PP/PPg systems was also observed by researchers [60]. Other researchers found that given certain PP, PPg and processing conditions, the clay interlayer expansion during compounding depended mainly on the interaction between the clay and the intercalate and between the polymers and the organic modifiers. Since the most important finding stated that the flow properties of composites were affected not only by the type and organisation of their components but also by the interactions between them, the linear viscoelastic response of the materials with time, temperature and frequency were analysed using an amplitude sweep test on the rheometer as shown in figure 2.11. The test was run at 180^{o}C and 1s^{-1} as a function of strain and shows that the nanoclay reduces the linear viscoelastic region of the PP/PPg blend that constitutes the matrix [52].

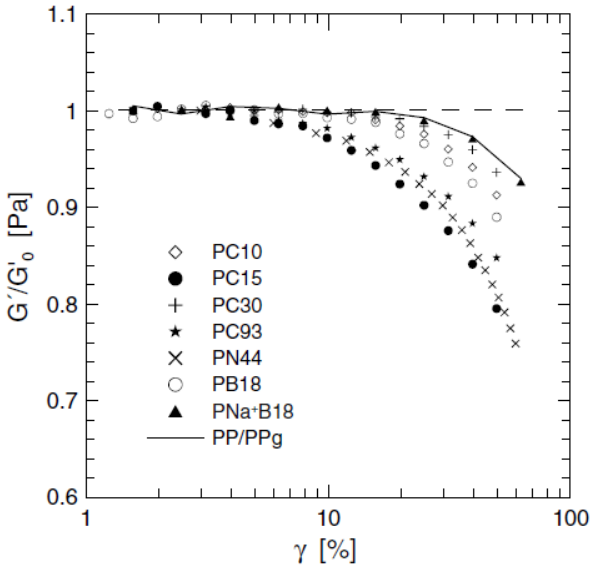

Figure 2.11: G'of PP/PPg vs.Strain at 1s^{-1}and 180^{o}C [52]

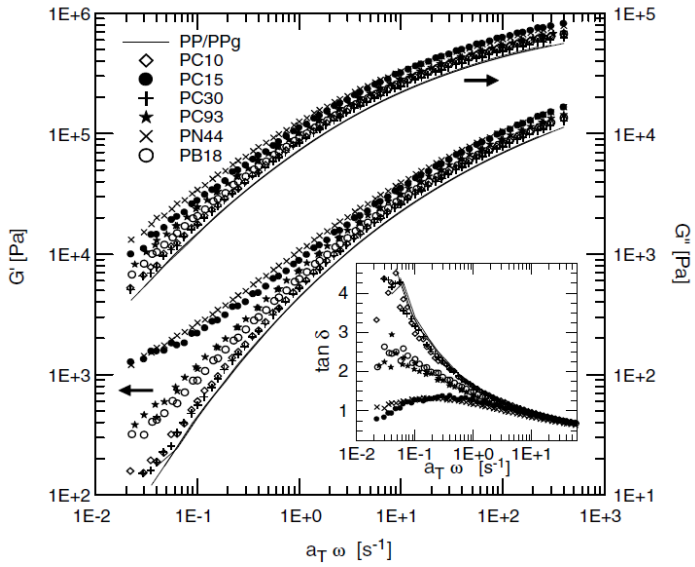

Figure 2.12: G' & tan δat 180^{o}C [52]

Figure 2.12 shows the G' & G'' values from the frequency sweep curves of the PP NC materials. All the materials display a thermo-rheologically simple behaviour in the range of temperatures considered. The time–temperature shift factors of each polymeric system follow an Arrhenius type of dependence with temperature. The agreement between the flow activation energies of the matrix and the hybrids indicate that the solid-like or quasi-solid-like behaviour of the annealed PNCs is due to the strong frictional interactions between clay layers above the percolation limit rather than confinement effects also shown by other researchers [52].

Another study by Hejazi et al. [53] mentioned earlier undertook a similar DOE study on a small scale by the addition of nanoclay blended with PP and a compatibilising agent in various concentrations from 1 to 7wt%.

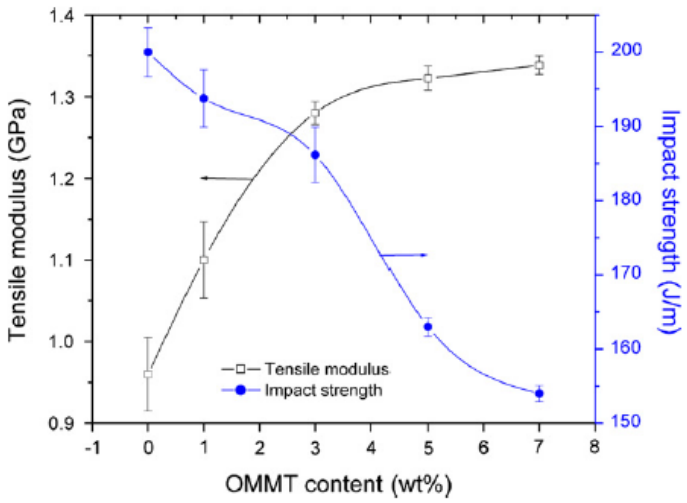

Figure 2.13: E'& Impact Strength of TPO vs. OMMT content [53]

The effects of clay loading on the tensile modulus and impact strength are shown in figure 2.13. The tensile modulus increases substantially with the lower concentrations of clay loading upto 3wt% and then levels off. Literature from other studies have also shown a similar trend that modulus of NC materials are sensitive to the aspect ratio and degree of exfoliation. The impact strength is drastically reduced with clay loading possibly due becoming more brittle with clay content.

Table 2.4: E', yield and impact strength of nanocomposites [53]

Processing conditions	Tensile modulus (GPa)	Yield strength (MPa)	Impact strength (J/m)
Rotor speed[a] (rpm)			
20	1.15	11.7	140
60	1.28	12.6	185
100	1.3	12.9	168
Time[b] (min)			
5	1.265	12.63	162
10	1.28	12.6	185
20	1.27	12.61	170

Table 2.4 shows the effects of shear rate (rotor speed) on the tensile modulus, yield and impact strength prepared at different processing conditions (a:Time = 10 min, b:Rotor speed = 60 rpm). It was found that the higher rotor speeds caused higher shear on the molten polymer possibly leading to higher degree of dispersion of OMMT particles in the system. This in turn resulted in an increase in the tensile modulus and yield strength values. Increasing the processing time also saw slight increases in the modulus values.

Lee et al [54] also undertook a small DOE approach with PP/clay loaded NC materials up to 10wt% shown in table 2.5.

Table 2.5: Pure PP, PP-g-MAH Compatibilizer & Organoclay (wt %) [54]

Sample	PP (wt %) (HP550K)	PP-*g*-MAH (wt %) (Polybond®3150)	Organoclay (wt %) (Closite 15A)
Pure PP	100	0	0
iPP/0/5[a]	95	0	5
iPP/5/5[b]	90	5	5
iPP/5/1	94	5	1
iPP/5/3	92	5	3
iPP/5/7	88	5	7
iPP/5/10	85	5	10
iPP/10/5	85	10	5
iPP/10/10	80	10	10

Intensive rheological data was gathered and one of the graphs showing the complex viscosity against the frequency is shown in figure 2.14. It can be clearly seen that with clay loading the complex viscosity is higher and the difference can be seen at the lower range frequencies which has been shown in other similar studies. This would point to higher shear thinning behaviours being observed in the PP-g-MAH compatibilised

nanocomposites at low frequency regions possibly due to the organo-clay content increasing the viscosity.

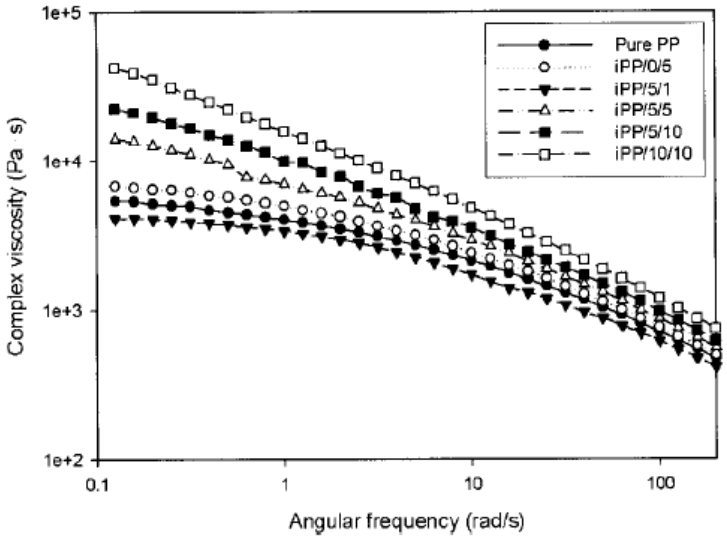

Figure 2.14: η* of various nanocomposites at 190^{o}C [54]

2.7 Assessing properties of PP nanocomposites

There is possibly no one scientific explanation or manner to describe or test the idealistic nanocomposite material since there is such a huge range of different materials with specific properties. The understanding to date has focused on trying to evaluate nanocomposite materials at the microscopic level and determining what has happened to their structural properties.

Many tests have been conducted on polymer nanocomposite materials to characterise their precise properties and what effect nanofiller blending has had on them. Since there are a range of improvements that can be introduced with the addition of these nanofillers, such as the improved modulus, strength or barrier properties a range of tests are routinely conducted which include XRD, SEM/TEM, DSC, DMA, Rheology and

Mechanical Testing [61]. Research into this area has found that assessing the quality of a nanocomposite material in a correct manner is possibly one of the most important stages involved in evaluating how successful the processing stages have been together with the various factors and materials used in making a good polymer nanocomposite.

Experimental trials undertaken by Tortora et al [62] found that the Young's modulus was increased from 120 to445MPa with the addition of 8 wt.% ammonium treated clay in PCL. Similarly Gorrasi et al. [63] reported a similar pattern with an increase in the Young's modulus from 216 to 390MPa for a polymer nanocomposite containing 10 wt.% ammonium-treated montmorillonite clay. Other testing techniques included measurements of the tensile strength which was shown to increase with the addition of nanofillers but this was not always the case due to certain polymer/clay morphologies.

The testing techniques are detailed below:

2.7.1 X-Ray Diffraction (XRD) is used to determine the crystalline structure and chemical composition of materials either naturally occurring or fabricated. Since nearly all solid materials consist of a crystalline structure at the atomic level, an X-ray beam is targeted at the material with a specific wavelength (λ) and at a particular angle (θ) resulting in diffraction but only when the ray distance reflected from many planes is different by a number (n) of wavelengths. Using a set angle and determining the intensity of diffraction from the radiation results in a specific pattern which can be plotted to depict a particular material. This would enable many of the materials chemical and physical properties to be found. Hejazi et al [53] reported that a very good degree of dispersion was noted for the organo-modified montmorillonite (OMMT) with the nanocomposite containing 3 wt.% OMMT and was also verified by X-ray diffractometry and transmission electron

microscopy. Other tests found that the tensile modulus and tensile strength both increased with the addition of OMMT using mechanical testing and that the optimum properties were observed at 3 wt.% OMMT using rheological tests.

2.7.2 SEM / TEM

Taking images using either SEM or TEM is a specialist area and requires a lot of experience in preparing the sample to undertaking images. These tools can thus provide the end user with very vital information about the processed nanocomposite material and any key features or negative aspects in regards to its structure at the nano level. It can also provide the composition of the different materials present within the material as a percentage. The vast majority of research papers have included either SEM or TEM images or a combination of both to highlight the blending of the nanofiller within the polymer matrix and how this could have affected the properties. A research study undertaken by Xie et al. [64] found a novel procedure to explain quantitatively the microstructure of processed polymeric nanocomposites by using their TEM and optical images. The degree of dispersion and mean inter-particle distance per unit volume of clay was used to describe the level of clay dispersion and gave the percentage of exfoliation that occurred.

2.7.3 Mechanical Testing is most commonly undertaken by tensile testing machines such as the Instron machine which measures various properties of the sample in the solid state while it is clamped between two grips in a vertical position. As each end pulls the sample which is T-bar shaped, it monitors the various properties in real time such as the modulus, strength, percentage elongation until the sample breaks. Kim et al [65] found that with the addition of 2-3% MMT to PP resulted in a significant increase in

stiffness but any higher loadings of MMT had only a minor effect. The similar trend was also found for PP/PP-g-MA/MMT nanocomposite materials together with an increase in the tensile modulus noted. Shelley et al. [66] found that with the addition of 5 wt.% clay in a nylon 6 nanocomposite caused the tensile modulus to increase by 200% and the yield stress increased by 175%. As for other tests, Liu et al [67] found that the tensile strength increased from 78MPa to 98MPa for 5wt. % clay addition but decreased with the addition of a higher quantity of nanoclay.

2.7.4 Differential Scanning Calorimetry (DSC) is used to monitor the different melting stages of the polymer (thermal transition stages) and especially the crystallinity values. This is achieved by inserting a small sample (10mg) into an aluminium pan and placing it into a heated chamber which measures the heat flow into or from the sample as it is either heated or cooled using nitrogen gas. A graph is generated from the heating or cooling trends and from this the crystallinity of the sample can be calculated by taking the area under the curve.

2.7.5 Dynamic Mechanical Analyser (DMA) works by gaining a response from a material as it is subjected to a periodic force and determines properties such as the modulus, stress and strain using a variety of testing techniques including the 3-point bending measurement. Many tests can be conducted with varying the factors such as temperature, frequency, testing time and different testing regimes.

2.7.6 Rheology is the measurement of the viscoelastic properties of a nanocomposite material to determine both the storage (G') and loss (G'') modulus properties of the sample in the melt state. It can precisely determine these and other properties including the creep and relaxation of the sample. It is also an important tool to evaluate quickly and efficiently if a feasible nanocomposite has been processed and the effects of nanofiller loading on the sample and the effects of various factors used to process the samples have had on the end product. Hwan Lee et al [68] investigated the melt rheology and processability of exfoliated polypropylene (PP)/layered silicate nanocomposites. He found that at low frequencies, the material showed some exfoliation properties with very good strain hardening behaviour in the uniaxial elongational flow. It was also found that the melt processability of exfoliated PP/layered silicate nanocomposites was significantly improved due to good dispersion of layered silicates and increased molecular interaction between the PP matrix and the layered silicate organoclay.

Galindo-Rosales [69] found that using rheological testing methods to assess the dispersion quality of a range of model nanocomposites prepared using different methods was successful. The finding that using selected linear and non-linear rheological properties as a function of volume fraction was a successful and accurate approach to distinguish different nanocomposite materials. Rather than just using imagery tools to look at nanocomposite materials or other labour intensive procedures, this could provide to be a feasible and quick alternative. The vast majority of research on polymer nanocomposites has focused their research by conducting their tests using the techniques listed above in a systematic way to help them understand and determine if a good or bad nanocomposite material has been processed and the reasoning's.

2.8 Additional work on PP nanocomposites

2.8.1 Biaxial stretching of polymer nanocomposites

Bi-axial stretching of a nanocomposite material is a unique feature that has gained popularity in recent times. Research has focused on using this as an additional step in trying to improve specific properties of the nanocomposite material by stretching it using specific conditions and settings to generate improvements. Research has proven that biaxial stretching of polymer/clay nanocomposites can result in delamination and orientation of the clay stacks/platelets. This is shown in figure 2.15 where TEM images clearly show that biaxial stretching helps delaminate clay stacks and causes orientation of the platelets. This in turn can improve the mechanical and permeability properties of the material. Table 2.6 shows that there is a significant increase in exfoliation number of clay platelets with increasing stretch ratio and the main improvements have been seen in the gas barrier effect. Finally the improvement in the yield strength could be associated to the modification in the crystallite size. This has been shown by studies undertaken both as part of this research project and also by other researchers and also companies who want to benefit from this technology.

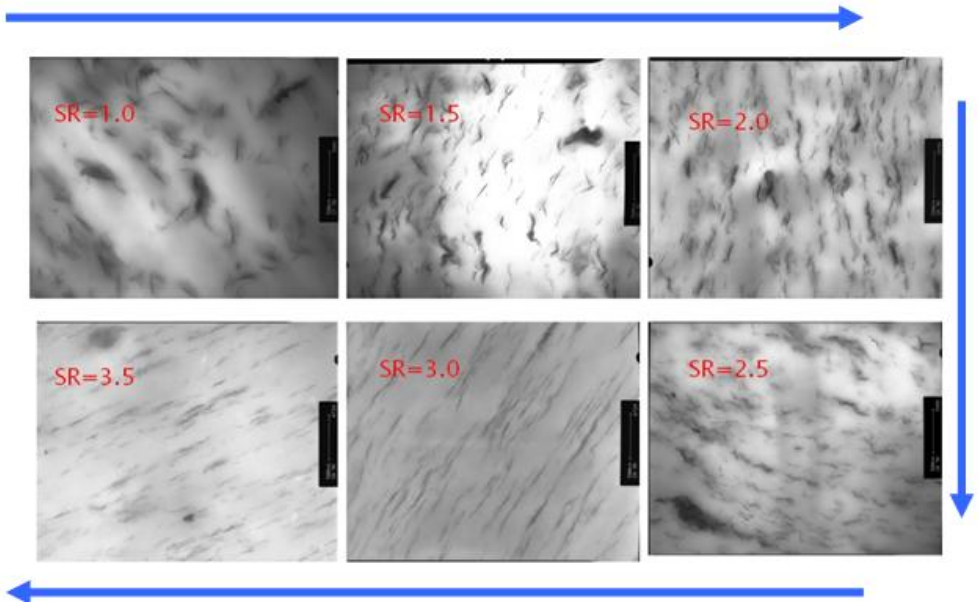

Figure 2.15: TEM Images of PP / Nanoclay materials with different Stretching Ratio's

(Courtesy of QUB)

Table 2.6: Effects of different stretch ratios on properties

Stretching ratio	Effect on Modulus (%)	Effect on Yield Strength (%)	Effect on stress at Break (%)	Effect on O_2 barrier (%)	Exfoliation number N
1.0	0	-27	-19	-	10
1.5	0	-24	-40	-	21
2.5	+4	+9	-17	+11	30
3.0	+10	+12	+4	+24	31
3.5	+15	+44	+15	+46	48

Currently only a handful of researchers have managed to successfully implement a complete system whereby the nanocomposite materials are processed and then biaxially stretched in one complete cycle. The typical researcher has used the process of manufacturing a nanocomposite material and then using an additional stage of biaixally stretching it using another piece of equipment.

A considerable amount of research papers have published work on this topic which has become a success both in academic and industrial institutions due to the simplicity involved. Abu-Zurayk et al. [70-71] undertook trials on bi-axially stretching PP nanocomposites to try and determine the relationship between the structure and properties of the materials. They found that the higher the biaxial stretch rates were used, the better the mechanical properties were observed. The degree of exfoliation increased possibly due to the exfoliation of the clay stacks thus resulting in a reduction in tactoid size which was reflected in an increase in yield and break stress. Another finding was that the elastic modulus did not change much with the unstretched sheets or the low stretching but over a 2.5 stretch ratio showed a linear increase. Anything over this made a significant change on the elastic modulus properties.

Other similar studies undertaken by Rajeev et al. [72] looked at PET nanocomposite materials and the effects of equi-biaxial stretching. Tests showed that the stretching improved the exfoliation of clay platelets by approximately 10% based on TEM observations. Other observations included finding longer tactoids after stretching possibly caused by the platelets slipping over one another but not completely separating thus an increase in length. Also as previously found the higher the stretch ratio, the greater improvement in mechanical and barrier properties was observed.

In industry, blown film processing is commonly used to manufacture biaxially orientated films and bags as shown in figure 2.16. It is a successful technique to produce polymer films with improved strength and barrier properties especially when nano-additives are added. The technique works by extruding a thin cylindrical film through an annular die and the inside pressure is slightly above ambient, causing the film to expand

(like a rubber balloon). The film is then flattened at "hauloff" and taken up at a linear speed higher than the linear extrusion velocity, so stretching occurs both in the machine and transverse directions. Solidification occurs prior to hauloff. The finished product can thus be used for film/bag production [73].

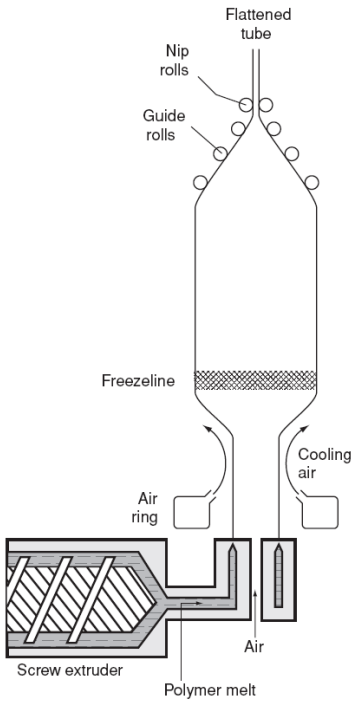

Figure 2.16: Diagram of the blown film process [73]

2.8.2 Recycling polymer nanocomposites

Reprocessing or recycling of polymer nanocomposites is a very small area as not many researchers have considered the outcome of trying to recycle or dispose of these materials. Very few studies have been conducted on trying to reprocess polymer nanocomposites once they have come to their end of life service or tried to understand what would happen to the nanocomposite material if it was to be processed for a second time. Studies so far have only concentrated on a single process stage and determining the properties of the material but not on what would happen if it were to be sent through the

processing stage for a second time. Some papers have vaguely pointed to the fact that processing polymer nanocomposites for a second time can show signs of degradation and lower the properties of the material.

Touati et al [74] studied the effects of reprocessing cycles on the structure and properties of PP/nanoclay materials with the addition of a compatibiliser. The various nanocomposite samples were prepared by melt intercalation, and were subjected to 4 reprocessing cycles.

The study showed that the repetitive reprocessing cycles modified the initial morphology of PP/OMMT nanocomposites by improving the formation of an intercalated structure, especially after the fourth cycle. The complex viscosity was found to decrease for the whole samples indicating that the main effect of reprocessing was a decrease in the molecular weight. Moreover, the thermal and mechanical properties of the nanocomposites were significantly reduced after the first cycle; nevertheless they remained almost unchanged during recycling. No change in the chemical structure was observed for both the nanocomposites and neat PP samples after 4 cycles.

A research project and presentation by Kozlowski et al. [75] showed that reprocessing of polymer nanocomposite materials resulted in thermo-mechanical degradation and that polymer sensitivity to degradation during processing differed according to the chemical structure. The mechanical properties of solid polymers were less sensitive to reprocessing than the viscoelastic ones in a molten state are were more sensitive to degradation caused by multiple extrusions than the matrix polymers. Polymer nanocomposites were also more resistant to recycling than micro-composites because of lower filler size.

Other such scenarios could be the extensive usage of nanofillers in car parts and the effect of trying to recycle or reprocess them.

2.8.3 Inline Monitoring

Inline monitoring is the process of gathering data in real time via probes, sensors or other hardware devices as shown in figure 2.17 and trying to assess and understand the specific conditions. This is especially important if producing polymer nanocomposites as they are a constituent of complex materials that require a clear understanding in real time measurements. Parameters such as the temperature, speed, torque of the extruder or the viscosity of the polymer melt within the barrel can be of significance to monitor. Researchers have looked into this area with great interest but have been vaguely successful in gaining any relevant or significant data. To capture data in real time requires a lot of expertise and understanding in the subject area. The knowhow of hardware/software systems is a requirement that has to be used with care.

Figure 2.17: Inline monitoring setup

Bur at al [76] used dielectric and optical transmission measurements to obtain the extent of clay exfoliation during the processing stage with online measurements. Measurements were made using an instrumented slit die and the data was correlated with off-line TEM images which showed that the transmission increased with the extent of exfoliation possibly due to the light scattering of aggregate clay particles being reduced as the particles exfoliated nano-size silicate flakes.

Bertolino et al [77] also conducted a similar study with the use of an inline optical detector to monitor the disaggregation of the MMT clay tactoids during the preparation of PP/MMT nanocomposites via polymer melt compounding. It was found that the signal of the detector was reduced with exfoliation because during this phase the tactoid size was reduced below the minimum particle size to produce light extinction.

Other work by Mould et al [55] used a computer controlled on-line rotational rheometer that was capable of collecting material samples from within an extruder at different axial locations and performing the usual measurements of typical bench top commercial instruments. Comparisons were made by undertaking measurements using both online and offline equipment and different parameters which showed consistent results.

2.9 Conclusions

For one to produce a good quality polymer nanocomposite material requires the successful integration of the nanofiller into the polymer matrix. This would have to include good distributive and dispersive incorporation of the nanofiller into the polymer matrix together with overcoming the compatibility issues between the nanofiller and the polymer materials by usually using a third party compatibilising agent to integrate both materials.

Also the aspect of selecting the correct equipment that could possibly undertake high shear mixing that would allow, in the case of nanoclays, the swelling or breakup of stacks of platelet layers to instigate the effect of intercalation or exfoliation as this has shown to improve various properties (Figure 2.18).

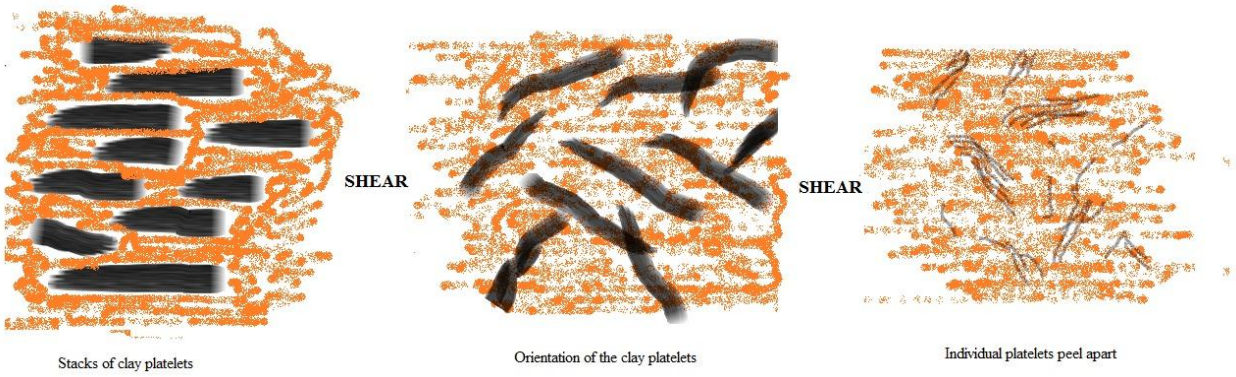

Figure 2.18: Shearing effect of clay platelets

In industrial mixers the main technique employed is to use large twin screw extruders which have a high power output coupled with large residence time to ensure the stress applied on the composites are large enough and sustained over a long time in the extruder to allow the platelets of nano-additives to be fully dispersed in the polymer matrix. An additional control in large extruders is the temperature control whereby as the temperature is decreased, one can develop higher stresses.

For smaller laboratory mixers the challenge has been to duplicate demanding conditions to create good distributive and dispersive mixing. An ideal situation would be to develop stresses similar to those on larger extruders so that enough dispersive power can break the clay platelets and create the intercalation and/or exfoliation of the nano-additive.

As for the testing phase of the nanocomposites it has been understood that using a set routine to undertake the tests are the norm. Studying the microstructure of such

materials using SEM/TEM coupled with XRD, Rheology, Mechanical testing, DSC, DMA are indispensable techniques to allow the user to determine the true qualities of the nanocomposite material.

Additional features include biaxial stretching of the nanocomposite materials that would allow more specialised improvements within certain properties of the material. Online monitoring could also prove a good technique to monitor the formation of such materials in real time with various measurements including Ultrasound, Viscosity or Photocell measurements to monitor the various changes taking place.

Usuki et al. [9] was one of the early researchers to record significant improvements in various properties including the tensile modulus of polymer nanocomposites over their neat polymer matrices. However, given all the benefits that are stated of polymer nanocomposites, in reality little has been put into practice on the industrial scale besides small amounts that have been produced for specific products. All research in this vast area has touched the surface with no definitive breakthrough to allow the mass production of such materials for applications. Another unknown is the difficulty in establishing the long term behaviour of these materials and if they can maintain their unique properties over a long period of time or if they will change.

Health and safety issues are also paramount as certain nanofillers have been known to interact with human cells and body tissue to cause specific problems and illnesses and also when inhaled these fine particles can enter the body and cause adverse reactions that can go undetected for prolonged periods of time. Recycling of these materials is also something reasonably new that has started to emerge as questions are being asked about the

ease at which these polymer nanocomposite materials can be recycled and the consequences.

Therefore this is still an area that has and will need substantial research work to totally understand the nature of the different types of polymer nanocomposite materials and their behaviour to utilise them as a beneficial end product.

Chapter 3 : EXPERIMENTAL METHOD

3.1 Introduction

This chapter describes the experimental method used in this research and centres on the use of a novel minimixer to produce polymer nanocomposites via the melt mixing route. This minimixer was developed at Bradford from previous studies to produce polymer master-batches. The production of master-batches relies on dispersing micron size particulates into polymer melts so it differs in the order of magnitude required to produce nanocomposites. The first objective was thus to establish the mixing conditions that lead to nano-composition. This required designing a set of experimental conditions for a given polymer and a nano-additive and measuring the properties of the compounds obtained from the programme. The measurements included microscopic observations of the samples, rheological and mechanical properties testing. There was however a particular emphasis on the rheological measurements. Additional to using mixing in the melt as a means to create nano-composition, the research also investigated the effect of biaxial orientation on the nanocomposites. The idea, as explained in the objectives, was to find if stretching induced further intercalation-exfoliation. Finally and as result of the importance of rheological measurement, an inline rheological cell was integrated as an attachment to the mini-mixer to be used to detect directly which mixing operating conditions resulted in the nanocomposite with the optimal properties. An ultra sound cell was also integrated within the mini-mixer to assess if such a method could help detect the optimum conditions. These and other aspects of the experimental method are described in this chapter.

3.2 The mini-mixer: Design and Operation Features

3.2.1 The original mini-mixer

Operating within a specialised field has always been challenging and for the team based at the University of Bradford, the conceptual challenge was to build a novel mini-mixer for producing polymer nanocomposites at the laboratory scale, in small quantities (10-30g) so as to facilitate research and development of a range of nanocomposites. The design challenge of this novel minimixer was that to guide industrial applications, it had to replicate the intensive mixing conditions achieved in the large industrial twin extruders, i.e. large stresses and residence times in shear and elongational flows to produce high levels of dispersive as well as distributive mixing. These are necessary to break the aggregated particulates making the nano-particles. As explained in the literature survey, other researchers have developed various devices aimed at this objective but none used the radical approach adopted in this novel design which was to use three screws, two to create the mixing necessary as in a standard twin extruder and a third screw placed underneath to circulate the mix melt continuously along the path of the twin screw system. Figure 3.1 explains the design which can then evolve in various other designs depending on how the melt is emptied from the device. The key aspect of the twin screw system is that it is fitted with the usual elongational dispersive elements typical of industrial twin extruders. The advantage of such a device is that not only does it produce intense mixing but effectively over an infinite residence time if so required. As the circulation is along the path of the twin screw system, the entire mass of the melt is recirculated and experiences the same mixing history. This is unlike the mini-mixers (see Figure 3.2) used conventionally which recirculate the melt via an external channel in which the melt is unequally sheared (more at the wall than at the centre). This original design was developed further and instrumented to

programme and measure the required temperatures for mixing and the mixing time and to measure the torque used during mixing. Figure 3.3 shows the entire experimental system, including the data logging (further details below). One practical and desirable feature of the minimixer is that on emptying it produces a continuous strand of nanocomposite ready for further measurements. The system thus provided user-friendly engineering information on the technique used. As torque dissipation is a good measure of the stresses developed, the device also acted as a semi-rheological tool able to distinguish between those systems developing high stresses and those that did not. It may also be possible with such an instrumentation to monitor torque, i.e. rheology in real-time which can be very useful in determining when the torque peaks for example (further details below), may be suggesting that a change of structure had been reached in the particular mix. From this, the operator may infer that the conditions for nano-composition have been reached and stop mixing at that point. Clearly these considerations are all inferences that were part of the research objectives to be verified by more precise measurements such the rheology of the actual nanocomposites formed.

As the minimixer was designed for materbatch testing and the demands of nanocomposites are more strident, suitable instrumentation was required and this was implemented as a new and integral part of this research.

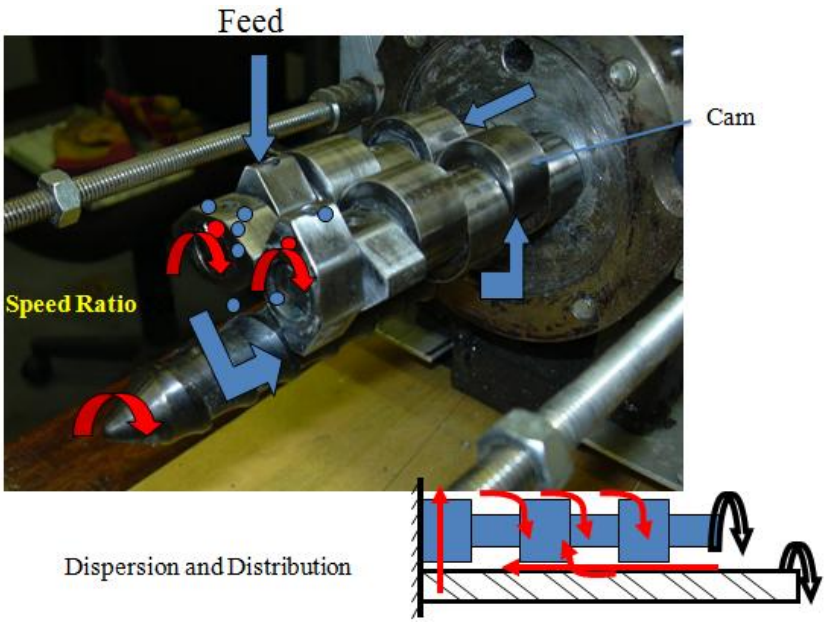

Figure 3.1: Designs of the minimixer showing various arrangements for operation.

Figure 3.2: The limitation of commercial minimixer (unequal mixing history in recirculation channel.

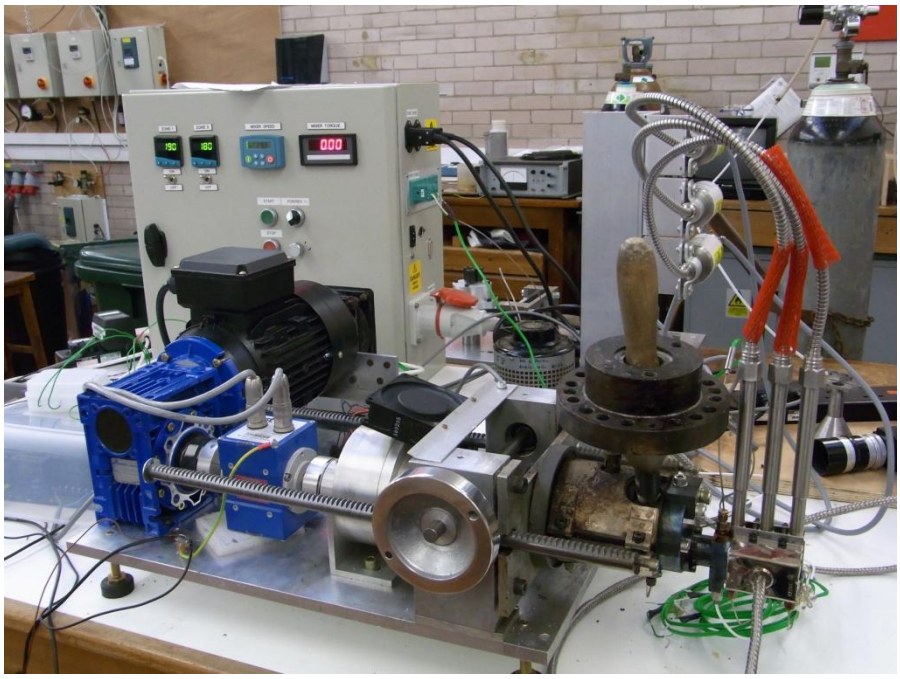

Figure 3.3: The minimixer setup in its entirety

3.2.2 New Instruments Data Logging of the mini-mixer

This part of the research project was critical and involved generating a software program for data acquisition in real-time. The main unit of hardware was a National Instruments NI-cDAQ-9172 data acquisition system (figure 3.4) that was connected to the various sensors on the test rig equipment i.e. temperature probes, speed control system, torque sensors, pressure transducers. In addition, Labview software was used to integrate with the hardware and control its features.

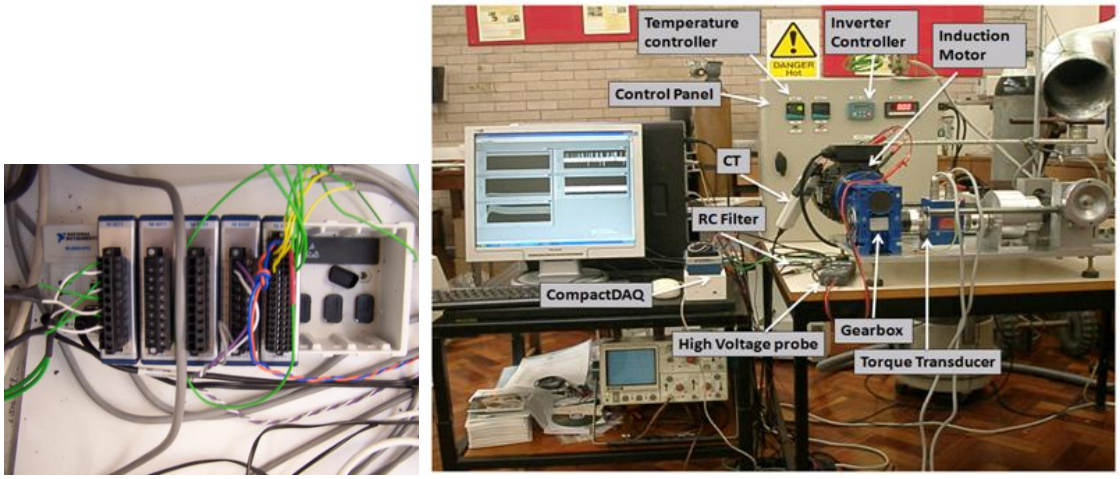

Figure 3.4: Picture of the NI-cDAQ-9172 and overall data acquisition setup

The Labview operating instructions are as follows:

(The Labview software was specifically developed for real-time measurements of the temperature, torque, screw speed, residence time & motor speed of the minimixer at Bradford University and later included the Viscosity and Ultrasound measurements).

To generate a new program in Labview:

- Open a new Labview program (Click on Labview icon)
- Right click on the centre of the new block diagram page and select [Exec. Control → While loop] and create a square window.
- Right click in the newly created window and select [Input → DAQ assist] and place anywhere in the box and a window appears
- Select [Aquire signal → Analog input → Voltage → aio (terminals on processing unit Ti) → Finish]
- Another window appears [Signal input range → Change (obtain from datasheet i.e. 0.2 max, -0.2 min volts)][Terminal configuration → Differential rate (change to i.e. 10k - obtain from datasheet)][Acquisition mode → Continuous samples]

- Click OK
- *DAQ Assistant logo appears*
- Go to “Icon window” on top of the page and select “Show front panel” (another page appears)
- Right click on the screen then select [Graph indicator → Graph]
- Place graph icon anywhere on the screen
- Go back to top of window and click on “Icon window” and select “Show block diagram”
- *Another icon appears “Waveform graph”*
- Click on this icon and place it parallel to the other icons
- Then click on the first icon at the “right hand side edge” and bring a line connection from one icon to the next
- A line is now connecting both the icons
- Go back to the front panel and enlarge the graph to the desired size
- Press the start / stop button to test
- Change Y scale by right clicking on the graph, selecting Y Scale and turning off Autoscale
- Change scale to the desired settings by clicking on the numbers and changing them

  To get a Output file: Right click → Output → Write assessment file → Select destination folder
- You can also add Filters by right clicking on the screen and adding a logo and linking it to the DAQ assist and putting in the preferred settings.

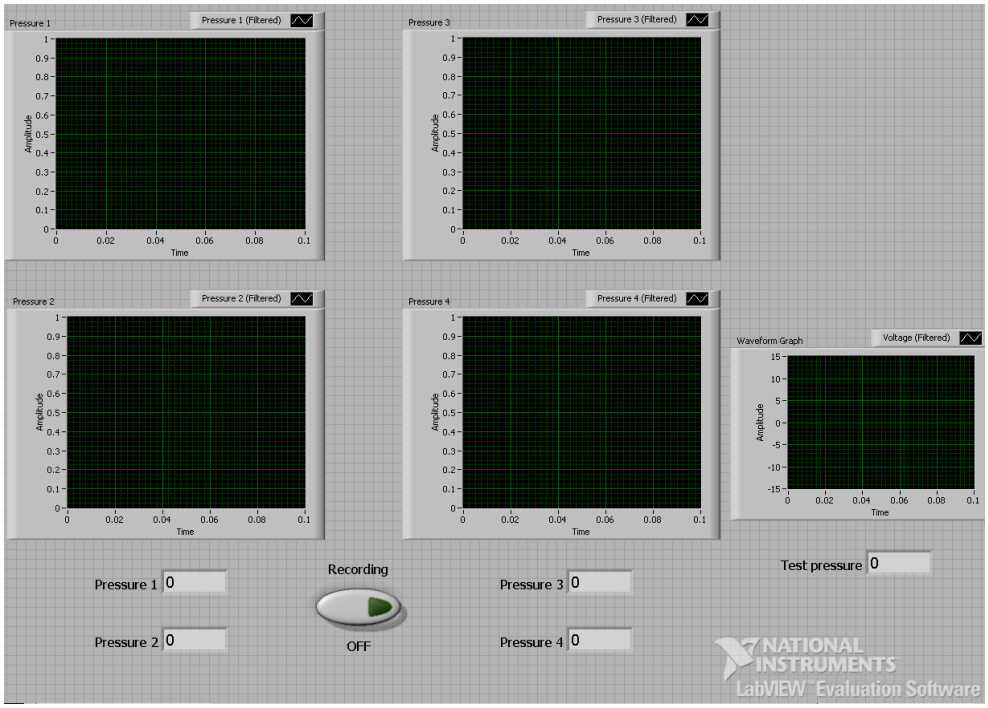

Figure 3.5: Front panel of VI for data acquisition Labview software

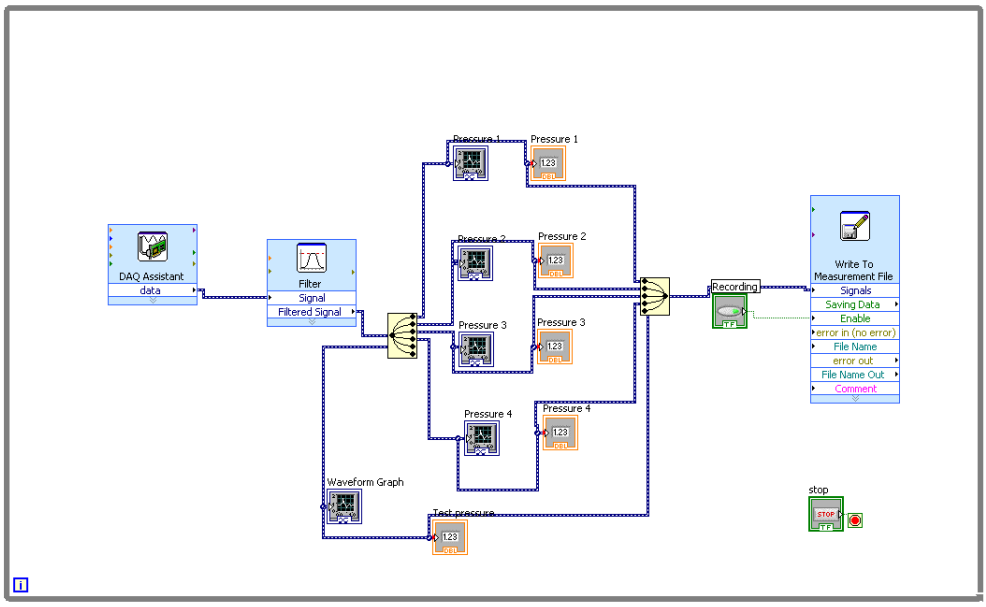

Figure 3.6: Block Diagram Containing Source Code of Labview software

3.3 Polymers & nano-additives used and their preparation

Previous studies dealing with polymer based nanocomposites have been conducted with a wide range of polymers and nano-fillers using different processing techniques and equipment, mainly small scaled twin screw extruders [78]. The majority of equipment use small batches of material since most of the raw materials are expensive and conducting small scaled tests are thus the preferred choice. The most crucial element of obtaining the ideal nanocomposite is having good dispersion and distribution of the materials and for them to be compatible with one another. By compatible we mean the materials should show signs of good chemical bonding at the microscopic scale as both polymer and nanofiller materials can be classed as either hydrophilic or hydrophobic etc [79]. The majority of tests that have been conducted using small scaled twin screw extruders have shown promising results with the nanocomposites showing improved properties. These processes however rely on the fact that the material can be mixed for only a short and specific period of time from the feeding within the hopper to the exit at the die end. This can thus result in poor mixing of the materials since there is a short mixing time within the extruder. Therefore the minimixer at Bradford was used to undertake the experiments due to its unlimited recirculation time and high shear mixing as previously mentioned [24]. This setup would make it ideal for processing nanocomposites since the desired mixing time and speed could be used to favour the manufacturing requirements of the nanocomposites. This scenario could also be ideal to mimic the processing conditions of the larger twin screw extruders which have a longer processing window.

3.3.1 Materials Used

The following polymers, nano-additives and compatibilisers were used:

- Two grades of Polypropylene (PP): 575P from Sabic with MFI=10.5 g/10min (homopolymer with a density of 905 kg/m^3) and Moplen HP420M from Basell with MFI=8g/10min (9003-07-0 1-propene homopolymer).
- Polyethylene terephthalate (PET) BP101 from Innovia.
- Polybond 3200 compatibiliser from Crompton (Maleic anhydride grafted polypropylene with melt flow rate of 115g/10min at 190^{o}C, density of 0.91g/cc at 23^{o}C) .
- Cloisite 20A & 10A nanoclays from Southern Clay Products for use with PP (Natural montmorillonite modified with a quaternary ammonium salt – 2M2HT with a typical dry particle size of 13µ by volume, density of 1.77g/cc & d_{001} = 24.2Å).
- Somasif MTE (surfactant: methyl trioctyl ammonium chloride) for use with PET.
- Polyurethane 80A and Single/Multi-walled Carbon nanotubes from Sichuan University, Chengdu, China (which were supplied separately).

3.3.2 Material preparation before extrusion

The PP & PET materials were obtained in fine powder form together with the clays and compatibilisers to ease the feeding and processing of the materials within the minimixer. In pellet form the materials were difficult to feed and caused variations in the torque readings and uneven running of the minimixer. The materials were weighed upto a total of 30 grams (maximum amount processable by the minimixer) using a Denver

instrument (DE 100A) to 4 decimal places and having an enclosed glass chamber to prevent any foreign contaminants from entering or discrepancies caused by fluctuations. The clays were kept in separated airtight containers to prevent air/moisture penetration and for health and safety reasons (toxic if inhaled in large quantities) and added to the PP/PET materials if and when required. The materials were thoroughly hand mixed in small containers to ensure there were no agglomerates present and masks were worn over mouth and nose so as not to inhale in any nanoclay dust.

Before carrying out any experiments it had to be made sure that no materials contained any moisture as this could cause variations in the results and therefore the materials were dried in a vacuum oven at 100^{o}C for 12 hours. [It was determined that it took the oven 1 hour to warm up and 5 hours to cool down so these settings were also taken into consideration]. Another issue was the transfer of the PET material from the oven to the minimixer hopper. This short interval could allow moisture to enter the material especially at the feeding point as PET is quick to retain moisture in a room environment. In order to prevent this occurring, a ring was placed over the hopper blowing nitrogen directly onto it thus preventing any air entering the minimixer. An attachment pipe was also linked to the vacuum oven so each time the door was opened to remove a sample nitrogen was pumped into the chamber to ensure no air could enter.

3.3.3 Extrudate samples preparation for testing

The preparation of the extrudate samples was critical to ensure accurate and consistent testing. This required first pelletising the strands and then pressing them into thin sheets approximately 1mm in thickness. This procedure ensured that the sheets could be cut out into a series of samples to be used for the necessary rheological and mechanical testing.

The procedure for rheological measurements involved placing cut sections of nanocomposite strands directly onto the parallel plate, melting them at the desired temperature and trimming off the excess material before conducting the testing. This procedure could result in slight inaccuracies due to the polymer being unevenly distributed between the parallel plates of the rheometer and most critically if any gaps or trapped air were present in the sample. Another issue, for tensile testing, was the injection moulding of the samples into the appropriate T-bars specimen. This clearly adds an additional processing step of the nanocomposite which could flaw the validity of the result. However as this is carried out for all the samples in the same manner, the added processing step was consistently present in all the samples.

An easier option, also used, was to cut out a T-bar shape from the compressed sheet using a sharp cutting tool. The pellets were placed onto a hotplate press set at 180^{o}C with 30cm^{2} diameter for 4 minutes until the pellets were sufficiently melted and a pressure of 10 tonnes was gradually applied (see figure 3.7). The equipment was water cooled to 30^{o}C to allow the sheet to be removed. Samples were cut out using sharp tailor made dies and also measured afterwards using vernier callipers to make sure the dimensions were correct.

Figure 3.7: Picture of the hot press

3.4 Experiments for producing nanocomposites

3.4.1 Design of Experiments for PP

Considering the large number of variables in the experimental programme (mixer temperature, residence time, screw speed; polymer type; clay type and loading; compatibiliser type and loading), a mathematically thorough approach was required to organise the experimental programme. Quarter fractional factorial experiments were thus constructed using Design-Expert software (Version 7.1.3; Statease Inc, USA) with 6 factors and 2 levels (low & high). Initial experimentation was carried out to ensure factor levels were appropriate and could be extended to half fractional if required. Three control runs with no nanoclay were also included in the DOE runs.

Factors and Factor Levels:

Table 3.1: Table of different factors and their levels

Factor	Name	Units	Type	Low	High
A	Speed	rpm	Numeric	20	60
B	Residence Time	min	Numeric	2	8
C	Temperature	oC	Numeric	190	230
D	Nanoclay Loading	%	Numeric	2	6
E	Compatibiliser	%	Numeric	2	6
F	Polymer MFI	g/10min	Categorical	8	10.5

Table of Experimental runs:

Table 3.2: Complete DOE runs

Run Order	Speed (RPM)	Residence time (Min)	Temp. (Deg)	Nanoday Load (%)	Compatibiliser Load (%)	Polymer MFI	Polymer mass (g)	Nanoclay mass (g)	Compatibiliser mass (g)
1	60	8	190	6	2	8.00	23.00	1.50	0.50
2	20	2	190	6	2	10.50	23.00	1.50	0.50
3	60	8	230	2	6	8.00	23.00	0.50	1.50
4	60	2	190	6	6	10.50	22.00	1.50	1.50
5	20	8	190	2	6	10.50	23.00	0.50	1.50
6	20	8	190	6	6	8.00	22.00	1.50	1.50
7	60	8	230	6	6	10.50	22.00	1.50	1.50
8	20	2	230	2	6	10.50	23.00	0.50	1.50
9	20	2	230	6	6	8.00	22.00	1.50	1.50
10	20	8	230	2	2	8.00	24.00	0.50	0.50
11	40	5	210	4	4	8.00	23.00	1.00	1.00
12	20	8	230	6	2	10.50	23.00	1.50	0.50
13	60	8	190	2	2	10.50	24.00	0.50	0.50
14	60	2	230	6	2	8.00	23.00	1.50	0.50
15	20	2	190	2	2	8.00	24.00	0.50	0.50
16	60	2	190	2	6	8.00	23.00	0.50	1.50
17	40	5	210	4	4	10.50	23.00	1.00	1.00
18	60	2	230	2	2	10.50	24.00	0.50	0.50
19	40	5	210	4	4	10.50	23.00	1.00	1.00
20	40	5	210	4	4	8.00	23.00	1.00	1.00
21	20	2	190	0	2	8.00	24.50	0.00	0.50
22	40	5	210	0	4	8.00	24.00	0.00	1.00
23	60	8	230	0	6	10.50	23.50	0.00	1.50

Each of the above 23 runs were repeated 5 times to ensure repeatability, consistency and more practically enough quantity of nanocomposite material was obtained for further analysis. The samples were obtained in approximately 1mm thick stands and pelletised for rheology, DSC, DMA and mechanical properties measurements.

3.4.2 Additional PP runs

An additional set of experiments were conducted using PP (10.5 MFI) polymer blended with Cloisite 20A nanoclay in 1% wt. increments upto a maximum weight of 10% clay. This was to determine the effect of nanoclay loading on the base PP polymer. Here the mixer parameters (screw speed, mixing time, temperature) as well as the compatibiliser loading were kept constant. Clearly a repeat series of experiments with different compatibiliser loading was necessary to build a complete picture but this was a recommendation for further work. The experiments were conducted exactly like the previous PP tests using the mini-mixer and collected in strand form which was later pelletised. The samples were then made into 1mm thick by 25mm diameter flat discs for further rheological testing using a hot press.

Table 3.3: Additional PP runs

Run	Speed (rpm)	Time (min)	Temp (°C)	Clay (%)	Comp. (%)	Comp. weight (g)	PP Weight (g)	Clay weight (g)
1	40	5	190	0	0	0.0	25.00	0.00
2	40	5	190	1	2	0.5	24.25	0.25
3	40	5	190	2	2	0.5	24.00	0.50
4	40	5	190	3	2	0.5	23.75	0.75
5	40	5	190	4	2	0.5	23.50	1.00
6	40	5	190	5	2	0.5	23.25	1.25
7	40	5	190	6	2	0.5	23.00	1.50
8	40	5	190	8	2	0.5	22.50	2.00
9	40	5	190	10	2	0.5	22.00	2.50

The programme of runs and testing was as follows:

1. Experimental runs using Polypropylene (575P from Sabic with MFI: 10.5 g/10min) mixed with 0-10wt.% Cloisite 20A clay and polybond 3200 compatibiliser were undertaken to determine the effect of clay loading on the virgin polymer (parameters used: 190 degC, mixing time 5min, mixing speed 20rpm, 2% compatibiliser)
2. Melt rheology of these samples were undertaken using a Bohlin CVO120 & Anton Paar Rheometers at 190 degC (in reference to the processing temperature of the nanocomposite materials) to identify any changes in the material properties that could suggest if *nano-composition* had taken place. Identified "*promising"* samples.
3. Solid bi-axial stretching of the extrudated samples was undertaken at 155 degC using a T M Long bi-axial stretcher (described in section 3.6 below) based at Bradford University with different stretch ratios of 2:1 and 4:1 stretch at constant speed.

4. The melt rheology of the stretched samples was re-measured again at 190 deg C to identify if biaxial stretching had any favourable or detrimental effect on the material and if it helped achieve nano-composition.
5. From a re-processing point of view to determine the effect of recycling the nanocomposite materials; a 6% clay loaded PP sample was produced using the mini-mixer, bi-axially stretched with a 4:1 stretch ratio, fed back into the mini-mixer and processed again. The melt rheology of the extrudate was then measured at 190 deg C and compared to the original sample.
6. The DMA, DSC and Mechanical properties of all the samples were tested to provide further comparative indicators on nano-composition.
7. The experimental runs were repeated once again but this time using a different clay (Cloisite 10A) again with 0-10% clay loading and the same settings to assess the effect of this clay type.
8. For all the above samples the PP/Clay/Compatibiliser was manually premixed by hand in a cup before being fed into the minimixer, thus for this step it was seen what the consequences would be if the samples were not premixed beforehand by feeding them directly into the minimixer individually. Therefore selective runs with 1, 3 and 6wt.% clay content were processed exactly as before without the initial premixing step, i.e. fed one after the other before start of mixing.
9. Additional runs were conducted on the minimixer including pressure measurements through a specialised slit die to determine the viscosity of the nanocomposite materials together with ultrasound measurements for real time data acquisition measurements.

3.4.3 Design of Experiment (DOE) for PET

The PET DOE set of experiments were conducted in a similar manner to the PP DOE runs and to distinguish the effect of adding Somasif MTE clay to PET polymer and the variation in different factors as shown in table 3.4.

PET Preliminary test runs

To find the ideal conditions of extruding the PET using the minimixer, preliminary test runs were conducted using different factors. The speed was kept constant at 60RPM for each experiment and the temperature was also kept constant at 290^{o}C. The processing time within the minimixer was changed in increments of ½ minute from 4 to 2.5 minutes. All samples were 30g in weight.

Table 3.4: Different factors used for PET runs

Factor	Name	Units	Type	Low	High
1	Temperature	°C	Numeric	270	285
2	Speed	rpm	Numeric	20	60
3	Residence Time	min	Numeric	1	3
4	Nanoclay Loading	%	Numeric	2	6

The results were inconclusive as the PET was relatively degraded at this temperature range (dark in colour & viscous composure) and could not be obtained in a reasonable form from the die end using either a air blower or a water bath (cooling aids) leading to the haul-off.

Therefore the experiments were slightly altered to try and alleviate the problem of the PET degradation by lowering the temperature from 290^{o}C to 285^{o}C and keeping all the other parameters the same. This resulted in a better and lighter appearance of the PET and the results are shown below.

Table 3.5: PET NC observations

Speed (RPM)	Temperature (^{o}C)	Time (Min)	Comments
60	285	4.0	Quite consistent with signs of degradation (darker colour change) and slightly unstable in viscosity
60	285	3.5	Similar in appearance to the 4 min run but showing lesser signs of degrading
60	285	3.0	Appearance is lighter in colour and flow is reasonably steady but still abit viscous in composure
60	285	2.5	Lighter and abit firmer in composure showing less signs of degrading

All the above experiments extruded within a reasonable state to allow a sample of constant sized strand to be collected. This was done using a water bath rather than an air ring blower due to the cooling period required for the PET. The torque readings were low throughout the experiments and before any experiments could be conducted, a thorough flush of the minimixer was required by fresh PET. For the experiments carried out at 270^{o}C; the PET was consistent in colour and appearance and showed no signs of degradation. It was cooled into strand format using a water bath as an air cooler had insufficient cooling power.

PET experimental procedure

The PET was accurately weighed and the clay was added to it by percentage weight. The total weight of both materials was 30g, sufficient for the Minimixer. The materials were vacuum dried for 12 hours at 100^{o}C and let to cool down for 5 hours to room temperature to remove all traces of moisture. The moisture content of both the PET and clay was measured by weighing them initially then placing them in a vacuum oven for 5 hours and reweighing them again. The difference in weight of the PET was 1.7g & for the clay 0.44g.

The experiments were carried out under strict conditions so not to allow any moisture to penetrate the PET & clay materials. This was done by swiftly removing the material from the oven and feeding it directly into the hopper through a nitrogen ring on the surface so not to attract any moisture in the process.

Table 3.6: PET runs

Standard Order	Run Order	Speed (RPM)	Temp. (°C)	Time (Min.)	Clay Loading (%)	PET Mass (g)	Clay Weight (g)
1	1	20	270	1	2	29.4	0.6
4	2	60	285	1	2	29.4	0.6
9	3	40	277.5	2	4	28.8	1.2
2	4	60	270	1	6	28.2	1.8
7	5	20	285	3	2	29.4	0.6
6	6	60	270	3	2	29.4	0.6
3	7	20	285	1	6	28.2	1.8
5	8	20	270	3	6	28.2	1.8
8	9	60	285	3	6	28.2	1.8
	10	20	270	1	0	30.0	0.0
	11	60	270	3	0	30.0	0.0
	12	20	285	1	0	30.0	0.0
	13	60	285	3	0	30.0	0.0

Initial tests conducted on the PET samples by Queens University Belfast showed that most of the samples had shown signs of degradation and so it was recommended that additional runs be conducted but with a run time of ½ minute. Therefore four additional runs were used as shown in table 3.7.

Table 3.7: Additional PET runs

Standard Order	Run Order	Speed (RPM)	Temp. (°C)	Time (Min.)	Clay Loading (%)	PET Mass (g)	Clay Weight (g)
14	14	20	270	0.5	2	29.4	0.6
15	15	60	285	0.5	2	29.4	0.6
16	16	60	270	0.5	6	28.2	1.8
17	17	20	285	0.5	6	28.2	1.8

Samples were sent to Queens University Belfast for further analysis.

Run 11 was repeated again at 60 RPM, 270 degrees, 3 min, 0% clay but the difference being that this time the PET would be vacuum dried for 6 hours at 150 degrees and fed hot into the minimixer. This was to see if this would have any effect on the outcome of the material since this was the worst experimental run. Intrinsic Viscosity (IV) tests were also conducted on these materials to determine if they had been processed correctly with no signs of degradation.

3.4.4 Experiments with PU and Carbon Nanotubes

Experiments were conducted on the mini-mixer using shore hardness grade 80A polyurethane and hydroxyl (OH) based carbon nanotubes, PU based carbon nanotubes and COOH based carbon nanotubes, singled walled nanotubes (SW), multi walled nanotubes (MW), SWCOOH, MWCOOH. Different concentrations of carbon nanotubes were mixed

with the PU polymer in stages of 0%, 1%, 3% & 5% and then fed into the mini-mixer and real-time data from the Labview software was obtained.

The key data included torque, screw speed, barrel temperature and mixing time. When the materials were added to the minimixer, the speed of the screw had a tendency to drastically slow down and the torque increased possibly due to the low viscosity and so as not to cause any damage to the equipment, the following parameters were implemented. After a few test runs it was decided that the PU and carbon nanotubes would be mixed at 20 RPM for 4 minutes (to ensure thorough mixing while keeping the torque low) and then for 2 minutes at 30 RPM (once the material became less viscous) giving a total time of 6 minutes in the barrel for mixing. All the materials were thoroughly dried using a vacuum drier for a couple of hours before each test and the mini-mixer was thoroughly cleaned between experiments to ensure no cross contamination took place. Carbon nanotubes were blended with the PU polymer in different concentrations (weight ratio) and the PU polymer quantity was kept constant at 25g for every experiment. The experimental setup together with the different factors that were used are shown in table 3.8.

Contamination

Cross contamination of the materials was a concern and thus steps were taken to combat such problems for the range of experiments. The mini-mixer was completely cleaned after a new batch material was used or at the end of the day so that it would contain no elements from the previous batch of materials that could possibly be residing on the inside of the screw or mixing elements or the die head.

The carbon nanotubes were initially added in lower concentrations and then gradually increased with the PU polymer with the latter runs. When a different grade/type of carbon

nanotube was used to conduct the experiments then the mini-mixer was flushed out with a cleaning agent and then flushed out a couple of times with the same PU grade virgin material.

Table 3.8: PU/CNT runs

Experiments Conducted

Date: 04-06/02/09

Polyurethane: Shore 80 A (Shenzhen Pepson Co, China), before mixing, the resin was vacuum dried for 2 h at 80 °C.

Carbon nanotubes: Chengdu Institute of Organic Chemistry

RUN order	Polymer	CNT type	CNT content (wt %)	Temp (°C)	Residence time (min)			Total Mass	PU Mass (g)	CNT Mass (g)
					At Speed 20 rpm	At Speed 30 rpm	Total			
1.	PU	None	0	195	4	2	6	25	25	0
2.	PU	MWNT-OH	0.5	195	4	2	6	25	24.875	0.125
3.	PU	MWNT-OH	1	195	4	2	6	25	24.75	0.25
4.	PU	MWNT-OH	3	195	4	2	6	25	24.25	0.75
5.	PU	MWNT-OH	5	195	4	2	6	25	23.75	1.25
6.	PU	MWNT-g-PU	0.5	195	4	2	6	25	24.875	0.125
7.	PU	MWNT-g-PU	1	195	4	2	6	25	24.75	0.25
8.	PU	MWNT-g-PU	3	195	4	2	6	25	24.25	0.75
9.	PU	MWNT-g-PU	5	195	4	2	6	25	23.75	1.25
10.	PU	MWNT	1	195	4	2	6	25	24.75	0.25
11.	PU	MWNT-COOH	1	195	4	2	6	25	24.75	0.25
12.	PU	SWNT	1	195	4	2	6	25	24.75	0.25
13.	PU	SWNT-COOH	1	195	4	2	6	25	24.75	0.25

All the experiments were repeated twice.

These samples were taken back to SKLPME at Sichuan University by Prof. Hesheng for further characterisation and tests which included: SEM, DSC, TGA, DMA and Tensile Tests.

3.5 Characterisation of nanocomposites obtained

3.5.1 Microscopy

The Scanning Electron Microscope (SEM) is possibly one of the most used apparatus for observing the microscopic structure of nanocomposites. It enables to determine if intercalation or exfoliation has occurred or if agglomerates are present. Also by using appropriate software, the SEM images can be processed to give quantitative evaluation of agglomeration, intercalation and exfoliation to enable a ranking of various stages of nanocomposite formation. The SEM observations were made with the following procedure. A small piece of the nanocomposite sample was cleaned to remove any contaminants on the surface, freeze dried using nitrogen and broken into small pieces so that a clean cut sub-sample with no abrasion marks could be obtained. This sub-sample was then placed in a holder and sputter-coated with a fine layer of silver paint that would act as a conducting agent. It was then put in the SEM chamber for observation to magnification up to 5000 times. One immediate note is that this procedure carries a bias as the sub-sample may not be representative of the sample. Strictly for the SEM observations to be an accurate reflection of the entire sample, several samples and sub-samples have to be processed. This is time consuming and expensive, hence the need to support these observations with other experimental methods.

3.5.2 Off-line rheology

Rheology is a simple but powerful method to measure structural properties of all materials (solid, liquid or gases) in the molten state. The broad principle it relies on is the measurement of the resistance to flow or deformation. With nanocomposites, dynamic oscillations are applied at small amplitudes and frequencies in order not to disturb the

structure whilst measuring it at approximately 190^{o}C. Thus the sample is put between (25mm) parallel plates at amplitude and frequency settings in the linear viscoelastic region (LVR) [10]. The amplitude sweep test is the preferred initial test whereby a gradual and increased strain is applied to the material and this allows the maximum strain that the material can handle to be determined. The two important parameters that are determined are the storage/elastic modulus (G') and loss/viscous modulus (G''). The frequency sweep is also very similar whereby G' and G'' are measured and can determine the properties of the material and how they change over a frequency range. As the frequency is steadily increased, both the G' and G'' parameters are measured and this can point to the material behaviour with controlled frequency rates. Other measurements include the phase angle and the complex viscosity which also tie in with the characteristic changes being undertaken within the material properties due to gradually increasing the frequency. Other property measurements with a rheometer include Creep and Recovery tests. These start with an initial stress (10MPa) being applied to the sample for a fixed time (180 sec) and then released and allowed to recover for a fixed time (30 sec). From this the creep and elastic properties of the material can be determined. Clearly, rheology is a powerful method of measuring structure and this makes it particularly useful in the study of nanocomposites. Unlike with the SEM observations, the sample measured here is larger and truly representative of the entire material. As note in the literature survey, the technique is widely used. For example, Lim et al. [80] used dynamic oscillatory shear in the linear viscoelastic regime of three different polymer systems in an attempt to identify the behaviour of exfoliated and intercalated nanocomposites. In agreement with previous studies the authors found an increase in yield behaviour with clay loading. It was also

found that for exfoliated silicate morphologies yield stress behaviour was caused by the formation of a percolated network structure.

The rheometers used:

First, all samples were prepared so that they were 25mm in diameter and 1mm in thickness and had no flaws or air gaps within them. The rheological tests were conducted mainly on the Bohlin CVO120 (figure 3.8) but the Anton Paar Rheometer was also used for some experiments using the 25mm parallel plate configuration and a temperature of 190^{o}C. The samples were placed between the parallel plates and allowed to melt completely for 15 minutes before running the tests. For each experiment a new sample was used and the results collected by the software were plotted.

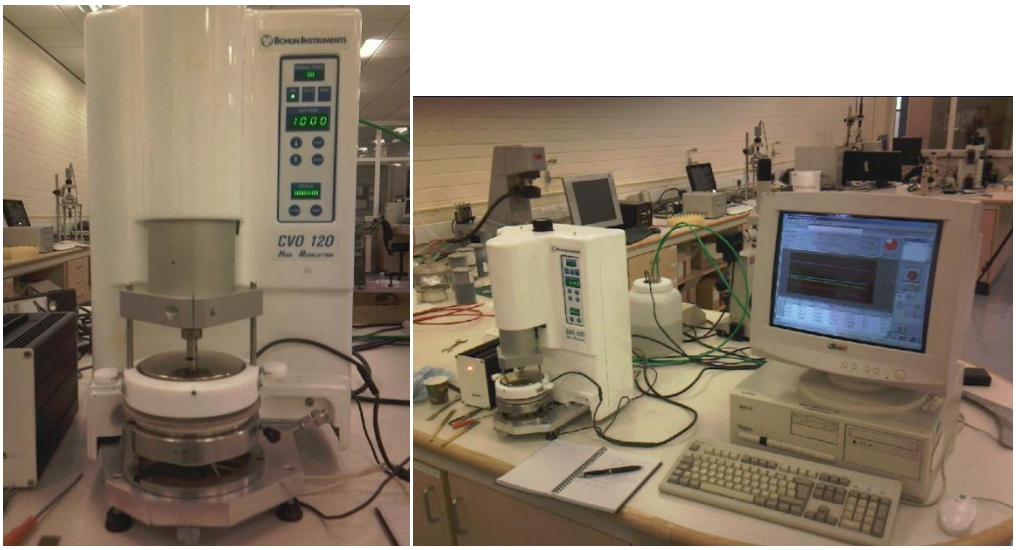

Figure 3.8: Bohlin CVO120 Rheometer

Amplitude Sweep Tests:

The strain values were set within a range of 0.001 to 20 as these were deemed to be the minimum and maximum values for the PP materials after running trials. The frequency was fixed at a constant value of 0.1 Hz as this was a desirable setting after a few test trials to establish that the flow-deformation was in the linear viscoelastic region (LVR). The temperature was set at 190^{o}C for the vast majority of runs as the DOE programme established that this temperature was the optimum mixing temperature.

Frequency Sweep Tests:

These tests were conducted with the frequency ranging from 0.1 Hz to 30 Hz with the same strain values as those used in the amplitude sweep tests to ensure the flow-deformation were in the LVR.

Creep and Recovery Tests:

These tests were undertaken with a Stress value of 10 MPa being applied to the samples in the Creep phase. This value for the stress was taken since it was within the LVR region. A time of 30 seconds was given for the Creep aspect of the measurement and allowed to recover for 300 seconds. The reason for undertaking such times was due to previous literature [81] stating that it was beneficial to have a short Creep time and a longer recovery time. Therefore after a few trial runs it was determined to use these time periods for the entire material range.

3.5.3 In-line rheology

As rheology was deemed to be a useful tool for determining the conditions leading to the formation of a nanocomposite, the mini-mixer was fitted with a slit die enabling an in-line monitoring of rheology. Three pressure sensors were used (MPI-MP201P0.75MSS; 750Psi; 80% fs; 10v), screwed into the die casing and with their heads sitting flush with the internal die surface. The transducers were powered by a 10V supply as shown in Figure 3.9 and linked up to a National Instrument (NI) 9205 module using specific pressure channels developed using the Labview software. This enabled the pressure readings to be recorded in real time. The experiments were conducted using three different screw speeds of 35, 25 & 15 rpm and the samples collected after every 2 minute intervals for a 30 second period and weighed. The pressure drop values were taken by the difference between pressure transducers 1 and 3.

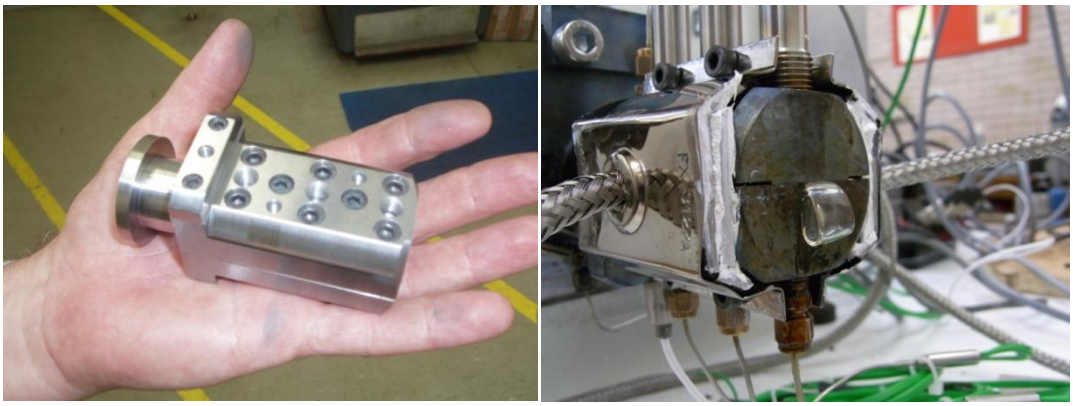

Figure 3.9: Slit die in bare form and in use

The principle of the slit die as a rheological technique is well established and is similar to that in a capillary die [82]. Essentially a pressure drop ΔP drop equivalent to a shear stress τ and a flow rate Q equivalent to a shear rate γ are measured and the apparent

viscosity η deduced from the two and the geometry of the die (width *w*, gap *h*and length *L*) as follows:

{1} $\gamma_{W(app)} = \frac{6Q}{wh^2}$ *Where* $\gamma_{W(app)}$ *is apparent shear rate*

{2} $\tau_{W(real)} = \frac{h}{2}\left(\frac{-\Delta P_{real}}{L}\right)$ *Where* $\tau_{W(real)}$ *is real shear stress*

{3} $\gamma_{W(real)} = \frac{6Q}{wh^2}\left(\frac{2}{3}+\frac{1}{3}b\right)$ *Where* $\gamma_{W(real)}$ *is rate of shear at the die wall after Walter correction for non – Newtonian liquids*

{4} $\tau_{W(real)} = \frac{wh}{2(w+h)}\left(\frac{-\Delta P_{real}}{L}\right)$ *Where* $\tau_{W(real)}$ *is wall shear stress*

{5} $\eta_{(real)} = \frac{\tau_{(real)}}{\gamma_{(real)}}$ *Where* $\eta_{(real)}$ *is real viscosity of polymer melt*

Q => Volumetric flow rate through slit die [(weight / time) / density of PP]

ΔP => Pressure drop along slit (initial pressure 1 - final pressure 3)

w => Width of slit die (8.44mm)

h => Thickness of slit die (0.84mm)

L => Length of slit die (45mm)

b => slope of log $\gamma_{W(app)}$ versus log τ_W

The following tables give an example of how the data were processed within Microsoft Excel.

Table 3.9: Pressure measurement calculations

Time (min)	Pressure 1	Pressure 2	Pressure 3	ΔP (Psi)	ΔP (Pa)
2	249.1	131.1	33.3	215	1487966
4	232.2	111.1	33.6	198	1369593

Table 3.10: Deriving Viscosity from Pressure data

Time (min)	Mass (g)	Q (m3/s)	ΔP (MPa)	γ (app.)	τ (real)	γ (real)	τ (real) at die wall	η (real)
2	0.660	2.59E-08	1.49	26.08	13888	8384	12631	1.51
4	0.455	1.78E-08	1.37	17.98	12783	5780	11626	2.01

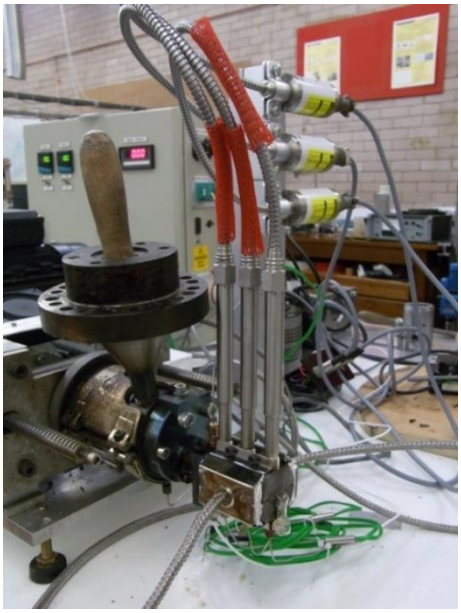

Figure 3.10: Slit die with pressure transducers

3.5.4 Ultrasound measurements

As explained in the objectives, preliminary experiments were carried out to assess the feasibility of using ultra-sound waves as an in-line measuring technique to help identify the conditions leading to the formation of nanocomposites using the mini-mixer. The ultra-sound measurements were thus undertaken using the same slit die as that used for in-line rheology. Initially, a single ultrasound probe was attached to the upper casing of the slit die in the centre position between the two pressure transducers. After testing it was noted that the signal was weak and unstable probably because of high levels of background electrical disturbances. A second probe was then added, situated directly underneath the first probe (in parallel). This improved the signal stability but background electrical disturbances remained. Both probes were linked to an oscilloscope and the difference in the signals between the two was measured.

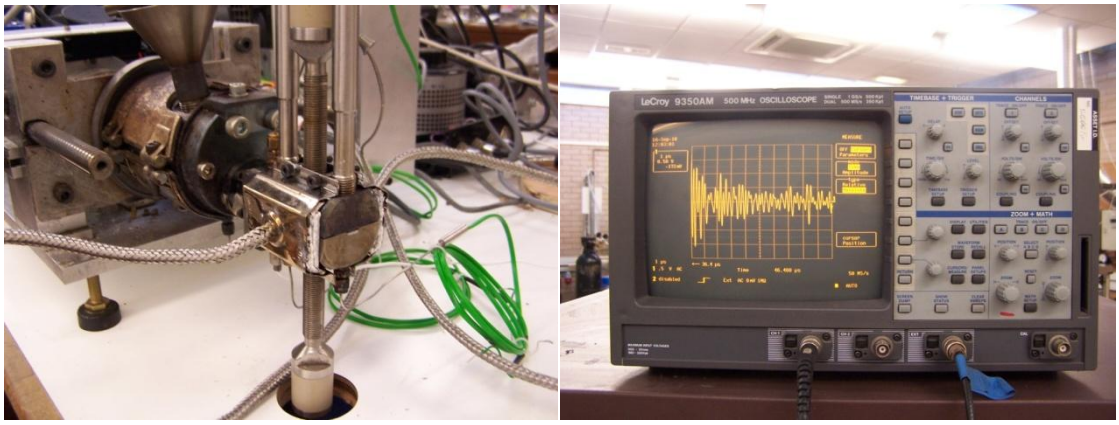

Figure 3.11: Slit die with ultrasound probes attached in parallel and Oscilloscope

3.5.5 Mechanical and Crystallisation properties measurements

Instron Testing

The tensile tests were conducted using an Instron testing machine. The T-Bar samples were cut out from the hot pressed discs prepared earlier using a sharp bladed die. Each sample was approximately 13mm in length by 2.5mm wide and 1mm thick. Each sample was initially measured using vernier calipers and these values were inserted into the computer software. The sample was vertically clamped tightly using air suction clamps and the Instron machine was operated using the PC (figure 3.12). The majority of settings were automated but the initial calibration of the equipment and the dimensions of the samples were of importance together with the stretching ratio with time as they would allow the test to be undertaken accurately. A variety of tests were conducted including the Elastic Modulus and Percentage Elongation of all the stretched and un-stretched samples.

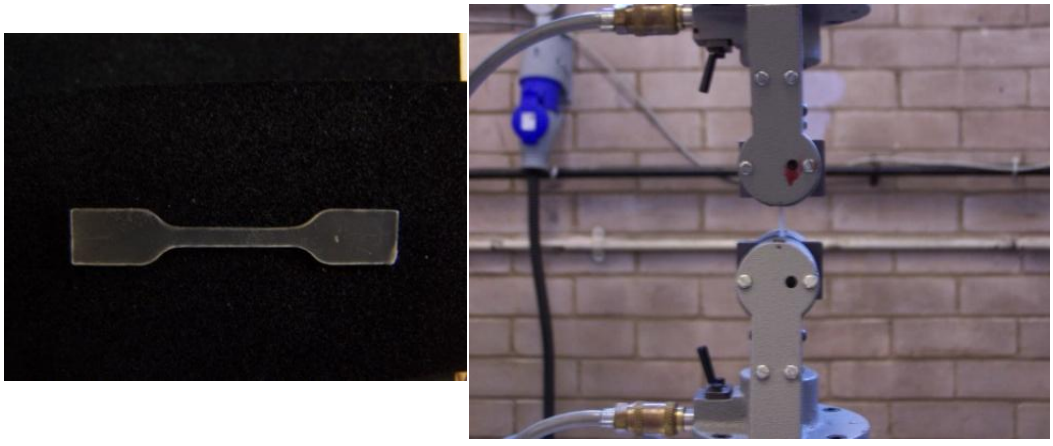

Figure 3.12: Picture of a cut out T-bar and Instron Machine clamps

DMA Testing

The equipment used was the DMA Q800 (TA Instruments) suitably calibrated according to the manufacturer's instructions. The sample dimensions were 60mm length,

10mm width and 1mm thickness. For testing the samples, the "force controlled" mode was used with a preload force of 0.001N being applied and an isothermal temperature set at 30^{o}C. The soak time was 5min with a force ramp rate of 2N/min and a force limit of 14N.

DSC Testing

The equipment used for the Differential Scanning Calorimetry (DSC) tests was the DSC Q20 (TA Instruments). The samples required careful preparation, cleaned and cut into tiny, evenly sized granules and weighing no more than 10mg before being placed into the aluminium pan of the instrument. Using the TA software a standard Heat-Cool-Heat cycle was applied from 30^{o}C to 250^{o}C, then back to 30^{o}C and then up to 250^{o}C before finally cooling back to 30^{o}C. Using the software package provided by TA, taking the area under the heat-cool-heat cycle curves gave the crystallinity values of the materials.

3.6 Stretching experiments

As explained earlier one of the objective was to assess the effect of stretching the extrudate sample from the minimixer on further intercalation-exfoliation. The equipment used was a commercial stretching machine manufactured by TM Long and modified with PC based data capture and control Labview software as shown in figure 3.13 [83].

The following procedure was used.

- The temperature was set at 155^{o}C (to allow the PP polymer to heat up enough to stretch but not melt it using air guns located on top and underneath the sample).
- The pneumatically operated chamber hood was opened and the sample (60mmx60mm x1mm) placed and held gripped by the clamps.

- The hood was then lowered and stretching was executed using an extensional program based on the Labview software from a PC that was directly linked to the equipment.

The samples were uni-axially and bi-axially stretched with either 2:1, 3:1 or 4:1 draw ratios, set at a fixed temperature of 155^{o}C for 3 minutes and at a speed rate of 40mm/sec. The equipment was run for a period of 3 minutes to allow the material to sufficiently warm up before the stretching step. All the stretched samples were once again made into 25mm diameter x 1mm thick discs for further rheological testing using the hot press and T-bars for mechanical testing as described earlier.

Figure 3.13: Setup of the biaxial stretcher

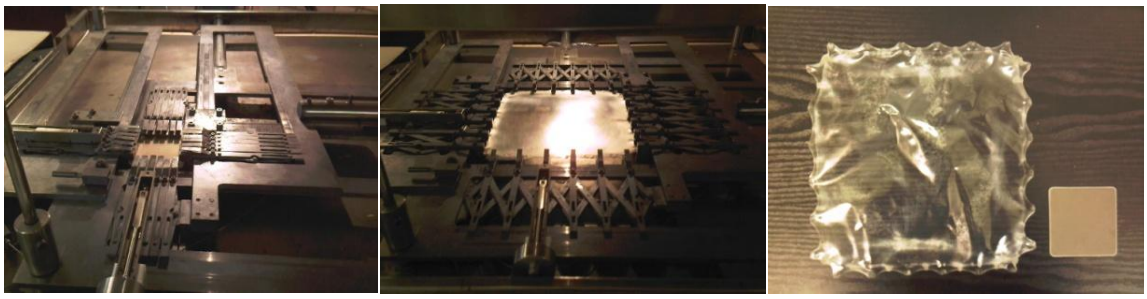

Figure 3.14: Different stages of the stretched samples

3.7 Extrusion scale-up: Equipment & method

Scaled up trials of the overall two best and two worst samples from the PP DOE runs 1-23 were conducted using the APV twin screw extruder. The operating conditions are listed in Table 3.9 and show a range of the number of passes on the APV to match the residence time in the mini-mixer. Thus extruded sampled from the APV had to be cooled, granulated and fed back into the APV. Calibration of the APV extruder was carried out using virgin PP (10.5 MFI) with the residence time measured using a tracer master-batch. The procedure for running the APV was as follows:

- 250g batches were prepared for the 4 runs (1kg for Run 4 and 1.5kg total for Runs 10, 12 & 13) and dried in a vacuum oven at 105^{o}C for 10 hours.
- Powder was fed in stages into the screw feeder to avoid segregation of fine clay particles.
- The polymer pellets were dried in a vacuum oven for over an hour at 110^{o}C before the next pass.
- The starved fed extruder flow was maintained at 40% of maximum torque.

Table 3.11: Scaled up runs undertaken on APV extruder

Scale up Trials on APV TSE (19mm)

Run No	MFI	Minimixer Screw Speed (rpm)	Minimixer Cam Speed (rpm)	Minimixer Shear Rate (s-1)	Minimixer Residence Time (min)	Temp ©	% N/clay	% Comp	APV Speed (rpm)	APV Flow Rate (kg/hr)	APV Residence Time (s)	No of Passes
4	10.5	60	186	2327	2	190	6	6	292	2.80	31.8	3.8
13	10.5	60	186	2327	8	190	2	2	292	2.80	31.8	15.1
10	8.0	20	62	788	8	230	2	2	97	2.22	54	8.9
12	10.5	20	62	788	8	230	6	2	97	2.22	54	8.9

Figure 3.15: Picture of the APV twin screw extruder

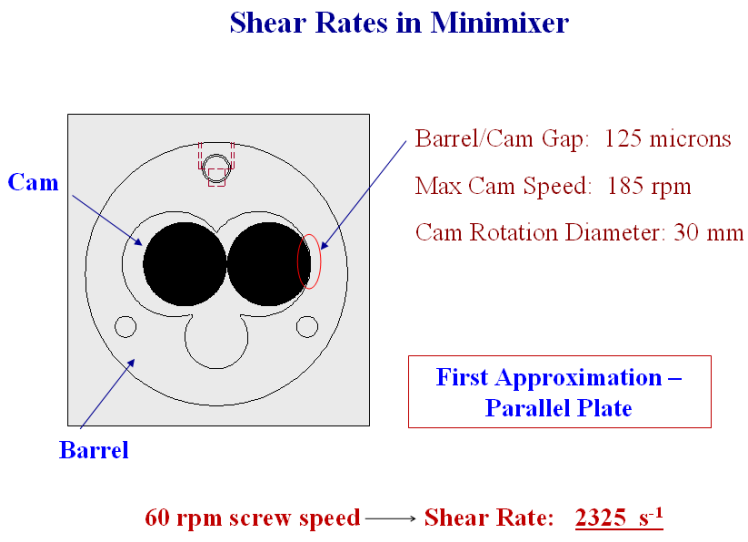

Figure 3.16: Illustration of shear rates within minimixer

Figure 3.17: The different colour complexity of each run after extrusion in the APV

Chapter 4 : RESULTS / DISCUSSION

4.1 Introduction

This chapter describes the results of the experiments carried out throughout this research. These were mainly on PP-clay nanocomposites organised first in a Design of Experiments (DOE) approach to assess the optimum operating conditions in the mini-mixer then complemented further once these conditions were established. The emphasis is on rheology as the means to establish conditions of nano-composition states. The characterisation was supplemented by further property measurements, most critically mechanical properties.

4.2 Results of DOE programme on PP in the Minimixer

The DOE experiments were conducted in the minimixer to optimise the 6 control factors of the mixer operating conditions (temperature, mixing time and screw speed), and the nanocomposite composition (PP MFI, %clay and % compatibiliser). These factors and the levels are depicted in Table 4.1.

Table 4.1: Table of different DOE factors and their levels

Factor	Name	Units	Type	Low	High
A	Speed	rpm	Numeric	20	60
B	Residence Time	min	Numeric	2	8
C	Temperature	oC	Numeric	190	230
D	Nanoclay Loading	%	Numeric	2	6
E	Compatibiliser	%	Numeric	2	6
F	Polymer MFI	g/10min	Categorical	8	10.5

Since a ¼ factorial approach was used, 23 experiments were carried out including the 3 control runs at 0% clay as shown in Table 4.2.

Table 4.2: DOE Runs

Run Order	Speed (RPM)	Residence time (Min)	Temp. (Deg)	Nanoclay Load (%)	Compatibiliser Load (%)	Polymer MFI	Polymer mass (g)	Nanoclay mass (g)	Compatibiliser mass (g)
1	60	8	190	6	2	8.00	23.00	1.50	0.50
2	20	2	190	6	2	10.50	23.00	1.50	0.50
3	60	8	230	2	6	8.00	23.00	0.50	1.50
4	60	2	190	6	6	10.50	22.00	1.50	1.50
5	20	8	190	2	6	10.50	23.00	0.50	1.50
6	20	8	190	6	6	8.00	22.00	1.50	1.50
7	60	8	230	6	6	10.50	22.00	1.50	1.50
8	20	2	230	2	6	10.50	23.00	0.50	1.50
9	20	2	230	6	6	8.00	22.00	1.50	1.50
10	20	8	230	2	2	8.00	24.00	0.50	0.50
11	40	5	210	4	4	8.00	23.00	1.00	1.00
12	20	8	230	6	2	10.50	23.00	1.50	0.50
13	60	8	190	2	2	10.50	24.00	0.50	0.50
14	60	2	230	6	2	8.00	23.00	1.50	0.50
15	20	2	190	2	2	8.00	24.00	0.50	0.50
16	60	2	190	2	6	8.00	23.00	0.50	1.50
17	40	5	210	4	4	10.50	23.00	1.00	1.00
18	60	2	230	2	2	10.50	24.00	0.50	0.50
19	40	5	210	4	4	10.50	23.00	1.00	1.00
20	40	5	210	4	4	8.00	23.00	1.00	1.00
21	20	2	190	0	2	8.00	24.50	0.00	0.50
22	40	5	210	0	4	8.00	24.00	0.00	1.00
23	60	8	230	0	6	10.50	23.50	0.00	1.50

4.2.1 Rheological Data of Nanocomposites Obtained

As already described in the Experimental Method chapter, the rheological tests were conducted in the dynamic oscillation mode so as not to destroy the samples while measuring their properties. These tests included the Amplitude Sweep (AS), Frequency Sweep (FS) and Creep and Recovery (CR) tests.

Amplitude Sweep (AS) Tests

The tests were conducted using a constant frequency value set at 0.1Hz to undertake measurements of the Elastic Modulus (G') and the Loss Modulus (G''). The results showing elastic / storage modulus are shown in Figure 4.1. The Linear Elastic Region (LVR) is observed at the lower strain ranges, then beyond a critical strain level, G' begins to drop signifying structural changes to the material. The highest G'values were for samples 4 and 6 which had a high clay and compatibiliser content. The control runs with 0% clay content had the lowest modulus values. A similar trend was observed for the G'' values which are in the appendices.

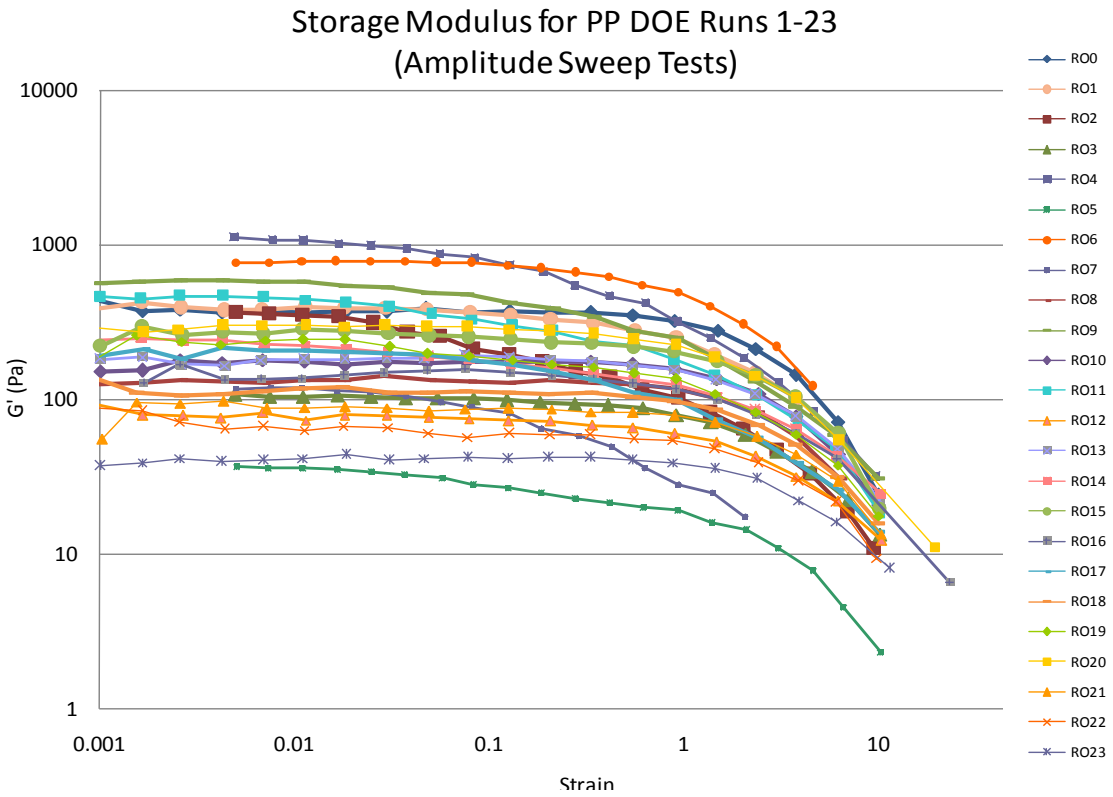

Figure 4.1: G' vs. strain rate from AS test

In order to make the comparison in the value of G' clearer, the data corresponding to the G'values in the LVR region are replotted as a bar chart in Figure 4.2. The control runs at % clay RO21, RO22, RO23 show lowest G' and give confidence in the approach. Runs RO12 and RO5 which together with RO21, RO22 and RO23 give the lowest G' point to large MFI as being conducive to poor performance. This however needs subtantiating further as the best performer also derives from an MFI of 10.5.

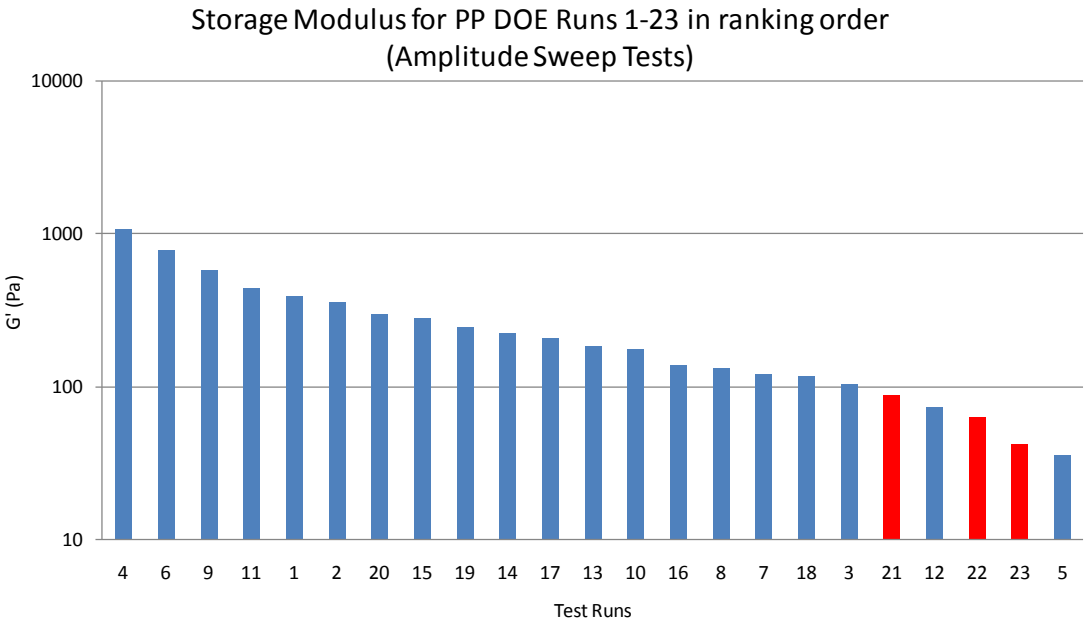

Figure 4.2: G' organised in descending order for AS

Frequency Sweep (FS) Tests

The frequency Sweep tests are equivalent to the Amplitude Sweep test, except that here we are effectively fixing the strain and increasing the time of application rather than fixing the time of application and increasing the load to break the structure. Frequency sweep tests in that effect are probably more sensitive to detectingthe structural strength level. Figures 4.3 and 4.4 show the original plot and the bar chart. Again we observe the

control runs RO21, RO22 and RO23 bunching in the lowest performance region. Again R05 is firmly in this region as is RO12 whereas R04 and R06 are best performers as revealed through the amplitude sweep tests

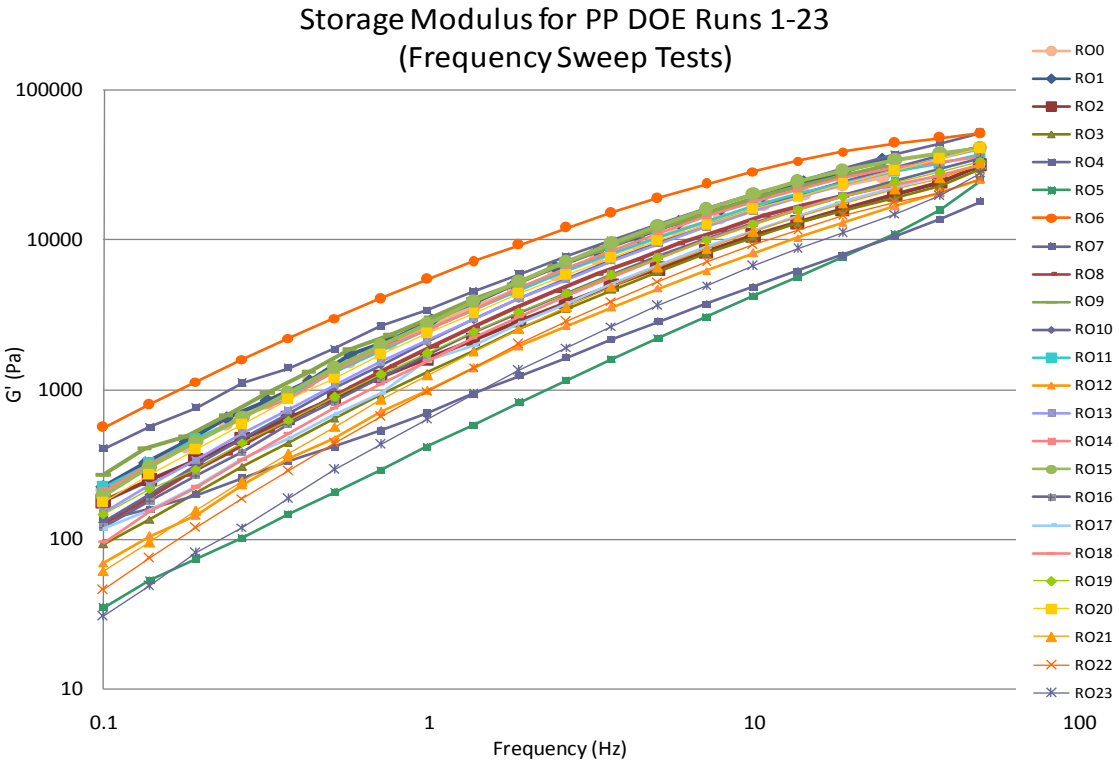

Figure 4.3: G' vs. frequency from FS tests

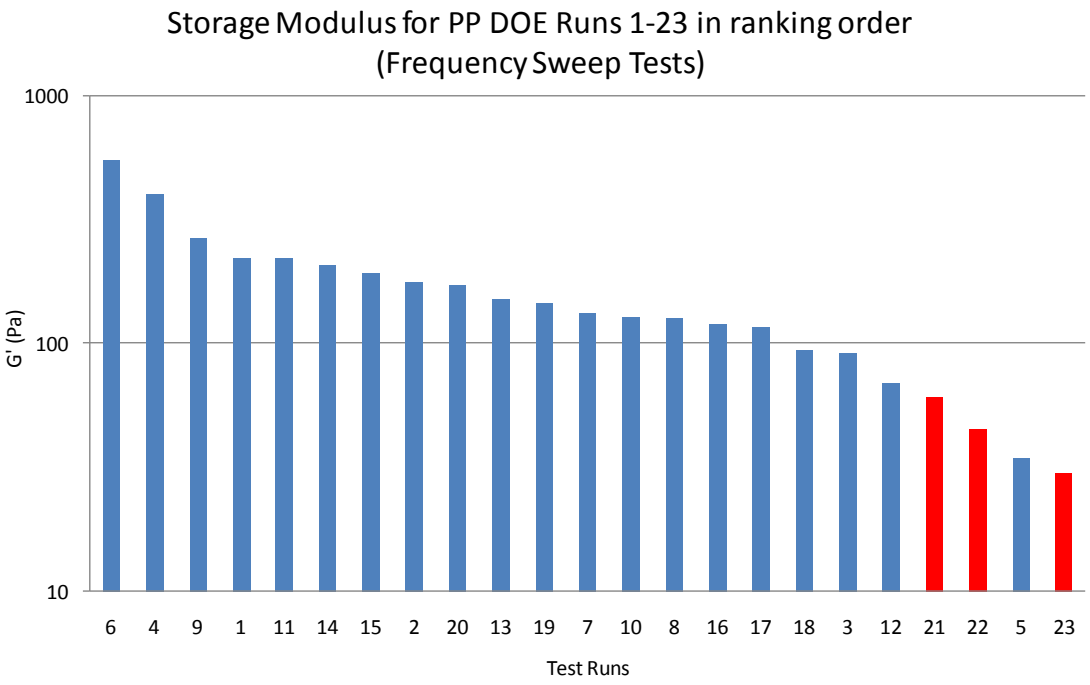

Figure 4.4: G' organised in descending order for FS

Similar trends are given when observing the loss modulus G'', complex viscosity η^* and phase angle data as shown in Figures 4.5, 4.6 and 4.7.

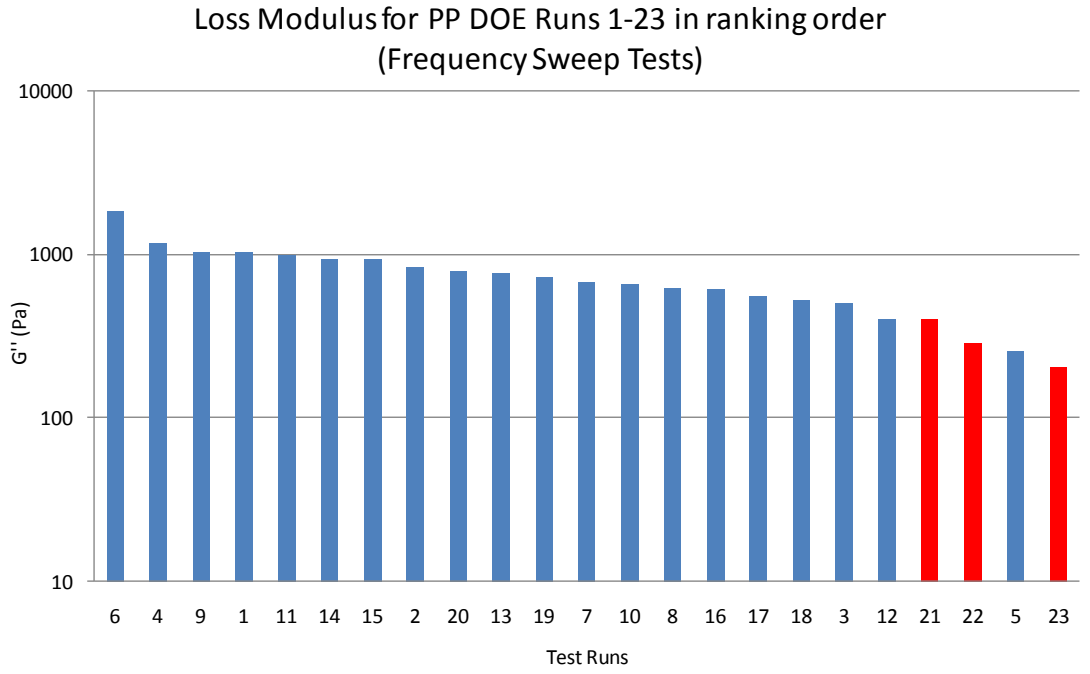

Figure 4.5: G'' organised in descending order for FS

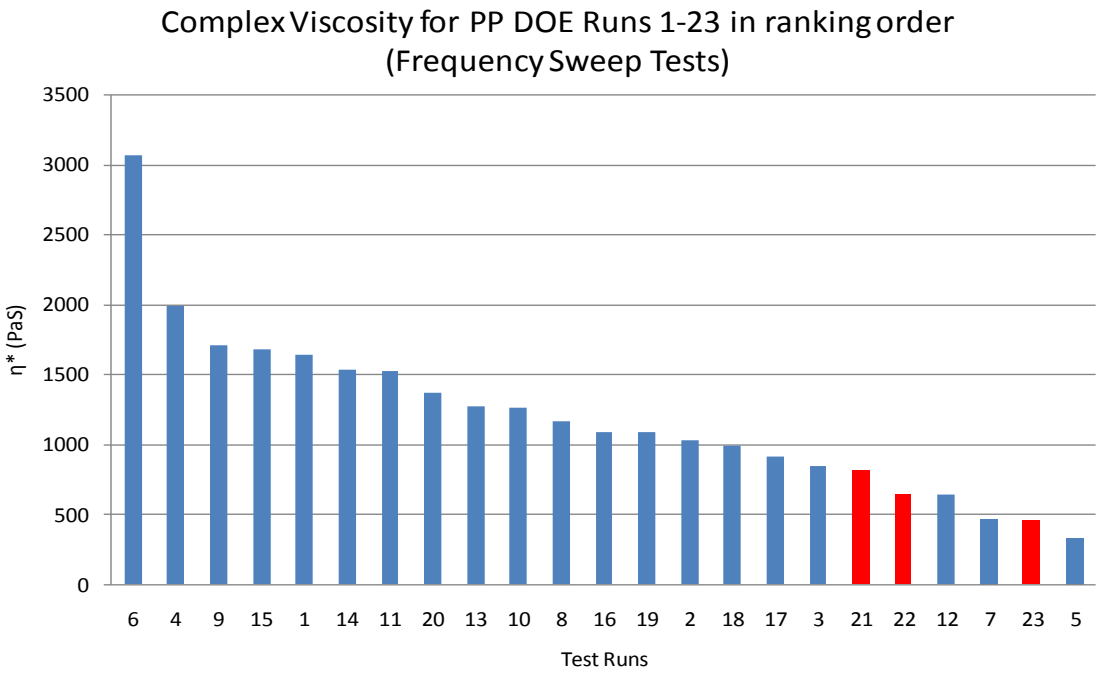

Figure 4.6: η* organised in descending order for FS

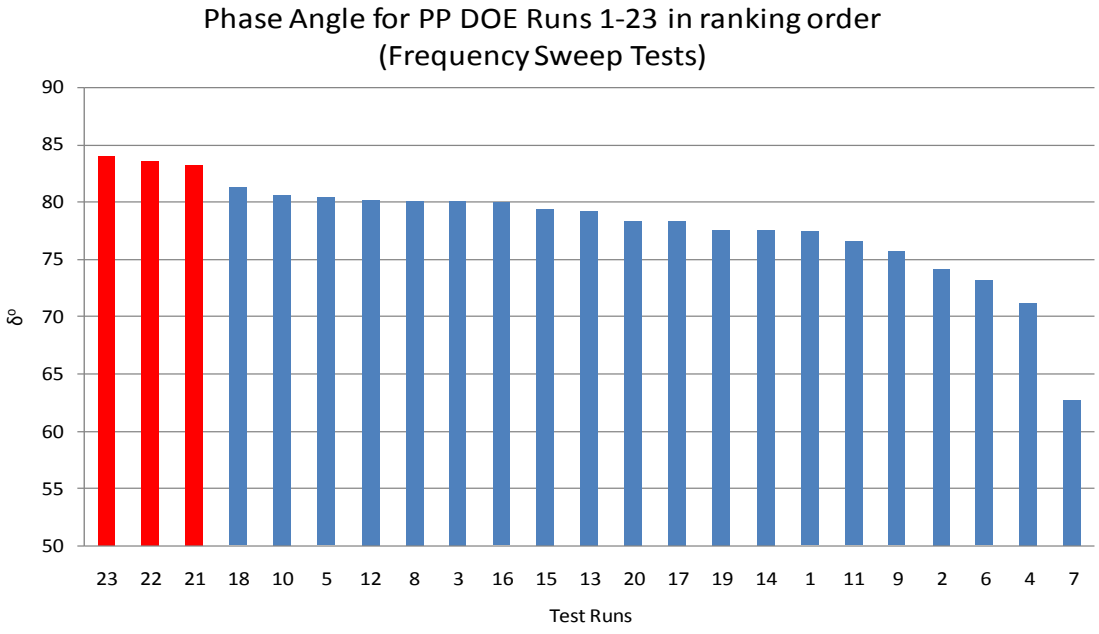

Figure 4.7: δ^{o}organised in descending order for FS

Creep & Recovery (CR) Tests

The creep and recovery tests were undertaken to distinguish the elastic properties of the materials in relationship to time. The creep conditions were fixed for a time period of 30 sec at a fixed stress of 10MPa and were followed by a relaxation time of 180 sec. Figure 4.8 shows the characteristics of the samples showing variation in creep compliance as depicted in Figures 4.8, 4.9 and 4.10. We note significant change in compliance but apparently little change in the recovery aspect. Interestingly however a similar ranking in performance of the various runs is observed as was with the Amplitude Sweep and Frequency Sweep tests. Again RO4 and RO6 show the lowest creep values as would be expected with high clay loading (stiffer material) and the control runs including run 5 being at the high end.

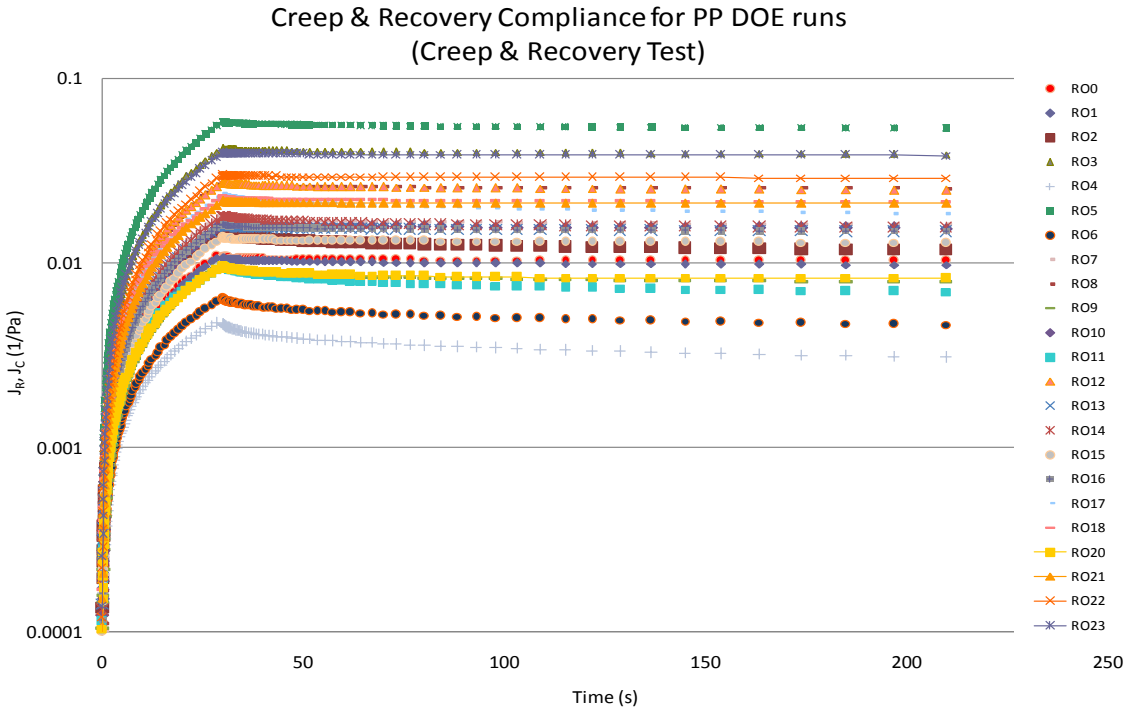

Figure 4.8: Creep & Recovery vs. Time

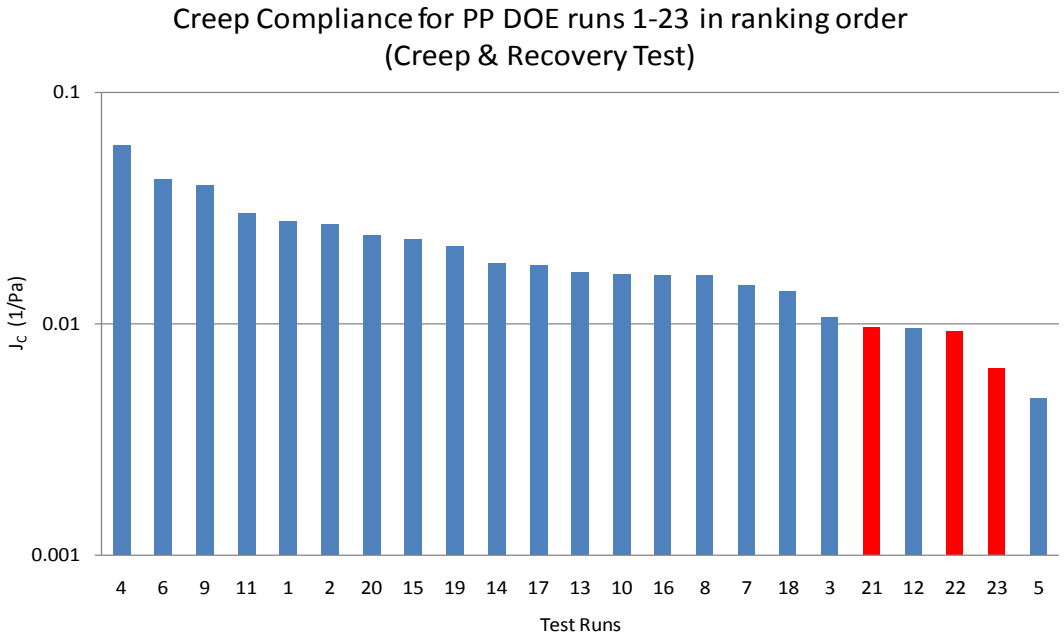

Figure 4.9: Creep tests in descending order

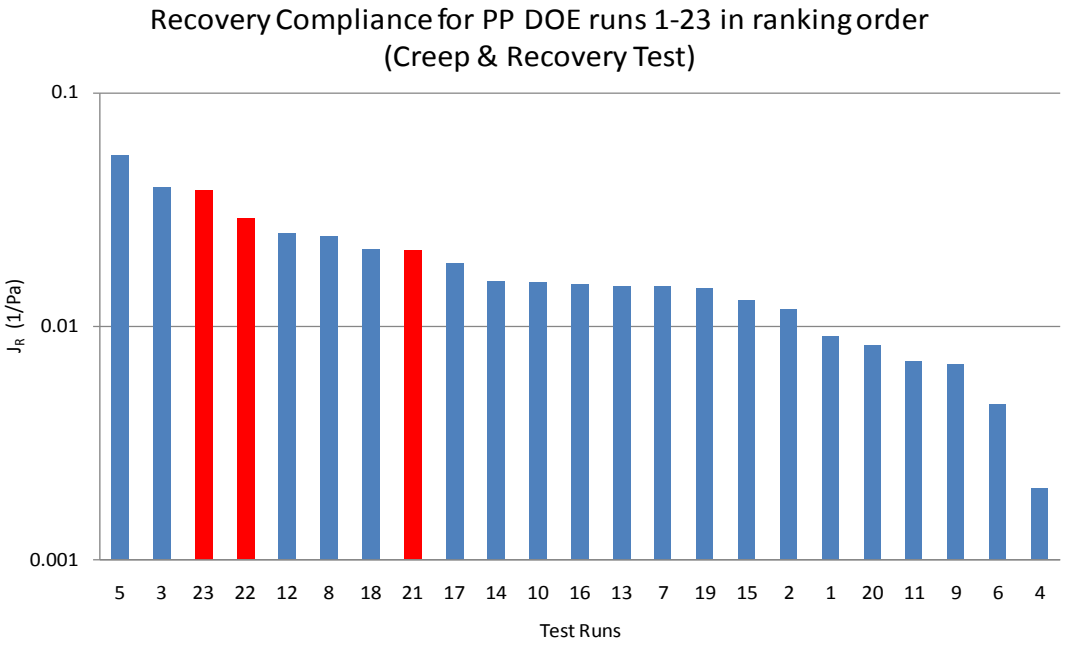

Figure 4.10: Recovery tests in descending order

Conclusions

Rheological testing has revealed that the nanocomposites produced at different conditions in the minimixer were distinguishable. Consistently, the various rheological methods of Amplitude Sweep, Frequency Sweep and Creep and Recovery, gave consistent ranking as to the best (RO4, RO6, RO9) and worst performers (RO5 together with the control runs at % clay, RO21, RO22, RO23).

In order to complement the work and validate the rheological approach, results from other testing methods (mechanical and microscopic) are now presented.

4.2.2 Mechanical Properties of the Nanocomposites Obtained[1]

These included the tensile modulus, tensile strength and elongation, all of which are shown in Figures 4.11-4.13. The runs with 0 % clays are seen to display consistently lower tensile modulus but higher strength and elongation. The addition of clay increased the modulus of PP up to a maximum of 32%. Interestingly and consistent with the rheological characterisation, RO4 was observed as performing highest in the tensile modulus, closely followed by RO9 and RO6 when we take experimental errors in consideration. This suggests that rheological characterisation which is relatively less laborious and less prone to experimental errors is a powerful tool in establishing and ranking the various states of nanocomposites.

What is also evident from these graphs is that the middle order ranking of the DOE samples is quite unclear due to the number of factors used so no firm discussions can be reached on these.

[1] This research was carried out in collaboration with Queens University Belfast as stated in the Introduction. In this part of the work, I prepared the DOE samples and performed the rheology. Colleagues at QUB then performed the mechanical and microscopic observations.

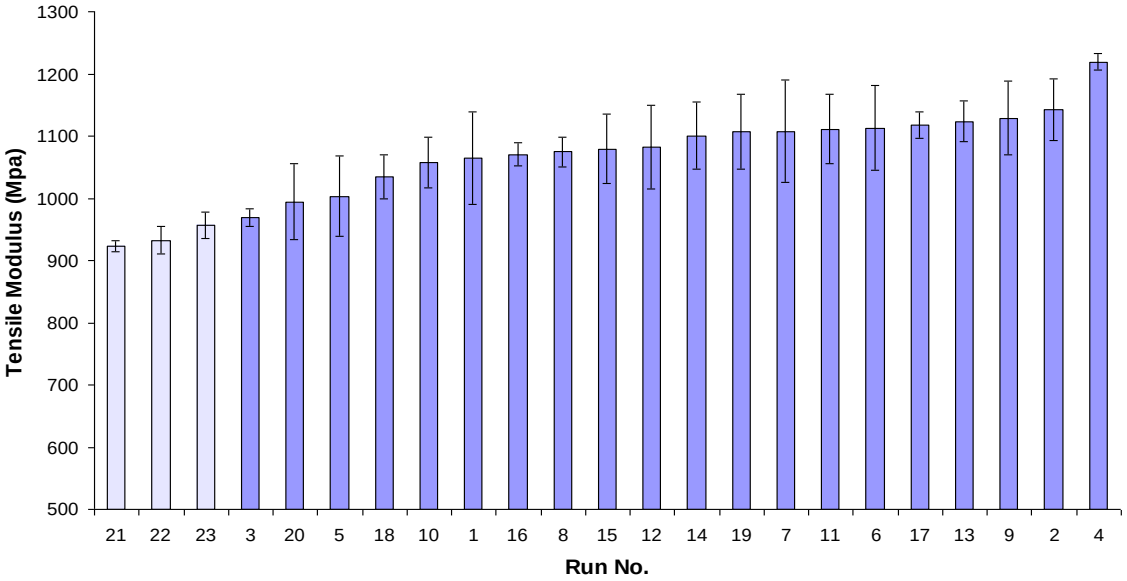

Figure 4.11: Tensile modulus of DOE runs in ascending order

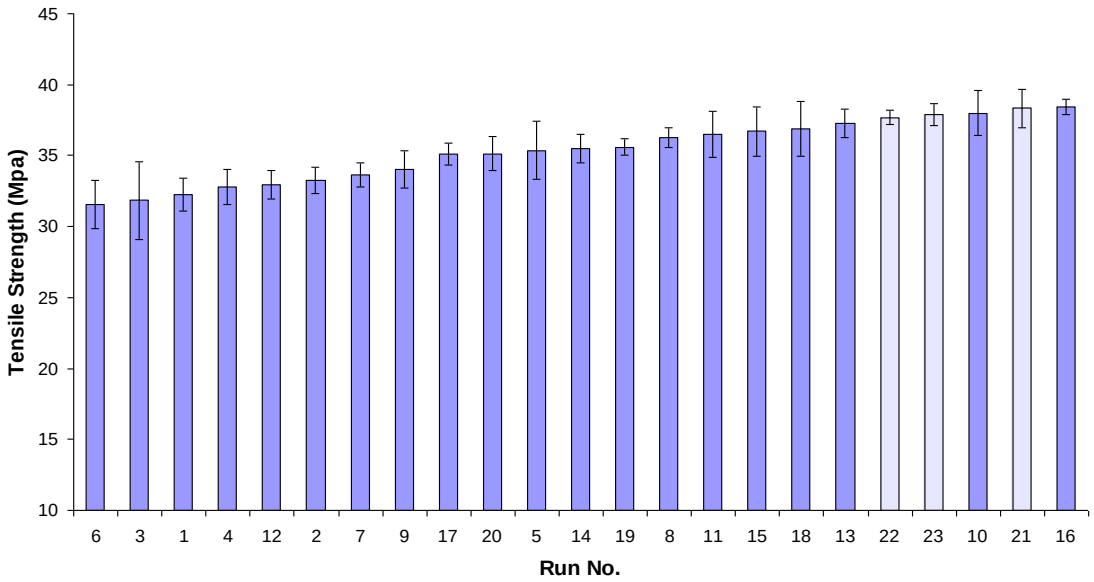

Figure 4.12: Tensile strength of DOE runs in ascending order

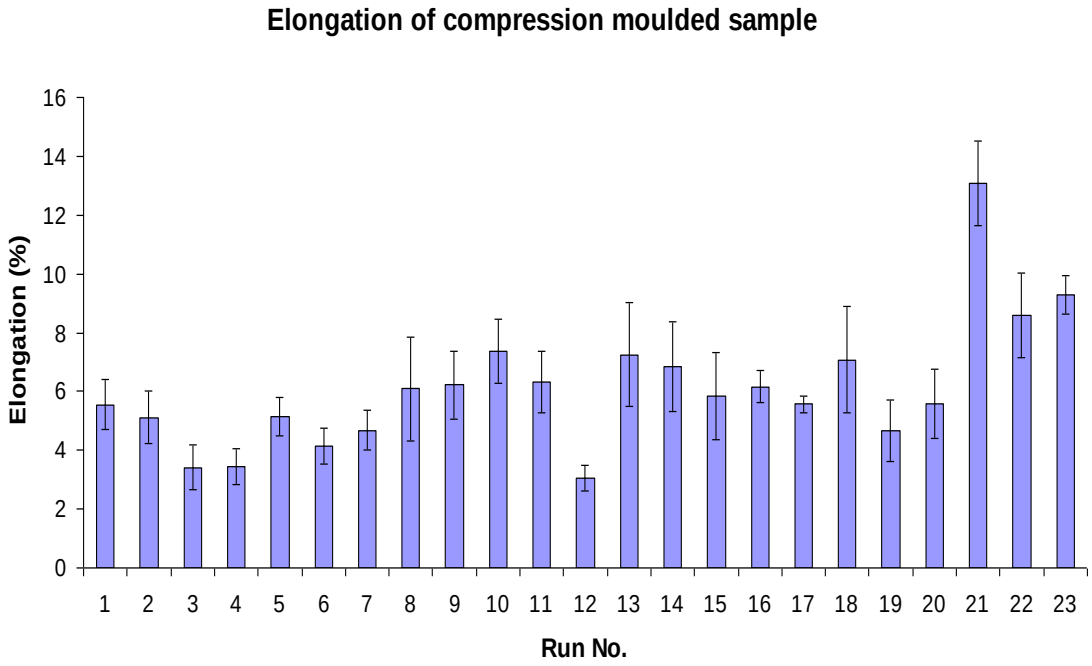

Figure 4.13: Mechanical properties of compression moulded samples

4.2.3 Microscopic Evaluation of the Nanocomposites Obtained[2]

Introduction

In order to guide the microscopic observations, an evaluation of all the samples from Table 4.3 shows that the temperature and clay loading contributed the most to the changes observed in rheological and mechanical properties. The most commonly occurring factor levels were 20rpm, residence time of either 2 or 8 minutes, 190^{o}C, 6% clay content, 6% compatibiliser content and an MFI of 10.5. Consequently, RO1, 2, 4 and 6 and RO7, 9, 12 and 14 were chosen for observation to reflect this. Figure 4.14 shows images obtained from TEM. It is evident from these images that RO4 and RO6 are the best performers.

[2] This research was carried out in collaboration with Queens University Belfast as stated in the Introduction. In this part of the work, I prepared the DOE samples and performed the rheology. Colleagues at QUB then performed the mechanical and microscopic observations.

However, this basis has to be quantified further in order to provide number ranking rather that broad observational ranking.

Table 4.3: DoE outcomes – responses

	Speed (rpm)	**Residence Time (Min)**	**Temperature (DegC)**	**Nanoclay Loading (%)**	**Compatibiliser Loading (%)**	**Polymer MFI (g/10min)**
E_{DMTA}	20	8	n/a	2	2	10.5
$\sigma_{Tensile}$	n/a	2	190	2	n/a	n/a
$E_{Tensile}$	n/a	2	190	6	6	10.5
$\varepsilon_{Tensile}$	20	8	n/a	6	2	8
η^*	n/a	n/a	190	6	6	n/a
G'	n/a	n/a	190	6	6	n/a
G''	n/a	n/a	190	6	6	n/a
$\%_{aggl}$	60	n/a	190	n/a	n/a	10.5

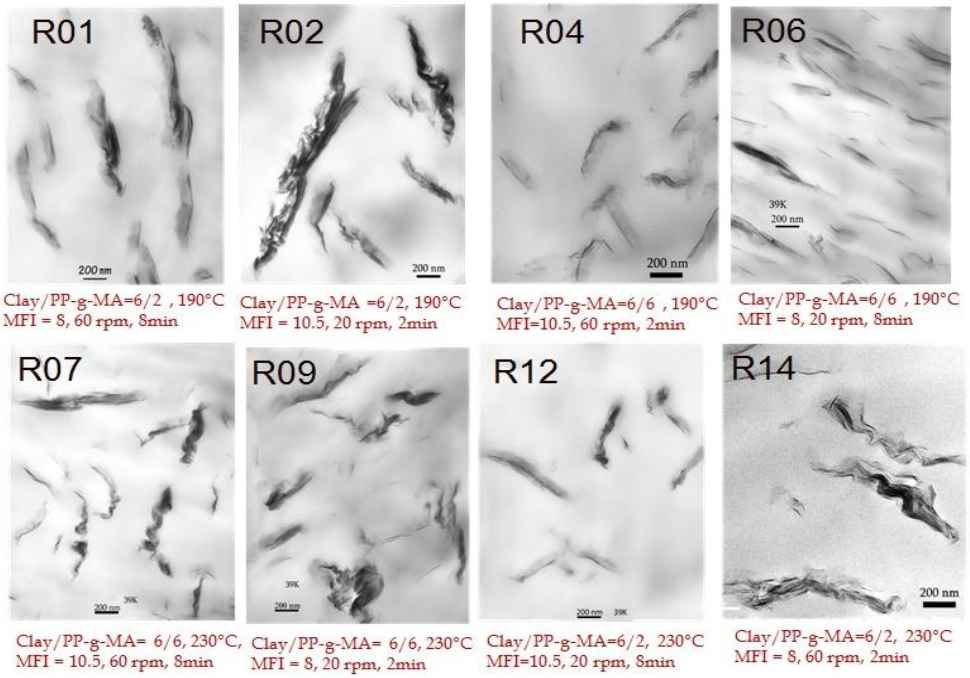

Figure 4.14: TEM images of various DOE runs

4.3 Rheological Evaluation at Optimum DOE conditions

Having established the optimum conditions of the minimixer, in particular the critical role of temperature, further rheological evaluation was now conducted but all at the optimum temperature of 190^{o}C. What was now being assessed systematically was the effect of changing the % clay loading keeping all other mini-mixer parameters constant and optimum as obtained from the DOE programme. This was carried for clay loading in the range 0-10% at 1% increment using again Amplitude Sweep, Frequency Sweep and Creep-Recovery tests starting in the appropriate Linear Viscoelastic Region (LVR). The results are shown in Figures 4.15-20. They show interestingly regions of significant change when the % clay is increased above 5% suggesting this as being the critical concentration. In order to evaluate this further, mechanical property testing was carried out as was done in

the DOE programme. The results are shown in Figures 4.21-22 again showing criticality near 5% clay addition. In addition to this, microscopic observations were also carried out using a high resolution field-emission scanning electron microscopy (SEM) with a maximum magnification of 5,000. An energy dispersive X-ray spectrometer (EDX) using an acceleration voltage of 15 kV and magnification of 5000× was used for elemental analysis purpose in order to confirm the appearance of Cloisite 20A nanoparticles. The samples were initially freeze dried using liquid nitrogen and broken into small pieces. They were then sputter coated with thin gold film and placed in a stub with silver paint for ground. The fracture surface of the samples were analysed at different magnifications and the observations are as shown in Figures 4.23-4.24. It is slightly unclear from these images to derive if good mixing has taken place of the nanoclay and polymer but they do show a good distribution of the platelets. However in order to zoom in further into the clay dispersion to observe and measure intercalation and exfoliation, TEM examination is necessary but was not in the scope of this research.

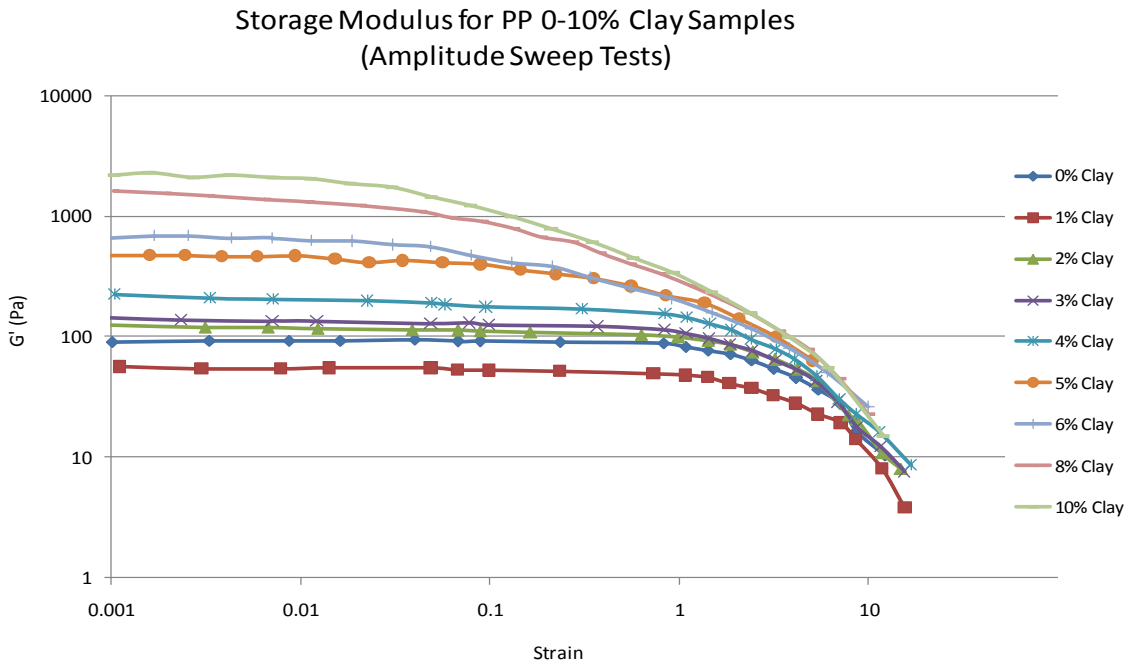

Figure 4.15: G' vs. Strain rate from AS test at 190°C and clay loading 0-10%

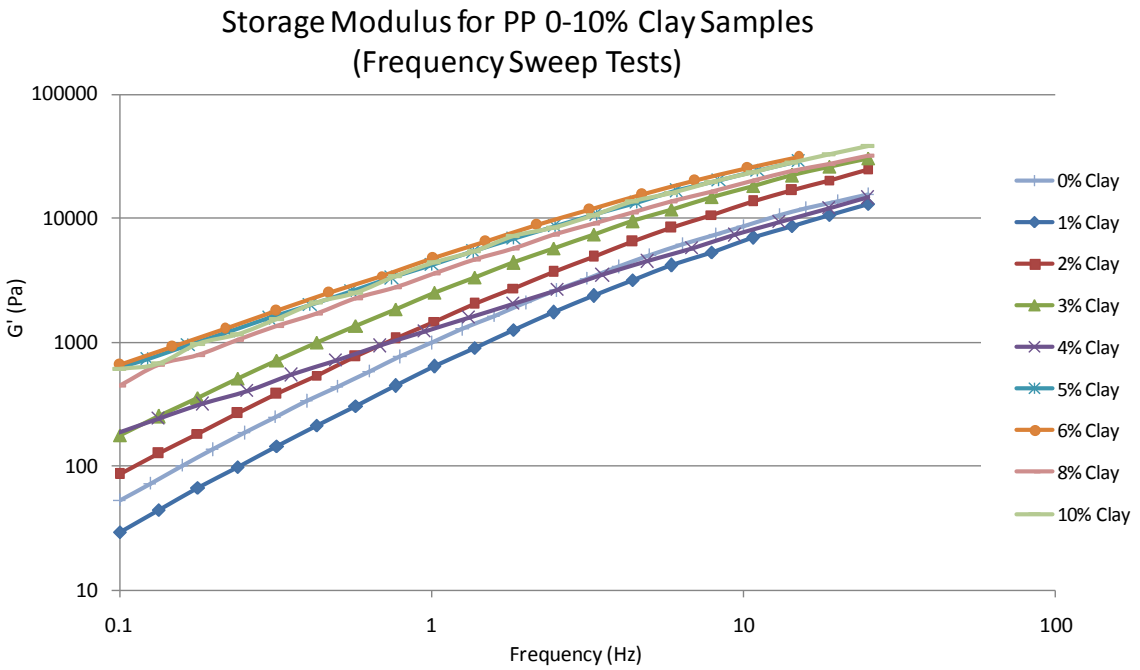

Figure 4.16: G' vs. Frequency from FS test at 190°C and clay loading 0-10%

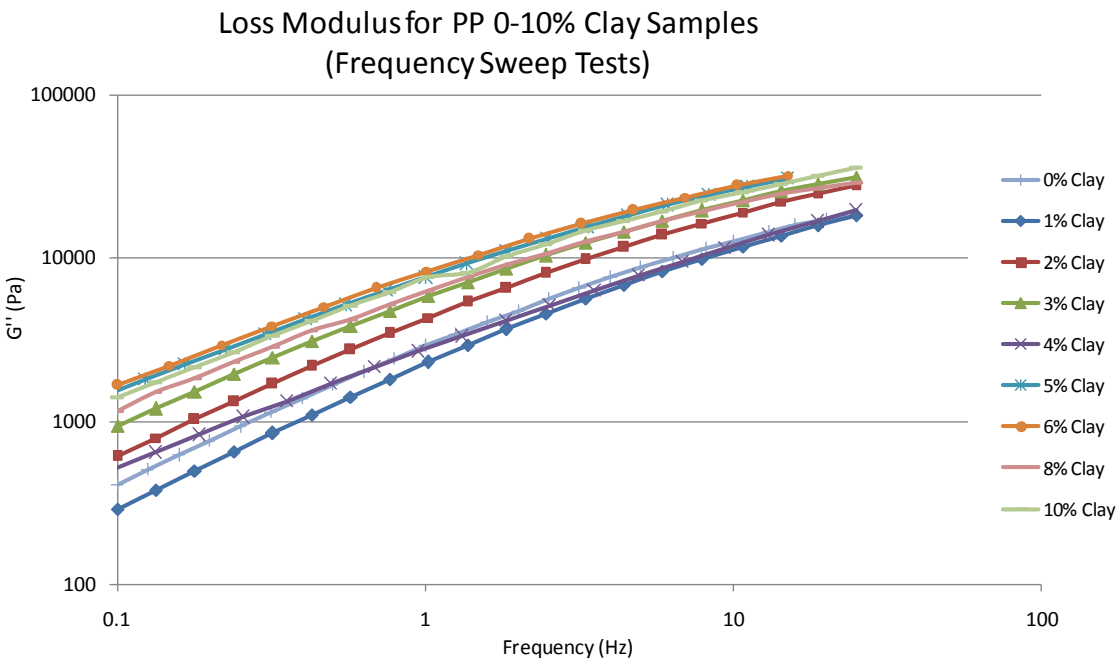

Figure 4.17: G'' vs. Frequency from FS test

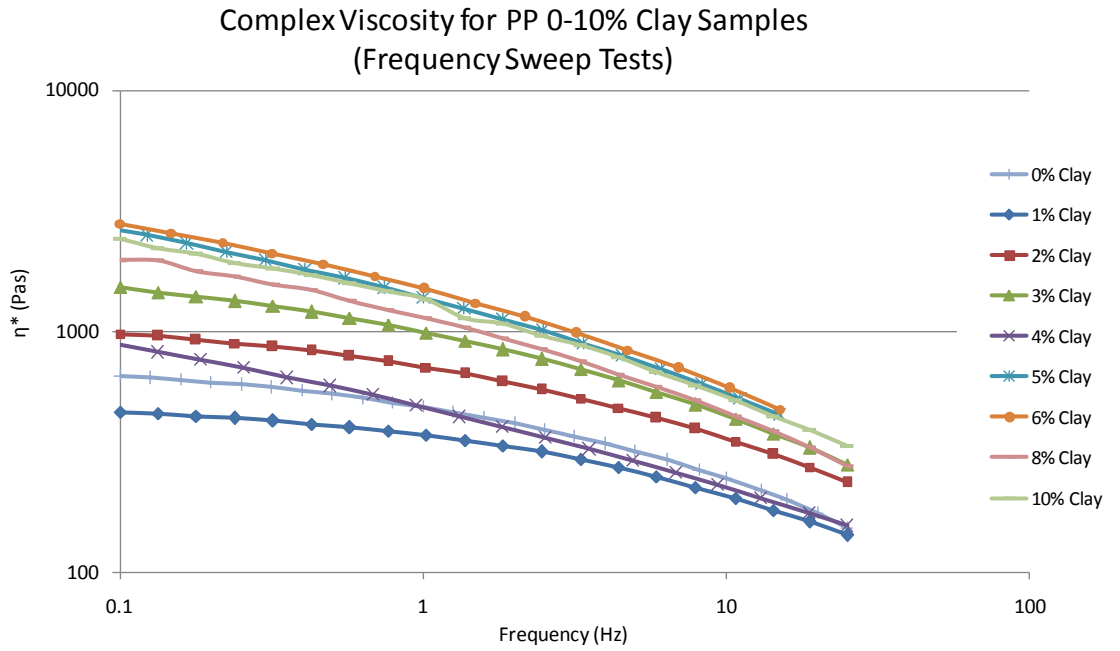

Figure 4.18: η* vs. Frequency from FS test

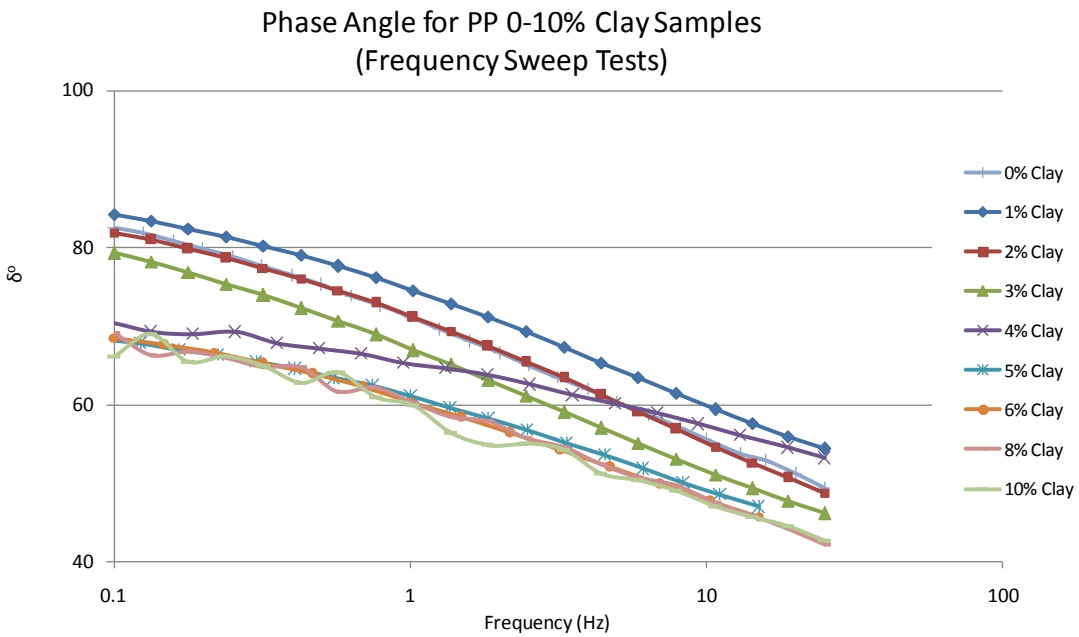

Figure 4.19: δ^{o} vs. Frequency from FS test

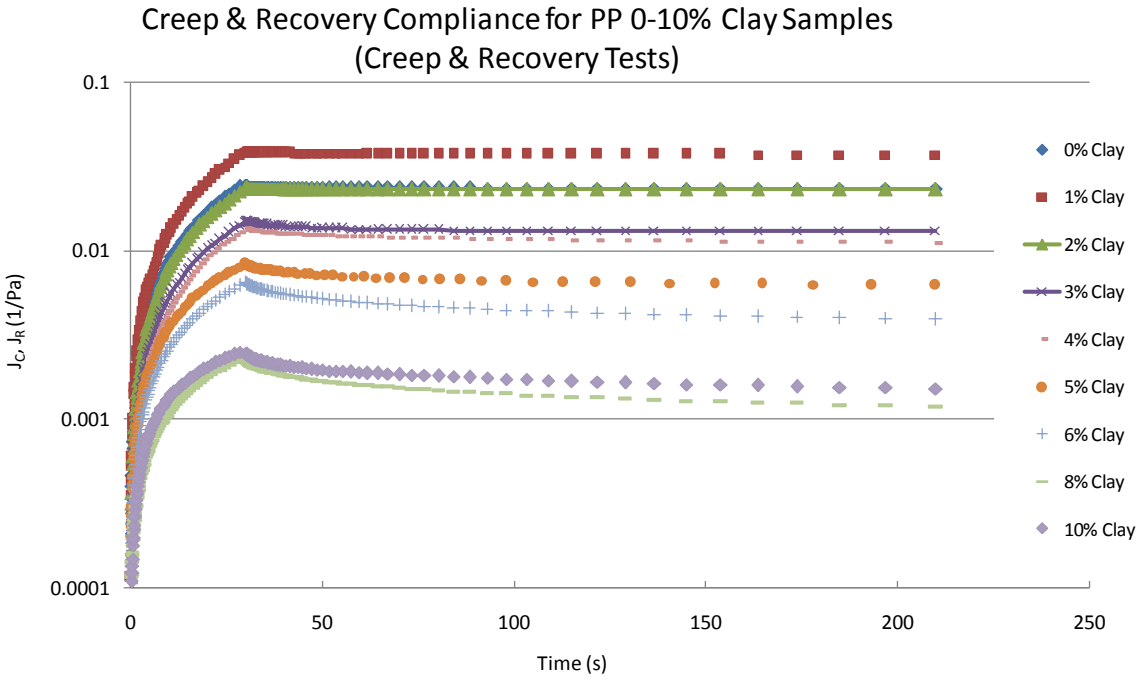

Figure 4.20: J_C& J_R vs. Time from CR test and clay loading 0-10%

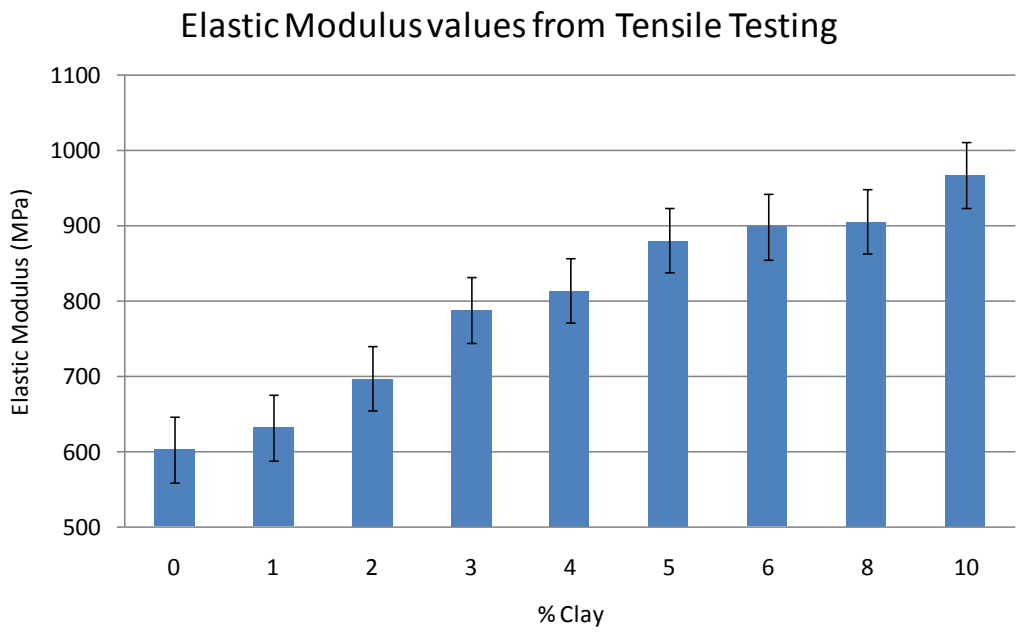

Figure 4.21: E' vs. % clay for PP

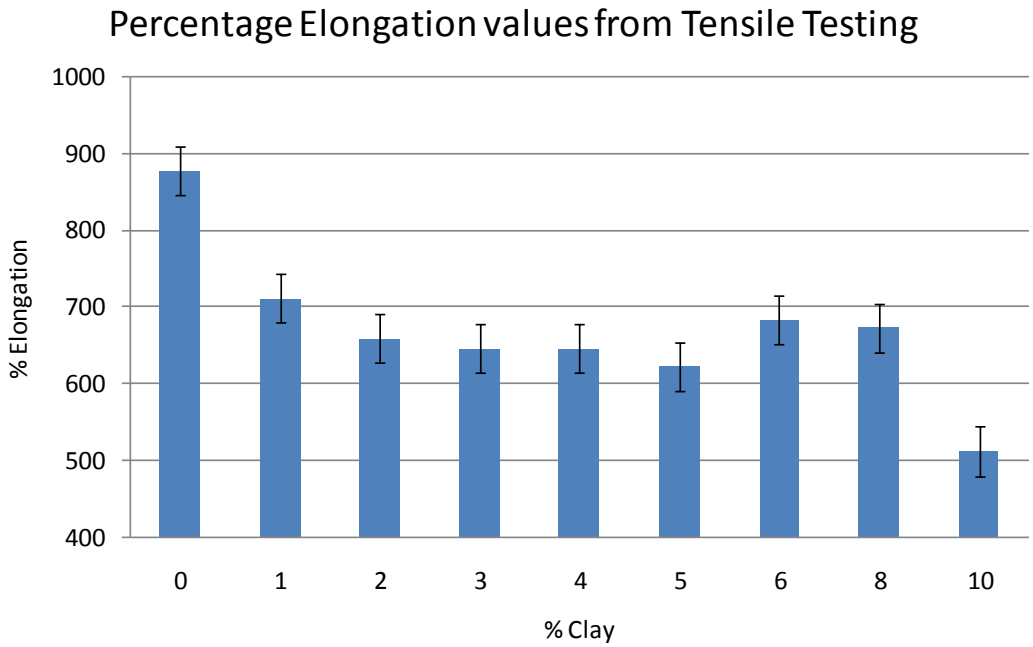

Figure 4.22: % Elongation vs. % clay for PP

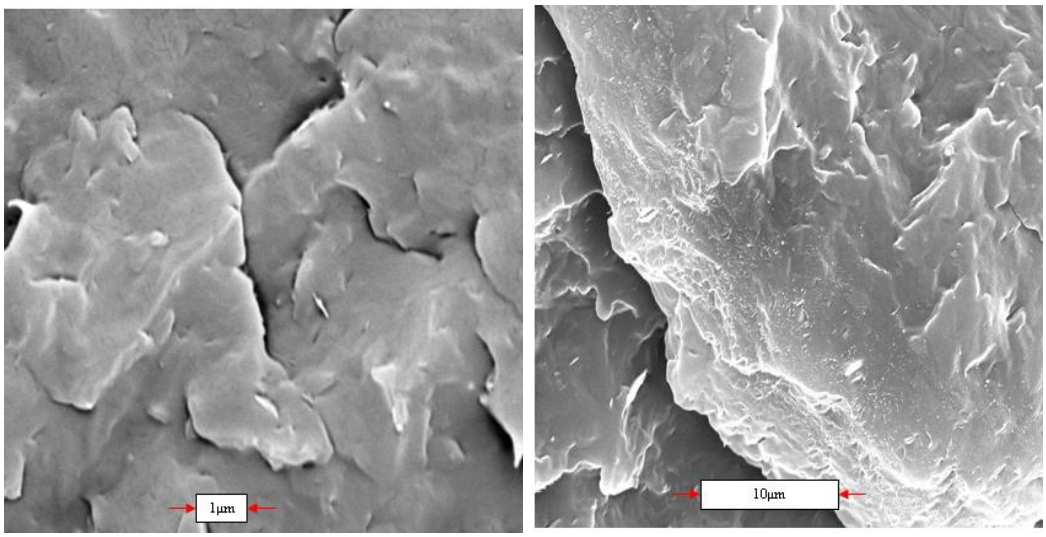

Figure 4.23: SEM images of fracture surface for 1% clay

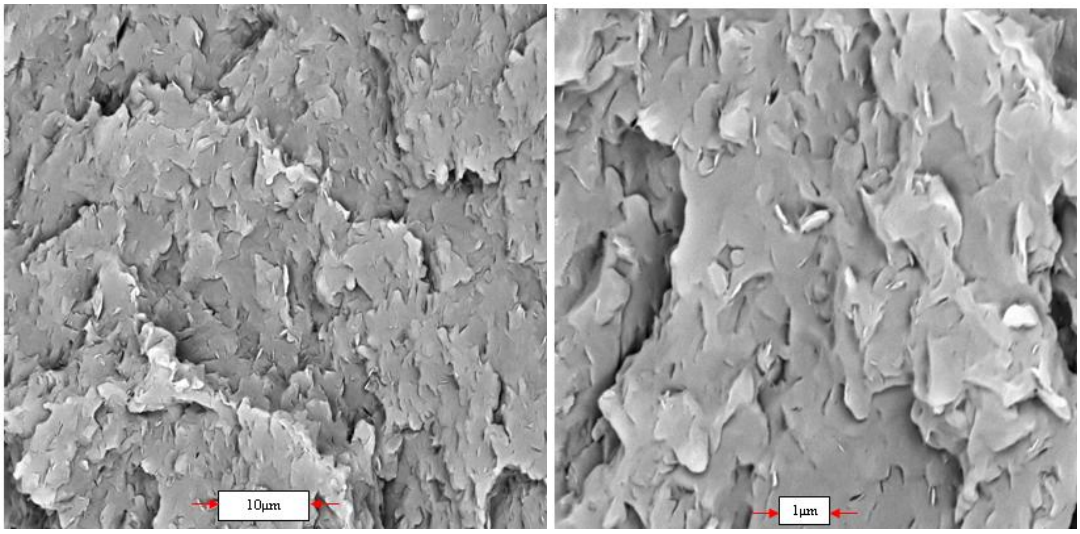

Figure 4.24: SEM images of fracture surface for 6% clay

4.4 Effect of Stretching on Nanocomposites

Having established from the DOE programme the ideal conditions required in the minimixer for obtaining the nanocomposite with the optimum properties, the next step as stated in the objectives was to assess the effect of stretching on nano-composition. The

question was to establish if with stretching, any improvements within certain properties could be observed. Here, it is important to note that the interest is not in stretching to achieve orientation but in enhancing intercalation and exfoliation. Consistent with this objective, the evaluation was assessed rheologically with melting after stretching erasing all memory of orientation. The range of conditions here were also 0-10% in 1% increments to compare with the performance in the unstretched state described above. The results are shown in Figures 4.25-41 at various stretch ratios obtained again using Amplitude Sweep, Frequency Sweep and Creep-Recovery tests and making comparison with un-stretched samples. The data were, as before, complemented with mechanical properties evaluation (see Figures 4.42-47) to validate the link between rheology and structure. Additionally, crystallinity of all the samples was also measured (0-10% clay in the un-stretched and stretched modes). As indicated in Table 4.4 and Figure 4.48, these show % crystallinity to reduce as the % clay addition increases. The stretched samples show only small differences.

The conclusions from these figures are as follows:

Conclusions from Rheological Tests

- At stretch ratio of 2:1, now 4% instead of 5% becomes the critical addition level as indicated in Figure 4.25 with G' attaining a value of 1000 Pa.
- Increasing the stretch ratio further to 4:1 shifts the G' values of all the samples. Now G'=1000 Pa when the % clay is 3%.
- Comparing the G' obtained in the non-stretched PP with the stretched PP at 2:1 and 4:1 (see Figure 4.27) shows clearly the significant (up to 10 fold increase) added

effect of stretching which is presumed here to have occurred as a result of further intercalation / exfoliation.

- The observations above related to the amplitude sweep data but the frequency sweep data also show similar effects (see G'', η^* and δ^0 variation with % clay in the un-stretched and stretched samples).
- Now considering the creep-recovery data in Figures 4.38-39, we observe that the creep decreases as the % clay loading is increased in all cases, un-stretched and stretched PP. However the effect of increasing stretching is to decrease further the creep in comparison with the un-streched sample. Again as indicated from the observation above, the stretching effect has increased the intercalation-exfoliation, as well as the alignment of the clay platelets leading to this reinforcement of structure. As for the recovery element of the test, no major recovery is seen in any sample thus suggesting that the material has a low elastic element to it regardless of clay loading or not. However for the biaxially stretched samples the recovery can be clearly observed from the curves.

Conclusions from Mechanical Properties Tests

- As observed in Figures 4.42-44 which give the variation of elastic modulus and elongation with clay loading, the stretched samples show appreciably a higher tensile modulus. For example at 3% clay loading, the un-stretched sample has a modulus of 780 Pa compared with a modulus of 810 Pa at 2:1 stretch ratio and 900 Pa at 4:1 stretch ratio. Similar variations are observed throughout at all % clay addition, again suggesting the added value of stretching on exfoliation-

intercalation, i.e. on elongational mixing as manifested on the stiffening of the structure.

- As for the elongation data, as shown in Figure 4.45-47, they show again the increased stiffening and reduced elasticity as the % clay and stretching ratio are increased.

Overall Conclusion

The important conclusion from these tests is the beneficial effect of stretching on elongational mixing which leads to enhanced intercalation-exfoliation and alignment of the clay platelets resulting in structural reinforcement of the nano-composites formed. This is an important conclusion from this research and a new finding which can be translated in recommending stretching as a processing step to be added to extrusion to reinforce nano-composites further. Again, it is important to note that this stretching effect is not the "usual" molecular alignment carried in the solid phase to enhance structure. Here stretching is used as a means to enhance elongational mixing. All samples once stretched were melted for rheological evaluation.

It is tempting from this overall conclusion to consider the following processing cycle to manufacture enhanced nanocomposites: extrusion-stretching-extrusion. This was considered in this research and experiments as the one just presented (rheological and mechanical properties evaluation) were conducted. The data obtained (see Figures 4.49-54) confirmed the importance of cycle extrusion-stretching but showed that cycle extrusion-stretching-extrusion leads to poor nanocomposites as indicated by the rheological and mechanical properties data. This can be attributed to degradation but further research is required to investigate this aspect further.

Interestingly and important to the realisation of the aim and objectives of this research is the ability of rheological testing of underpinning performance. In these extrusion-stretching-extrusion tests, rheology was as good as mechanical testing in establishing that the nano-composites formed were comparatively poorer than in the cycle extrusion-stretching.

DATA ON EFFECT OF STRETCHING ON NANO-COMPOSITION

The figures here refer only to the cycle extrusion-stretching

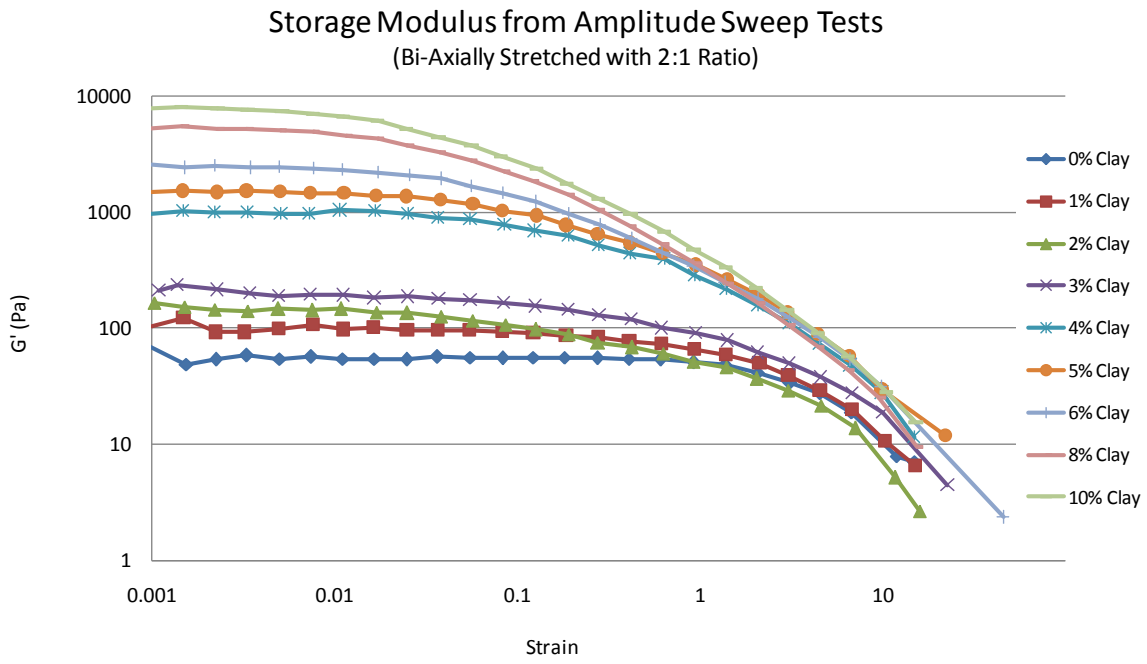

Figure 4.25:G' vs. Strain rate from AS test (2:1)

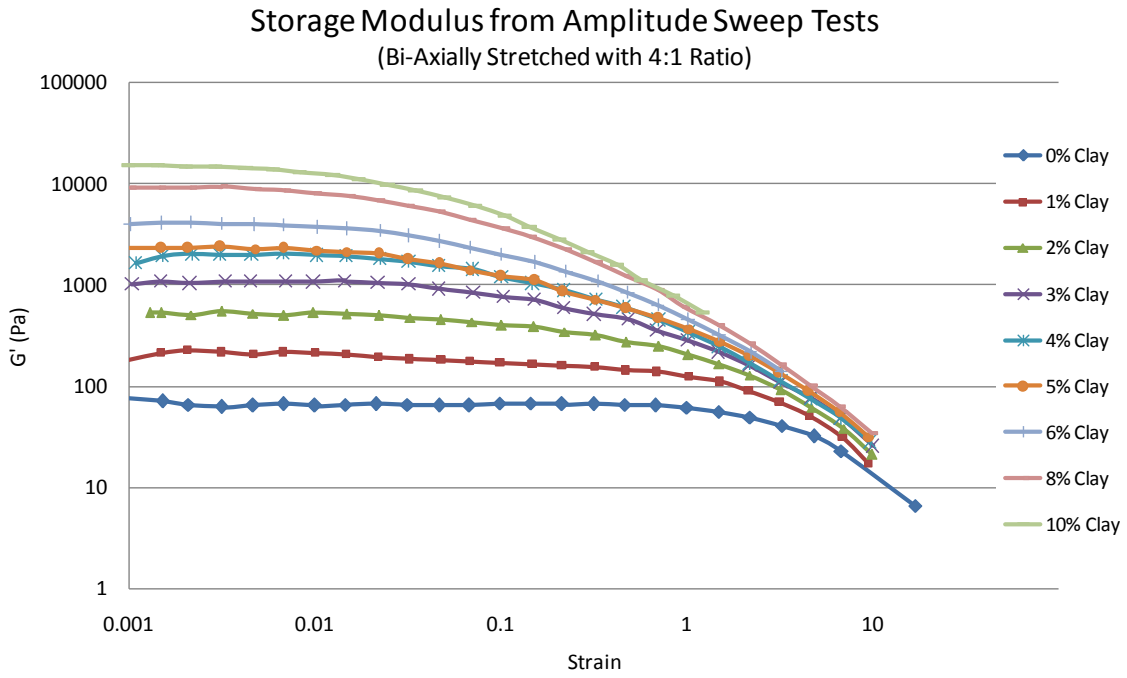

Figure 4.26: G' vs. Strain rate from AS test (4:1)

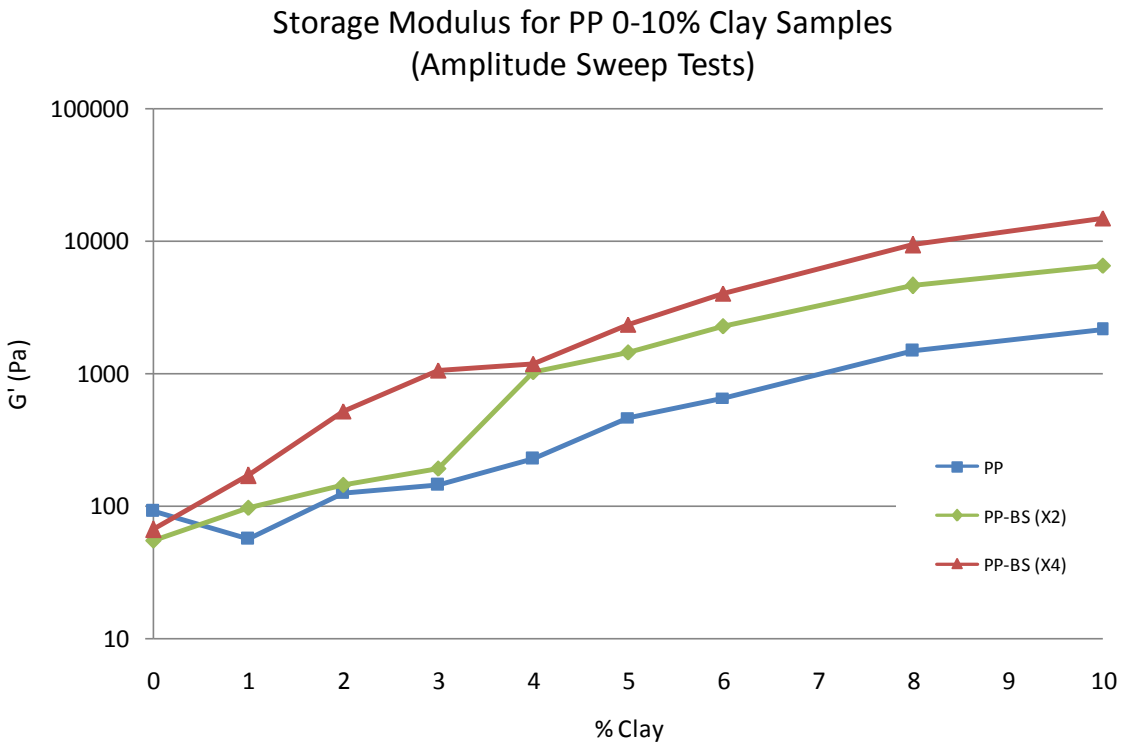

Figure 4.27: AS comparison chart for G'

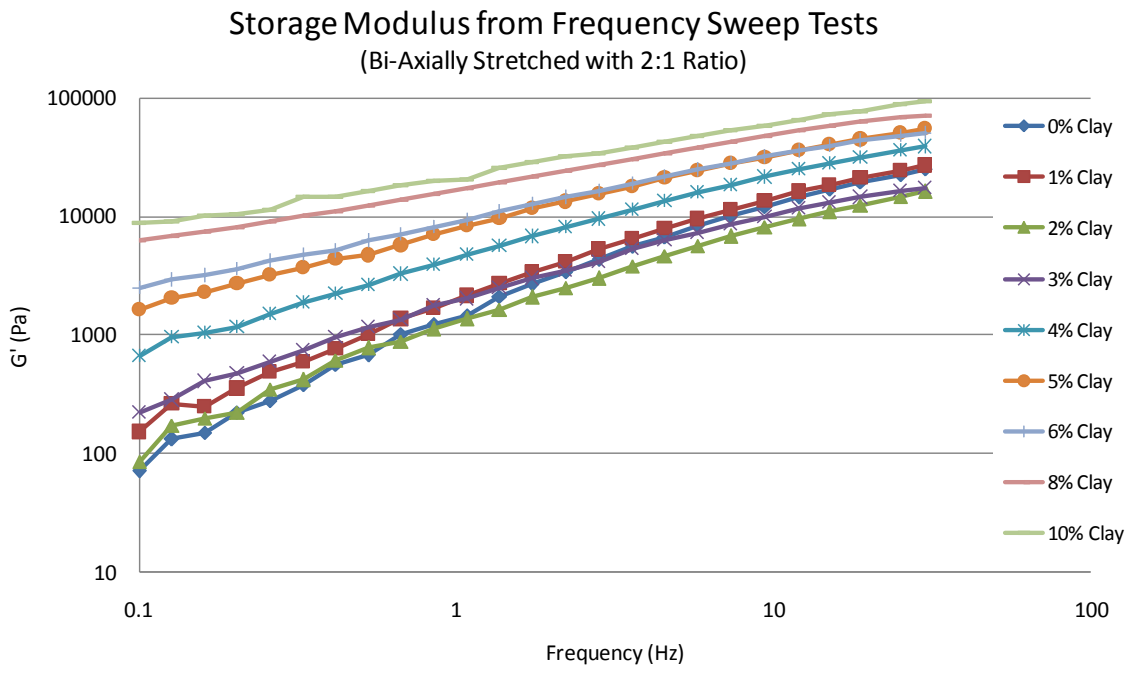

Figure 4.28: G' vs. Frequency from FS test (2:1)

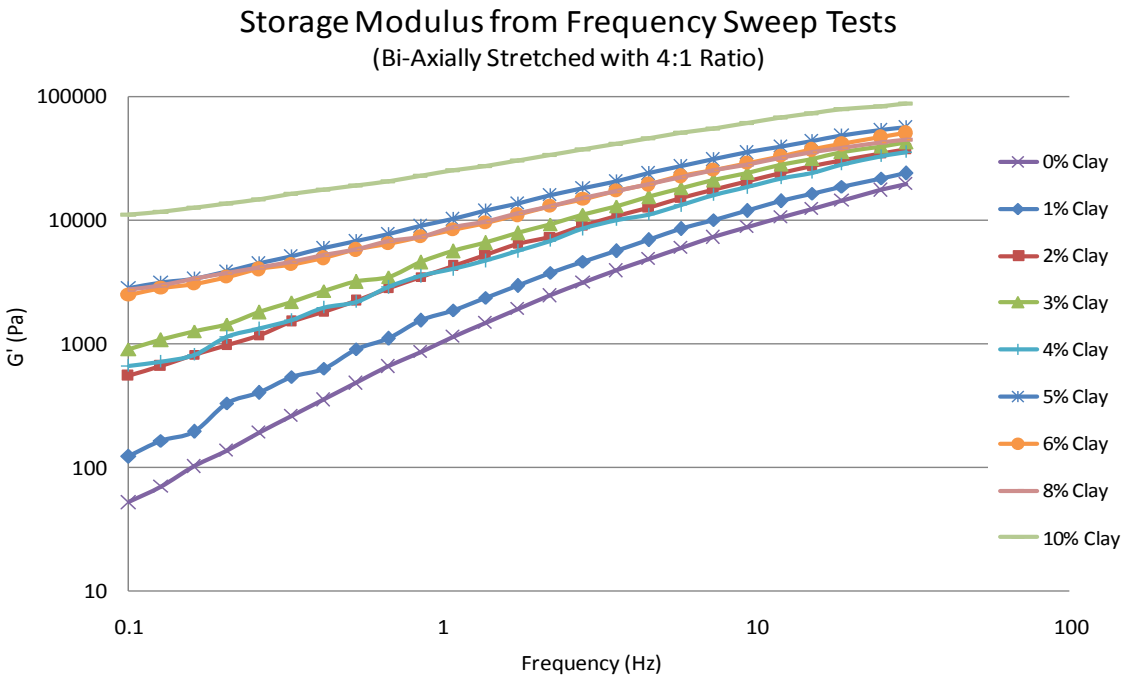

Figure 4.29: G' vs. Frequency from FS test (4:1)

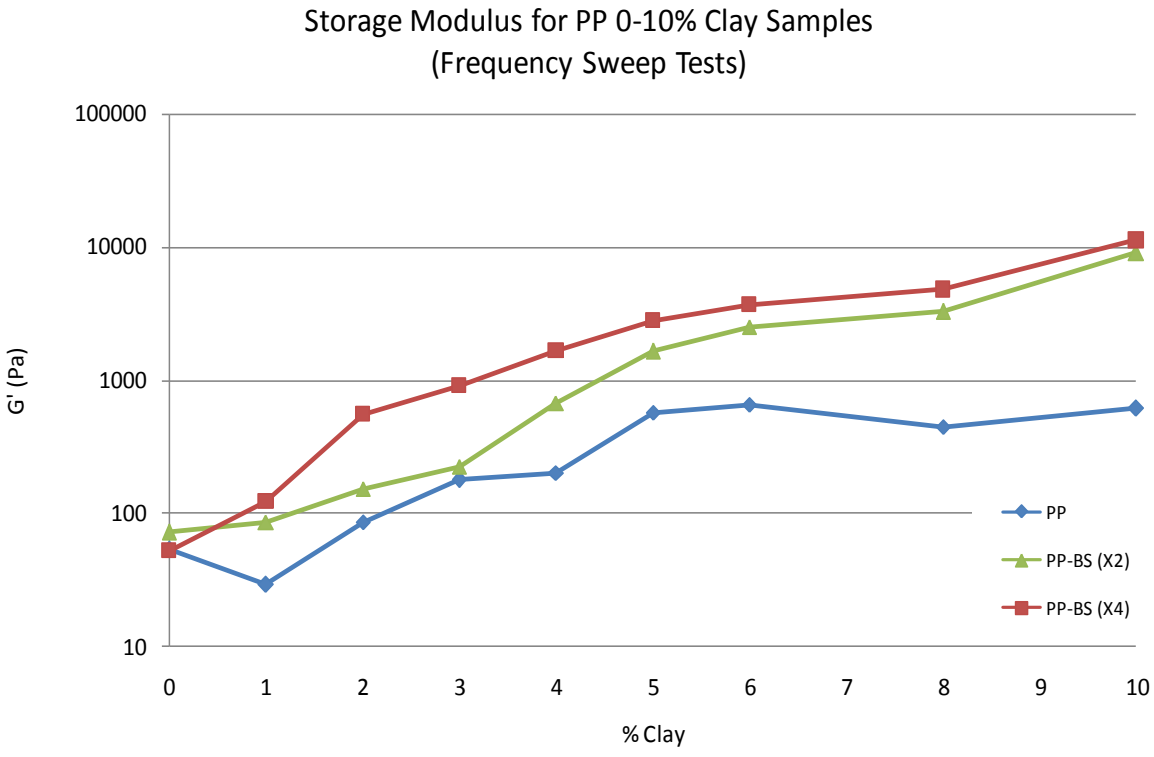

Figure 4.30: FS comparison chart for G'

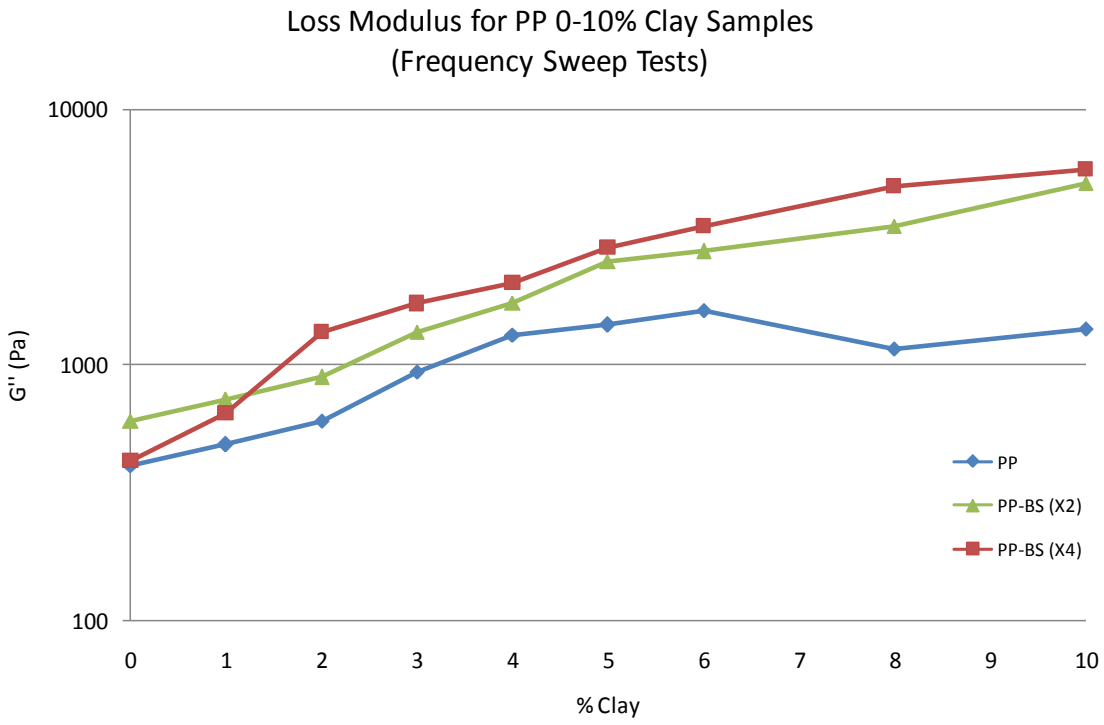

Figure 4.31: FS comparison chart for G''

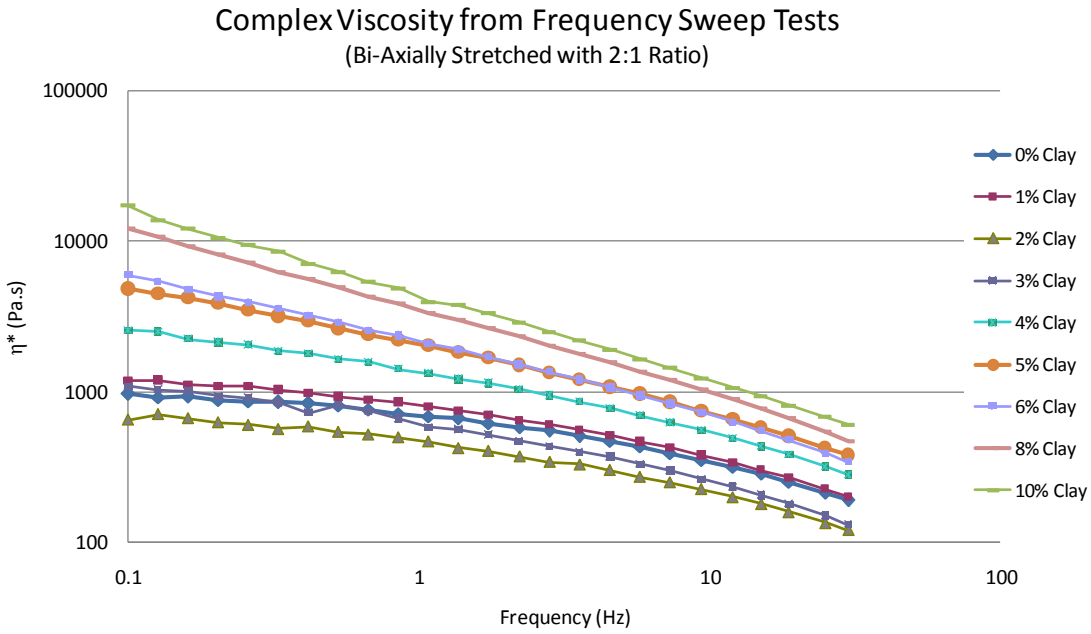

Figure 4.32: η* vs. Frequency from FS test (2:1)

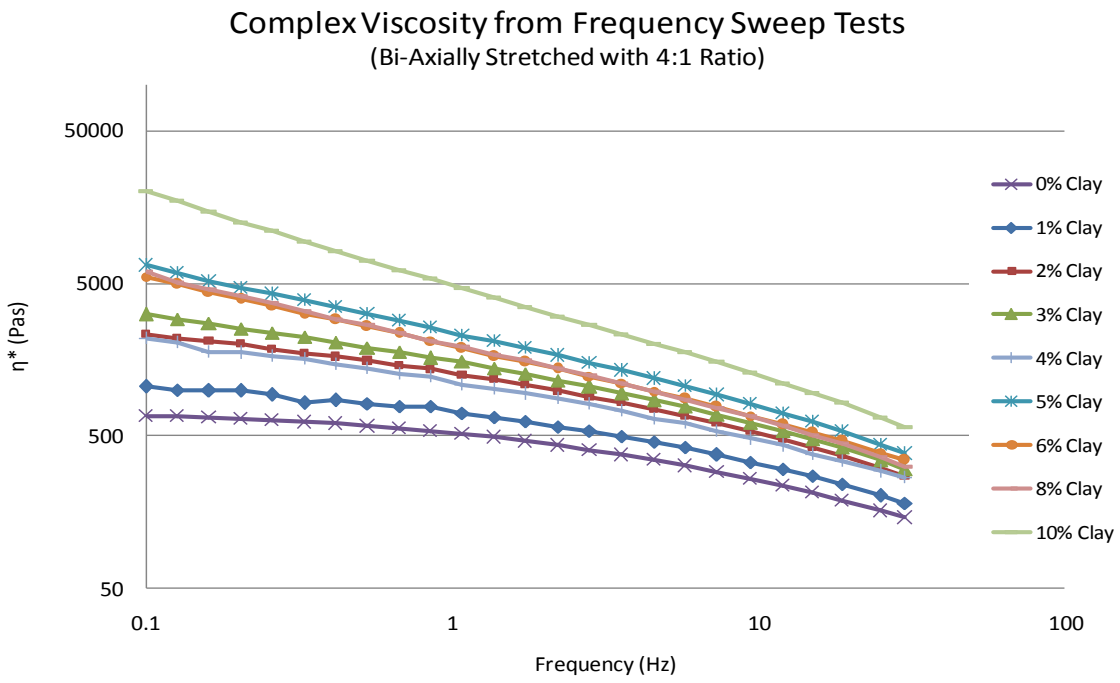

Figure 4.33: η* vs. Frequency from FS test (4:1)

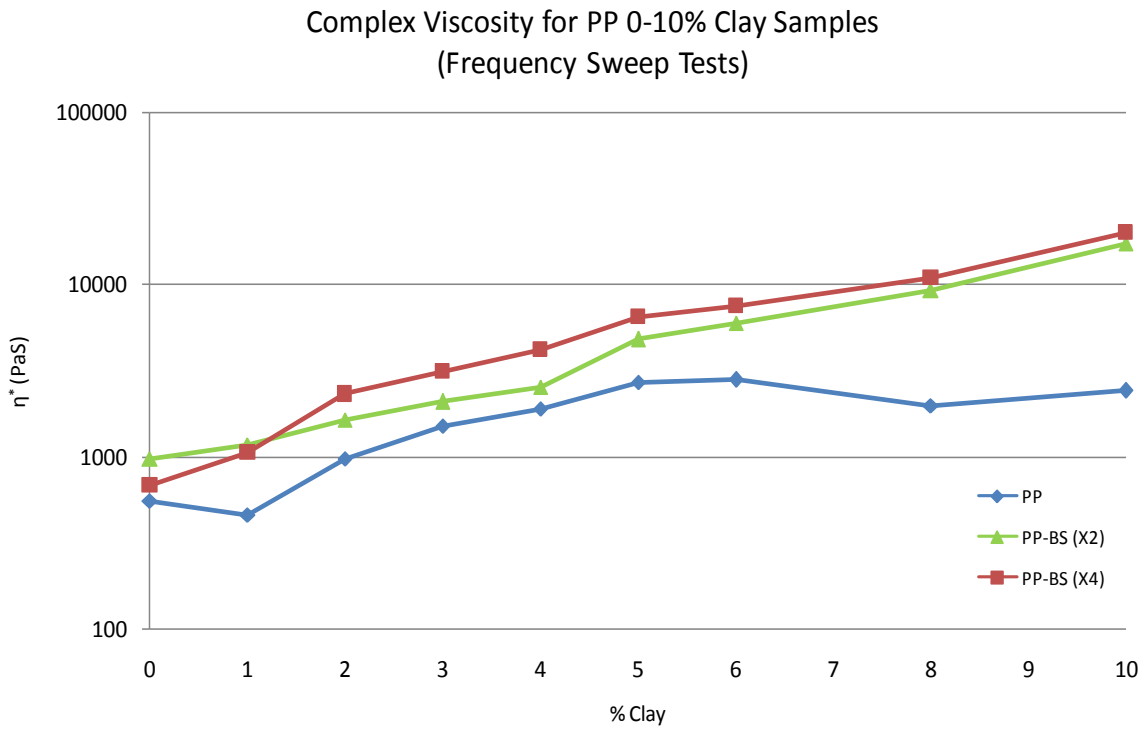

Figure 4.34: FS comparison chart for η*

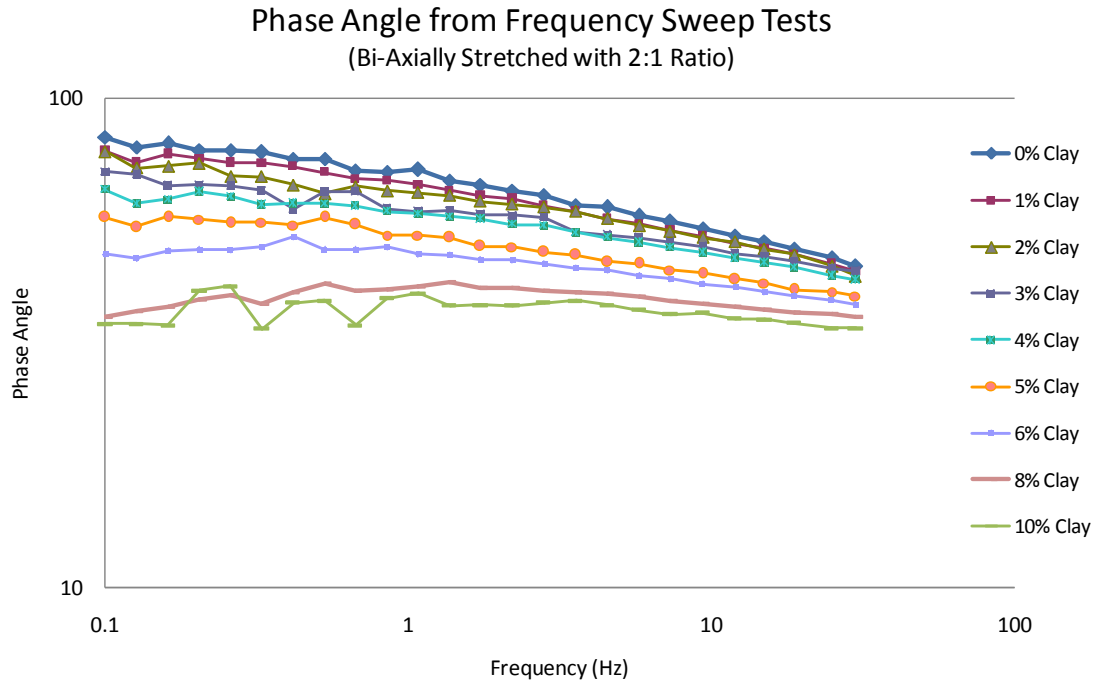

Figure 4.35: δ^o vs. Frequency from FS test (2:1)

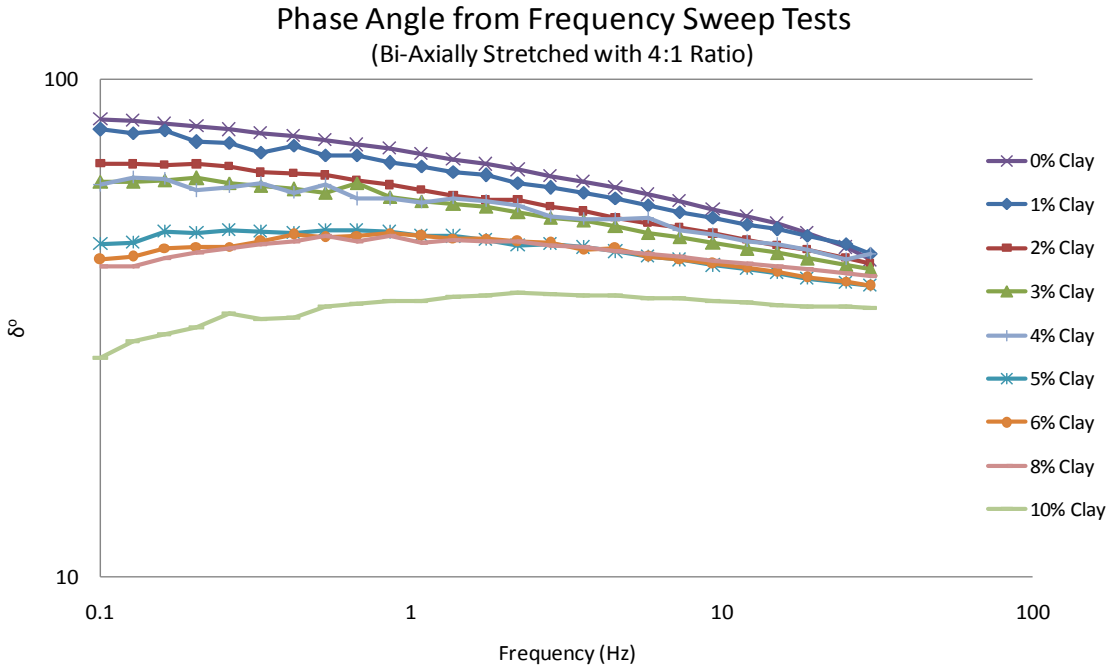

Figure 4.36: δ^o vs. Frequency from FS test (4:1)

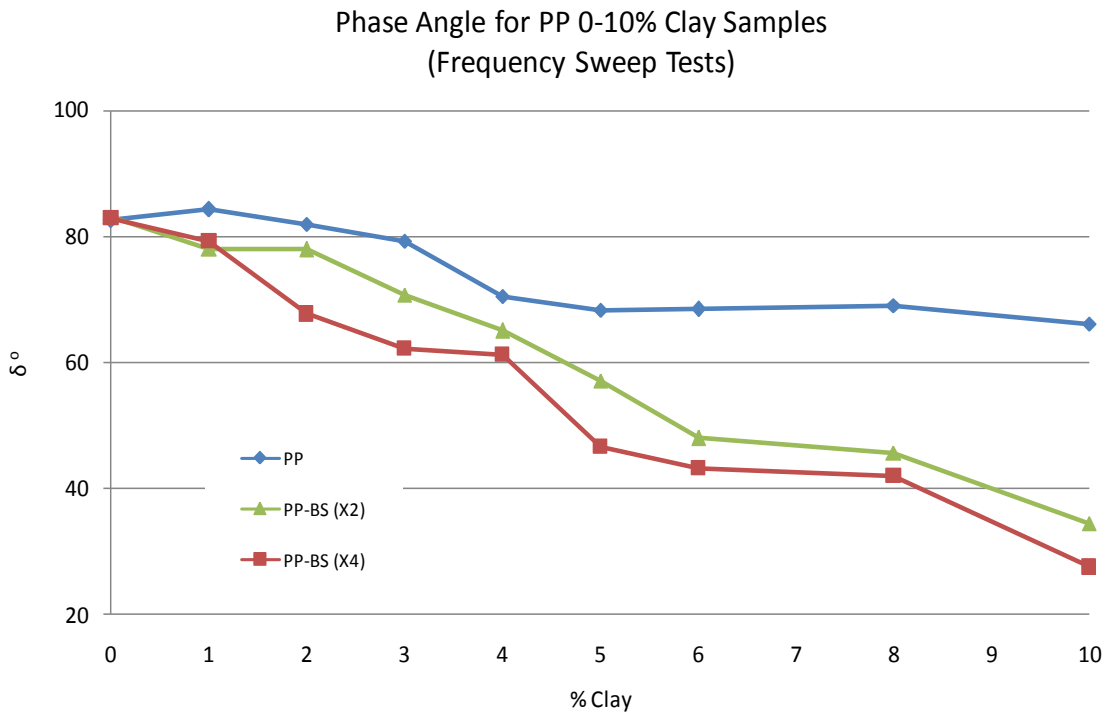

Figure 4.37: FS comparison chart for δ^{o}

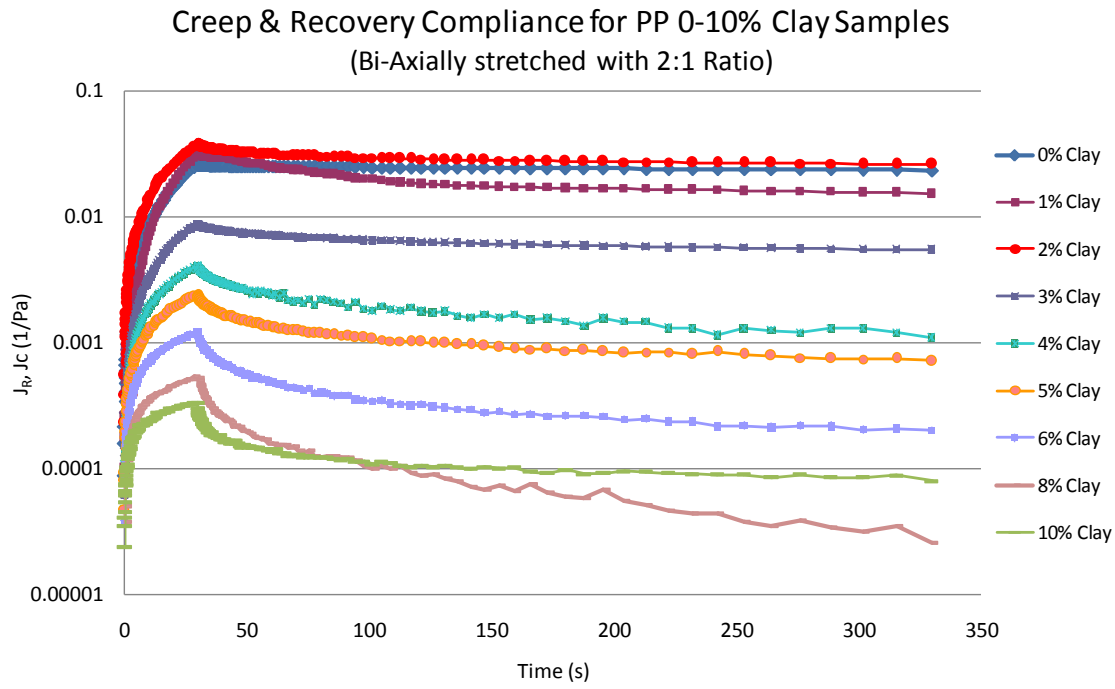

Figure 4.38: J_C& J_R vs. Time from CR test (2:1)

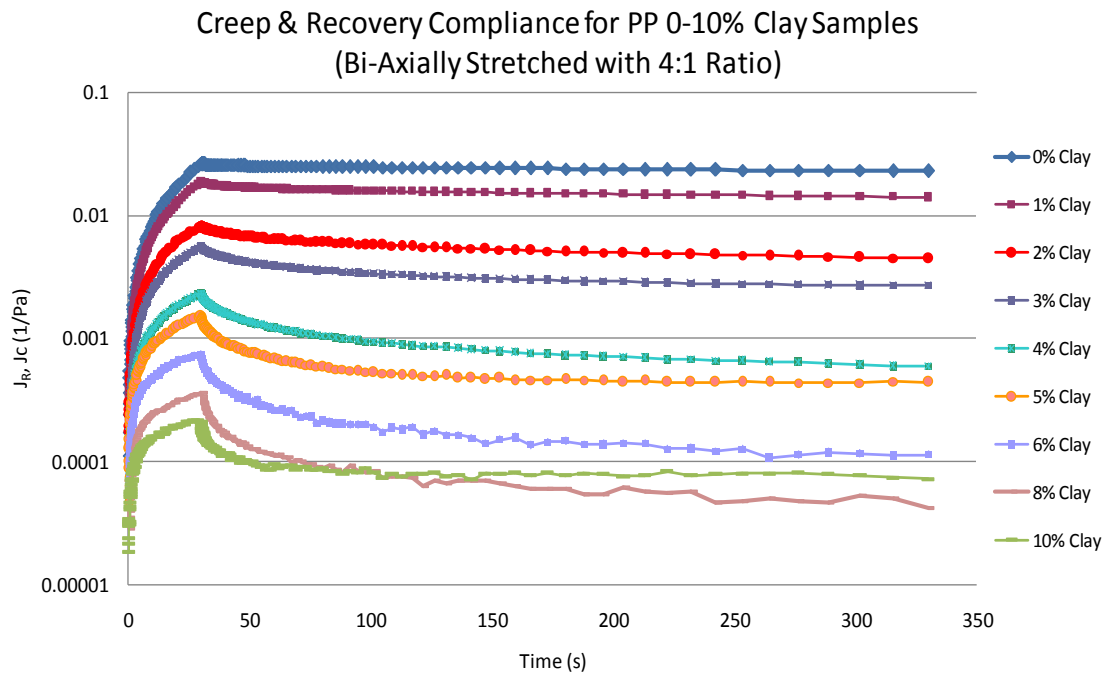

Figure 4.39: J_C& J_R vs. Time from CR test (4:1)

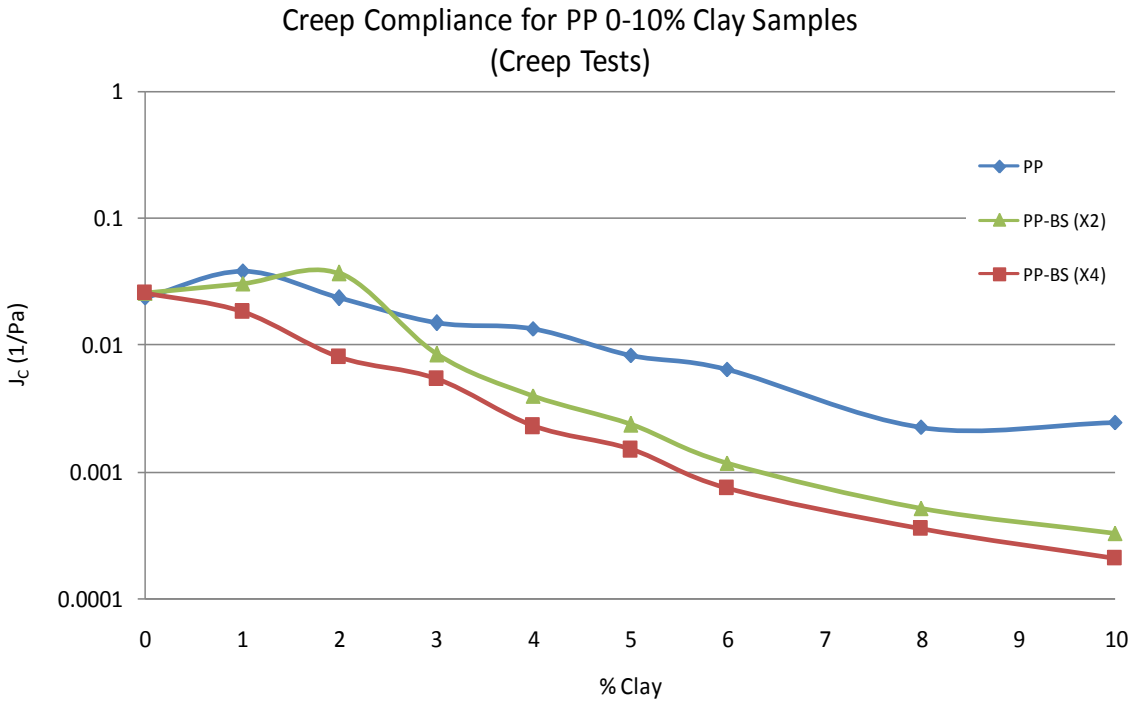

Figure 4.40: Creep tests comparison chart

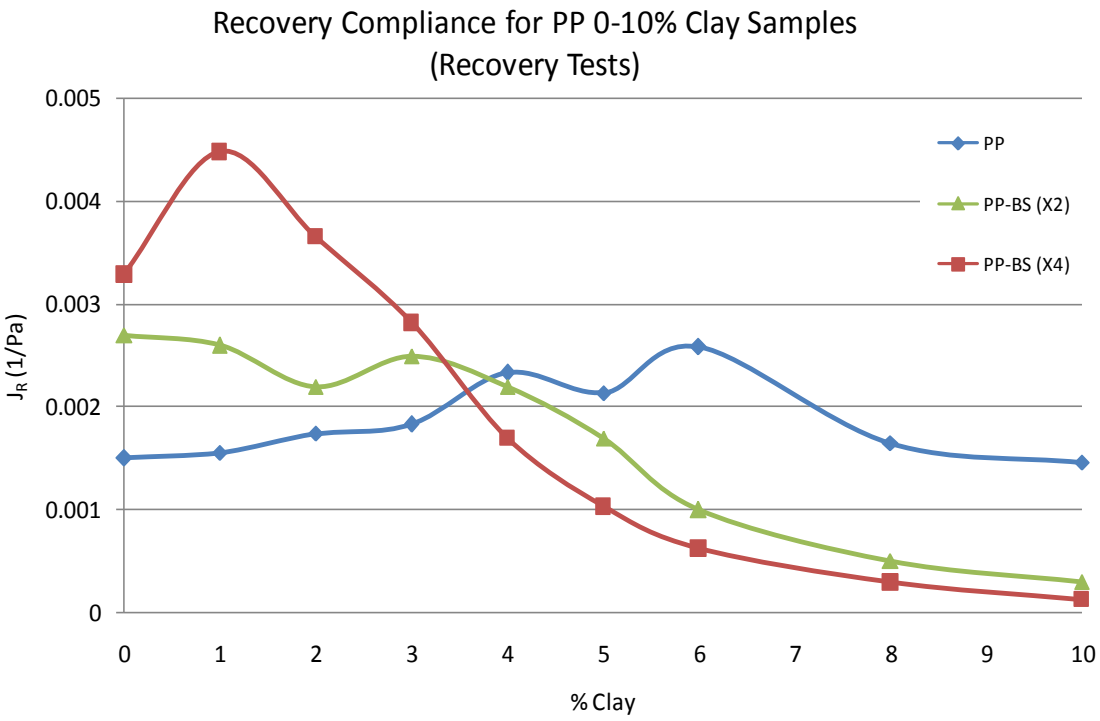

Figure 4.41: Recovery tests comparison chart

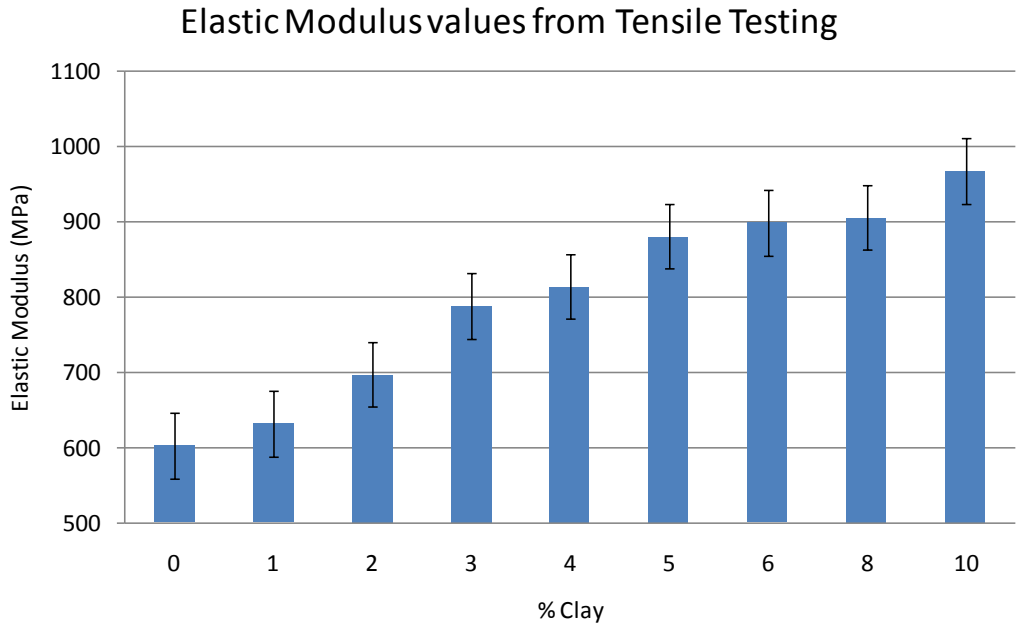

Figure 4.42: E' vs. % clay for unstretched PP

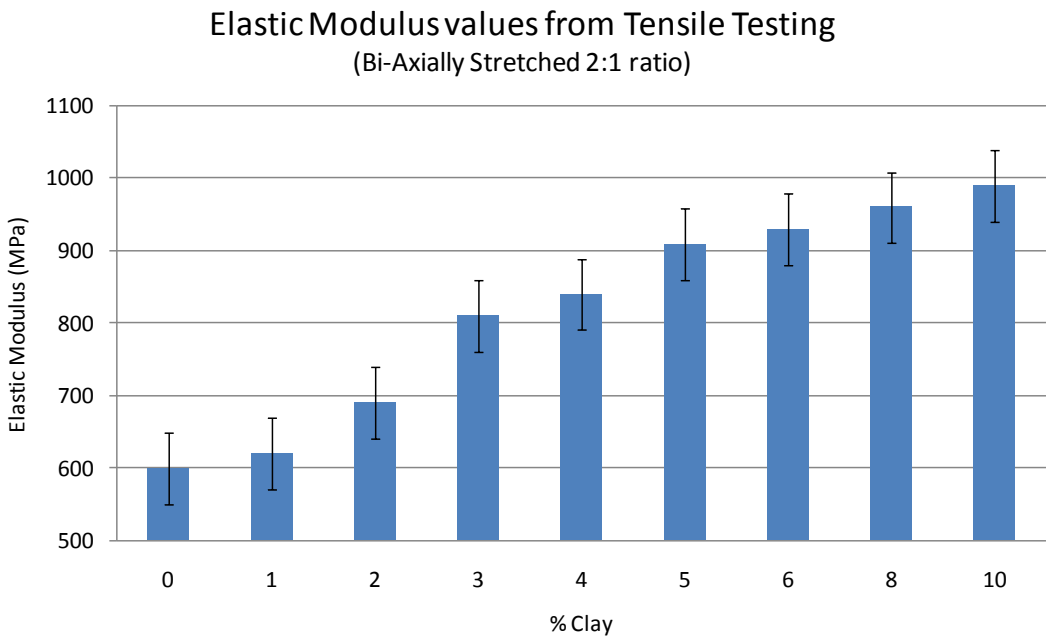

Figure 4.43: E' vs. % clay for 2:1 stretched PP

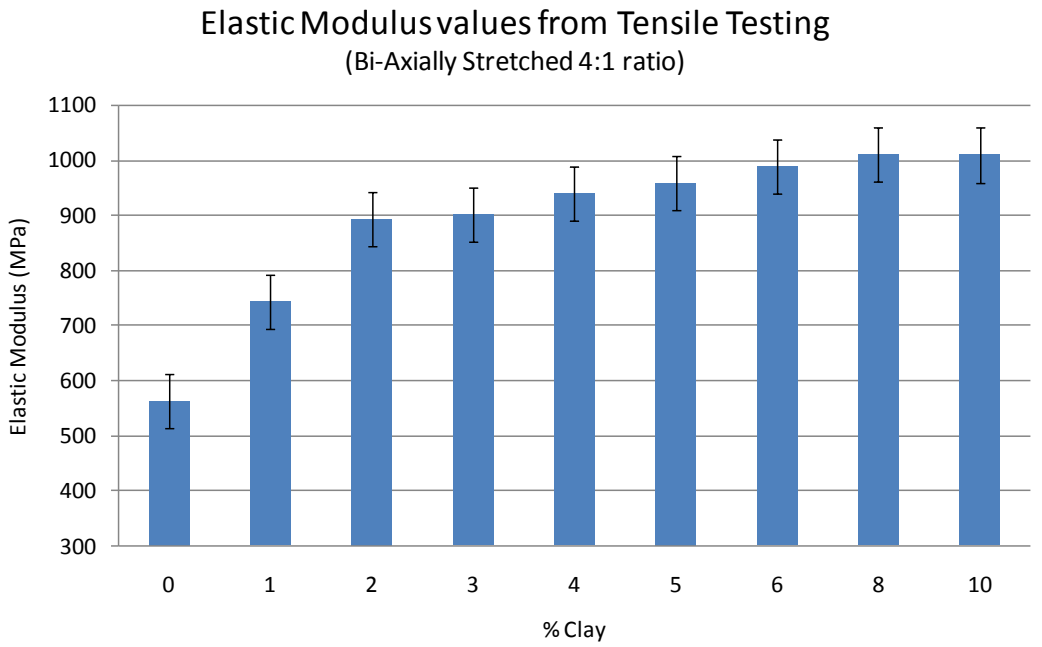

Figure 4.44: E' vs. % clay for 4:1 stretched PP

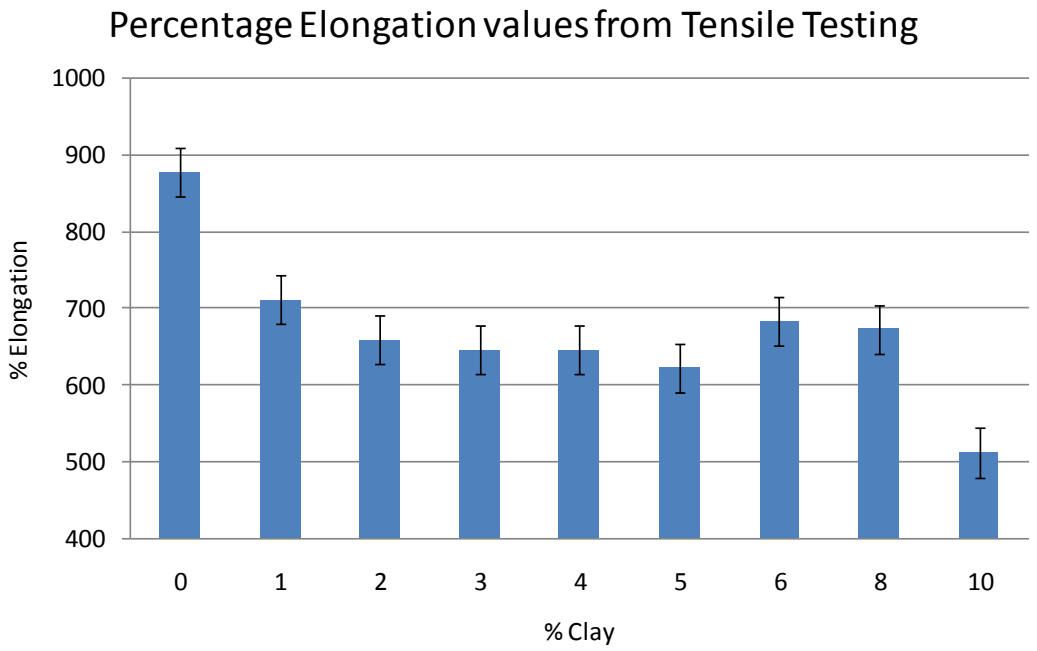

Figure 4.45: % Elongation vs. % clay for unstretched PP

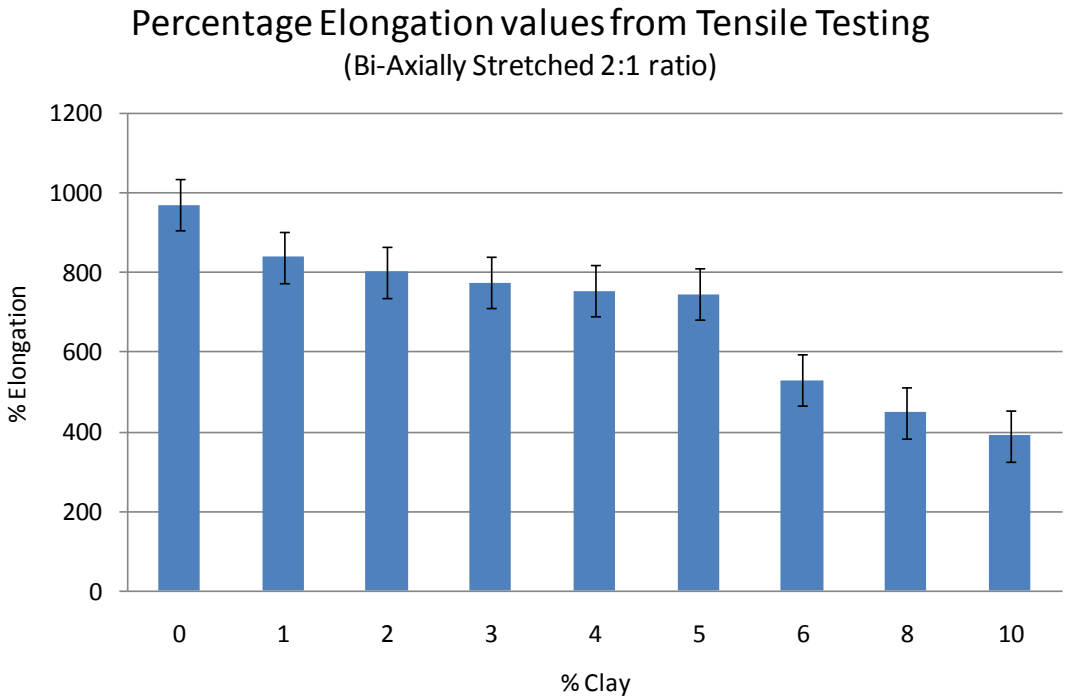

Figure 4.46: % Elongation vs. % clay for 2:1 stretched PP

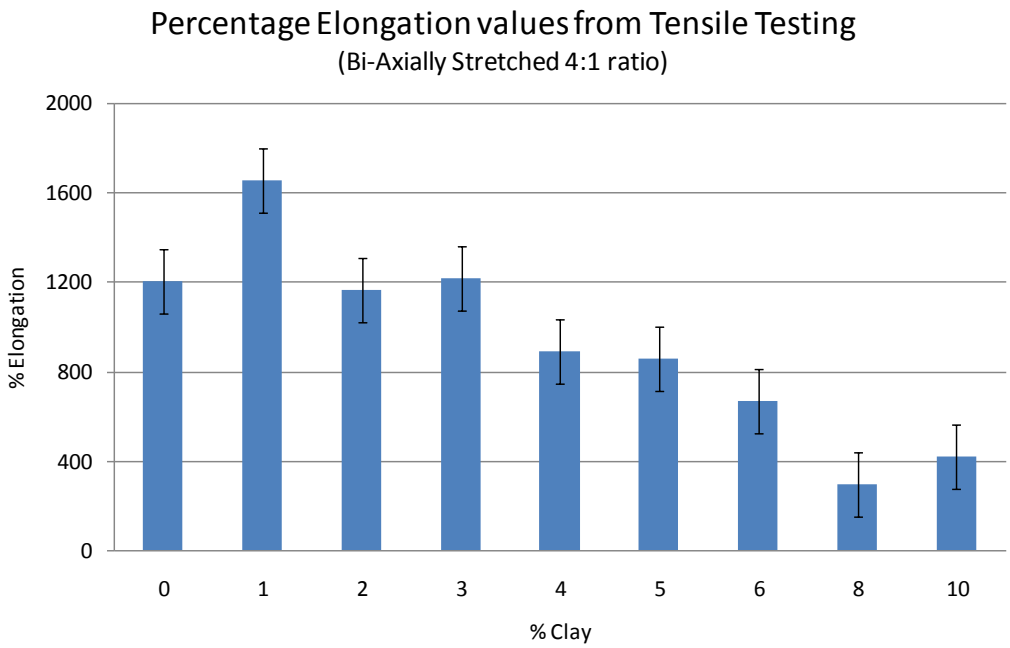

Figure 4.47: % Elongation vs. % clay for 4:1 stretched PP

DSC Test

Table 4.4: Crystallinity and Standard Heat values

PP Samples			PP BS (X2) samples		PP BS (X4) samples	
% Clay	% Crystallinity	Std Heat (J/g)	% Crystallinity	Std Heat (J/g)	% Crystallinity	Std Heat (J/g)
0	54.35	112.6	45.85	94.95	43.11	89.28
1	52.63	109	45.28	93.77	40.29	83.43
2	44.02	91.18	43.27	89.61	43.75	90.61
3	43.52	90.14	41.31	85.54	43.07	89.19
4	40.88	84.66	40.97	84.85	43.08	89.22
5	41.95	86.87	41.71	86.39	39.38	81.55
6	39.16	81.07	40.33	83.53	40.9	84.7
8	41.54	86.03	41.02	84.96	41.95	86.88
10	39.29	81.36	39.27	81.32	38.56	79.85

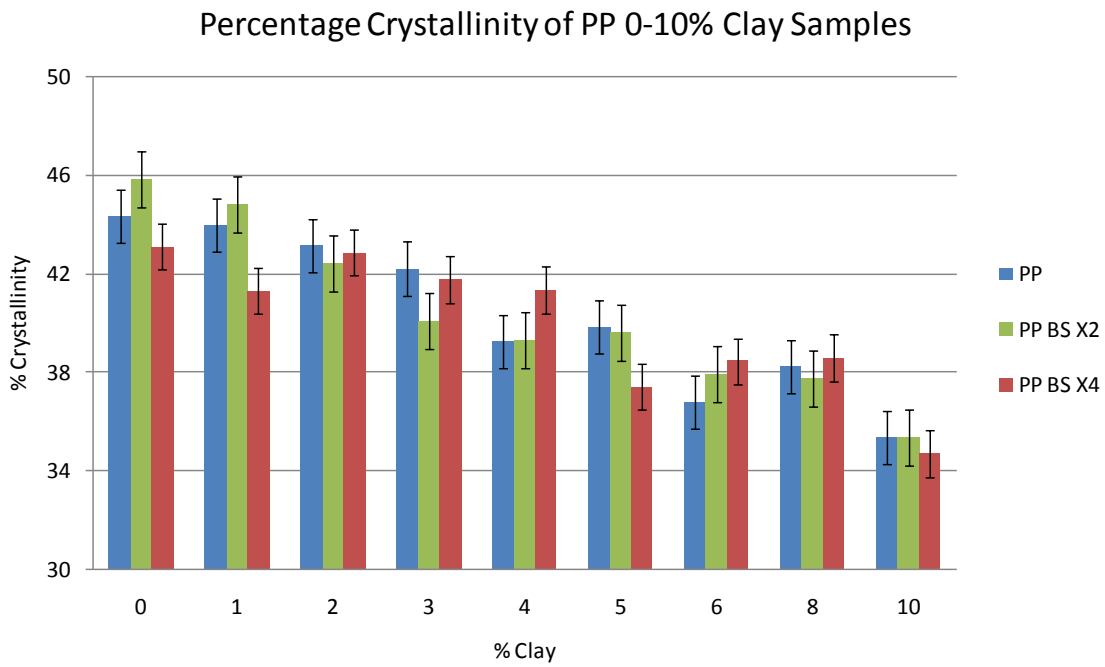

Figure 4.48: % Crystallinity from DSC data

DATA ON CYCLE EXTRUSION-STRETCHING-EXTRUSION

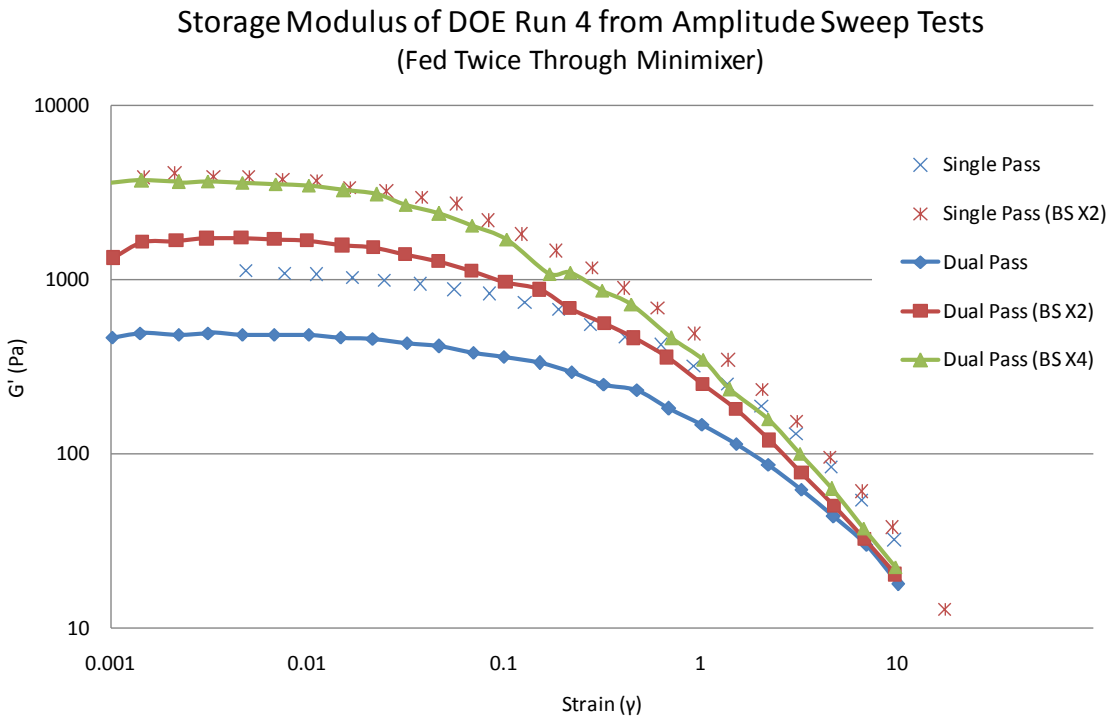

Figure 4.49: G' vs Strain from dual processing of run 4

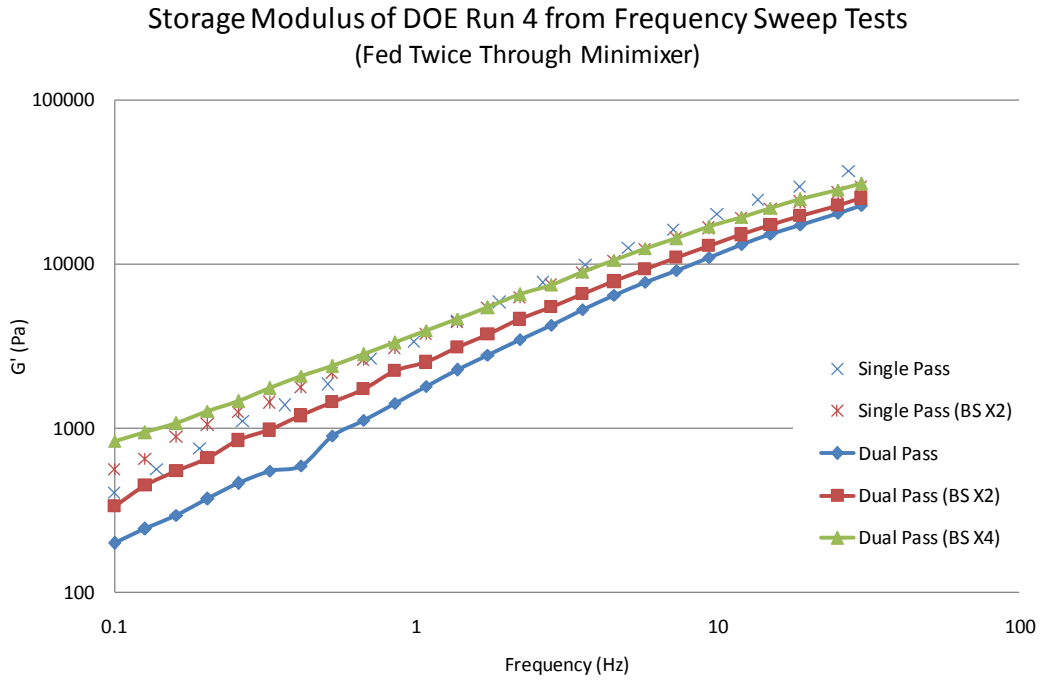

Figure 4.50: G' vs Frequency from dual processing of run 4

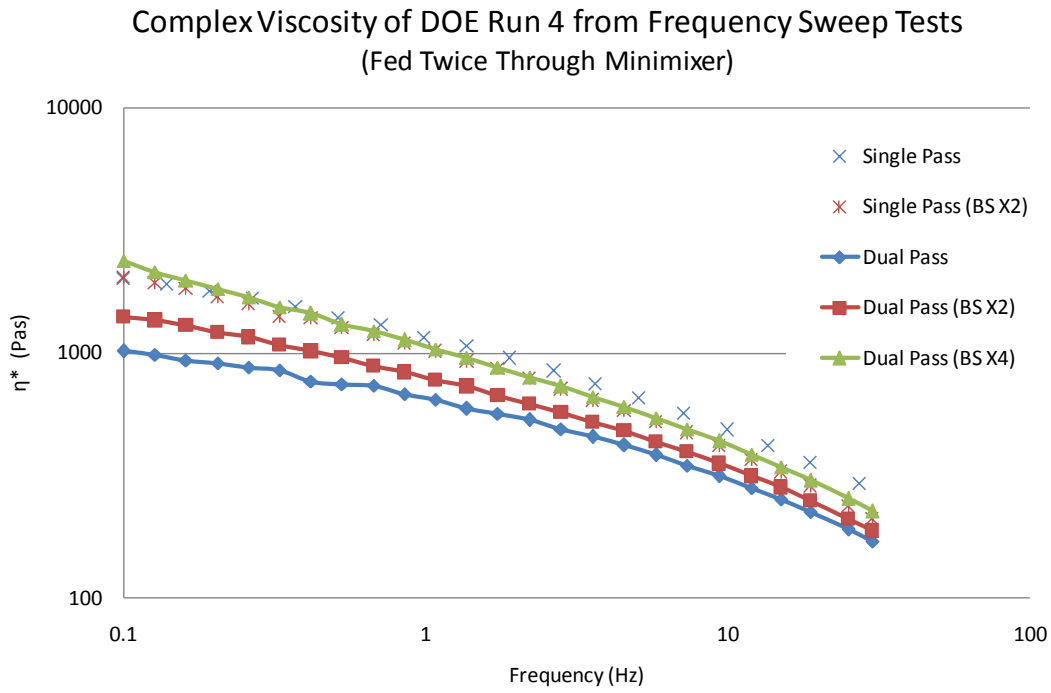

Figure 4.51: η* vs Frequency from dual processing of run 4

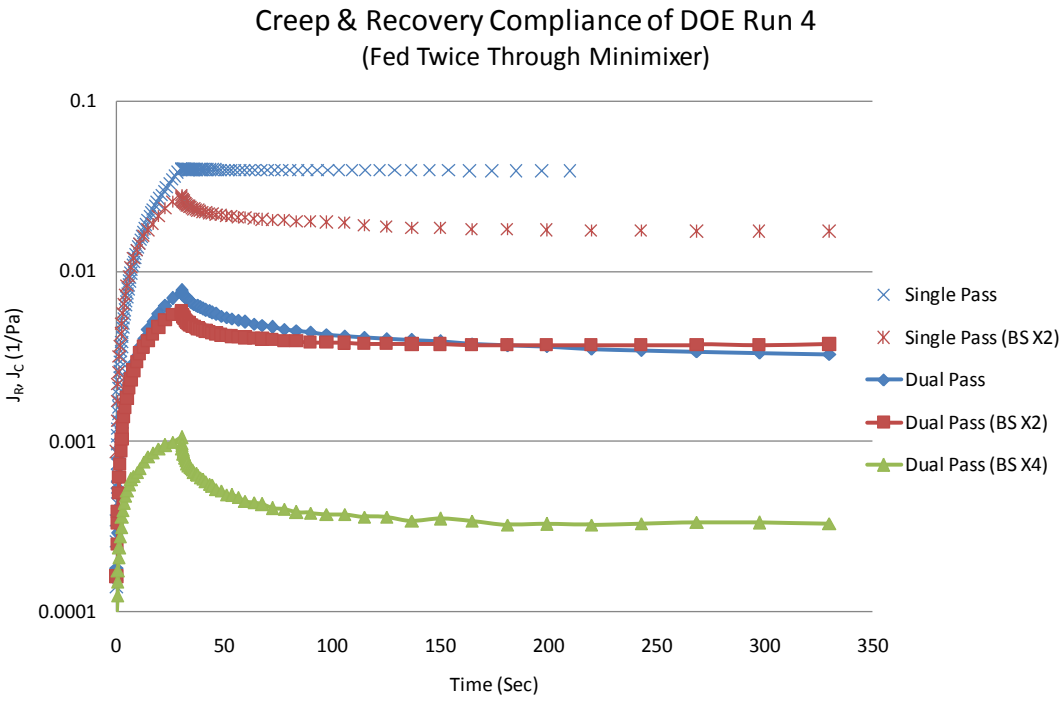

Figure 4.52: J_C &J_R vs Time from dual processing of run 4 (AS test)

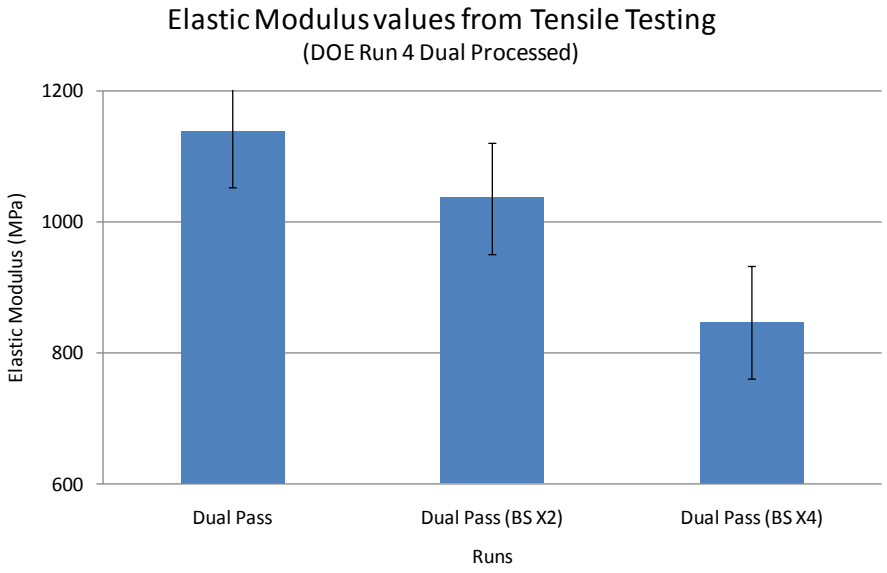

Figure 4.53: E' from tensile tests of dual processed run 4

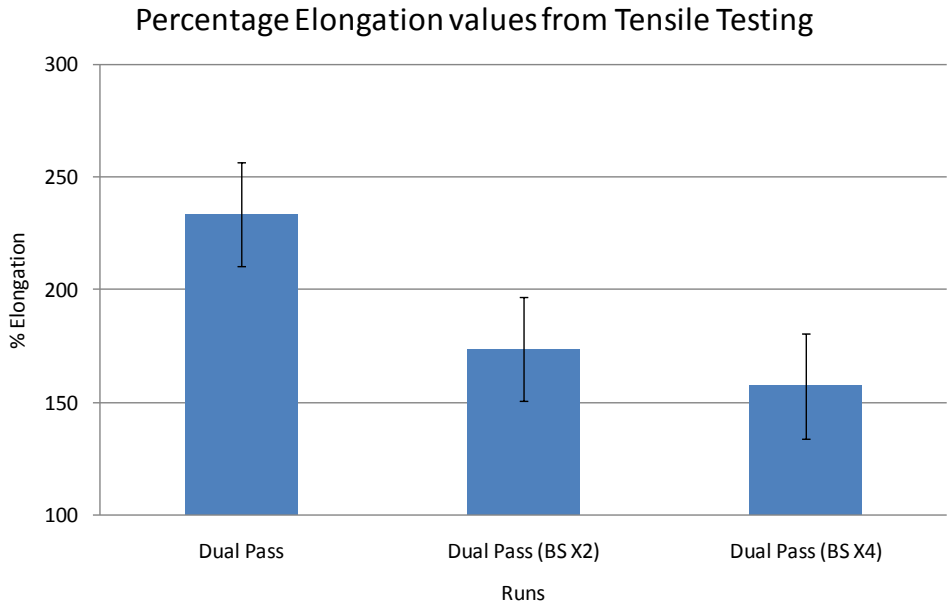

Figure 4.54: % Elongation from tensile tests of dual processed run 4

4.5 Further Evaluation of Mixing Processes

4.5.1 Effect of Mixing Materials Prior to Feeding into Mini-mixer (Extrusion)

In these experiments, the objective was to assess if there was a need to mix the polymer and nano-additive prior to feeding into the mini-mixer. Arguably, it is clearly more beneficial to do so, however in practice this step is not always followed hence the importance of these experiments to guide processing.

For this set of experiments, only 3 clay loadings were investigated 1wt%, 3wt% and 6wt%. The polymer-nanoclay-compatibiliser however were not hand mixed as in the previous tests but fed directly into the mini-mixer; polymer first followed by nanoclay and compatibiliser. The rheological and mechanical properties evaluation, including the effect of stretching was carried out in exactly the same manner as in the mixed samples. The data obtained is shown in Figures 4.55-59 and give as before results of the Amplitude sweep, Frequency sweep and Creep-Recovery tests.

The findings are as follows:

- Prior mixing is critical according to the data which show significant difference in properties between mixed and unmixed raw material. An explanation for this is that although a considerable amount of mixing is generated once the materials are introduced, prior non-mixing has probably caused agglomeration of the nanoclay and limited distribution into the polymer melt. Clearly a pre-requisite for good mixing is first a good distribution to facilitate further dispersion on application of high shear in the minimixer.
- Biaxial stretching of the samples also had very little effect on improving the properties which could suggest a badly mixed nanocomposite in this instance.

- Once again the rheological tests have confirmed that they are able to inform on structure as evidence from the data.

4.5.2 Effect of Nanoclay Type

Clearly, the effect of the nano-additive type is an important aspect, so far not considered in this research. Here a preliminary assessment of this effect is carried out by testing a different clay, Cloisite 10A type instead of the Cloisite 20A used so far. All other measurement techniques remained the same and prior mixing was carried out in order to conduct a fair assessment.

The conclusions which derive from the rheological and mechanical properties evaluations shown in Figures 4.60-71 are as follows:

- Cloisite 10A performed badly in both the un-streched and stretched samples.
- Upon further research, it was establish that Cloisite 10A is incompatible with the Polybond 3200 compatibiliser used. This opens an interesting area for further research to establish on the basis of performance which of the clay-compatibiliser systems is best suited for various polymers.
- Again, rheological testing has proved to be as useful a tool as the mechanical properties tests in underlining this effect.

FURTHER EVALUATION OF MIXING ASPECTS

1. DATA ON EFFECT OF PRIOR MIXING

2. DATA ON EFFECT OF CLAY TYPE

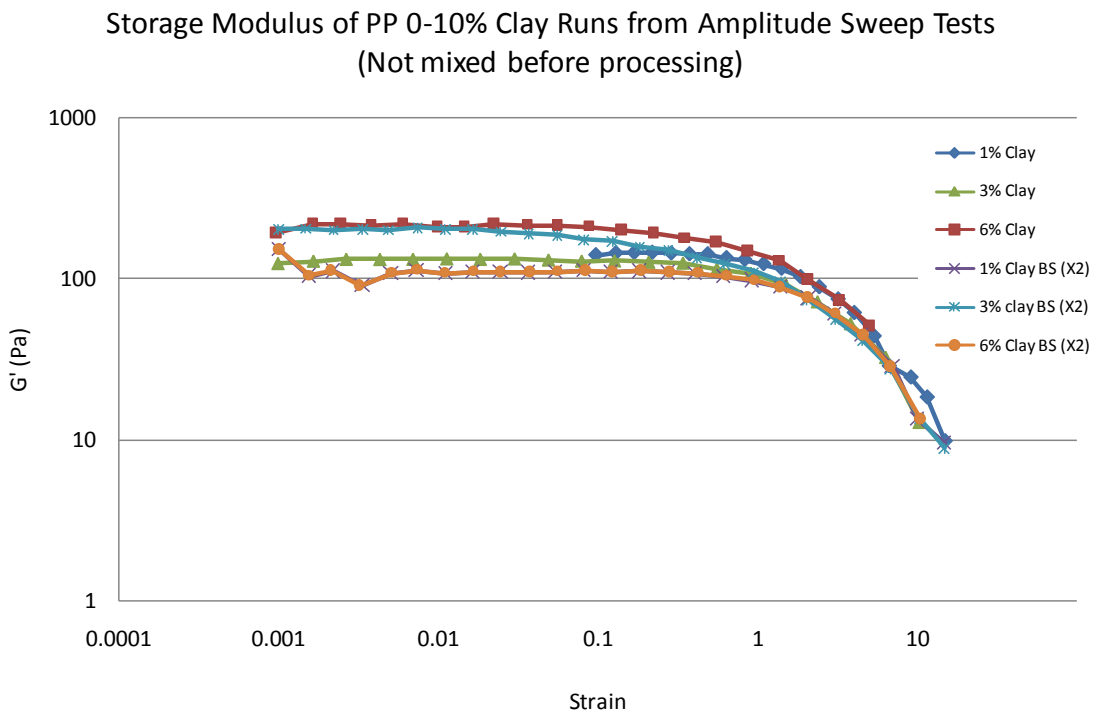

Figure 4.55: G' vs. Strain for unmixed samples

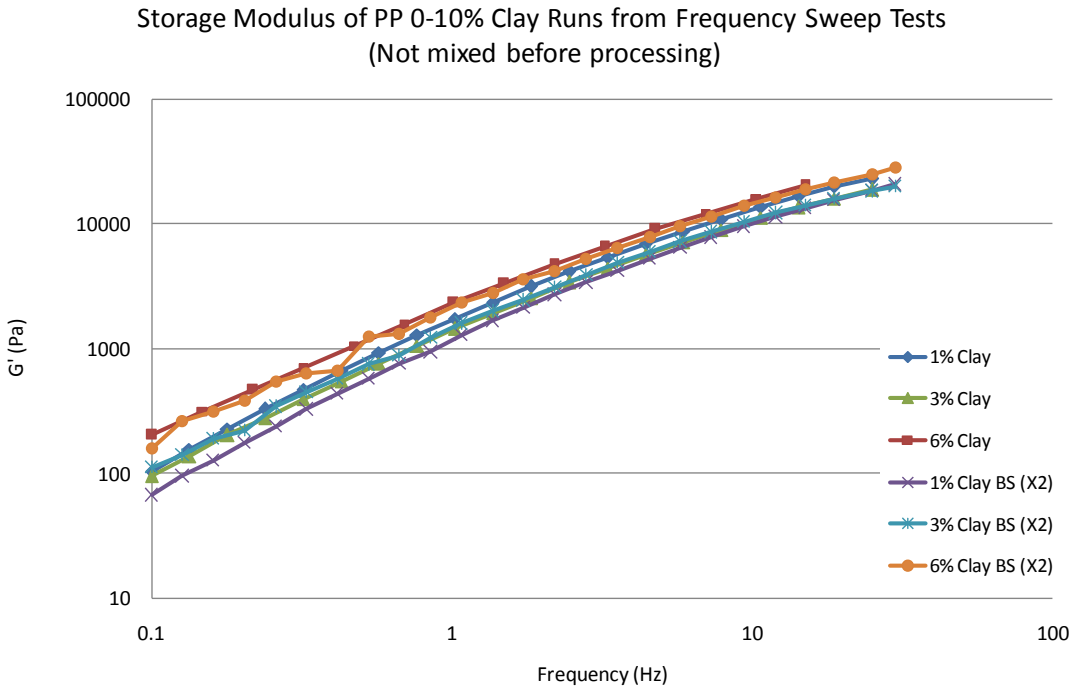

Figure 4.56: G' vs. Frequency for unmixed samples

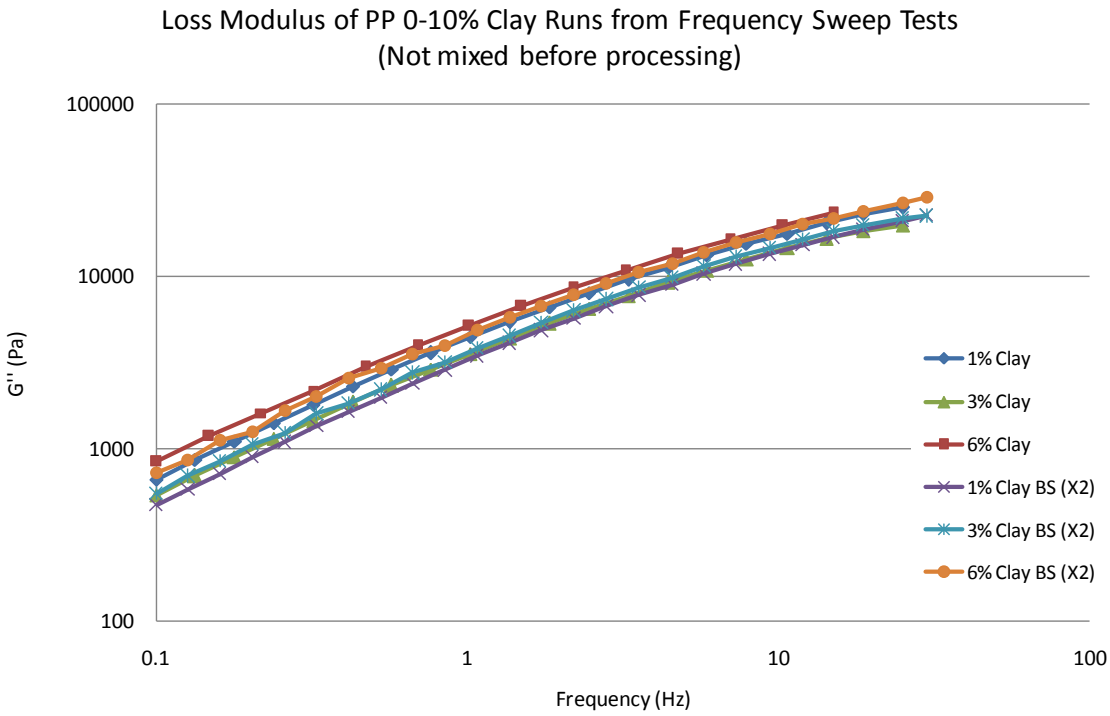

Figure 4.57: G'' vs. Frequency for unmixed samples

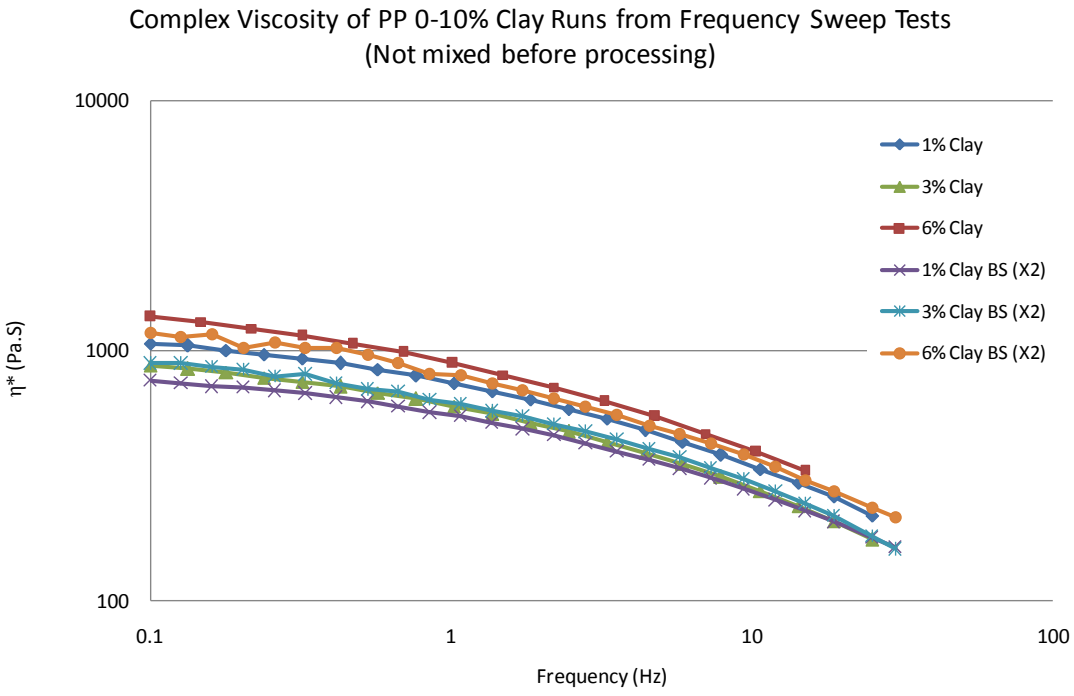

Figure 4.58: η* vs. Frequency for unmixed samples

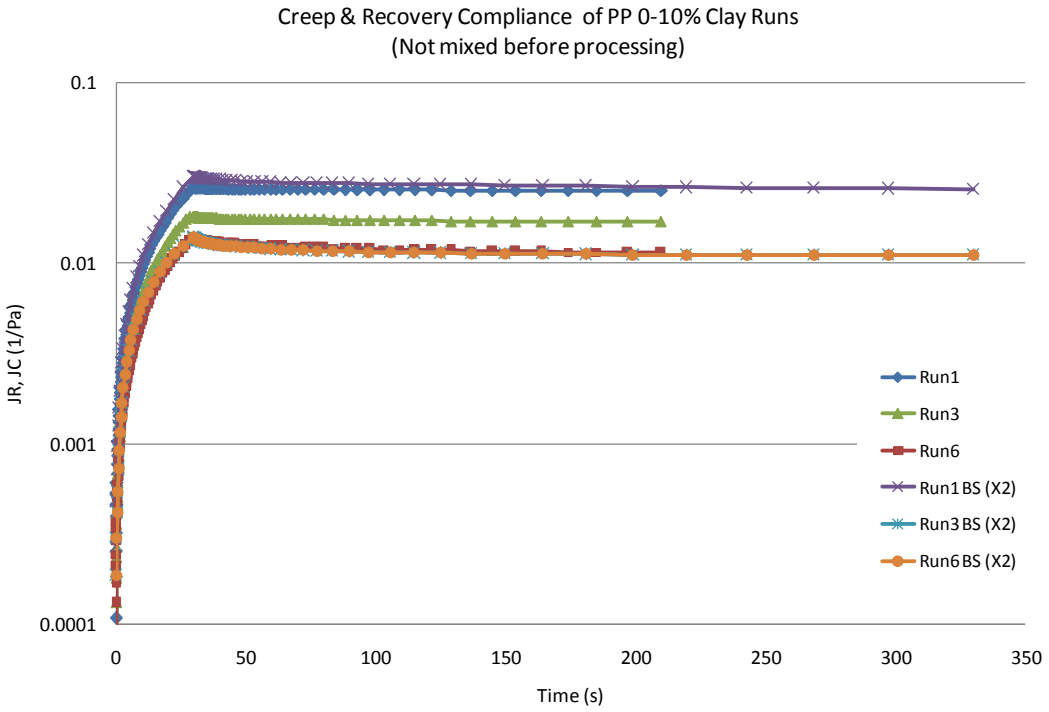

Figure 4.59: J_C& J_R vs. Time for unmixed samples

DATA ON EFFECT OF CLAY TYPE

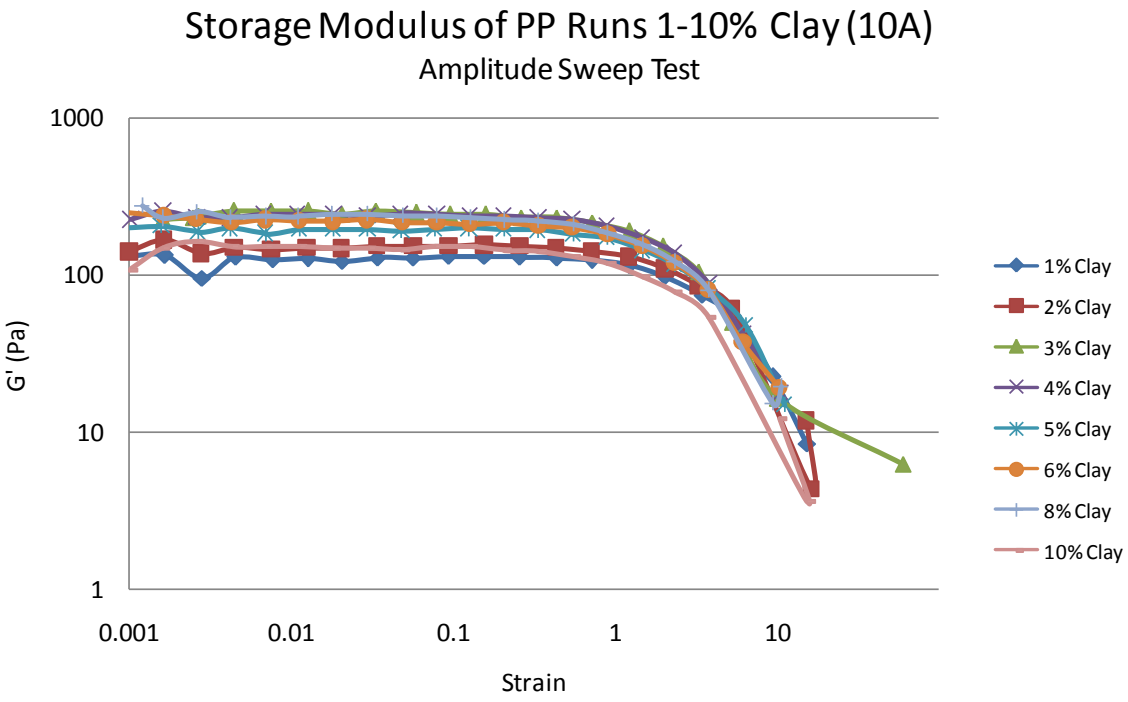

Figure 4.60: G' vs. Strain for Cloisite 10A

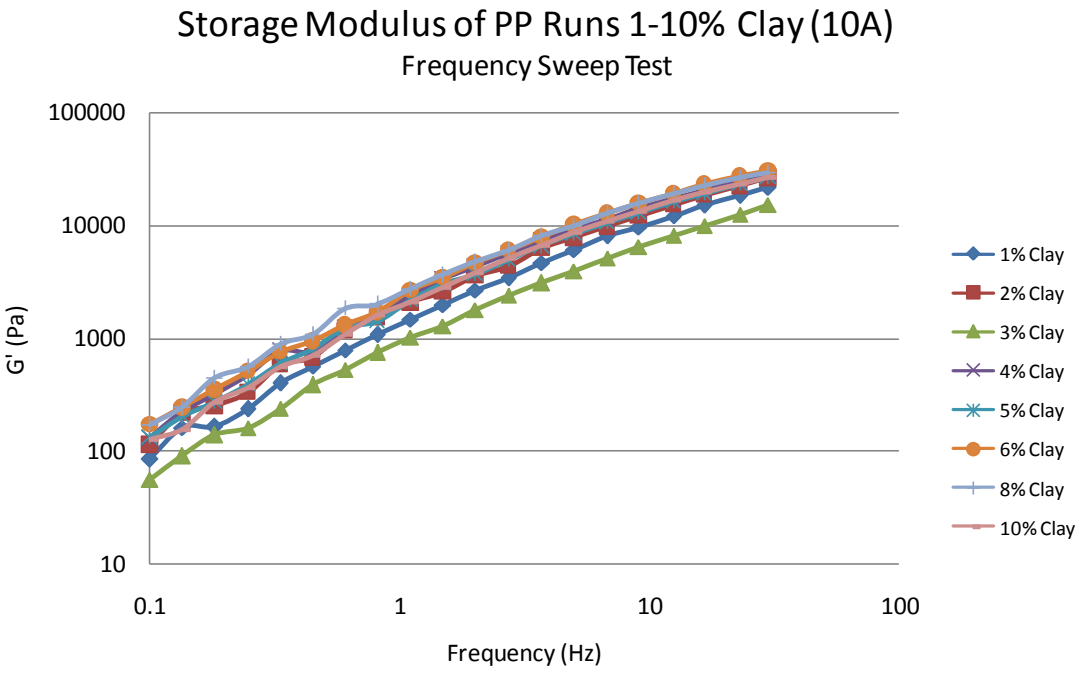

Figure 4.61: G' vs. Frequency for Cloisite 10A

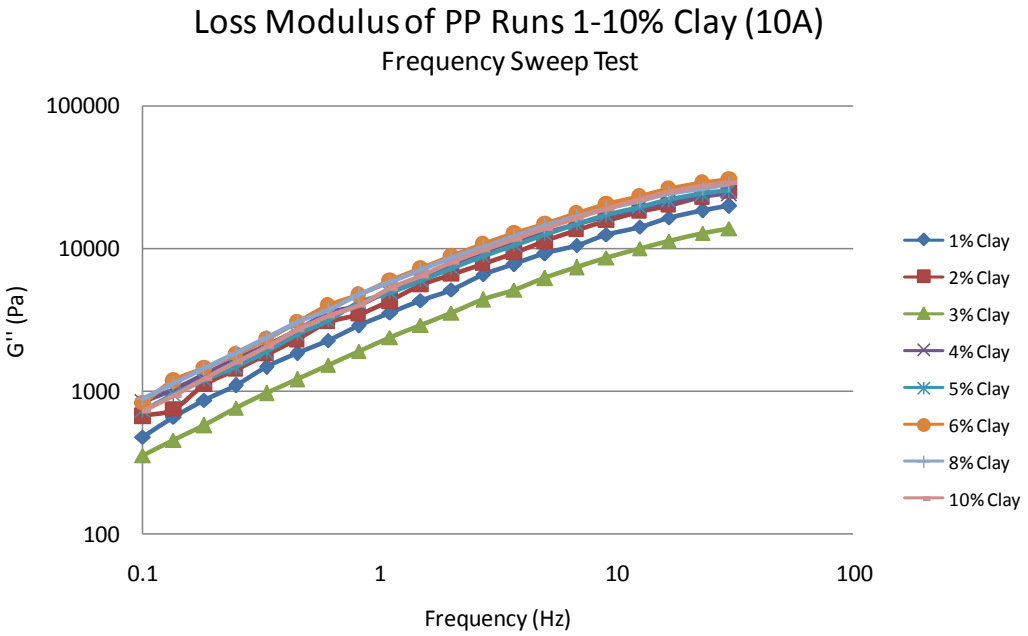

Figure 4.62: G'' vs. Frequency for Cloisite 10A

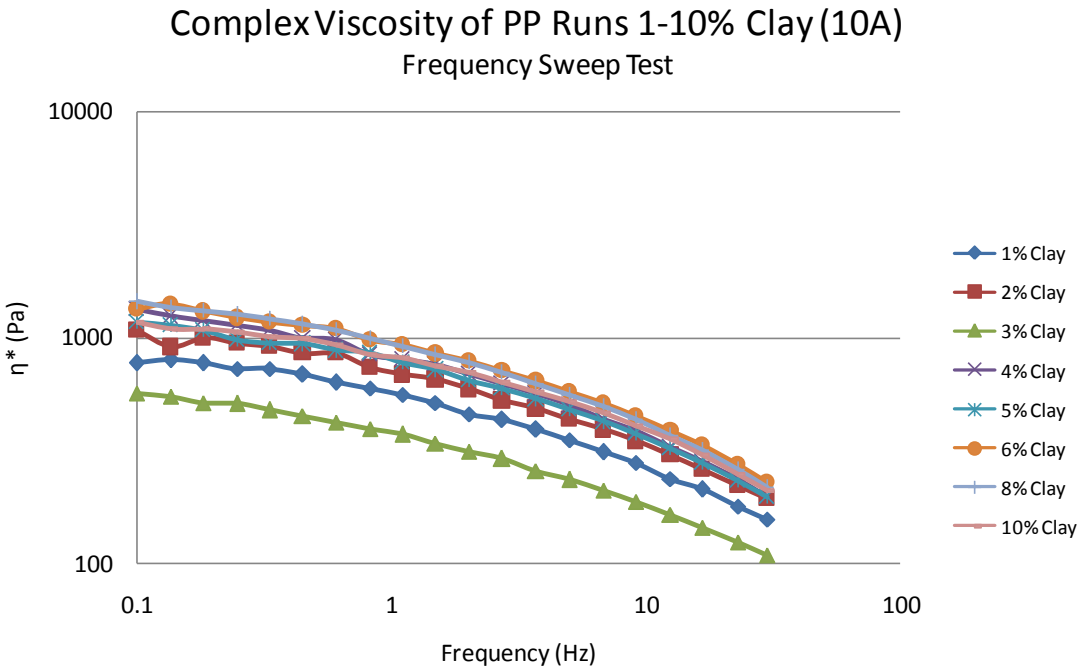

Figure 4.63: η* vs. Frequency for Cloisite 10A

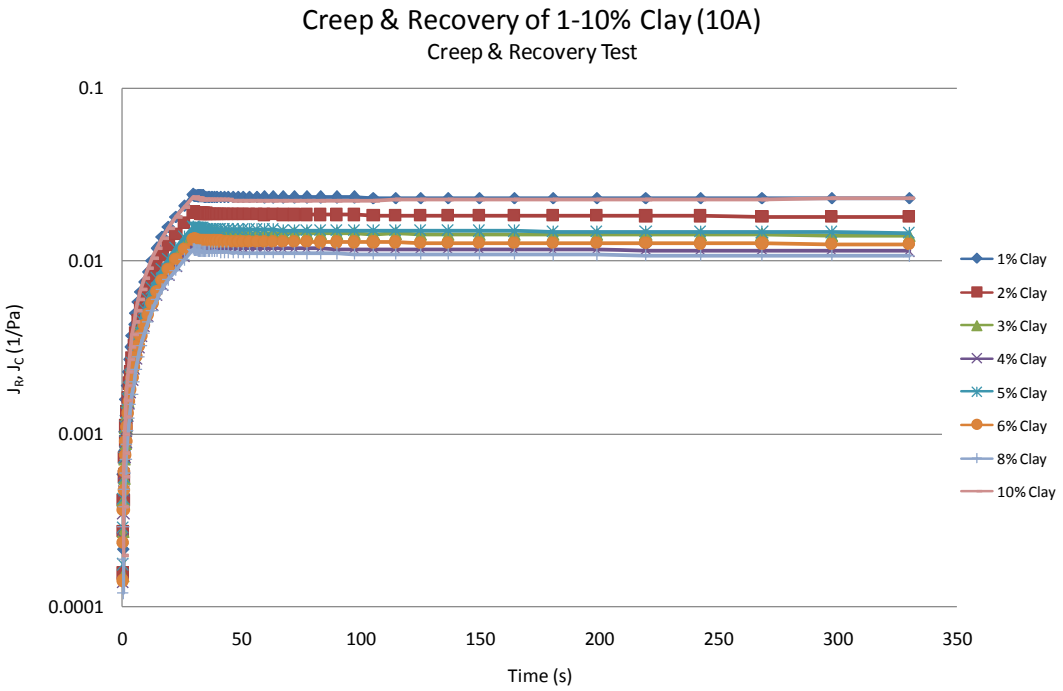

Figure 4.64: J_C & J_R for Cloisite 10A

Bi-axially Stretched with 3:1 ratio

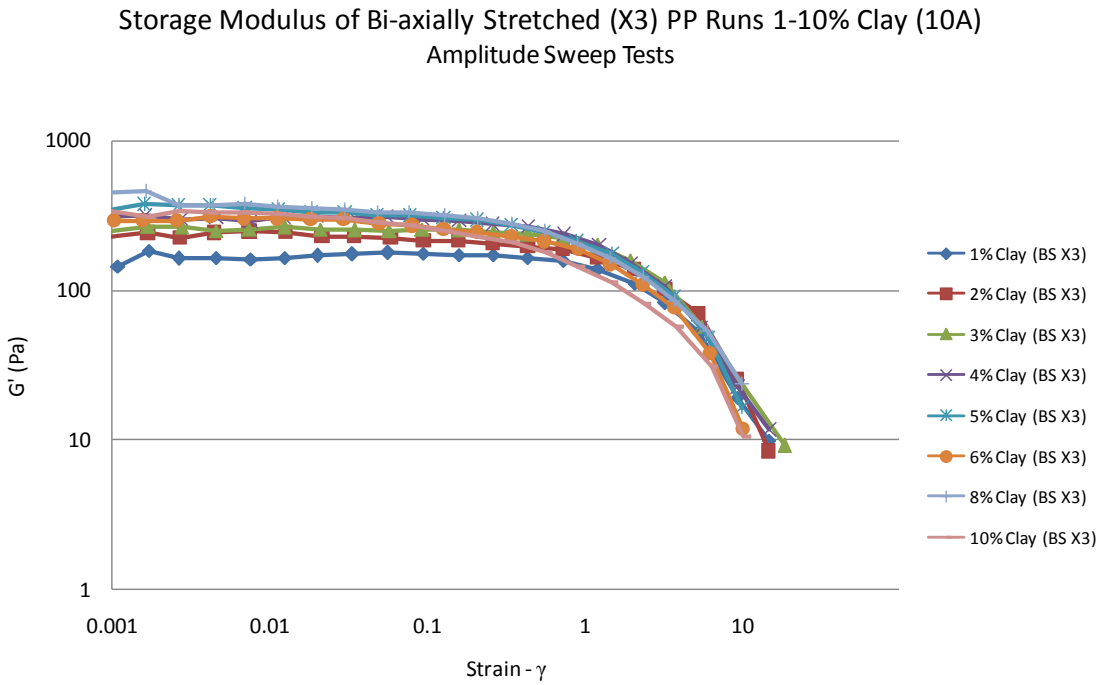

Figure 4.65: G' vs. Strain for Cloisite 10A (3:1)

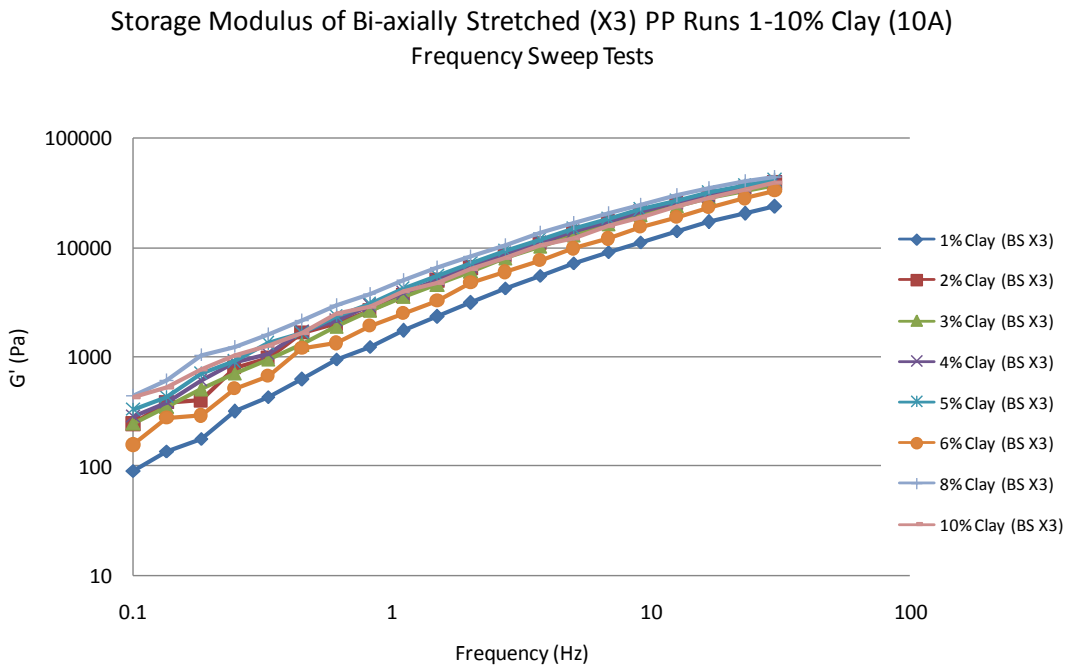

Figure 4.66: G' vs. Frequency for Cloisite 10A (3:1)

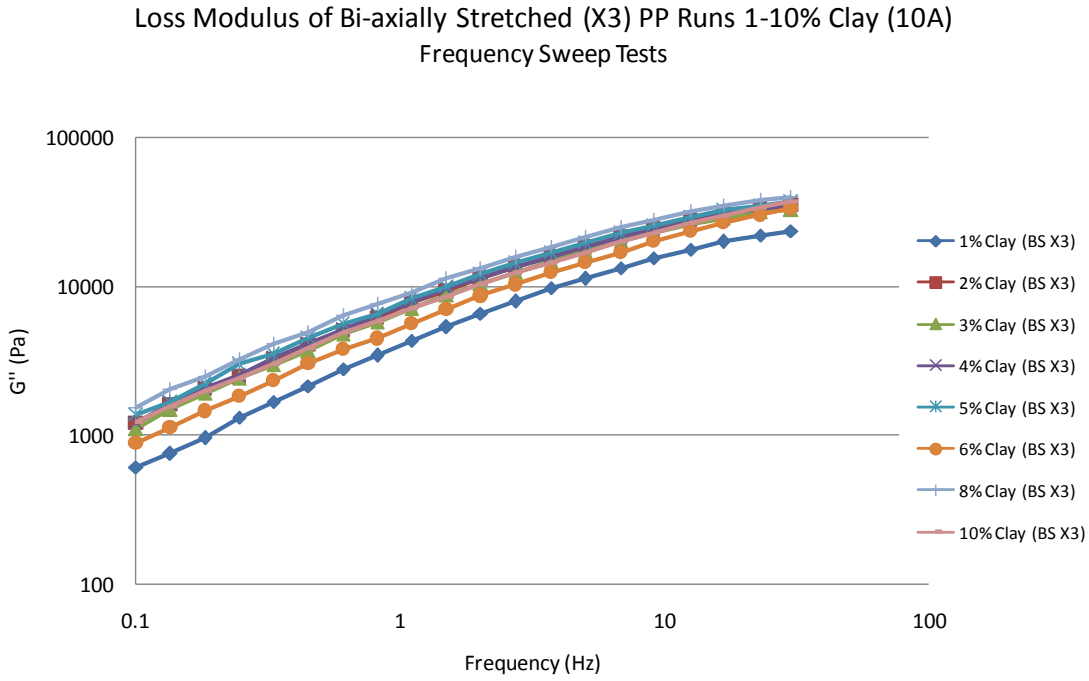

Figure 4.67: G'' vs. Frequency for Cloisite 10A (BS 3:1)

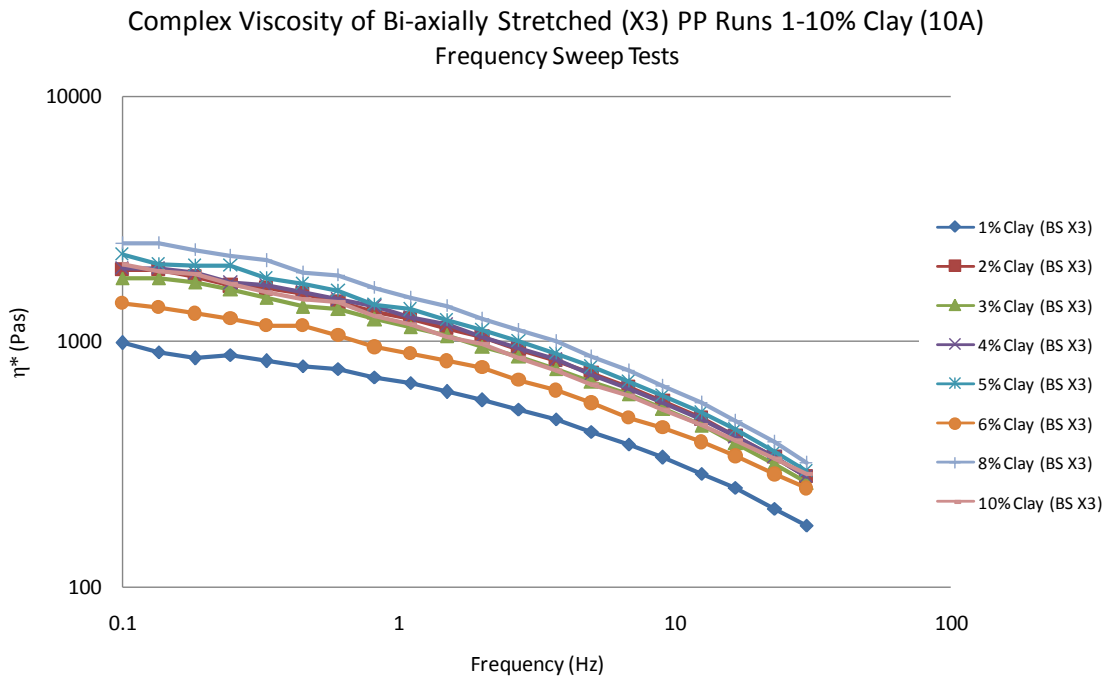

Figure 4.68: η* vs. Frequency for Cloisite 10A (BS 3:1)

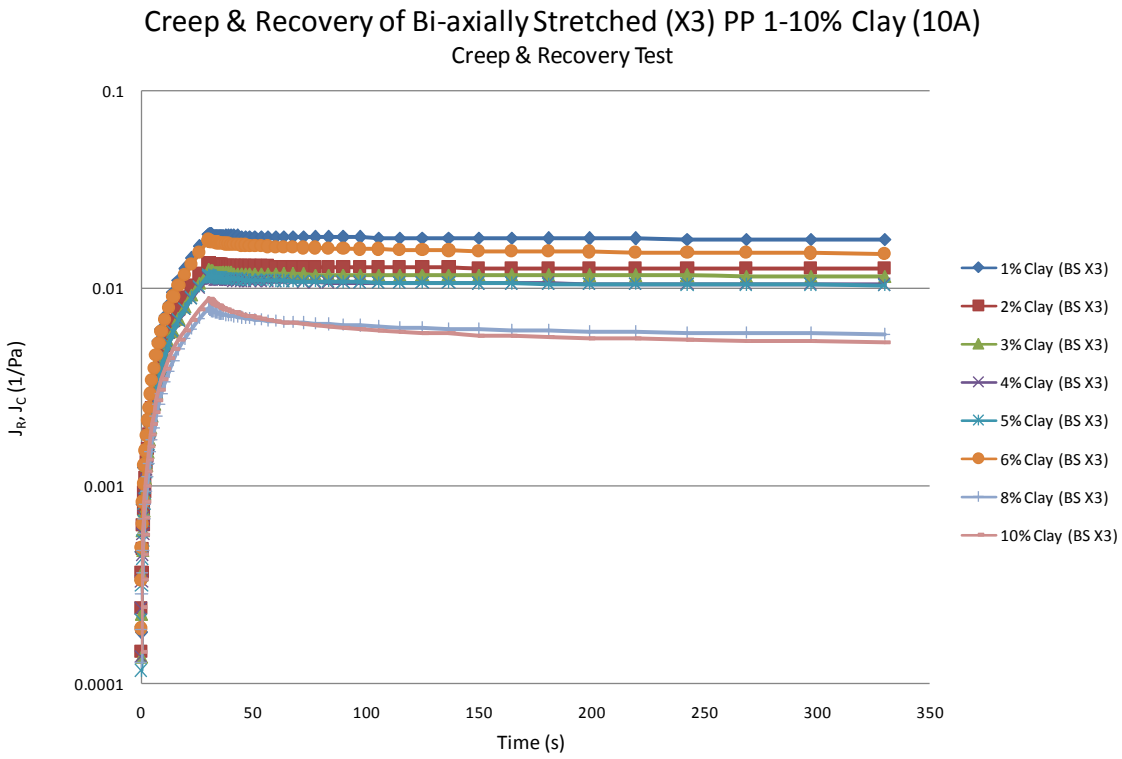

Figure 4.69: J_C& J_R for Cloisite 10A (BS 3:1)

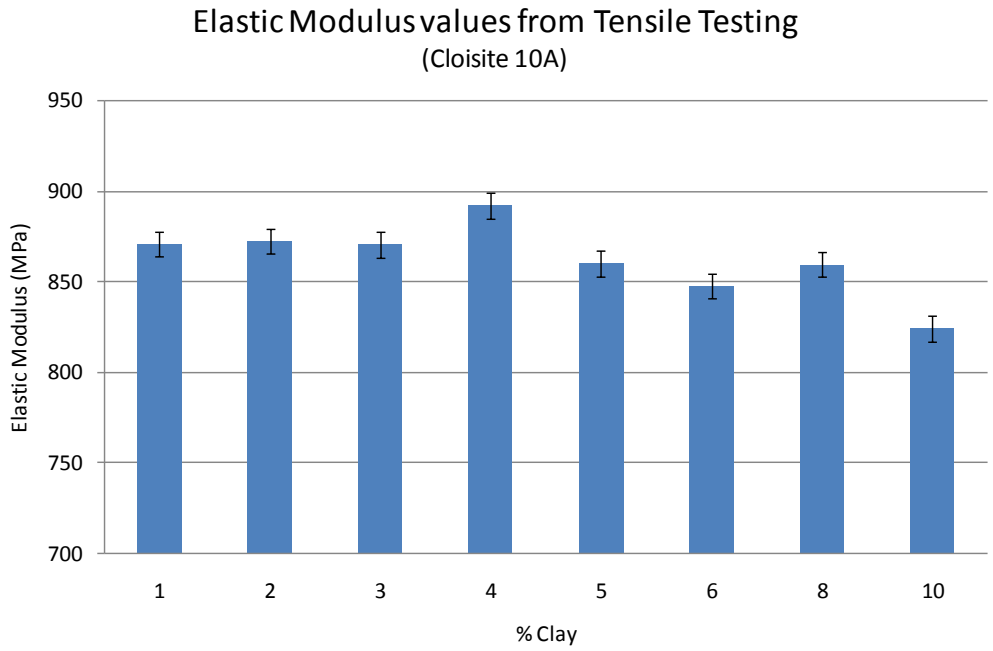

Figure 4.70: E' from tensile tests of Cloisite 10A

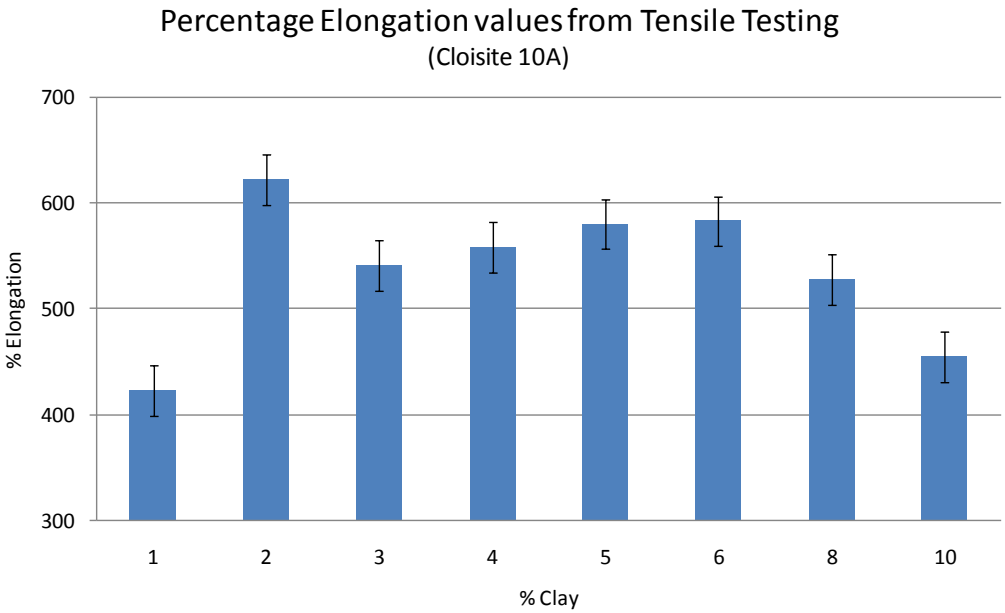

Figure 4.71: % Elongation from tensile tests of Cloisite 10A

4.6 Repeatability Tests of Rheological Evaluation

One of the main objectives of this research was to assess the feasibility of rheology as a means of distinguishing between various states of nano-composition. The results presented so far have shown that it is the case. However it is important to assess the repeatability of the data not only to check experimental errors but also to assess if using the same mini-mixer, the same operating conditions, the same formulation, we obtain the same nano-composite with the same rheology using two different rheometers. This is not only important for practical applications but would also give confidence in the ability of rheological tests to give broader, less operator bias data as for example microscopic observations.

In order to test this effect, RO4 and RO10 from the DOE programme were repeated. Recall that RO4 was found to be the best performing and RO10 was found to lie in the mid-range of performance (see Figure 4.1). Also, testing at 0 and 6% clay loading was conducted at the optimum mini-mixer operating conditions (i.e. at 190^0C, 40 rpm screw speed, 5 mins mixing time and 2% compatibiliser loading) to provide further data. As these tests have been assessed previously with the Bolin CVO120, we present here the data obtained with a different rheometer, the Anton Paar Rheometer.

The results, giving G', G'' & η^* for RO4 and RO10 as shown in Figures 4.72-77 together with runs 0% & 6% clay loading (Figures 4.78- 81) allow the following overall conclusion to be made: The small discrepancy between the actual values and the similar trend confirm that rheology is an accurate tool to be used in ranking the performance of nanocomposites. Thus it can be used to gauge which operating conditions during extrusion are best suited to produce the "best" nanocomposite.

RHEOLOGICAL REPEATABILITY DATA ON RO4 AND RO10

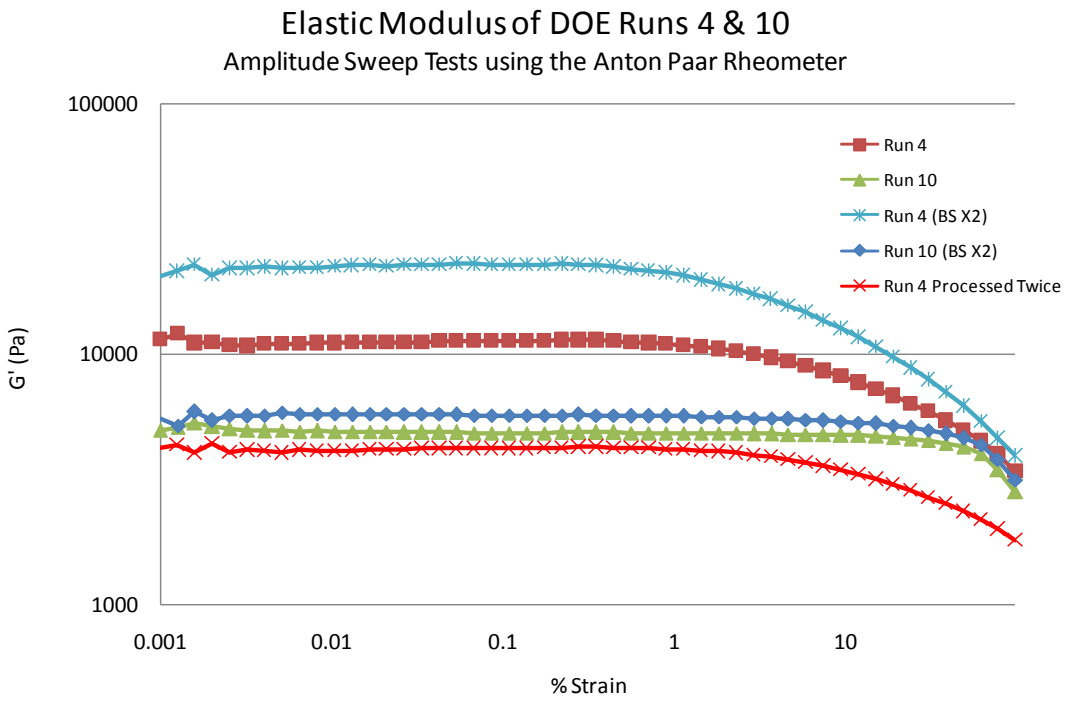

Figure 4.72: G' vs. Strain using Anton Paar

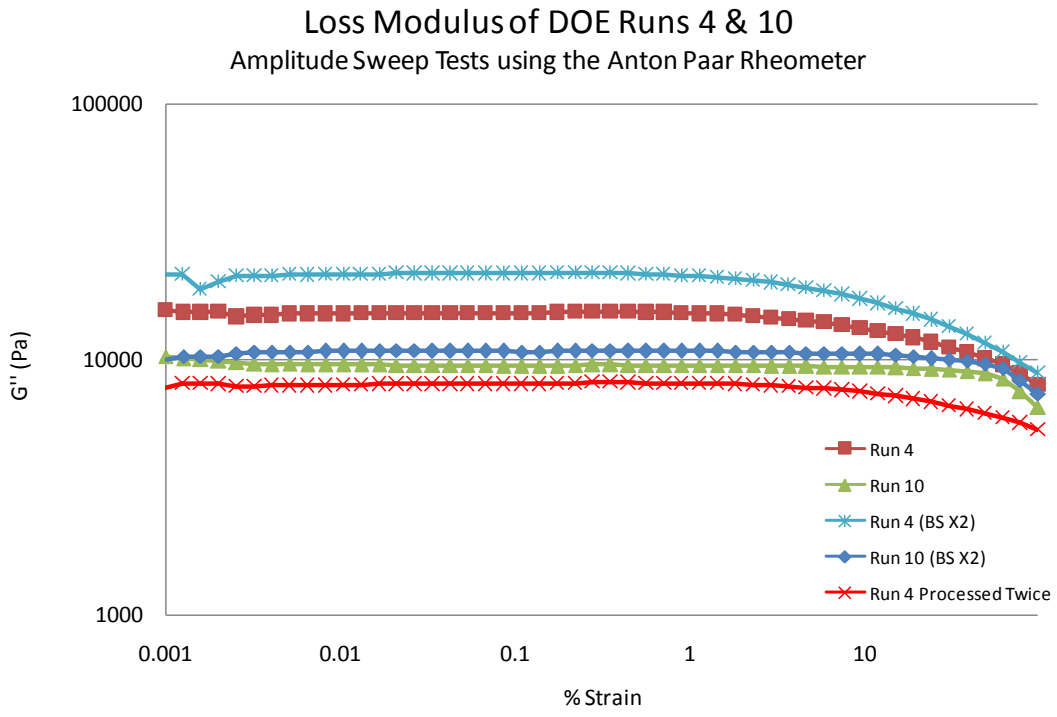

Figure 4.73: G'' vs. Strain using Anton Paar

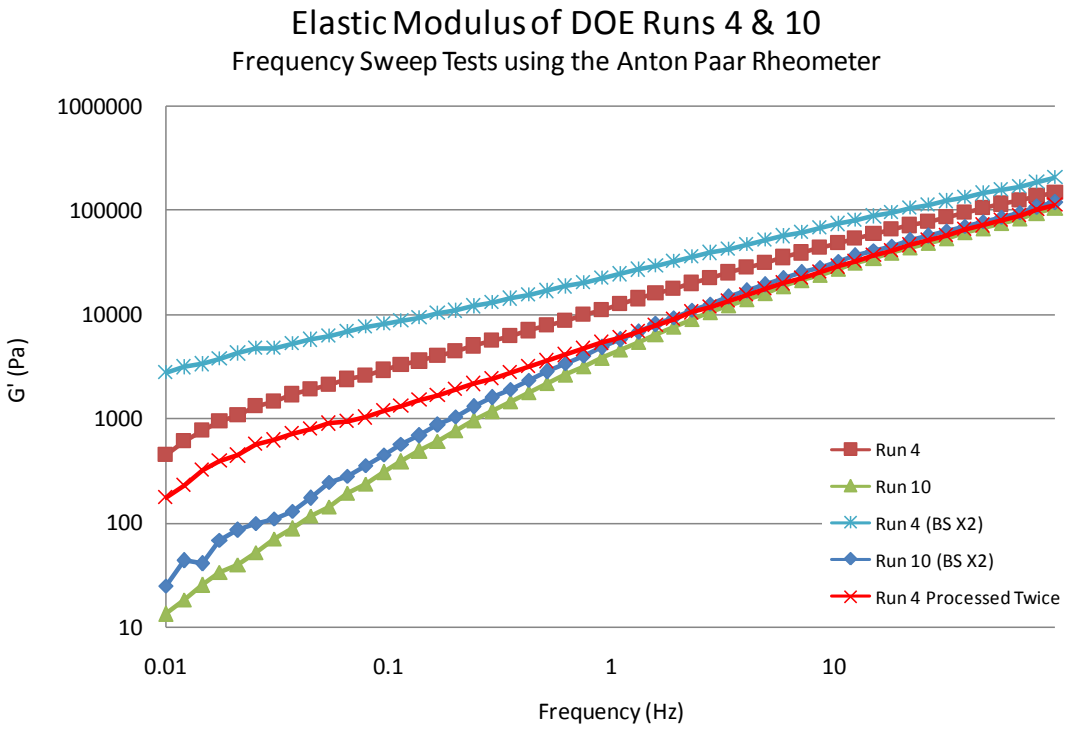

Figure 4.74: G' vs. Frequency using Anton Paar

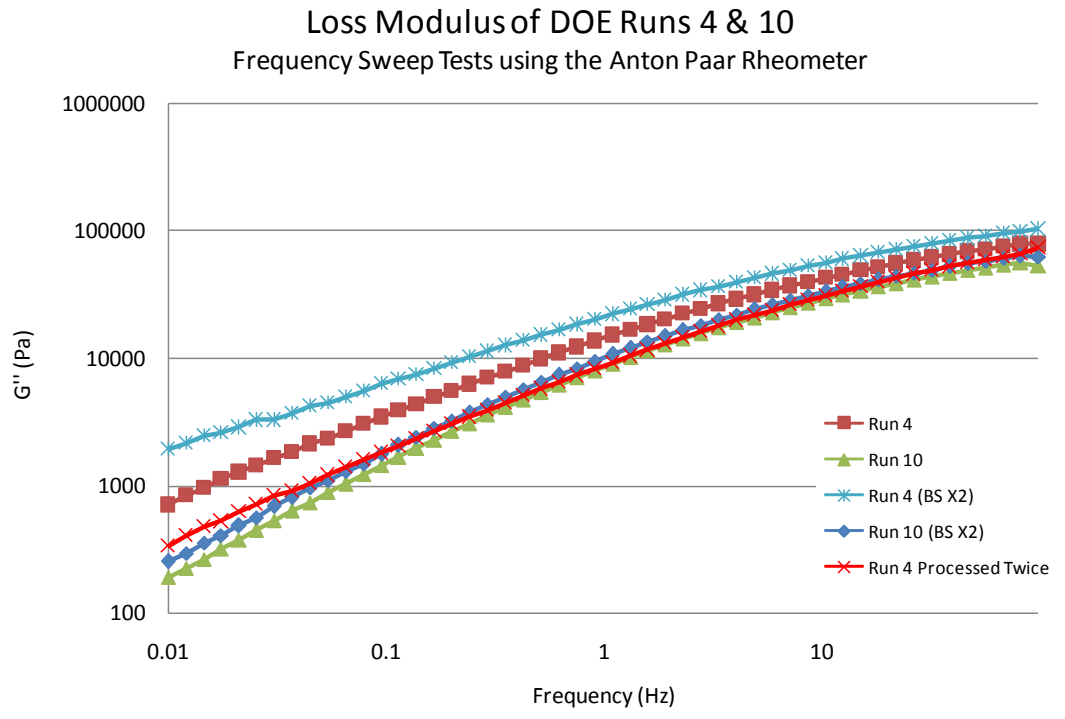

Figure 4.75: G'' vs. Frequency using Anton Paar

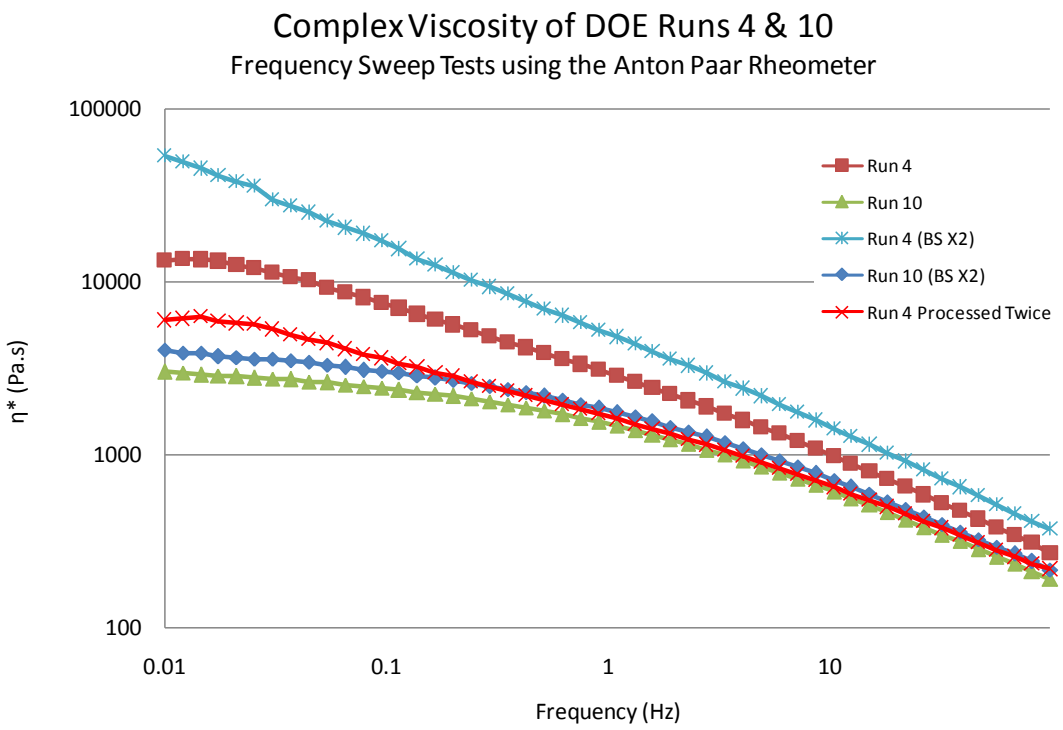

Figure 4.76: η* vs. Frequency using Anton Paar

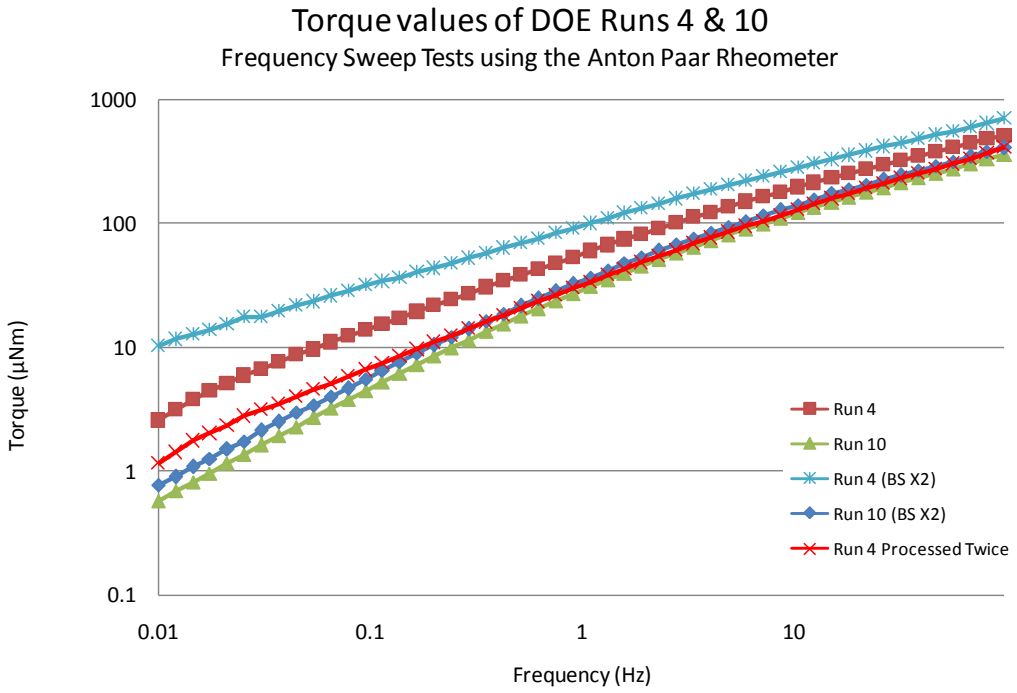

Figure 4.77: Torque vs. Frequency using Anton Paar

0% & 6% Clay Samples

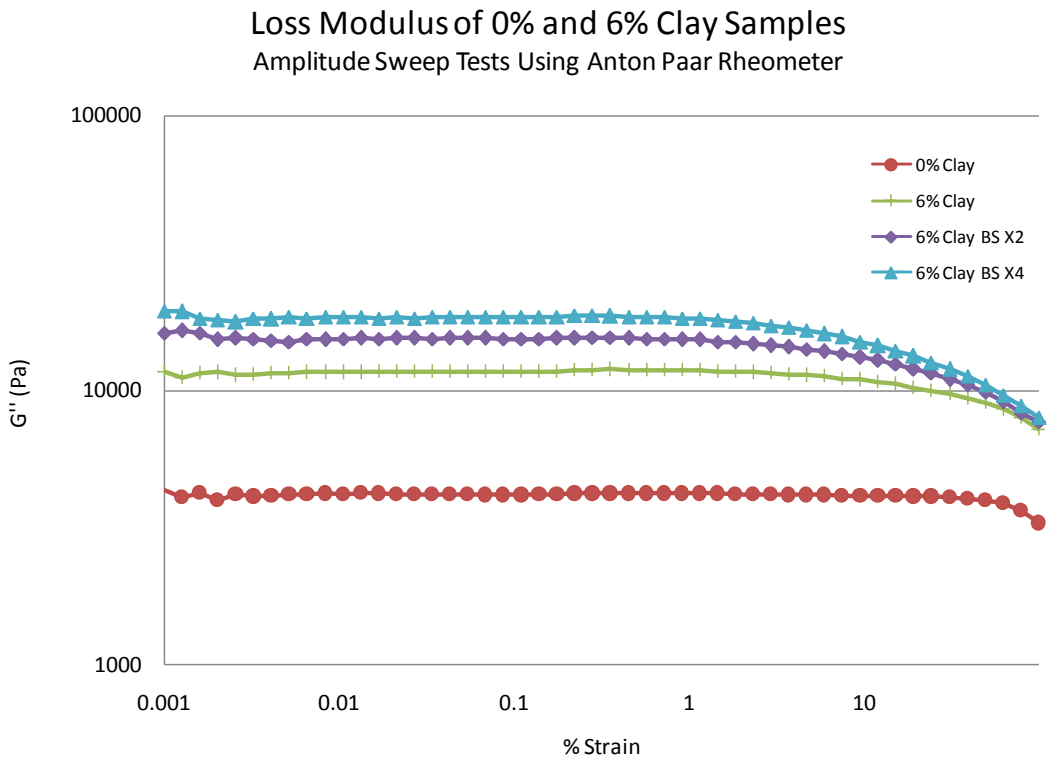

Figure 4.78: G'' vs. Strain using Anton Paar

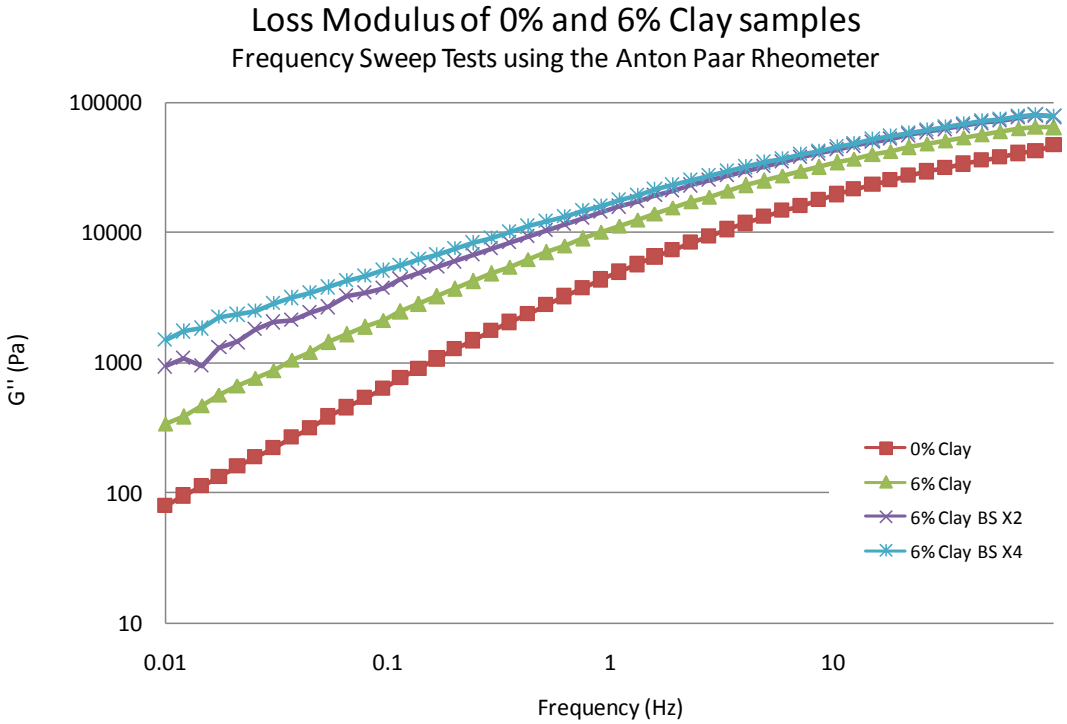

Figure 4.79: G'' vs. Frequency using Anton Paar

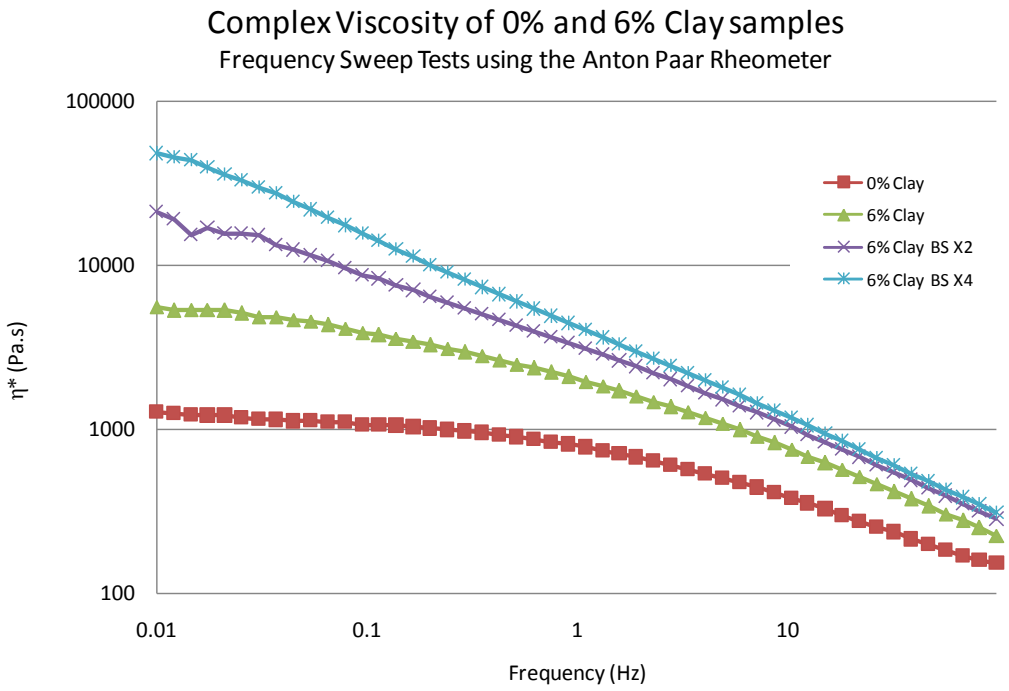

Figure 4.80: η* vs. Frequency using Anton Paar

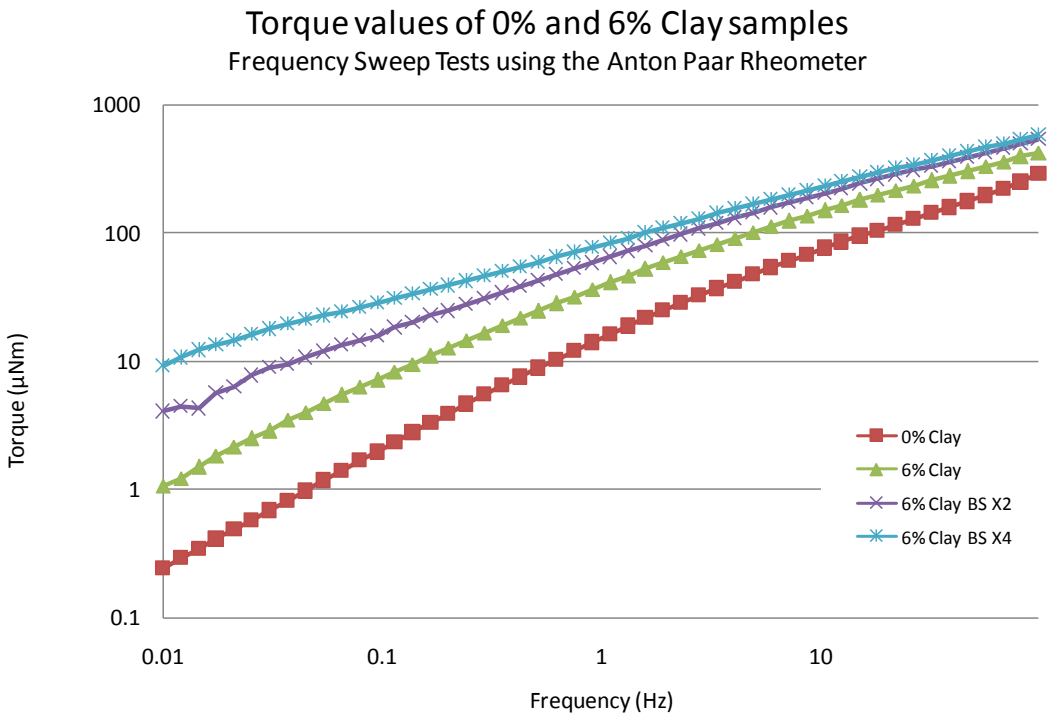

Figure 4.81: Torque vs. Frequency using Anton Paar

4.7 In-Line Rheological Evaluation using a Slit Die

Having established the usefulness of rheology in assessing nano-composite states and leading to finding optimum operating conditions, the next part of the work as stated in the objectives was to attempt an in-line rheological evaluation using the purpose made slit die attached to the end of the mini-mixer and the torque transducer fitted on the shaft of the screws. The arrangement was described in the Experimental Method chapter which also describes the data generation using Labview software. The results are displayed in Figures 4.82-85. The conclusions from these are as follows:

- The slit die as designed and operated is unable to give clear information on the data collected although a trend appears when comparing the data with those obtained from a rheometer (see Figure 4.84).
- The torque transducer also reveals unclear information suggesting that the viscosity increases from 0 to 2% loading then flatten thereafter only to drop suddenly at 8-10% clay loading.

Clearly on the basis of this information further research is required. It is noted here that the flow in the slit die is fully sheared so any structure that may have formed and would be detectable at very low shear rates (i.e. corresponding to the Linear Viscoelastic Region) would have been destroyed hence the difficulties in assessing the effect. Also, the slit die is not as precise instrument as a rheometer (temperature variation (see Figure 4.85), accuracy of pressure and flow measurement, accuracy of flow channel, etc.). As for the torque transducers it measures other frictional losses as well as those dissipated during mixing. More research is needed in this area to develop a more precise means of measuring rheology in-line. This is an interesting challenge and an important recommendation to

address, as if possible, it will complement the mini-mixer as an effective tool for nano-composite research.

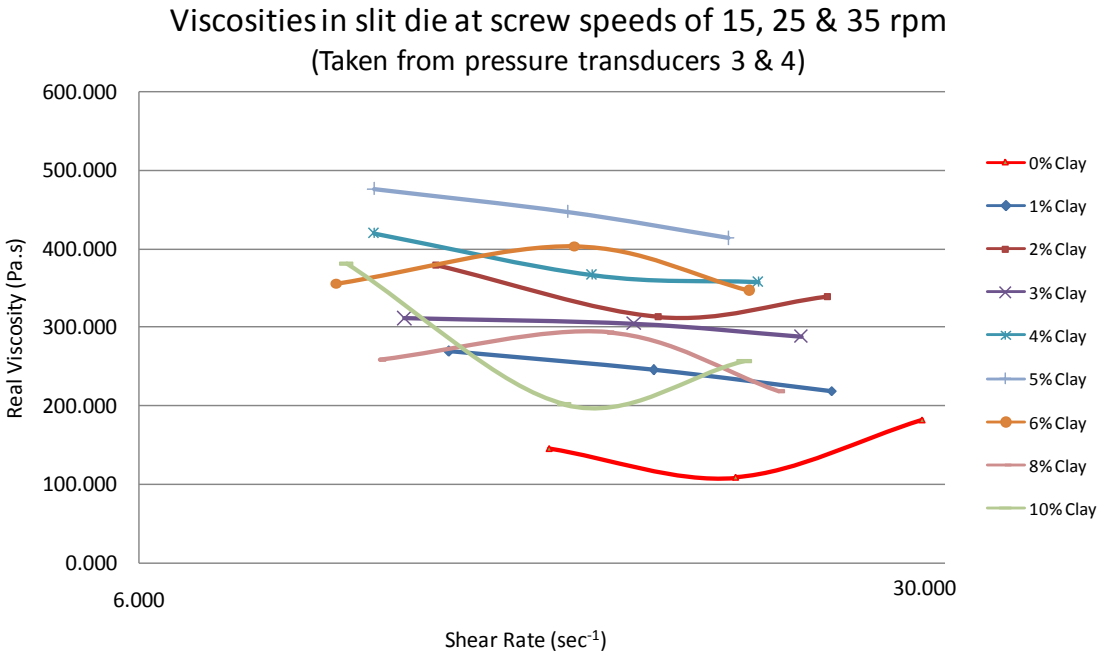

Figure 4.82: Viscosity vs. Shear rate from Pressure measurements

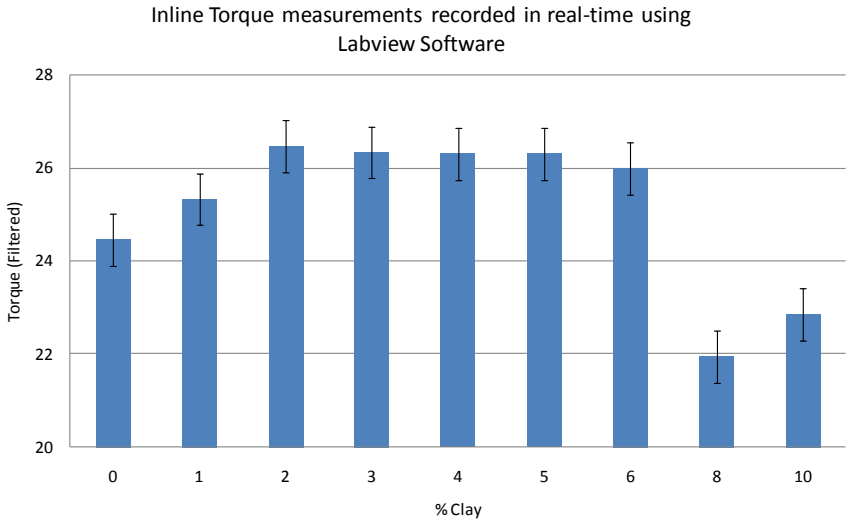

Figure 4.83: Inline Torque measurement in real time

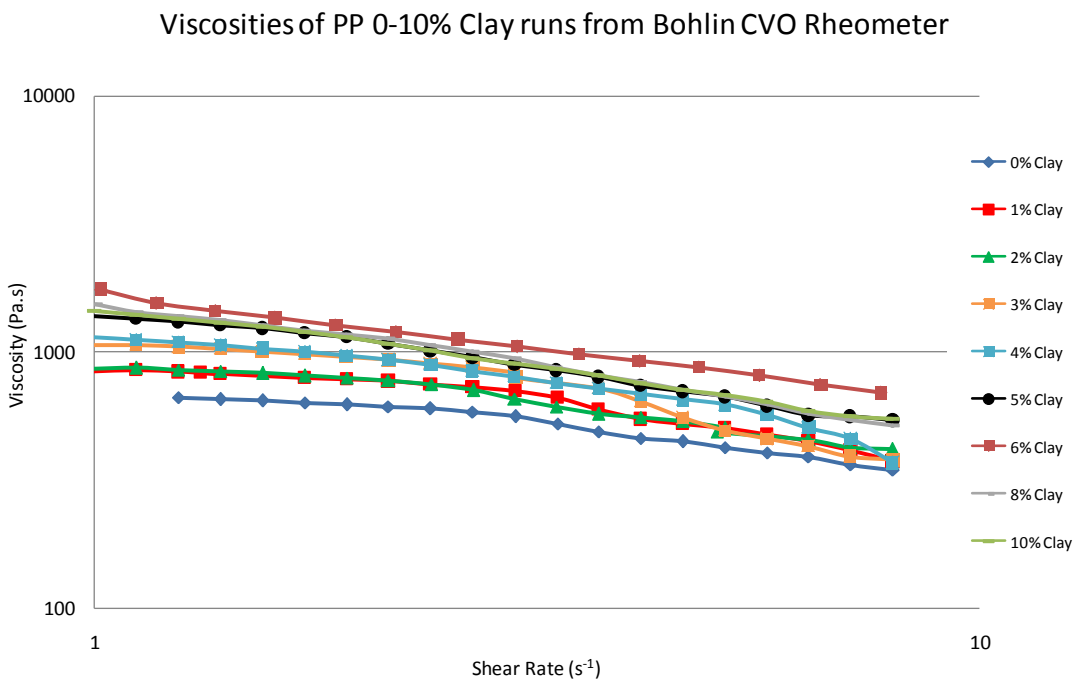

Viscosity vs. Shear rate of 0-10% clay samples

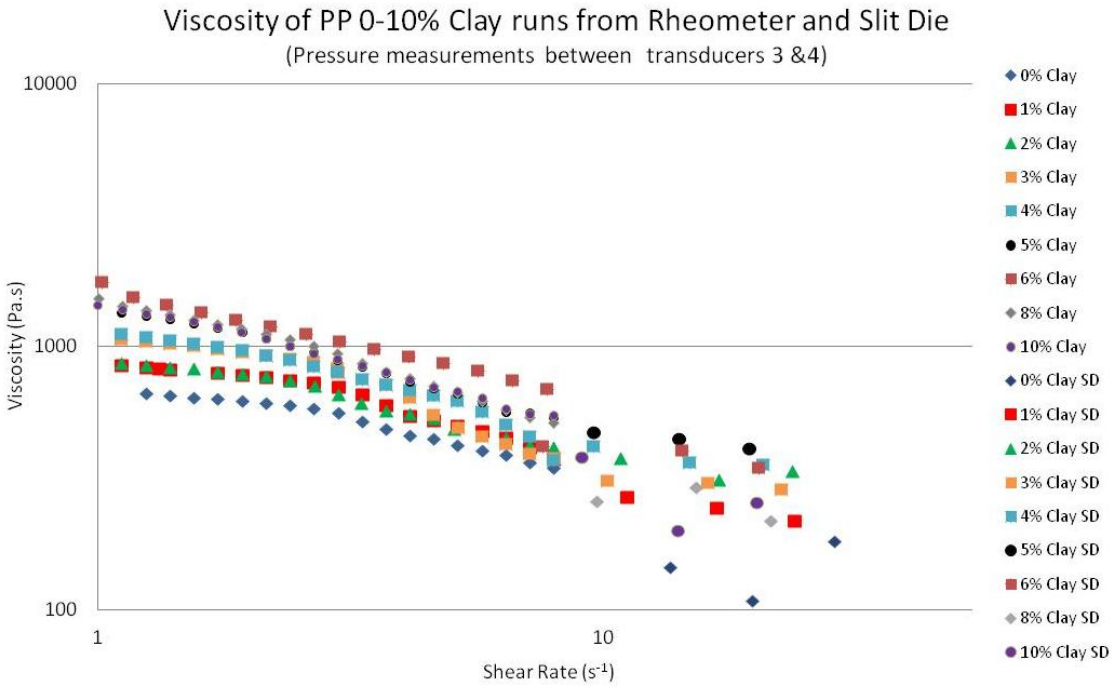

SD (Slit Die)

Figure 4.84: Viscosity vs. Shear Rate comparison

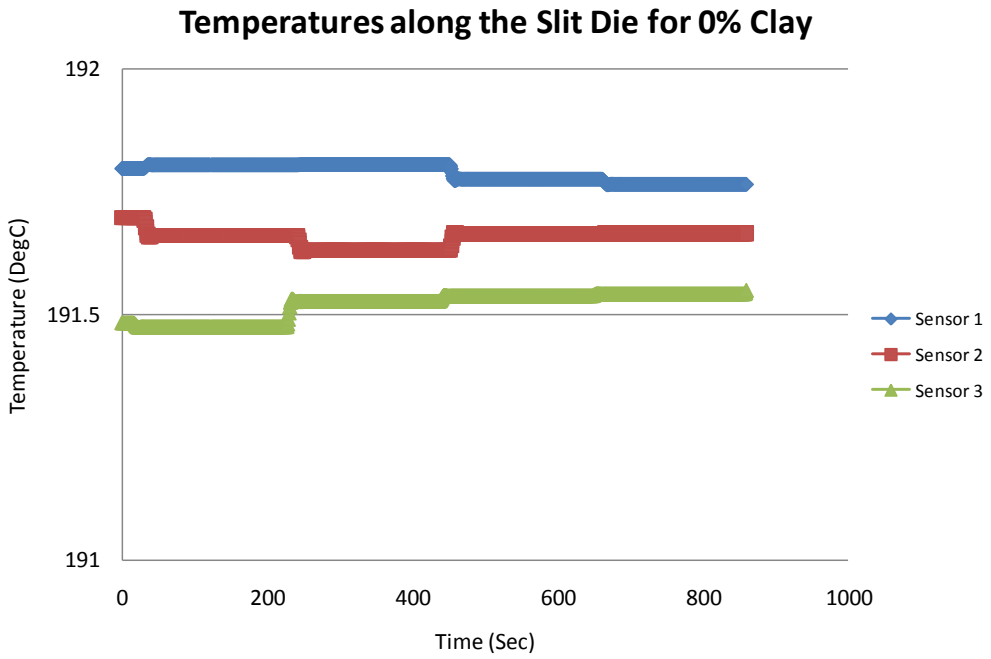

Figure 4.85: Temperature along slit die

4.8 In-line Evaluation of Nanocomposites using Ultrasound

This too was part of preliminary work aimed at complementing the ability of the mini-mixer. The ultrasound measurement ports used the same holes as those used for the pressure measurements. This is described in the Experimental Method chapter. The corresponding data are displayed in Figures 4.86-88 and the following conclusion can be made:

A correlation appears between the transit time of the ultrasound applied and the % clay added suggesting that ultra sound may be able to detect the percolation point. However, this evaluation needs further research and is part of the recommendations identified for further research.

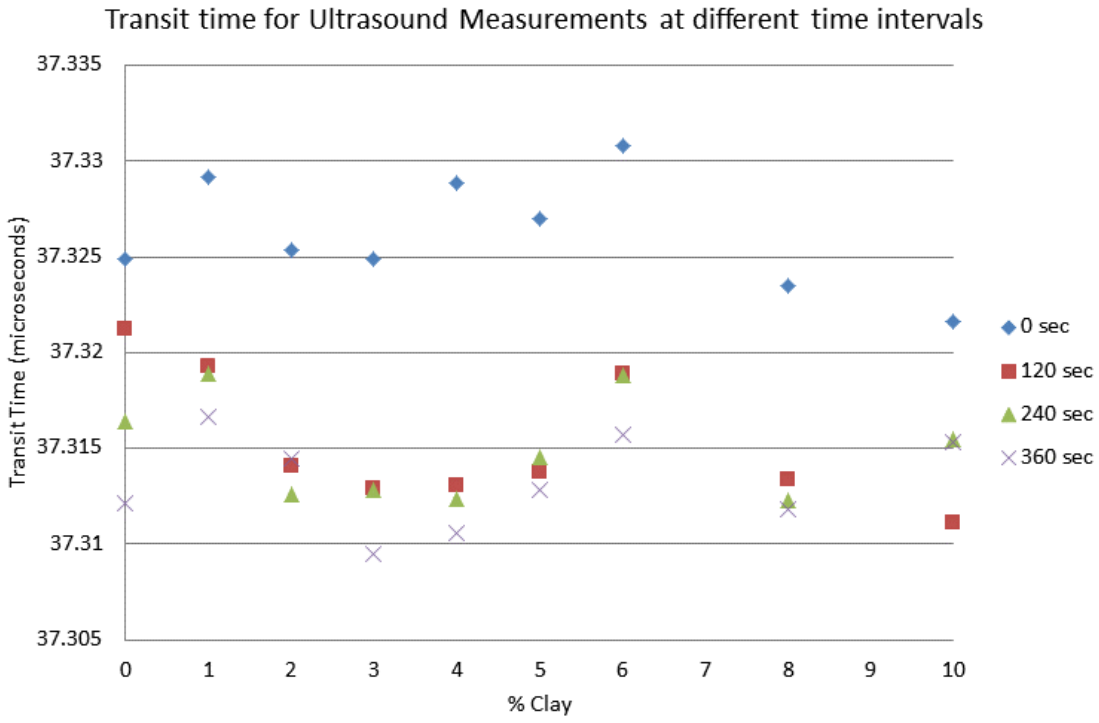

Figure 4.86: Ultrasound measurements of PP 0-10%wt Clay

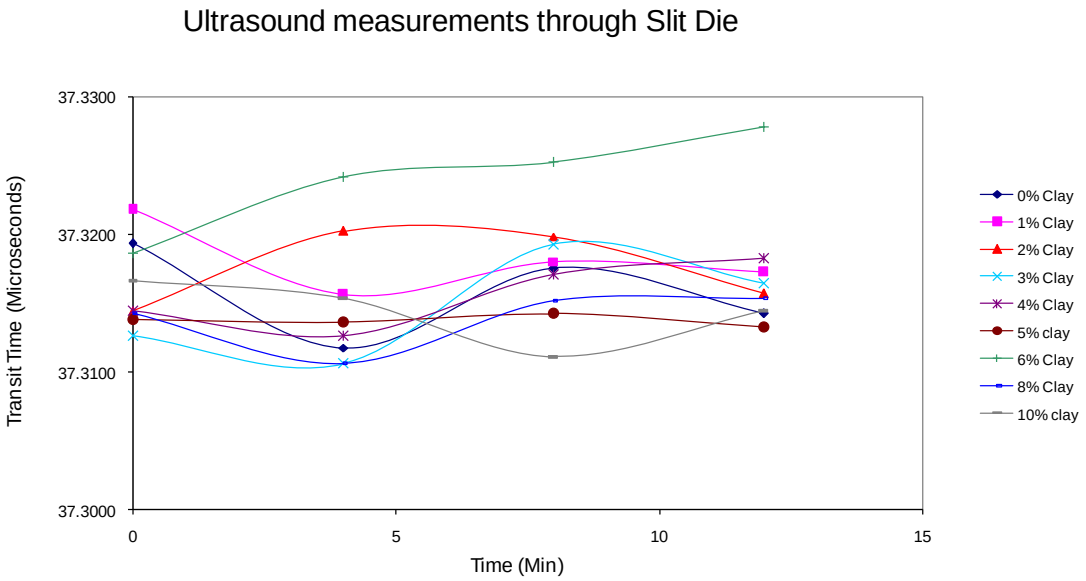

Figure 4.87: Ultrasound measurements of 0-10% clay samples

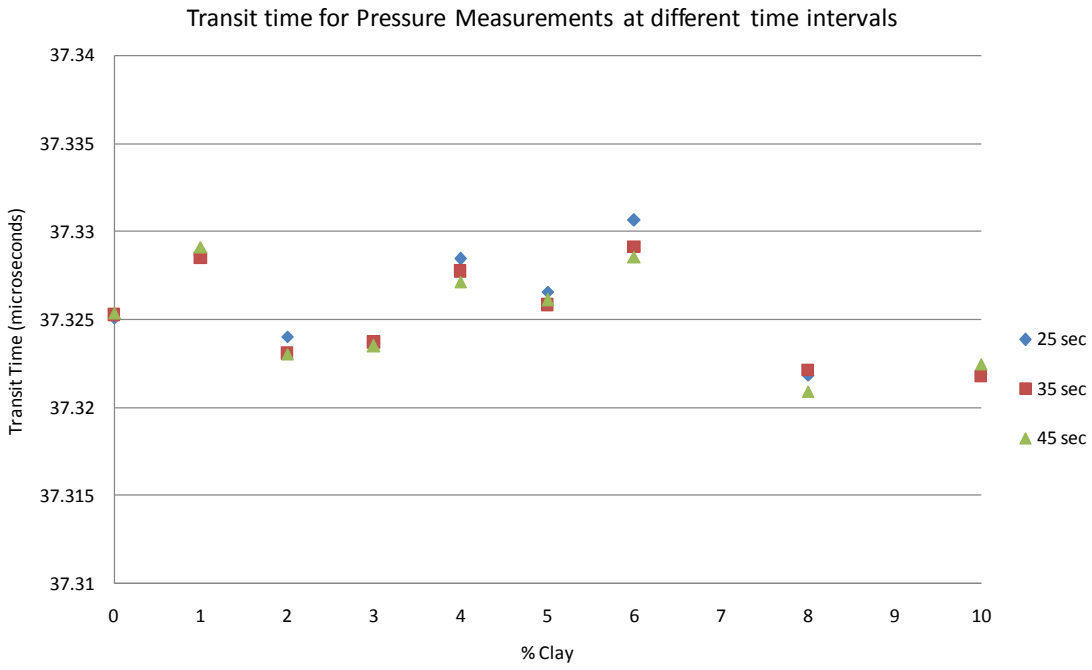

Figure 4.88: Ultrasound measurements of 0-10% clay samples

Chapter 5 : CONCLUSION / RECOMMENDATIONS

This comprehensive research project based on the processing and testing of PP polymer nanocomposite materials has included some unique research and findings that have not been carried out before, especially using a wide-ranging DOE experimental approach. It has been demonstrated that the development of polymer nanocomposite materials is a complex process that requires attention to detail and is sensitive to the slightest of changes in any of the factors being used e.g. temperature, residence mixing time, nanoclay / compatibiliser loading or the type of materials used.

It was shown that the minimixer was capable of undertaking high shear mixing for a range of time scales to generate a variety of polymer nanocomposite materials. Undertaking rheological measurements on these samples as an initial testing tool to determine the quality of these materials and ranking them in order of their properties was a positive way of determining the advantages of using this technique to quickly and efficiently find the best or worst materials. This in turn could be linked to the factors used in making those particular samples and thus distinguishing which factors could be used to advance the development of the nanocomposite materials with the optimum properties. The rheological testing procedure was also found to be accurate when compared with most of the other testing techniques and clearly highlighted the fact that experimental runs 4 and 6 from the DOE trials had the highest G' and G'' values and the control runs 21, 22 & 23 with 0 wt. % clay loading had the lowest values shown in figures 4.1 - 4.4. This outcome was also backed up by the various other tests including the mechanical testing.

Other findings that tied in well were the Creep and Recovery data that showed higher clay loaded samples had the highest creep values due to the materials becoming stiffer with clay loading.

The additional range of experiments undertaken which included the 0-10% clay loading of the PP material was also a very important procedure with interesting findings. The rheological data shown in figures 4.15 – 4.20 clearly showed a trend whereby the G' and G'' values increased with clay loading. The mechanical tests also confirmed these findings and the Creep & Recovery data also highlighted the stiffer material with clay loading through rheological testing. The other tests which included not pre-mixing the raw materials before processing in the minimixer, using Cloisite 10A clay, processing the material through the minimixer twice, again highlighted how sensitive small changes could affect polymer nanocomposites and how using rheological measurements could easily identify any weaknesses or strong points in a given number of their properties.

Another important finding was the significance of bi-axially stretching the polymer nanocomposite materials. This additional step substantially increased the G' and G'' values when compared with the original nanocomposite materials including certain mechanical properties and this finding was clearly observed from the vast majority of experimental trials undertaken on the bi-axially stretched samples. Comparisons between the G' values of PP tested in the non-stretched and stretched states at 2:1 and 4:1 stretch ratios (see Figure 4.27) clearly showed a significant increase (up to 10 fold) in the values which was presumed to have occurred as a result of further intercalation/exfoliation. Other observations including the frequency sweep data also showed similar effects (see G'', η^* and δ^0 variation with % clay in the un-stretched and stretched samples). The stretched

samples also showed an improvement in the elastic modulus and elongation values from mechanical testing. For example at 3% clay loading, the un-stretched sample has a modulus of 780 Pa compared with a modulus of 810 Pa at 2:1 stretch ratio and 900 Pa at 4:1 stretch ratio. Similar variations were observed throughout at all % clay addition. The important conclusion from these tests is the beneficial effect of stretching on elongational mixing which leads to enhanced intercalation-exfoliation and alignment of the clay platelets resulting in structural reinforcement of the nano-composites formed.

The inline tests carried out for the Viscosity & Ultrasound measurements through the slit-die did have some promising data as shown in figure 4.84 which showed that the viscosity using both the inline & offline methods followed a similar trend. The Ultrasound data was quite inconsistent due to background electrical disturbances but could be improved with further work.

In summary the ability of using rheology as an initial testing tool for nanocomposite materials has been proved to be desirable and able to distinguish between different materials at the nano scale.

As for the recommendations, further work looking into the in-line monitoring of both the Viscosity and Ultrasound measurements of the melt flow of the nanocomposite materials through the slit die attachment could be improved. This area of the research was not studied in great depth due to a busy schedule but would be of great importance in quickly and effectively determining the significance of various nanocomposite materials being processed by the minimixer if implemented correctly. It would of course require

further development of both hardware and software systems but could pose as a useful tool for both academic and industrial partners in the long term with many beneficial outcomes.

Another course of action could be the addition of a unit to the minimixer that can undertake stretching of the exiting extrudate material in a variety of directions. This could therefore allow the material to be stretched without the added step of stretching it later using separate equipment. This could potentially generate a polymer nanocomposite with improved properties but would need to be thoroughly researched.

The continued research into the electrical conductivity trials of polymer nanocomposites would be advantageous. Due to an increased demand for new products especially conductive polymers for many markets, further work into the testing of conductive polymer nanocomposites could be utilised by the use of the Keithley 610C electrometer at Bradford. This equipment allows the resistance of the nanocomposite sample to be measured which in turn would be used to calculate the resistivity and thus the conductance and is highlighted in the appendix in further detail.

REFERENCES

1. Pinnavaia, T.J. and Beall G.W., (2002) Polymer-Clay Nanocomposites, John Wiley & Sons, Ltd, New York.
2. Giannelis, E.P., (1998) Polymer-layered silicate nanocomposites: synthesis, properties and applications, Applied Organomettalic Chemistry, 12, 675–680.
3. Mirabella M. Francis, Jr., (2004) Polypropylene and TPO Nanocomposites, Dekker Encyclopedia of Nanoscience and Nanotechnology, 5, pp. 3015-3038
4. Oriakhi, C.O. (1998) Nano Sandwiches, Chem. Br., 34: 59–62.
5. Keegan, J., (2004) A history of warefare. Pimlico ISBN 978-1844137497.
6. Hall, A., (2006) The development of reinforced composites, journal of the society of Antiquaries 49, 65-77.
7. Guedes, R.M., Morais, J.J.L., Marques, A.T., Cardon, H.C. (2000). Prediction of long-term behaviour of composite materials. New York.
8. Gerstale. F., (1985) Composites: Encyclopedia of polymer science and technology, vol. 3, New York: Wiley.
9. Usuki, A., Kawasumi, M., Kojima, Y., Okada, A., Kurauchi, T. and Kamigaito, O.J. (1993) Swelling Behavior of Montmorillonite Cation Exchanged for V-amino Acids by E-caprolactam, Mater. Res., 8(5): 1174.
10. Usuki A, (1995) `Interaction of nylon-6 clay surface and mechanical-properties of nylon-6 clay hybrid', J. Appl. Polym. Sci. 55: 119±123.
11. Kojima Y, (1993) `One-pot synthesis of nylon-6 clay hybrid', J. Polym. Sci. A Polym. Chem, 31: 1755±1758.
12. Ijima, S. (1991) Nature 354 p. 56-58.

13. Liu, H.; Brinson, C. (2008); Composite Science Technology. 68(6) 1463-1470.
14. Krishnamoorti, R.; Vaia, R.A.; Giannelis, E.P. (1996) Chem. Mater. 8 p. 1728-1734.
15. Hussain, F.; Hojjati, M.; Okamoto, M.; Gorga, R.E. J. (2006) Composite Materials 40(17) p.1511-1565.
16. Krishnamoorti, R. and Yurekli, K., (2001) Rheology of polymer layered silicate nanocomposites. Current Opinion in Colloid & Interface Science, 6(5-6): p. 464-470.
17. Sinha, R.S, Okamoto K. and Okamoto M., (2003) Structure–property relationship in biodegradable poly(butylenes succinate)/layered silicate nanocomposites Macromolecules, 36, pp. 2355–2367.
18. Alexandre, M. and P. Dubois, (2000) Polymer-layered silicate nanocomposites: preparation, properties and uses of a new class of materials. Materials Science and Engineering: R: Reports, 28(1-2): p. 1-63.
19. Vaia, R.A., Ishii H. and Giannelis E.P., (1993) Synthesis and properties of two-dimensional nanostructures by direct intercalation of polymer melts in layered silicates, Chemistry of Materials, 5, pp. 1694–1696.
20. Breuer, O., U. Sundararaj, and R.W. Toogood, (2004) The design and performance of a new miniature mixer for specialty polymer blends and nanocomposites. Polymer Engineering and Science, 44(5): p. 868-879.
21. Harold F. Giles, J., E.M.M. III, and J. John R. Wagner, (2005) Extrusion: The Definitive Processing Guide and Handbook: William Andrew Publishing.

22. Yao, C.H. and I. Manas-Zloczower, (1998) Influence of design on dispersive mixing performance in an axial discharge continuous mixer - LCMAX 40. Polymer Engineering and Science, 38(6): p. 936-946.
23. Covas, J.A. and P. Costa, (2004) A miniature extrusion line for small scale processing studies. Polymer Testing, 23(7): p. 763-773.
24. Benkreira, H., Butterfield, R., Gale, M. and Patel, R. (2008) Replication of mixing achieved in large corotating screw extruders using novel laboratory 10-100g minimixer. Plastics Rubber and Composites, 37(2-4): p. 74-79.
25. Butterfield, R., (2009) A Novel Laboratory Dispersive & Distributive Minimixer & Applications, in IRC, University of Bradford: Bradford.
26. Ma, J.S., Qi, Z.N., and Hu, Y.L., (2001) "Synthesis and characterization of polypropylene/clay nanocomposites", Journal of Applied Polymer Science, 82, pp. 3611-3617
27. Manias, E., (2001) "A direct-blending approach for polypropylene/clay nanocomposites enhances properties", Materials Research Society Bulletin, 26, pp. 862 – 863
28. Lei, S, Hoa, S. V.G., Ton, That M.T, (2006) "Effect of clay types on the processing and properties of polypropylene nanocomposites", Composites Science and Technology, 66, pp. 1274-1279
29. Ding, C., Jia, D., Hui, H., Guo, B., and Hong, H., (2004) "How Organo-Montmorillonite Truly Affects The Structure And Properties Of Polypropylene",Polymer Testing, 20, pp. 1-7.

30. Mirabella M. Francis, Jr., (2004), “Polypropylene and TPO Nanocomposites”, Dekker Encyclopedia of Nanoscience and Nanotechnology, 5, pp. 3015-3038
31. Schmidt, D., Shah, D. and Giannelis, E.P. (2002). New Advances in Polymer/Layered Silicate Nanocomposites, Current Opinion in Solid State and Materials Science, 6(3): 205–212.
32. Fedullo, N., Sorlier, E., Sclavons, M., Bailly, C., Lefebvre, J.M., Devaux, J., (2007) Polymer-based nanocomposites: Overview, applications and perspectives. Progress in Organic Coatings, 58(2-3): p. 87-95
33. Peter J. T. Morris (2005). Polymer Pioneers: A Popular History of the Science and Technology of Large Molecules. Chemical Heritage Foundation. p. 76.
34. Vaia R.A, Jant K.D., Kramer E.J., Giannelis E.P., (1996) Microstructural evaluation ofmelt-intercalated polymer-organically modified layered silicate nanocomposites, Chemical Materials, Vol.8,pp. 2628–2635.
35. Zhu, S., Chen, J., Zuo, Y., Li, H and Cau, Y., (2011) Montmorillonite/polypropylene nanocomposites: Mechanical properties, crystallization and rheological behaviours. Applied clay science, (52), p171-178.
36. Ellis, T.; D’Angelo, J. (2003) Thermal and Mechanical Properties of a Polypropylene Nanocomposite. Journal of Applied Polymer Science, 90: 1639–1647.
37. Demin J., Chao D., Hui H., Baochun G., Haoqun H., (2005) “How organomontmorillonite truly affects the structure and properties of polypropylene”, PolymerTesting,Vol.24,pp. 94-100.

38. Gianelli, W., Ferrara, G., Camino, G., Pellegatti, G., Trombini, R.C., (2005) Effect of matrix features on polypropylene layered silicate nanocomposites, Polymer, Volume 46, Issue 18, p. 7037-7046
39. Lei, S, Hoa, S. V.G., Ton-That M.T, (2006) "Effect of clay types on the processing and properties of polypropylene nanocomposites", Composites.
40. Sinha, R.S, Okamoto K. and Okamoto M., (2003), "Structure–property relationship in biodegradable poly(butylenes-succinate)/layered silicate nanocomposites" Macromolecules, 36, pp. 2355–2367.
41. Peter, R., Hansjörg, N., Stefan, K., Rainer, B., and Ralf, T. R., (2001) "Poly(propylene)/organoclay nanocomposite formation: Influence of compatibilizer functionality and organoclay modification", Macromolecular Materials and Engineering, 1, pp. 8-17
42. Sinha Ray S, Okamoto M. (2003) Polymer/layered silicate nanocomposites: a review from preparation to processing. Polymer Science 28:1539–1641
43. Hoa, S.V., Lei, S.G., Ton That, M.T., (2001) Effect of clay types on the processing and properties of polypropylene nanocomposites, Composite Science and Technology, Vol. 66, pp.1274-1279
44. Kawasumi M, Hasegawa N, Kato M, Usuki A, Okada A. (1997) Preparation and mechanical properties of polypropylene-clay hybrids. Macromolecules 30:6333-6338
45. Dennis, H.R.; Hunter, D.L.; Chang, D.; Kim, S.; White, J.L.; Cho, J.W.; Paul, D.R. (2001) Polymer 42 p. 9513-9522.

46. Chin, I.J., Thurn, A. T., Kim, H.C., Russel, T.P. and Wang, J. (2001). On Exfoliation of Montmorillonite in Epoxy, Polymer, 42: 5947–5952.
47. Sinha Ray S, Okamoto M (2003) Polymer/layered silicate nanocomposites: a review from preparation to processing. Prog Polym Sci 28:1539–1641
48. Manas-Zloczower, I. and H.T. Cheng, (1996) Analysis of mixing efficiency in polymer processing equipment. Macromolecular Symposia, 112: p. 77-84.
49. Cho, J.W., Paul D.R., (2001) Nylon 6 nanocomposites by melt compounding. Polymer ;42:1083–94.
50. Park, J.U., Kim, J.L., Kim, D.H., Ahn, K.H. & Lee, S.J., (2006) Rheological behaviour of Polymer / Layered Silicate Nanocomposites under Uniaxial Extensional Flow, Macromolecular Research, Vol. 14, No. 3, pp 318-323.
51. Kim, D.H., Fasulo, P.D., Rodgers, W.R and Paul, D.R., (2007) Structure and properties of polypropylene-based nanocomposites: Effect of PP-g-MA to organoclay ratio, Polymer 48, pp. 5308-5323
52. Rohlmann, C.O., Horst, M.F., Qunizani, L.M. & Failla, M.D., (2008) Comparative analysis of nanocomposites based on polypropylene and different montmorillonies, European Polymer Journal, 44, pp 2749-2760.
53. Hejazi, I., Seyfi, J., Sadeghi, G.M.M. & Davachi, S.M., (2011) Assessment of rheological and mechanical properties of nanostructured materials based on thermoplastic olefin blend and organoclay, Materials & Design, vol. 32, pp. 649-655

54. Lee, S.H., Cho, E. & Young, J.R., (2006) Rheological behaviour of PP/layered silicate nanocomposites prepared by melt compounding in shear and elongational flows, Wiley Interscience, DOI 10.1002/app.25204
55. Mould, S., Barbas, J., Machado, A.V., Nobrega, J.M. & Covas, J.A., (2011) Measuring the rheological properties of polymer melts with online rotational rheometry, Polymer Testing, Vol. 30, pp. 602-610.
56. Liaw, J.H., Hsueh, T.Y., Tan, T.S., Wang, Y. and Chiao, S.M., (2007) Twin-screw compounding of poly(methyl methacrylate)/clay nanocomposites: effects of compounding temperature and matrix molecular weight. Polymer International, 56(8): p. 1045-1052.
57. Padmanabhan, B., (2008) Understanding the Extruder Processing Zone: the heart of a twin screw extruder. Plastics, Additives and Compounding, 10(2): p. 30-35.
58. Y. Lui, N. Nishimura and Y. Otani, (2011) Computational Material Science.
59. Tang Y, Hu Y, Song L, Zong R, Gui Z, Chen Z, (2003) Preparation and thermal stability of polypropylene/montmorillonite nanocomposites. Polymer Degradation Stab ;82:127–31.
60. Benetti EM, Causin V, Marega C, Marigo A, Ferrara G, Ferraro A, (2005) Morphological and structural characterization of polypropylene based nanocomposites. Polymer; 46:8275–85.
61. Anastasiadis, S.H., K. Chrissopoulou, and B. Frick, (2008) Structure and dynamics in polymer/layered silicate nanocomposites. Materials Science and Engineering: B,. 152(1-3): p. 33-39.

62. Tortora M, Vittoria V, Galli G, Ritrovati S, Chiellini E. (2002) Transport properties of modifiedmontmorillonite–poly(_-caprolactone) nanocomposites. Macromol Mater Eng; 287:243–9.
63. Gorrasi G, Tortora M, Vittoria V, Pollet E, Lepoittevin B, Alexandre M, (2003) Vapor barrier properties of polycaprolactone montmorillonite nanocomposites: effect of clay dispersion. Polymer; 44:2271–9.
64. Xie, S., Harkin-Jones, E., Shen, Y., Hornsby, P., McAfee, M., McNally, T., Patel, R., Benkreira, H., and Coates, P, (2010) Quantitative characterization of clay dispersion in polypropylene-clay nanocomposites by combined transmission electron microscopy and optical microscopy. Materials Letters, Volume 64(Issue 2): p. Pages 185-188.
65. Kim, D.H., Fasulo, P.D., Rodgers, W.R. and Paul, D.R., (2007) Structure and properties of polypropylene-based nanocomposites: Effect of PP-g-MA to organoclay ratio. Polymer, 48(18): p. 5308-5323.
66. Shelley JS, Mather PT, DeVries KL. (2002) Reinforcement and environmental degradation of nylon 6/clay nanocomposites. Polymer; 42:5849–58.
67. Liu X,Wu Q. (2002) Polyamide 66/clay nanocomposites via melt intercalation. Macromolecular Material Engineering; 287:180–6.
68. Hwan Lee, S., E. Cho, and J. Ryoun Youn, (2007) Rheological behavior of polypropylene/layered silicate nanocomposites prepared by melt compounding in shear and elongational flows. Journal of Applied Polymer Science, 103(6): p. 3506-3515.

69. Galindo-Rosales, F.J., P. Moldenaers, and J. Vermant, (2011) Assessment of the Dispersion Quality in Polymer Nanocomposites by Rheological Methods. Macromolecular Materials and Engineering, 296(3-4): p. 331-340.
70. Abu-Zurayk., R, Harkin-Jones E, McNally T, Menary G, Martin P, Armstrong C. (2009) Biaxial deformation behavior and mechanical properties of a polypropylene/clay nanocomposite. Composite Science & Technology; 69:1644–52.
71. Abu-Zurayk., R, Harkin-Jones E, McNally T, Menary G, Martin P, Armstrong C. (2010) Structure–property relationships in biaxially deformed polypropylene nanocomposites. Composite Science & Technology; 70:1353–59.
72. Rajeev, R.S., Harkin-Jones. E., Soon, K., McNally. T., Menary. G., Martin P, Armstrong C., (2009) Studies on the effect of equi-biaxial stretching on the exfoliation of nanoclays in polyethylene terephthalate. European Polymer Journal, 45(2): p. 332-340.
73. Rosato, Marlene, G., (2000) Concise encyclopedia of plastics, Springer, p.245, ISBN 9780792384960
74. Touati, N., Kaci, M., Bruzaud S., Grohens. Y., (2011) The effects of reprocessing cycles on the structure and properties of isotactic polypropylene/cloisite 15A nanocomposites. Polymer Degradation and Stability, 96(6): p. 1064-1073.
75. Kozlowski, M., and Iwanczuk, A., (2008) "Recycling of polymer and polymer nanocomposites", Wroclaw University of Technology; Faculty of Environmental Engineering; Materials Recycling Center of Excellence; Polish Structural Fund Innovative Economy POIG 01.03.01-00-018/08, (Presentation)

76. Bur, A.J., Lee, Y.H., Roth, S.C., Start, P.R., (2005) Measuring the extent of exfoliation in polymer/clay nanocomposites using real-time process monitoring methods.Polymer, 46(24): p. 10908-10918.
77. Bertolino, M.K. and S.V. Canevarolo, (2010) Preparation of extruded melt-mixed polypropylene/montmorillonite nanocomposites with inline monitoring. Polymer Engineering & Science, 50(3): p. 440-445.
78. Utracki, L.A., (2008) Polymeric nanocomposites: Compounding and performance. Journal of Nanoscience and Nanotechnology, 8(4): p. 1582-1596.
79. Wang, Y., Chen, F.B., Li, Y.C., Wu, K.C., (2004) Melt processing of polypropylene/clay nanocomposites modified with maleated polypropylene compatibilizers. Composites Part B: Engineering, 35(2): p. 111-124.
80. Lim, Y.T., Park. O., (2001) Phase morphology and rheological behaviour of polymer/layered silicate nanocomposites. Rheologica Acta 40(3): p. 220-229.
81. Wang, K., Liang, S., Zhao, P., Qu. C., Tan, H., Du, R., Zhang, Q. and Fu, Q., (2007) Correlation of rheology-orientation-tensile property in isotactic polypropylene/organoclay nanocomposites. Acta Materialia, 55(9): p. 3143-3154.
82. Chen, S.C., Tsai, R.I., Lin, T.K., (2005) Preliminary study of polymer melt rheological behaviour flowing through micro channels; Dept. of Mech. Eng.; Taiwan; Vol. 32; Issue 3-4; Elsevier
83. Sweeney, J., Spares, R., Woodhead, M. (2009), A constitutive model for large multiaxial deformations of solid polypropylene at high temperature. Polymer Engineering Science 49; 1902.

84. Martin, P.J., Tan, C.W., Tshai, K.Y., McCool, R., Menary, G. & Armstrong, C.G., (2005) Biaxial characterization of materials for thermoforming and blow molding. Plastic Rubber Composites, 34: p. 276-282.

85. Capt, L., Kamal, M.R., Munstedt, H., Stopperka, K. and Sanze, J., (2001) Morphology Development during Biaxial Stretching of Polypropylene Films. Proceedings of 17th Annual Meeting of the Polymer Processing Society, Montreal.

APPENDICES

DSC Results

The following curves were generated for the PP0-10% clay samples using the DSC TA software.

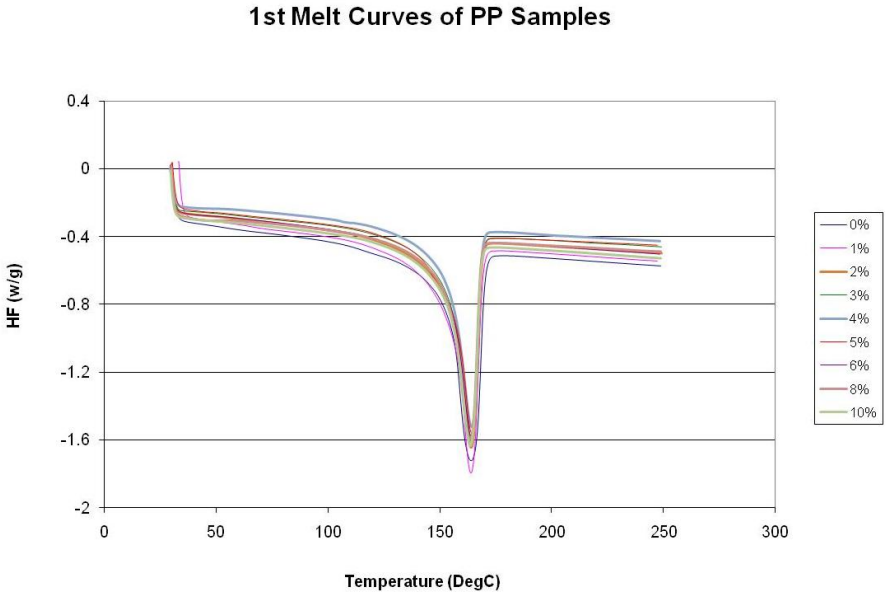

1st melt curves from DSC

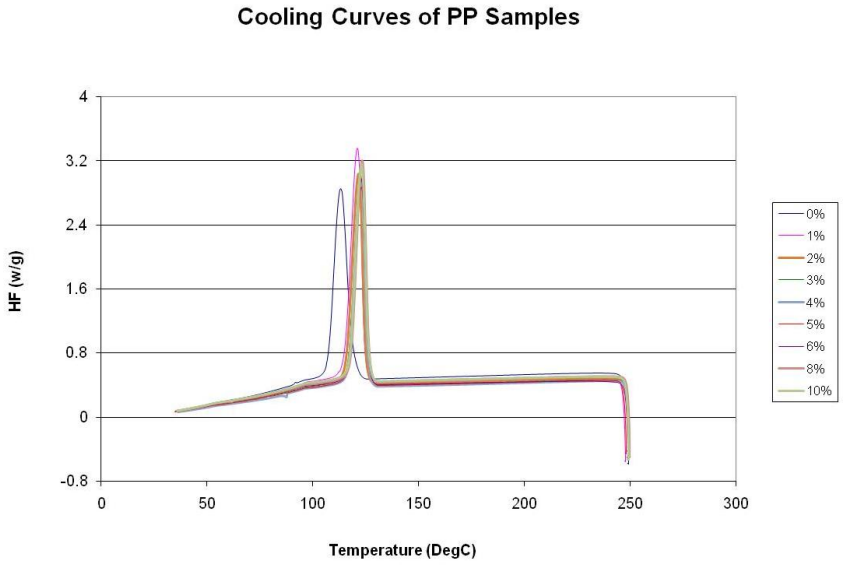

Cooling curves from DSC

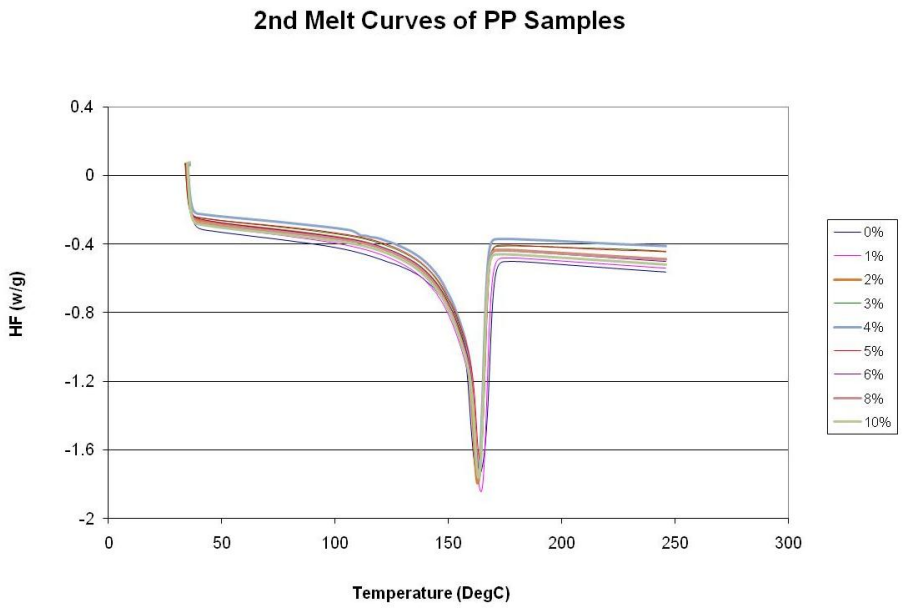

2nd melt curves from DSC

From these it can be seen that the 1st and 2nd melt curves for all the samples are very much overlapping at the same melting temperature. From this it can be stated that clay % does not play a major part in altering the melting temperatures. For the cooling temperature, this once again shows all the samples to be closely packed together.

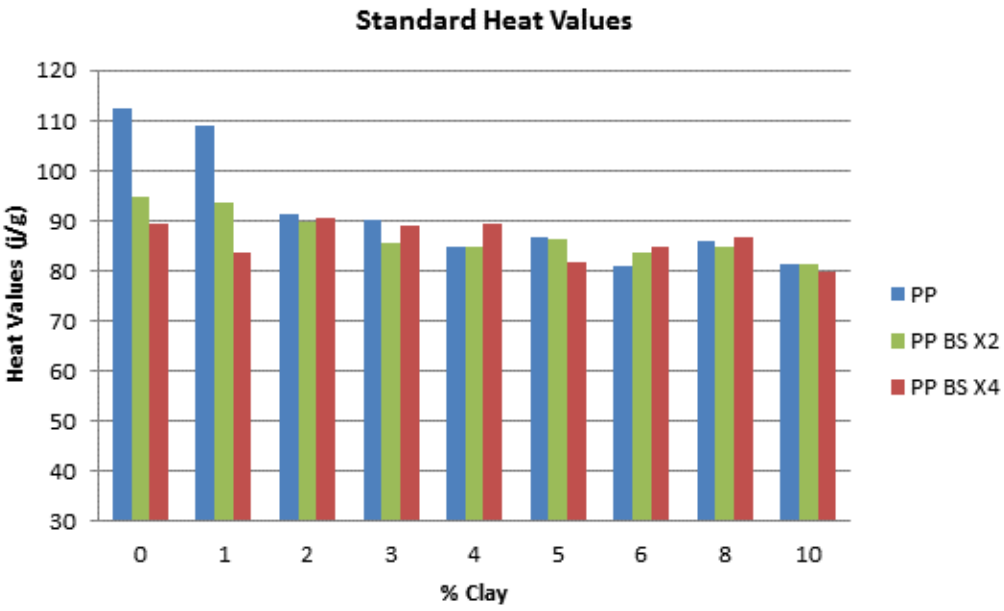

Heat vs. % Clay for 0-10% clay samples

DMA Results

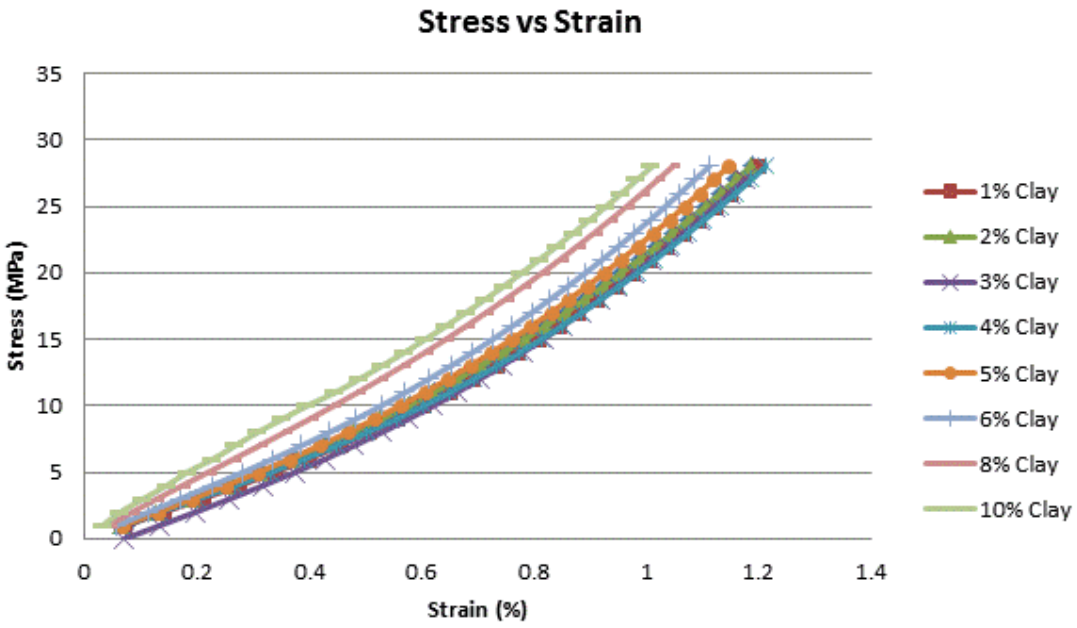

Stress vs Strain chart from DMA data

Additonal DMA tests using Multi-Frequency Strain (MFS) and Multi Strain (MS) Modes were conducted. For MFS the strain was kept constant at 0.1% and the frequency changed from 0.1 to 100Hz at room temp. The following graph was generated from the test data.

From the observations there was no distinct pattern for clays 0-6% but the 8 and 10% clay samples showed higher Storage Modulus values. This would indicate that the testing of such nanocomposites at room temperature could yield good mechanical property results with the addition of high quantities of clay, preferably 8/10% clay or higher.

On the other hand melt testing the samples could yield good results with the addition of much lower clay concentrations, as observed in the rheolocial experiments.

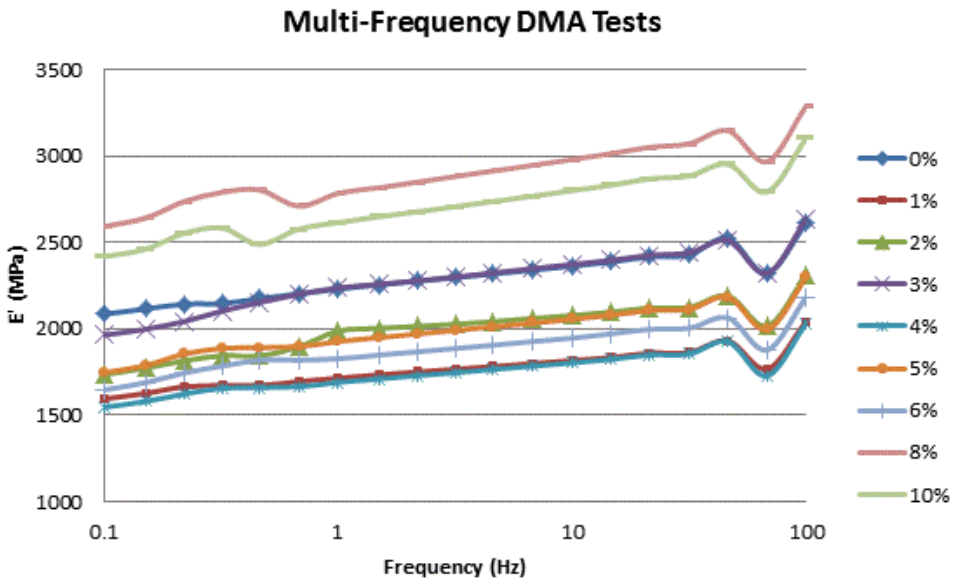

Multi-Frequency from DMA tests

For the MS tests, the frequency was kept constant at 1Hz but the amplitude was increased from 10 to 500 µm at room temp. With this data the following graph was plotted.

Once again there was no distinct pattern that could be observed, but higher storage modulus values were observed with the 8 and 10% clay samples. The same scenario as above could be taken into consideration.

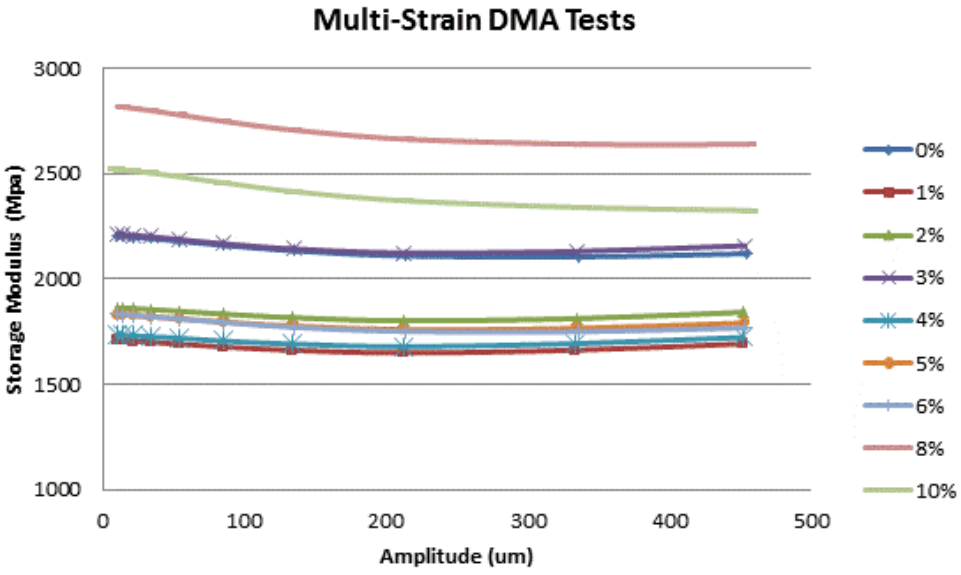

Multi-Strain from DMA tests

PET DOE trials

The following Design of Experiment (DOE) results were undertaken using the PET base material together with Somasif MTE as the nano-additive. The different factors that were used are shown in the table below. The range of factors used was lower than the PP trials since the processing conditions of PET were more difficult using the minimixer equipment after initial trial runs. The overall experimental setup consisted of 13 runs with the different factors and an additional 4 runs with a reduced residence mixing time of ½ minute. The testing of these nanocomposite materials together with the entire results was undertaken by the research team based at Queens University, Belfast.

Different factors used for PET trails

Factor	Name	Units	Type	Low	High
1	Temperature	°C	Numeric	270	285
2	Speed	rpm	Numeric	20	60
3	Residence Time	min	Numeric	1	3
4	Nanoclay Loading	%	Numeric	2	6

PET DOE runs

PET Design of Experiment (1/2 Factorial)				
Run	Speed	Temperature	Time	Clay Loading
Order	(rpm)	(Deg C)	(min)	(%)
1	20	270	1	2
2	60	285	1	2
3	40	277.5	2	4
4	60	270	1	6
5	20	285	3	2
6	60	270	3	2
7	20	285	1	6
8	20	270	3	6
9	60	285	3	6
10	20	270	1	0
11	60	270	3	0
12	20	285	1	0
13	60	285	3	0
14	20	270	0.5	2
15	60	285	0.5	2
16	60	270	0.5	6
17	20	285	0.5	6

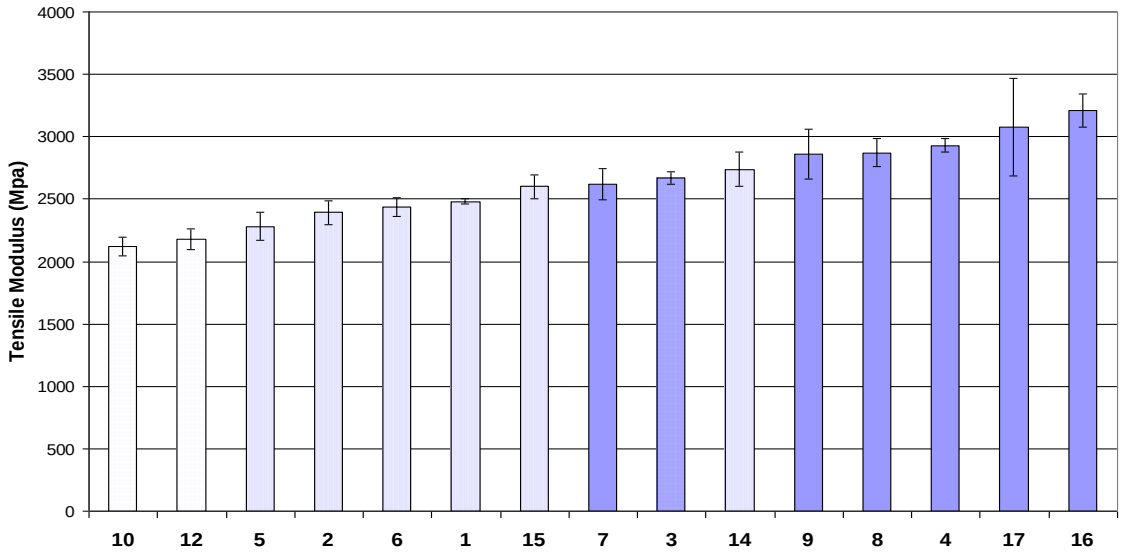

Tensile modulus of PET samples

The Modulus showed an increase with clay loading (Max.~51% difference)

The Modulus increased ~ 10% after reducing time from 1 to 0.5 min

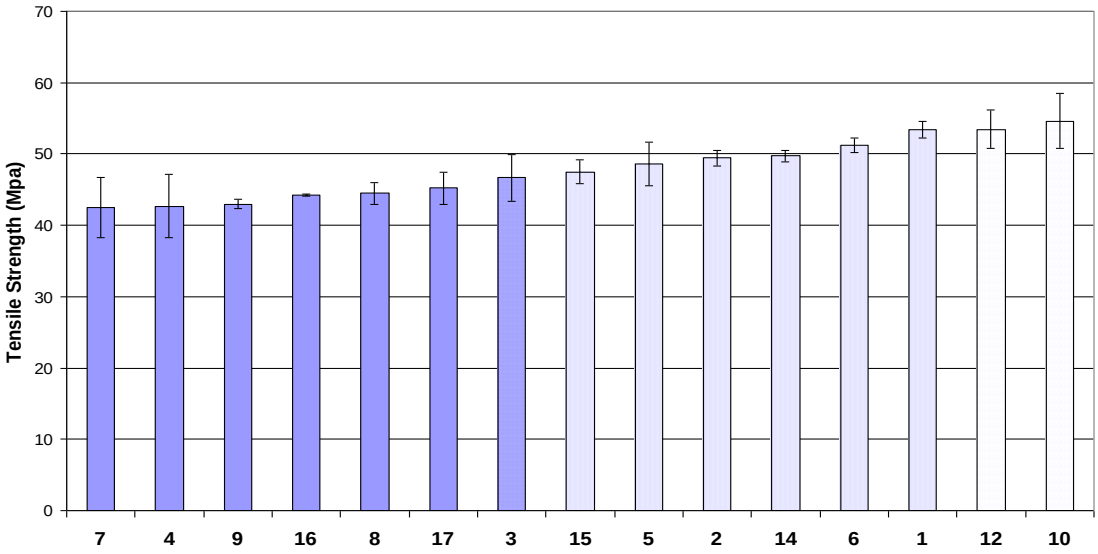

Tensile strength of PET samples

The Tensile strength decreased with clay loading (Max.~28% difference)

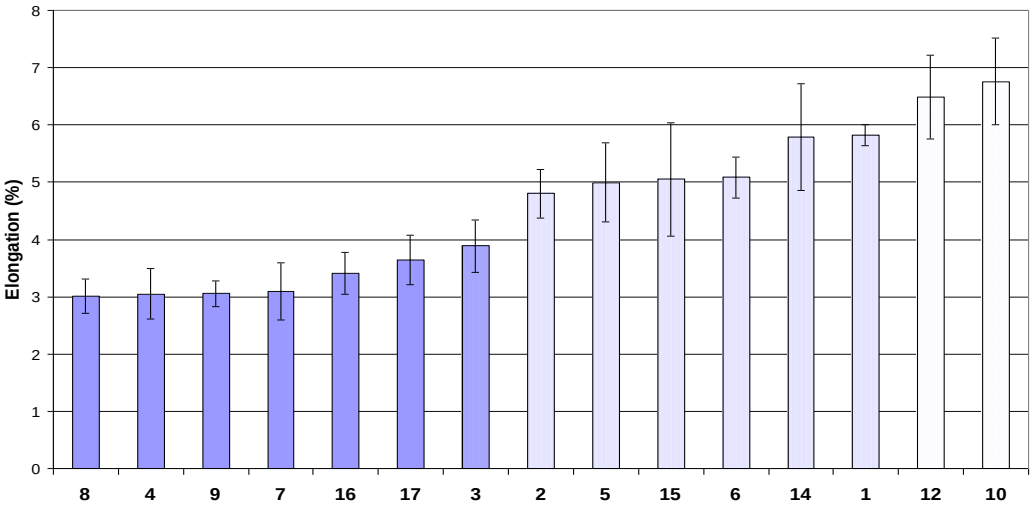

Elongation of PET samples

The Elongation decreased with clay loading (Max.~125% difference)

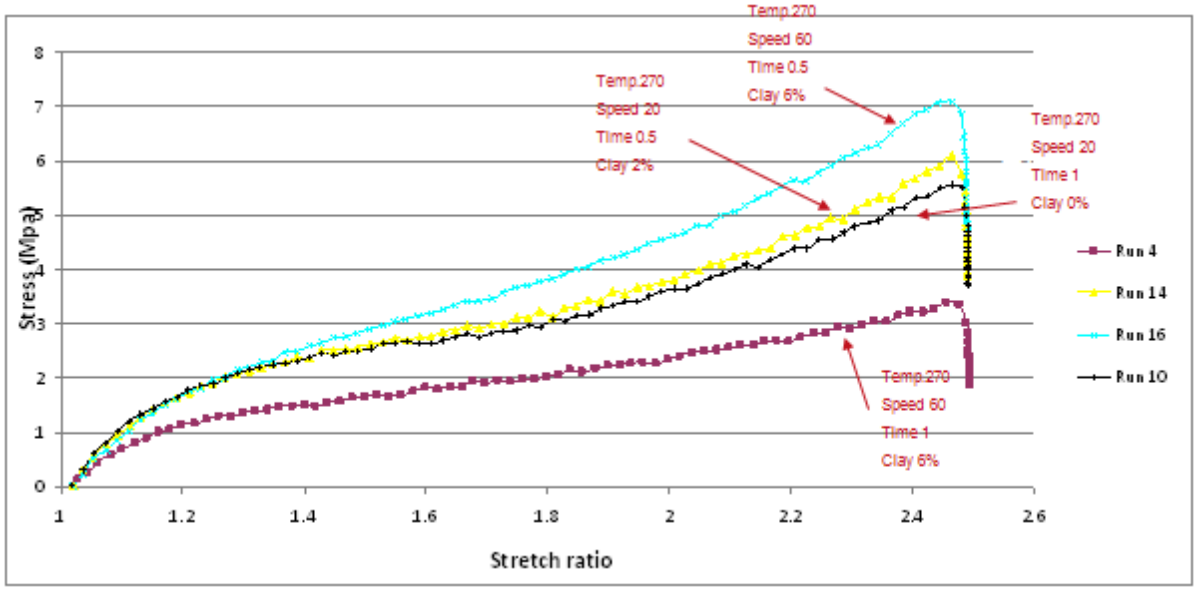

Biaxial stretch curves of PET samples

The biaxial stretching parameters were:

- Stretch ratio: $\lambda = 2.5$
- Strain rate: $\dot{\varepsilon} = 2\ /s$
- Temperature: $T = 100\ °C$
- Heating time: 2min

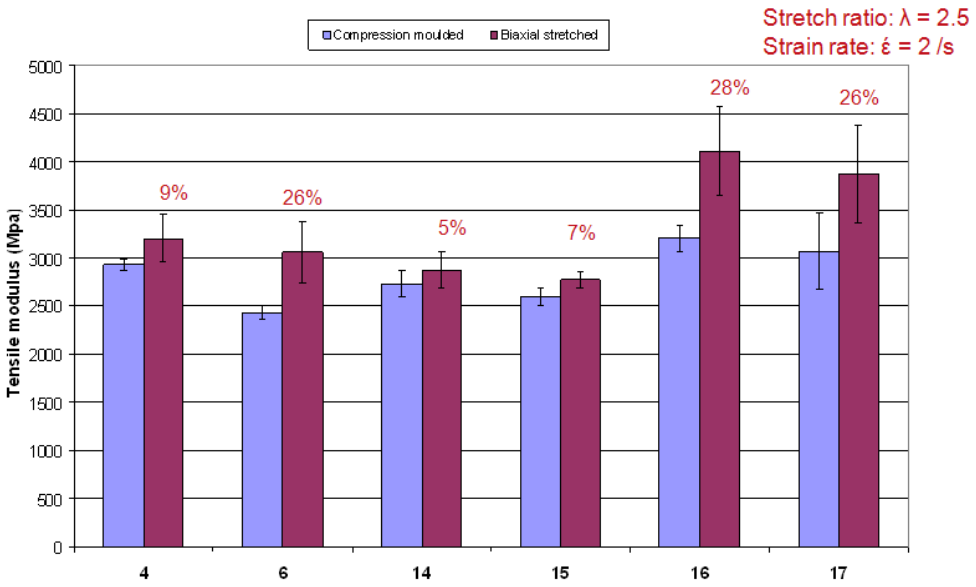

Tensile modulus of PET samples

The Modulus increased up to 28% over the compression moulded sheets and seemed to improve with higher clay loading

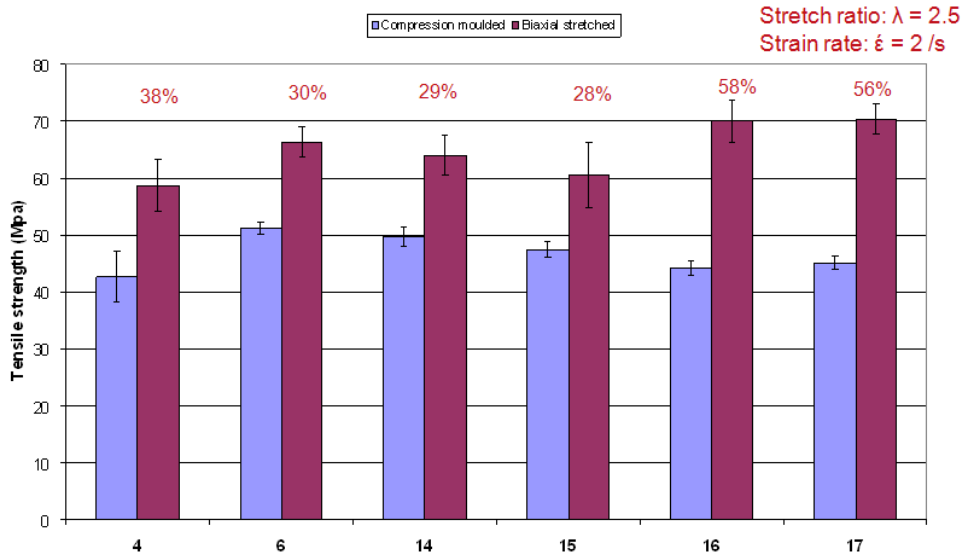

Tensile strength of PET samples

The Strength increased up to 58% over the compression moulded sheets and improved further on clay loading

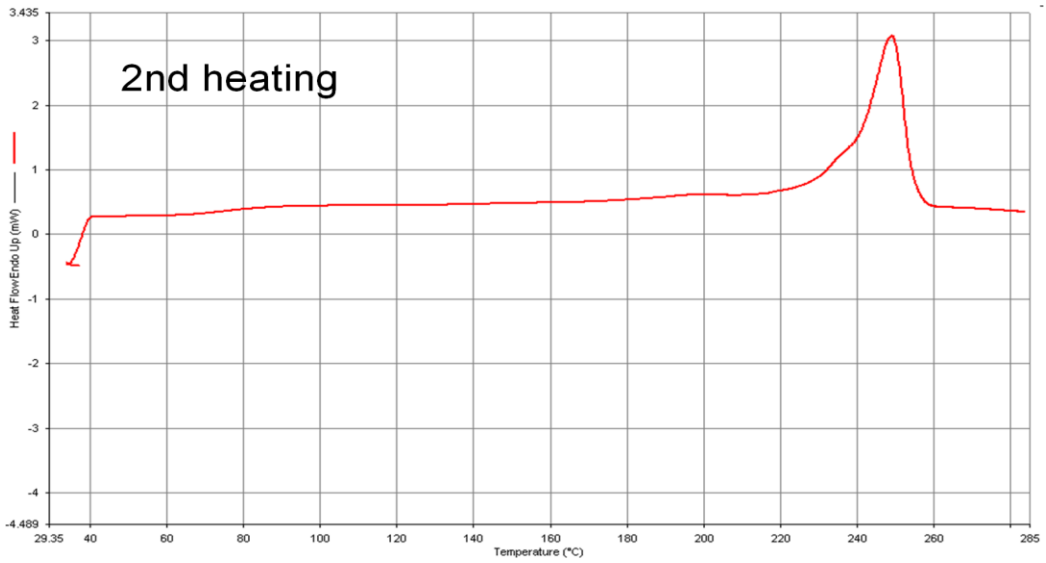

DSC of PET sample

The settings were as follows:

- Heating from 30 C to 285 C, 10C/min
- Held for 2 min
- Cooling from 285 C to 30 C, 10C/min
- Heating from 30 C to 285 C, 10C/min

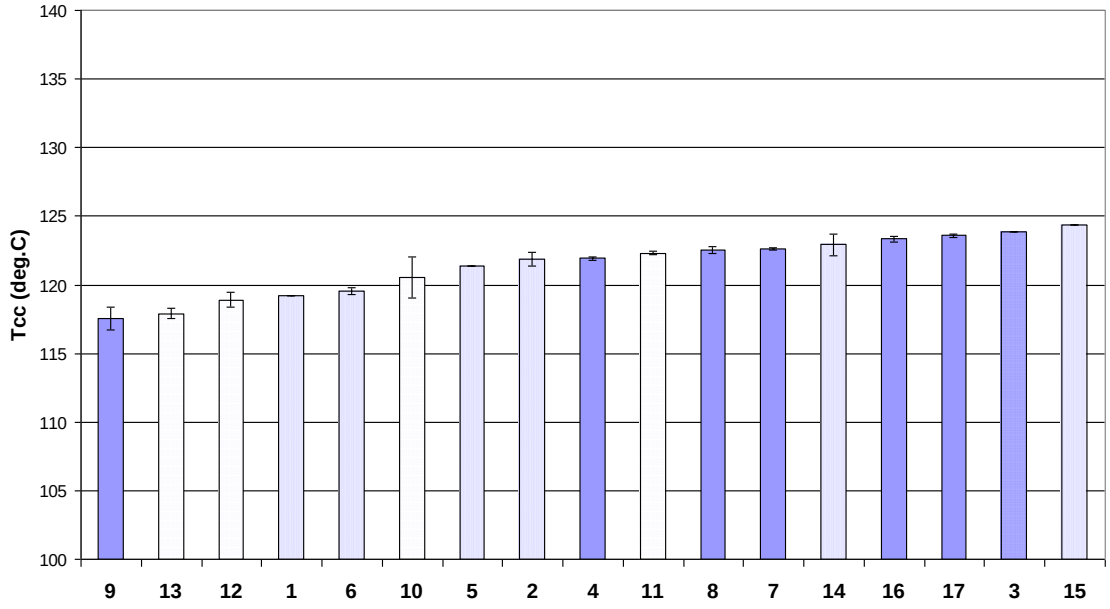

Cold crystallisation of PET samples

Difference of Tcc ~7 deg.C

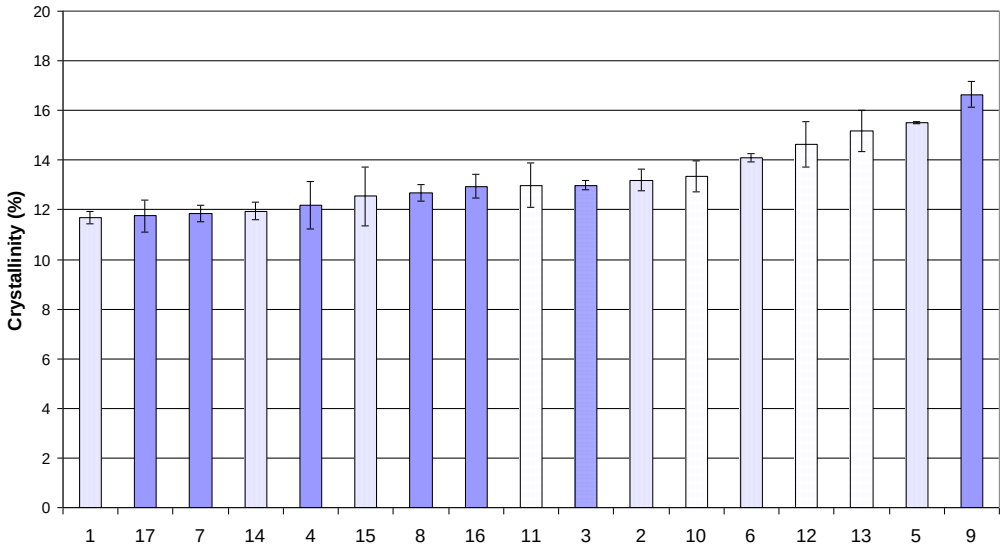

Crystallinity of PET samples

Difference of crystallinity was within 5%

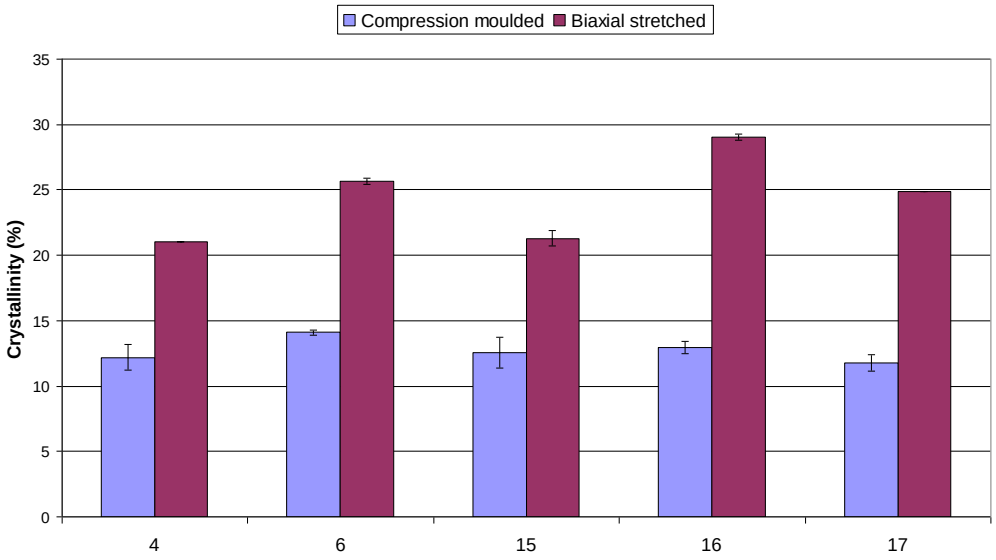

Crystallinity of PET samples

The Crystallinity doubled after biaxial stretching the samples

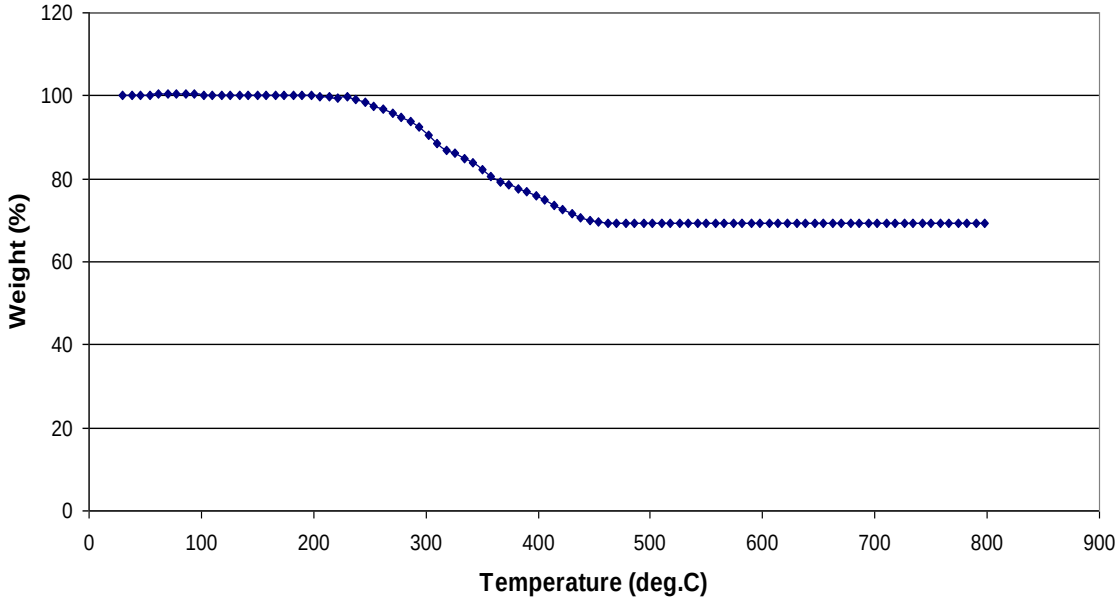

TGA of PET samples

The following settings were used:

- Heating from 30 °C to 800 °C in nitrogen atmospheres
- Heating rate 20°C /min

The Onset of degradation was ~230 °Cand the Organic surfactant: ~30%

XRD values

Sample	d (A)
MTE	23.28
Run1	22.30
Run2	22.14
Run3	22.09
Run4	22.12
Run5	22.17
Run6	22.09
Run7	22.20
Run8	22.20
Run9	22.02

The d-spacing decreased in the DOE runs compared to the clay and this may have resulted from degradation of the surfactant during processing.

There was only slight difference in the d-spacing between different runs.

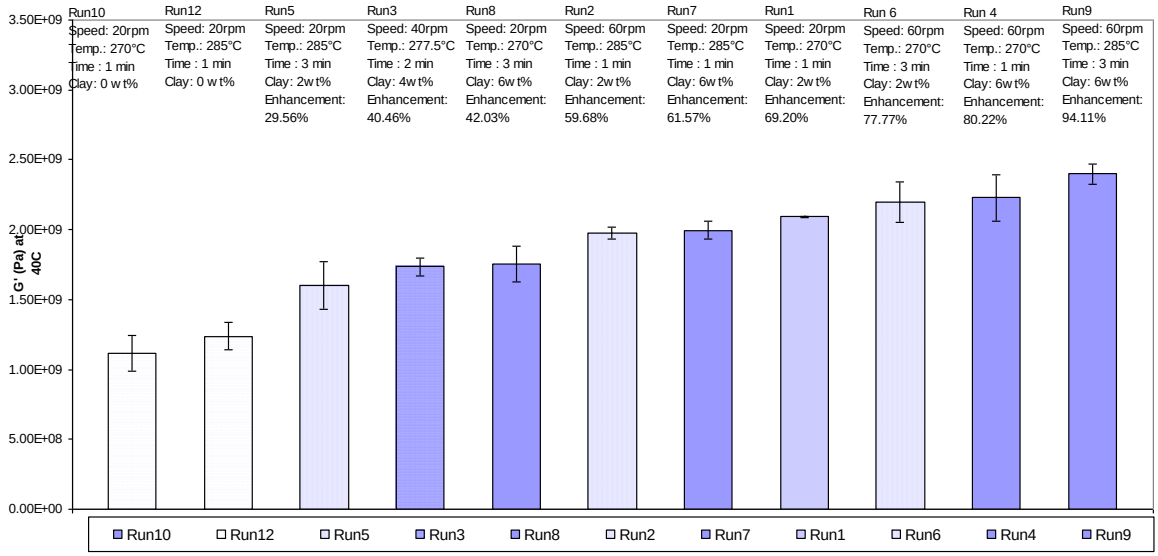

DMTA of PET samples at 40^{o}C

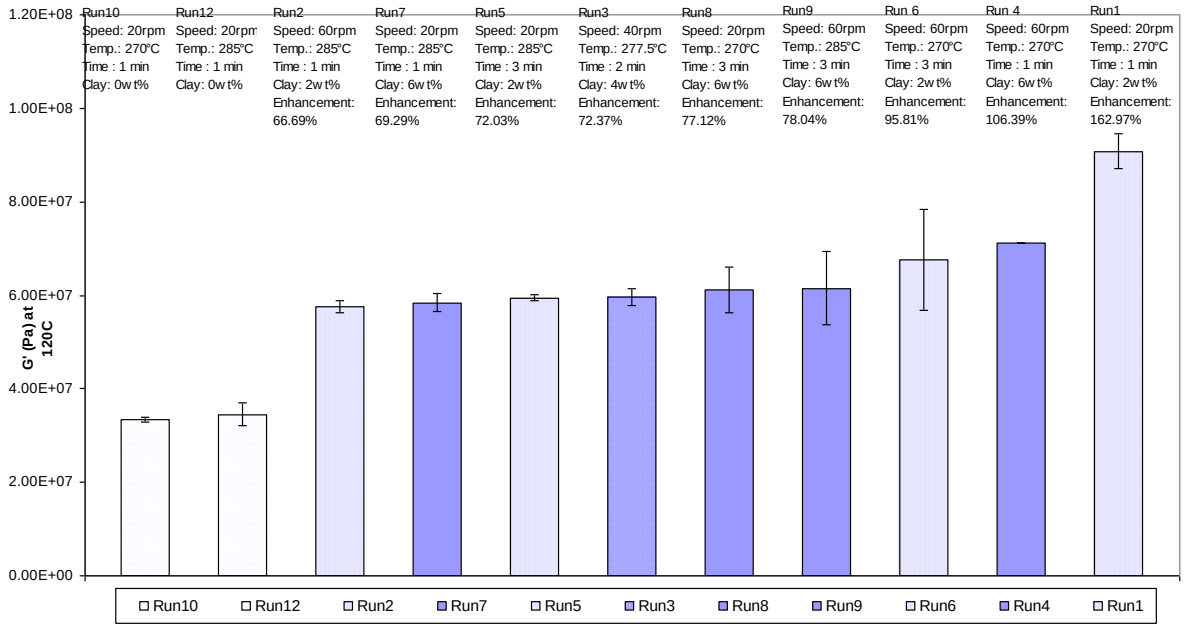

DMTA of PET samples at 120^{o}C

Overall summary

At both chosen temperatures (40°C, 120°C), there was a good enhancement in G' compared to the unfilled PET. At 40°C, the best enhancement of 94% was found in run 9 (60rpm, 285°C, 3 min, 6wt%). At 120°C, the best enhancement of 163% was found in run1 (20rpm, 270°C, 1 min, 2wt%).

At both temperatures runs 1, 4, 6, 9 showed the best four enhancements. There was a decrease in Tg with the addition of clay. Runs 10 and 12 (unfilled PET) had the highest Tg among all the runs with runs 4 and 9 having the lowest Tg values.

Overall the PET samples showed some interesting results but not as in depth as the PP data. This could have been due to a number of attributes but the main one was possible degradation of the PET material due to high shear mixing within the minimixer. Other

causes could have been from the moisture content within the material or the difficulty in testing the samples. A few alterations were made to the processing conditions of the PET including lowering the mixing time of the PET to ½ minute and drying the base materials at higher temperatures and for shorter time periods and also feeding them into the minimixer while still hot. These made a very slight improvement to the material properties but were not clear in distinguishing which DOE run had the optimum properties.

Polyurethane and Carbon nanotube trials

For the Polyurethane and Carbon nanotube experiments the following results were obtained from the online torque data obtained in real time.

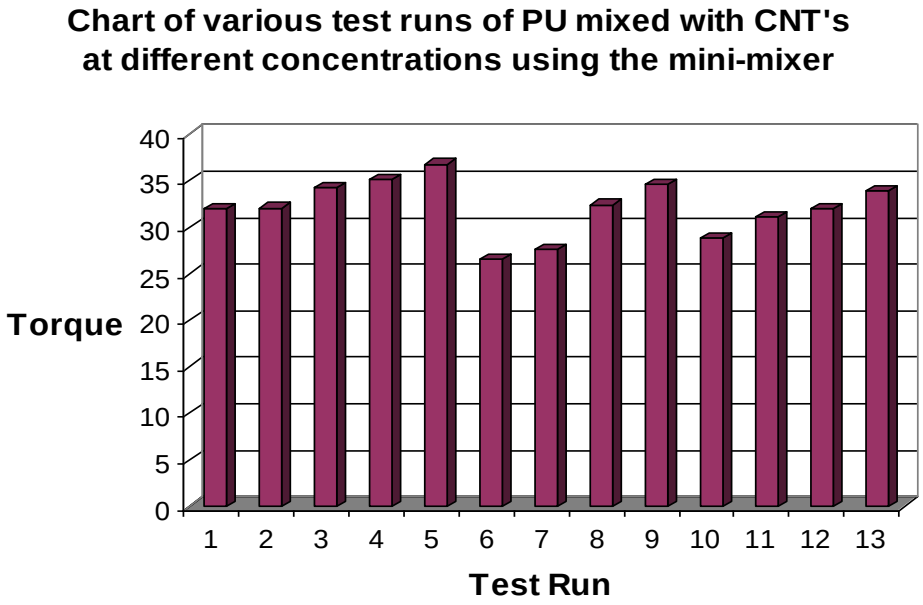

Graph of online torque readings

Chart highlighting the different torques generated in the test runs using various CNT's blended with PU.

Test Runs 1	
Test	Torque
1	31.94
2	32.08
3	34.2
4	35.1
5	36.8
6	26.55
7	27.58
8	32.39
9	34.64
10	28.89
11	31.05
12	31.99
13	33.95

Test Runs 2	
Test	Torque
1	27.33
2	27.61
3	30.83
4	32.44
5	34.62
6	28.89
7	30.16
8	32.83
9	36.5
10	28.33
11	32.39
12	33.64
13	34.15

CNT Type
PU (O%)
MWNT-OH (0.5%)
MWNT-OH (1%)
MWNT-OH (3%)
MWNT-OH (5%)
MWNT-g-PU (0.5%)
MWNT-g-PU (1%)
MWNT-g-PU (3%)
MWNT-g-PU (5%)
MWNT (1%)
MWNT-COOH (1%)
SWNT (1%)
SWNT-COOH (1%)

Torque values

Conductivity of PU/CNT

To test the electrical conductivity of the Polyurethane and Carbon nanotube samples that were prepared using the mini-mixer, a Keithley 610C electrometer was used. This equipment would allow the resistance of each sample to be measured which in turn would be used to calculate the resistivity and thus the conductance.The Keithley apparatus had to be initially calibrated to ensure accurate readings and this was done by resetting it to zero and then testing different values of resistors to ensure the readings were accurate.

All 13 samples were prepared in the same manner as highlighted below before conducting the tests to ensure that valid results could be obtained.

- The samples were measured and cut into 10cm strips
- Diameter size of each sample was ~1.5mm
- Samples were cleaned with acetone and the tips were coated with silver paint to allow better contact
- Three tests were conducted for each sample and the average taken

Once the average diameter of the 3 strands of PU/CNT was measured using Vernier callipers and the resistance measured of the 3 samples using the Keithley instrument and averaged; the conductivity of each set of sample could be obtained using the following equations.

$\rho = AR / L$ where

ρ = Resistivity (Ωm)

R = Resistance (Ω)

L = Length of sample (m)

A = Cross sectional area of sample (m^2) = $\pi D^2/4$ (D = diameter of sample)

i.e. $\rho = AR / L$

$\rho = [[3.14 \times (0.0015)^2 / 4] \times 12x10^{11}] / 0.1$

$\rho = 21.20 \times 10^6\ \Omega m$

Therefore the opposite of Resistivity (ρ) is Conductivity (σ) thus:

$\sigma = 1 / \rho$

$\sigma = 1 / 21.20 \times 10^6 = 4.72 \times 10^{-8}\ S.m^{-1}$

Sample	Average Diameter	Average Resistance	Resistivity	Conductivity
	(mm)	Ω	Ωm	S.m-1
		(1×10^{11})	(1×10^{6})	(1×10^{-8})
PU Only - No CNT	1.52	10.00	17.66	5.66
0.5% MWNT-OH	1.25	12.33	15.12	6.61
1% MWNT-OH	1.40	12.00	18.46	5.42
3% MWNT-OH	1.43	10.33	16.58	6.03
5% MWNT-OH	1.46	14.33	23.98	4.17
0.5% MWNT-PU	1.38	11.33	16.94	5.90
1% MWNT-PU	1.66	13.67	29.57	3.38
3% MWNT-PU	1.32	10.33	14.13	7.08
5% MWNT-PU	1.68	14.00	31.02	3.22
1.0% MWNT-OH	1.52	10.67	19.35	5.17
1.0% MWNT-OH	1.34	9.00	12.68	7.89
1.0% MWNT-OH	1.71	8.67	19.90	5.03
1.0% MWNT-OH	1.46	10.67	17.85	5.60

The Resistance, Resistivity & Conductivity values of each sample

From the results shown above it can be concluded that there were no signs of conductivity shown in any of the samples. This could have been due to certain factors ranging from too low concentrations of CNT's to bad dispersion or incompatibility.

Some papers have shown CNT's in concentrations as low as 1% to bring about drastic changes in conductivity within the polymer as CNT's are a good source of conductive material due to their carbon structure and high aspect ratio. However some of the experiments that have been conducted in the past using twin screw extruders and where the CNT's have been melt blended into the polymer directly have shown low conductivity levels. This could explain our scenario plus also the fact that Polyurethane is a very good conductor and so large concentrations of CNT's would be required for any conclusive results. Other techniques that have yielded positive results include doping the materials or coating them.

Further tests would have to be carried out with different parameters to understand the full concept of Polyurethane and Carbon nanotubes and their interactions.